Nalini M. Rajamannan
Editor

Molecular Biology of Valvular Heart Disease

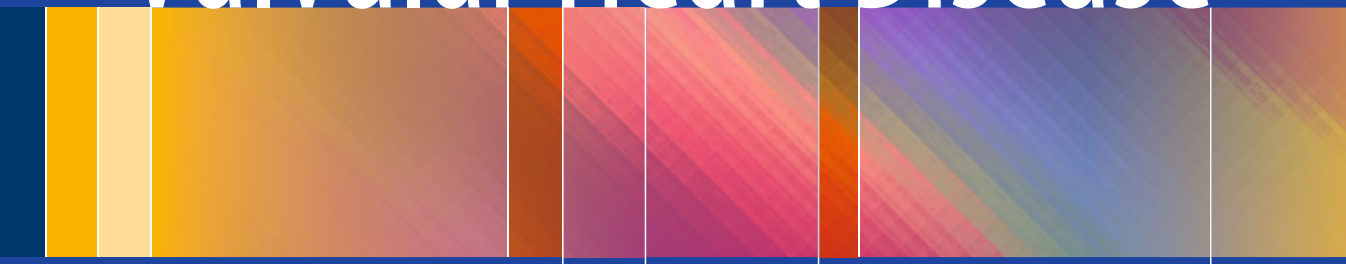

Springer

Molecular Biology of Valvular Heart Disease

Nalini M. Rajamannan
Editor

Molecular Biology of Valvular Heart Disease

Springer

Editor
Nalini M. Rajamannan, MD
Division of Biochemistry and Molecular Biology
Mayo Clinic
Rochester, MN
USA

ISBN 978-1-4471-6349-7 ISBN 978-1-4471-6350-3 (eBook)
DOI 10.1007/978-1-4471-6350-3
Springer London Heidelberg New York Dordrecht

Library of Congress Control Number: 2014937313

Printed on acid-free paper

Springer is part of Springer Science+Business Media (www.springer.com)

Dr. Harry and Concie Rajamannan, Lohini, Chapman, Hugh and Hazen Mayo and My Catholic Faith

My Mentors and Colleagues, Dr. Thomas Spelsberg and Dr. Christopher Johnson

Members of the NHLBI Working group

The co-authors of the Molecular Biology of Valvular Heart Disease and Cardiac Valvular Medicine

Foreword

The history of cardiac valve cellular biology experiments began in the early 1980s with pioneering studies from the Mayo Clinic's Department of Pediatrics by Dr. Christopher Johnson. Dr. Johnson developed *in vitro* cell culture systems to study the cellular biochemistry and molecular biology of the heart valve. The development of these porcine cell culture systems took several years to isolate, and clone the valvular sub-populations. It was clear from the start that there were two morphologically distinct layers of cells resident in the valve tissue, an endothelial cell layer and a subendothelial cell layer. These studies describing the meticulous isolation of cardiac valve cells were reported in several seminal publications. Since then, Dr. Johnson's cell culture techniques have been utilized in valve biology laboratories around the globe and have provided the foundation for understanding the cellular expression of extracellular matrix proteins both *in vitro* and *in vivo*. His pioneering work determined the optimal technique for valve cell isolation and identified subtle changes in cellular morphology by light microscopy. These early studies also provided some initial biochemical and molecular characterization of both endothelial and subendothelial cell populations.

In 1983, Johnson's laboratory established culture lines of porcine endothelial cells derived from the aortic valve. These cells had the typical morphology of vascular endothelial cells in culture and contained angiotensin-converting enzyme activity found in other endothelial cells. However, they differed from endothelial cells derived from the ascending aorta in a unique way: aortic valvular endothelial cells were deficient in their ability to synthesize fibronectin. This finding was confirmed *in vivo* using immunohistochemical staining of tissues. This was an intriguing find because fibronectin is a major biosynthetic product of other vascular endothelial cell types. Aortic valve cells are relatively deficient in this ability, a finding that carries significant implications for aortic valvular disease

In 1987, Johnson's laboratory established culture lines derived from the subendothelial region of the porcine aortic valve. These cells were isolated by extensive collagenase digestion of valvular tissue and were serially propagated *in vitro* with stable morphology. In sparse culture by phase contrast microscopy valve, subendothelial cells, later termed myofibroblasts, morphologically resembled skin fibroblasts. When confluent in the culture dish, however, the valve subendothelial cells assumed a morphology similar to that of cultured vascular smooth muscle cells, in that they formed ridges and piles. Subendothelial cells also formed calcifying nodules *in vitro*, the first description in the literature of this potentially significant phenomenon.

In 1988, Rajamannan and Johnson reported cell culture experiments that identified potential cell to cell communication occurring between valve endothelial cells and subendothelial myofibroblasts. The experiments examined materials released into the culture supernatant by endothelial cells that would affect growth and other behaviors of myofibroblast cells. This *in vitro* culture model evolved over the next 25 years to identify the role of the components of this conditioned media, including isolation of mitogenic proteins, and to characterize the expression of endothelial nitric oxide synthase in the aortic valve endothelium. The cell-cell architecture assays set the foundation for the evolving hypothesis that the endothelial cell, under conditions of oxidative stress, is responsible for the initiation event of the myofibroblast cell to signal extracellular matrix synthesis, which is then responsible for the calcification process in the valve. This cell-cell communication hypothesis has now evolved into the concept of the stem cell niche in the aortic valve.

The field evolved rapidly in the 1990s with the published findings from large databases, such as the Cardiovascular Health Study from the University of Washington. These findings demonstrated that the risk factors for valvular heart disease are similar to those for vascular atherosclerosis, including the traditional risk factors – lipids, hypertension, obesity, male gender. From 2000 to the present, *in vivo* and *in vitro* models have been described to determine the cellular basis of the calcification in the aortic valve. This included the appearance of an osteoblast-like phenotype, the phenotype of the myxomatous changes in the mitral valve, and a chondrogenic-like phenotype, as described by investigators at the University of Pennsylvania, the Mayo Clinic, Rice University, and Northwestern University. This work all began with the *in vitro* cell culture systems first described by Johnson and Rajamannan 30 years ago.

Over the past decade, animal models have been developed to study the cellular processes of the cardiac valve. These have included rabbits and genetic knock-out mice using different concentrations of experimental hypercholesterolemia diets, different lengths of diets, and renal failure to determine the critical findings of apoptosis, cell proliferation, atherosclerosis, early mineralization, chondrocyte hypertrophy, and finally calcification. The specific cell assays, both *in vivo* and *in vitro*, as well as *ex vivo* models, and techniques presented in this textbook, *Molecular Biology of Valvular Heart Disease,* will become a handbook for current and future valve biologists throughout the world.

Rochester, MN, USA Nalini M. Rajamannan, MD, FACC, FAHA
Santa Fe, NM, USA Christopher M. Johnson, MD, MA, FAAP

Preface

The National Heart, Lung, and Blood Institute (NHLBI) convened a Working Group of investigators on September 21, 2009, in Chicago, Illinois, to advise the NHLBI on the state of the science and on new research directions to improve the understanding, and ultimately, the treatment of calcific aortic valve stenosis.

Calcific aortic valve disease (CAVD) covers a spectrum of disease from initial changes in the cell biology of the valve leaflets, through early calcification, tissue remodeling and aortic sclerosis, to outflow obstruction and aortic stenosis. The later stages are characterized by fibrotic thickening of the valve leaflets and the formation of new blood vessels and calcium nodules – often including the formation of actual bone – throughout the valve leaflets but concentrated near the aortic surface. Although CAVD is more common with age, it is not an inevitable consequence of aging. CAVD appears to be an actively regulated disease process that cannot be characterized simply as "senile" or "degenerative."

Epidemiological studies show that some of the risk factors for CAVD are similar to those for vascular atherosclerosis. Age, gender, and certain clinical factors are all associated with an increased risk of CAVD. Clinical risk factors associated with the presence of CAVD include elevated low-density lipoprotein (LDL) cholesterol, but the association is relatively weak in those over 65 years old, the group at greatest risk of progressing to aortic stenosis. Other factors include smoking, hypertension, shorter height, lipoprotein (a) level, metabolic syndrome, type II diabetes, end-stage renal disease (but not mild to moderate renal disease), and imbalances in calcium or phosphate metabolism. However, the factors associated with disease initiation may differ from those that promote disease progression.

Although aortic stenosis may occur in individuals with otherwise anatomically normal aortic valves, congenital valve abnormalities markedly increase the risk. Nearly half of the individuals with aortic stenosis have a bicuspid aortic valve (BAV), an aortic valve that developed with two functional leaflets instead of the normal three. BAV occurs in about 0.6 % of the population and is the most common congenital cardiac malformation. Although the causes of BAV are unclear, genetic factors have been identified in some cases. CAVD tends to develop at an earlier age in individuals with BAV and to progress more rapidly for reasons that are poorly understood. Genetic mutations associated with BAV that cause cellular dysfunction may also predispose an individual to other congenital heart defects or to dilation and dissection of the ascending aorta.

CAVD may progress to a point-of-no-return, a stage of severe calcification where damage to the valve leaflets is too severe to be reversed by drug therapy. Whether a point-of-no-return really exists, and if so, whether it is a fundamental aspect of CAVD biology or only the limit of therapeutic ingenuity is not known.

The biology of the aortic valve is regulated by valve endothelial cells and valve interstitial cells (VICs). These cells maintain the health of the valve and mediate valve disease. VICs may behave differently in different locations within the valve and in different stages of valve development or disease. The normal signals between valve cells and the signals that trigger activation and differentiation have not been fully established. Possible triggers for VIC differentiation or dysfunction include hemodynamic shear stress, solid tissue stresses, reactive oxygen species, inflammatory cytokines and growth factors, and the cellular environment caused by other disease states, such as metabolic syndrome, diabetes mellitus, hypercholesterolemia, chronic renal disease, and disorders of calcium or phosphate metabolism. Once activated, VICs can differentiate into a variety of other cell types, including myofibroblasts and osteoblasts, although valve osteoblasts may respond to cellular signals differently than skeletal osteoblasts.

The study of bioprosthetic valves may serve as a "purer" model of calcification or VIC injury and may improve our understanding of the mechanisms of CAVD and the early events of calcification.

Mouse models of hypercholesterolemia demonstrate various features of human CAVD at the molecular and organ levels, and at least one develops stenosis. However, is only one of several conditions – including other risk factors for atherosclerosis and specific genetic mutations – that contributes to aortic stenosis, and may not be the most common. Therapies developed in high-cholesterol animal models may fail in human clinical trials unless the therapies target final common pathways leading to CAVD, which remain to be elucidated. The implications are important for the design of future clinical trials. Large animal models, possibly including non-human primates, would be helpful but are limited by technical difficulties, expense, and the likelihood that development of disease will be slow.

Prospective clinical studies of CAVD are hampered by the typically slow and variable progression of the disease. Patients who present with aortic stenosis are already in the later stages of the disease. Echocardiography is the standard for evaluating the severity of aortic stenosis and is a useful surrogate endpoint for clinical studies in the later stages. CT is a relatively high-resolution and high-sensitivity technique for evaluating aortic valve calcium and is a useful endpoint for clinical studies in the earlier stages. However, molecular imaging, with sub-millimeter resolution, may be able to identify and study the mechanisms of even earlier subclinical aortic valve calcification.

Current information does not yet support a specific pharmacological target or design of a large CAVD treatment clinical trial. Recent studies showing lipid reduction to be ineffective may have been limited by the late stage of the disease or by an insensitive measure of effect. Whether patients at an earlier stage, e.g., with aortic sclerosis, or with specific known risk factors such as BAV, should be treated with lipid lowering therapy, angiotensin converting enzyme inhibitors, or novel pharmacological interventions – even if they do not meet the current criteria for therapy – remains an open question.

Rochester, MN, USA Nalini M. Rajamannan, MD, FACC, FAHA

Contents

Contributors

Elena Aikawa, MD, PhD Division of Cardiovascular Medicine, Center for Excellence in Vascular Biology, Brigham and Women's Hospital, Harvard Medical School, Boston, MA, USA

Francesco Antonini-Canterin, MD Preventive and Rehabilitative Cardiology, Cardiologia ARC, Azienda Ospedaliera "S. Maria degli Angeli", Pordenone, Italy

Yohan Bossé, PhD Laboratoire d'Études Moléculaires des Valvulopathies (LEMV), Groupe de Recherche en Valvulopathies (GRV), Quebec Heart and Lung Institute/Research Center, Laval University, Quebec, QC, Canada

Department of Surgery, Laval University, Québec, QC, Canada

Grace Casaclang-Versoza, MD Departments of Surgery, Mayo Clinic, Rochester, MN, USA

Marie-Chloé Boulanger, PhD Laboratoire d'Études Moléculaires des Valvulopathies (LEMV), Groupe de Recherche en Valvulopathies (GRV), Quebec Heart and Lung Institute/Research Center, Laval University, Quebec, QC, Canada

Department of Surgery, Laval University, Québec, QC, Canada

Muzaffer Cicek Division of Biochemistry and Molecular Biology, Mayo Clinic, Rochester, MN, USA

Patrick S. Connell, BS Department of Bioengineering, Rice University, Houston, TX, USA

Dietmar Glogar, MD Department of Cardiology, Medical University of Vienna, Vienna, Austria

K. Jane Grande-Allen, PhD Department of Bioengineering, Rice University, Houston, TX, USA

Mariann Gyöngyösi, MD, PhD Department of Cardiology, Medical University of Vienna, Vienna, Austria

John R. Hawse Division of Biochemistry and Molecular Biology, Mayo Clinic, Rochester, MN, USA

Rayyan Hemetsberger, MD Department of Cardiology, Medical University of Vienna, Vienna, Austria

Kurt Huber 3rd Department Medicine, Wilhelminen Hospital, Vienna, Austria

Christopher M. Johnson, MD, MA Pediatric Intensive Care Unit, CentraCare Health Systems, Santa Fe, NM, USA

University of Kansas Medical School, Kansas City, KS, USA

Varun K. Krishnamurthy, PhD Department of Bioengineering, Rice University, Houston, TX, USA

Chaim Lotan, MD, FACC, FESC Division of Cardiology, Hadassah Hospital, Hadassah, Israel

Ablajan Mahmut, MD, MSc Laboratoire d'Études Moléculaires des Valvulopathies (LEMV), Groupe de Recherche en Valvulopathies (GRV), Quebec Heart and Lung Institute/Research Center, Laval University, Quebec, QC, Canada

Department of Surgery, Laval University, Québec, QC, Canada

Eduardo Martínez-Martínez Division of Cardiovascular Medicine, Center for Excellence in Vascular Biology, Brigham and Women's Hospital, Harvard Medical School, Boston, MA, USA

Patrick Mathieu, MD Laboratoire d'Études Moléculaires des Valvulopathies (LEMV), Groupe de Recherche en Valvulopathies (GRV), Quebec Heart and Lung Institute/Research Center, Laval University, Quebec, QC, Canada

Department of Surgery, Laval University, Québec, QC, Canada

Institut de Cardiologie et de Pneumologie de Québec/Quebec Heart and Lung Institute, Quebec, QC, Canada

Gerald Maurer, MD Department of Cardiology, Medical University of Vienna, Vienna, Austria

Jordan D. Miller, PhD Departments of Surgery, Mayo Clinic, Rochester, MN, USA

Department of Physiology and Biomedical Engineering, Mayo Clinic, Rochester, MN, USA

Jeffrey Park, MD Division of Biochemistry and Molecular Biology, Mayo Clinic, Rochester, MN, USA

Jeff Park, MD Division of Biochemistry and Molecular Biology, Mayo Clinic, Rochester, MN, USA

Noemi Pavo, MD, MSc Department of Cardiology, Medical University of Vienna, Vienna, Austria

Imre J. Pavo, MD Department of Cardiology, Medical University of Vienna, Vienna, Austria

Ors Petnehazy Diagnostic Imaging and Radiation Oncology, University of Kaposvar, Kaposvar, Somogy, Hungary

Zsolt Petrasi, PhD Diagnostic Imaging and Radiation Oncology, University of Kaposvar, Kaposvar, Somogy, Hungary

Philippe Pibarot, DVM, PhD, FAHA, FACC, FESC, FASE Laboratoire d'Études Moléculaires des Valvulopathies (LEMV), Groupe de Recherche en Valvulopathies (GRV), Quebec Heart and Lung Institute/Research Center, Laval University, Quebec, QC, Canada

Department of Surgery, Laval University, Québec, QC, Canada

Aniko Posa, PhD Department of Cardiology, Medical University of Vienna, Vienna, Austria

Nalini M. Rajamannan, MD Division of Biochemistry and Molecular Biology, Mayo Clinic, Rochester, MN, USA

Mony Shuvy, MD Division of Cardiology, Hadassah Hospital, Hadassah, Israel

Konstantinos Spargias, MD, PhD, FESC Department of Transcatheter Heart Valves, Hygeia Hospital, Athens, Greece

Thomas C. Spelsberg, PhD, BA Division of Biochemistry and Molecular Biology, Mayo Clinic, Rochester, MN, USA

Rembert Pogge von Strandmann, PhD Department of Clinical, Eurocor GmbH, Bonn, Germany

Malayannan Subramaniam Division of Biochemistry and Molecular Biology, Mayo Clinic, Rochester, MN, USA

Philippe Sucosky, PhD Department of Aerospace and Mechanical Engineering, Eck Institute for Global Health, University of Notre Dame, Notre Dame, IN, USA

Kristian Wachtal, MD, PhD Department of Medicine, Glostrup Hospital, University of Copenhagen, Copenhagen, Denmark

Bin Zhang, MD Department of Surgery, Mayo Clinic, Rochester, MN, USA

Calcific Aortic Valve Disease: The Role of the Stem Cell Niche

1

Nalini M. Rajamannan and Christopher M. Johnson

Introduction

Calcific Aortic Valve Disease is the most common indication for surgical valve replacement in the world [1]. For years, this disease was thought to be a passive degenerative phenomenon. Understanding of the cellular mechanisms of this valve lesion will provide new cellular therapeutic options to slow disease progression. Until recently, the etiology of valvular heart disease has been thought to be a degenerative process related to the passive accumulation of calcium binding to the surface of the valve leaflet. Recent descriptive studies have demonstrated the critical features of aortic valve calcification, including osteoblast expression, cell proliferation and atherosclerosis [2–5] and mitral valve degeneration, glycosaminglycan accumulation, proteoglycan expression, and abnormal collagen expression [6–9]. Studies have also demonstrated that specific bone cell phenotypes are present in calcifying valve specimens in human specimens [10, 11]. This phenotype is the foundation for the studies focused on the cellular mechanism for osteoblastogenesis in the heart and the foundation for the Molecular Biology of Valvular Disease.

Calcifying Stem Cells Responsible for Aortic Valve Calcification

Over the past decade, scientific publications have demonstrated that cardiac stem cells of mesenchymal origin are responsible for the bone formation in the heart. These data provide the evidence that the aortic valve calcification follows the spectrum of bone formation secondary to stem cells which have the potential to differentiate to bone, fat and cartilage. The presence of calcification in the aortic valve is responsible for valve stenosis. Severe aortic stenosis can result in symptomatic chest pain, as well as syncope and congestive heart failure in patients with severe aortic valve stenosis. For years, aortic valve stenosis was thought to be a degenerative process. However, the pathologic lesion of calcified aortic valves demonstrate the presence of complex calcification in the valve leaflet [2, 3, 12].

N.M. Rajamannan, MD (✉)
Division of Biochemistry and Molecular Biology,
Mayo Clinic, 200 First St SW,
Rochester 55905, MN, USA
e-mail: rajamannan.nalini@mayo.edu

C.M. Johnson, MD, MA
Pediatric Intensive Care Unit,
CentraCare Health Systems,
1850 Bandelier Court, Santa Fe, NM 77505, USA

University of Kansas Medical School,
Kansas City, KS, USA

N.M. Rajamannan (ed.), *Molecular Biology of Valvular Heart Disease*,
DOI 10.1007/978-1-4471-6350-3_1,

The Role of Lrp5/Beta-Catenin Activation in Cardiovascular Calcification and Osteoblast Bone Formation

Bone and cartilage are major tissues in the vertebrate skeletal system, which is primarily composed of three cell types: osteoblasts, chrondrocytes, and osteoclasts. In the developing embryo, osteoblast and chrondrocytes both differentiate from common mesenchymal progenitors in situ, whereas osteoclasts are of hematopoietic origin and brought in later by invading blood vessels. Osteoblast differentiation and maturation lead to bone formation controlled by two distinct mechanisms: intramembranous and endochondral ossification, both starting from mesenchymal condensations. To date, only two osteoblast-specific transcripts have been identified: (1) Cbfa1 and (2) osteocalcin (OC). The transcription factor Cbfa1 [13] has all the attributes of a 'master gene' differentiation factor for the osteoblast lineage and bone matrix gene expression. During embryonic development, Cbfa1 expression precedes osteoblast differentiation and is restricted to mesenchymal cells destined to become osteoblasts. In addition to its critical role in osteoblast commitment and differentiation, Cbfa1 appears to control osteoblast activity, i.e., the rate of bone formation by differentiated osteoblasts [13]. Rajamannan et al., have shown previously that cholesterol upregulates Cbfa1 gene expression in the aortic valve, and atorvastatin decreases the gene expression [5] in an animal model. The studies also demonstrated that Sox9 and Cbfa1 are expressed in human degenerative valves removed at the time of surgical valve replacement [10]. The regulatory mechanism of osteoblast differentiation from osteoblast progenitor cells into terminally differentiated cells is via a well-orchestrated and well-studied pathway which involves initial cellular proliferation events and then synthesis of bone matrix proteins, which requires the actions of specific paracrine/hormonal factors and the activation of the canonical Wnt pathway [14].

Recently, studies [10, 15–19] have shown that the Lrp5/Wnt/beta-catenin pathway plays an important role in the development of vascular and valvular calcification. Studies have shown that different mutations in Lrp5, an LDL receptor related protein, develop a high bone mass phenotype and an osteoporotic phenotype [20, 21]. In the presence of the palmitoylation of Wnt, an active beta-catenin accumulates in the cytoplasm, presumably in a signaling capacity, and eventually translocates to the nucleus via binding to nucleoporins [22] where it can interacts with LEF-1/TCFs in an inactive transcription complex [23, 24]. The Wnt/Lrp5/frizzled complex turns on downstream components such as Dishevelled (Dvl/Dsh) which leads to repression of the glycogen synthase kinase-3 (GSK3) [25]. Inhibition of GSK3 allows beta-catenin to accumulate and translocate to the nucleus. In the nucleus, beta-catenin interacts with members of the LEF/TCF class of architectural HMG box of transcription factors, including Cbfa1 and Sox9 involved in cell differentiation, osteoblast activation and chrondrocytic cell differentiation [26–31].

Translating the Calcifying Aortic Valve Mechanistically

Currently, there are three fundamental mechanisms defined in the development of aortic valve disease: (1) oxidative stress via traditional cardiovascular risk factors [5, 19, 32–39], (2) cellular proliferation [40] and (3) osteoblastogenesis in the end stage disease process [3, 4]. Previously, the Wnt/Lrp5 signaling pathway has been identified as a signaling mechanism for cardiovascular calcification [10, 19, 41]. Recently, a stem cell niche has been added to the mechanisms to define the role of cell-cell communication necessary to develop the disease [18].

The corollaries necessary to define a tissue stem cell niche include (1) physical architecture of the endothelial cells signaling to the adjacent subendothelial cells: the valve interstitial cell along the valve fibrosa, and (2) an oxidative-mechanical stress gradient necessary to activate Wnt3a/Lrp5 in this tissue stem niche to induce disease.

Cardiac Stem Cell Origins: Circulating Systemic Stem Cells Versus Resident Myofibroblast Cells

There are two specific cell types of interest for understanding the role of the cell types responsible for bone formation. First is the circulating stem cell, and second is the resident mesenchymal cell, which maintains potential to differentiate to bone. A recent study by Egan et al. [42], identifies for the first time in human calcifying aortic valves a population of circulating osteogenic precursor cells(COP) in calcified human aortic valves. Their finding of these $CD45^{+}$ OCN^{+} COP cells in areas of calcification and not in the unaffected calcified tissues provides another level of evidence that mesenchymal derived cell populations are responsible for the development of osteogensis in the calcified aortic valve. Specifically, the study demonstrated that these cells were localized to areas of confirmed endochondral ossification and bone formation. Fig. 1.1 demonstrates the two types of cardiac stem cells which have the capacity to differentiate to bone via osteogenic differentiation. Within the regions of interest, there were areas of mature bone with the characteristic architecture including osteocytes and bone lining cells. However, within the limits of the study there was no consistent involvement of the valve leaflet layers as the areas of endochondral ossification was found to extend to variable depths. The conclusions from this study provide the first evidence in human calcifying aortic valve tissue that a novel cellular origin is found on the calcific aortic valve and that these COP cells play a role in the cellular mechanisms of osteogensis. Tanaka et al. [44], have demonstrated in an in vivo experimental cholesterol model that the number of circulating stem cells is approximately 17 %. Therefore, this population of stem cells contributes to a portion of the calcification process.

The studies to date indicate that the cellular origins of bone forming cells in the calcifying aortic valve have two distinct pathways as shown in Fig. 1.1. The cells can be the COP cell capable of differentiating to bone at the site of calcification and disease. The other cell type of interest to form bone in the valve is the interstitial aortic valve cell that is capable of differentiating to bone in vivo. This cell type is described in the most recent NHLBI working group paper on calcific aortic valve disease, and this position paper provides a framework to study the cellular mechanisms of this disease process [45].

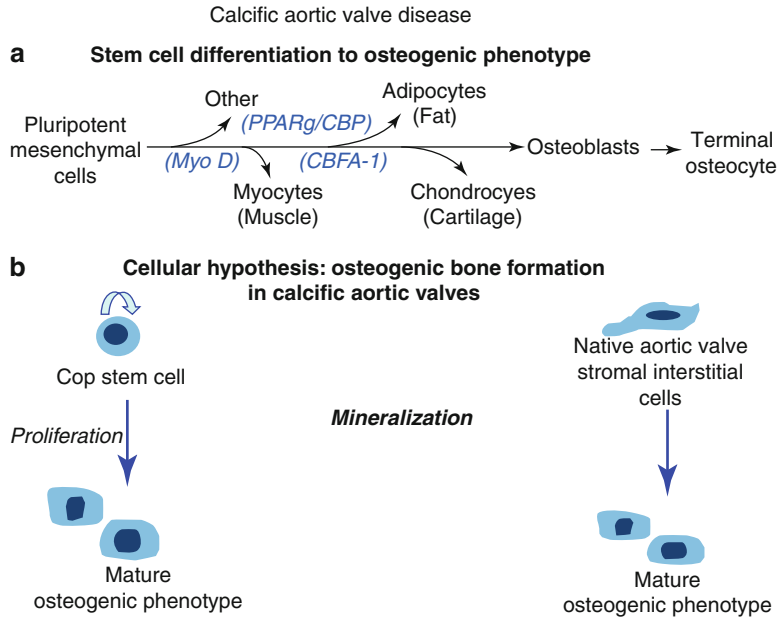

Fig. 1.1 Demonstrates the calcific aortic valve disease: cellular origins of valves calcification and the mechanisms of osteogensis in these cell types. Panel (**a**) The potential cellular phenotypes for mesenchymal derived cells, Panel (**b**) The two different cell origins for valve calcification: the COP cell versus the native interstitial cell both contributing to the hypothesis of osteogenesis in calcific aortic valve disease [43]

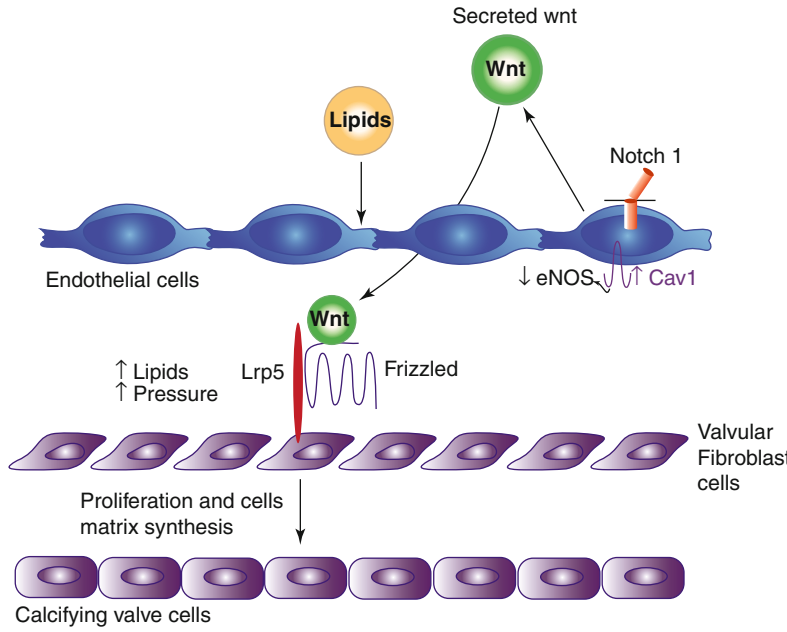

Fig. 1.2 Demonstrates the cellular architecture necessary for a stem cell niche including the cell-cell communication between valvular endothelial cells and myofibroblast cells [16]

Cardiac Valve Stem Cell Niche

Recently, the role of a stem cell niche present within the aortic valve has been identified [18]. There are two corollaries necessary for an adult stem cell niche. The first is to define the physical architecture of the stem-cell niche and second is to define the gradient of proliferation to differentiation within the stem-cell niche. Figure 1.2, demonstrates the cell architecture necessary for the stem cell niche. The endothelial lining cell located along the aortic surface is responsible for the secretion of a growth factors [46]. In the aortic valve, the endothelial cell then interacts with the subendothelial cells which are resident below the endothelial layer of cells. These cells have been characterized as myofibroblast cells [47–49].

Adult tissues stem cells are a population of functionally undifferentiated cells, capable of (i) homing (ii) proliferation, (iii) producing differentiated progeny, (iv) self-renewing, (v) regeneration, and (vi) reversibility in the use of these options. Within this definition, stem cells are defined by virtue of their functional potential and not by a specific observable characteristic. The COP cells have the potential to migrate or home to the niche once the gradient of oxidative stress develops to form bone, or the resident myofibroblast cell can differentiate to bone. Both cell types self renew via cell proliferation and then form bone via osteogenesis.

The two corollary requirements necessary for an adult stem cell niche is to first define the physical architecture of the stem-cell niche and second is to define the gradient of proliferation to differentiation within the stem-cell niche. The aortic valve endothelial cell communicates with the myofibroblast cell to activate the myofibroblast to differentiate to form an osteoblast-like phenotype [4]. This concept is similar to the endothelial/mesenchymal transition critical in normal valve development [50]. These data are the first to implicate a cell-cell communication between the aortic valve endothelial cell and the myofibroblast cell to activate the canonical Lrp5/Wnt pathway. Lrp5 is important in normal valve development [51]. In this stem cell niche, reactivation of latent Lrp5 expression [10, 19] regulates osteoblastogenesis in these mesenchymal cells.

These data fulfill the main corollaries of the plausibility of a stem cell niche as another mechanism for the development of valvular heart disease. Within a stem cell niche there is a delicate balance between proliferation and differentiation.

Cells near the stem-cell zone are more proliferative, and Wnt likely plays a role in directing cell differentiation. Endothelial cell derived Wnt3a secretion into the micro-environment is capable of activating quiescent stem cells into differentiation [52].

An important inhibitor in this model is Notch1. Notch1 plays a roll in cellular differentiation decisions. In the osteoblast cell, it serves as an inhibitor of osteoblast differentiation [53, 54]. In the aortic valve, it serves to turn off bone formation via the cell-cell crosstalk between the endothelial and the myofibroblast cells [55]. Normal Notch1 receptor functions to maintain normal valve cellular composition and homeostasis. In the presence of lipids, Notch1 is spliced and therefore activates osteoblastogenesis. In turn, the Wnt3a is secreted and binds to Lrp5 and Frizzled on the extracellular membrane to regulate the osteoblast gene program. This developmental disease process follows a parallel signaling pathway, which has been described in normal embryonic valve development. It has also been well delineated by previous investigators [50]. A similar cell-cell communication is necessary for the development of valve disease [46].

In the aortic valve, the communication for the stem cell niche would be between the aortic valve endothelial cell and the adjacent myofibroblast cell located below the aortic lining endothelial cell. Initial experiments from the 1980s characterized the initial publications isolating the cells, defining the protein expression and the potential role of the proteins in the development of CAVD [56–58]. Conditioned media was produced from untreated aortic valve endothelial cells for the microenvironment that activates signaling in the myofibroblast cell. A mitogenic protein (Wnt3a) was isolated from the conditioned media and then tested directly on the responding mesenchymal cell, the cardiac valve myofibroblast [18, 47, 59]. This transfer of isolated protein to the adjacent cell was necessary to determine if the cell would proliferate directly in the presence of this protein. This system is appealing because the responding mesenchymal cell is isolated from the anatomic region adjacent and immediately below that of the endothelial cells producing the growth factor activity along the fibrosa surface. Very little is known regarding the characterization of the endothelial cell conditioned media.

The second corollary for identifying a stem cell niche is to define the gradient responsible for the proliferation to differentiation process. The main postulate for this corollary stems from the risk factor hypothesis for the development of aortic valve disease. If traditional atherosclerotic risk factors are necessary for the initiation of disease, then these risk factors are responsible for the gradient necessary for the differentiation of myofibroblast cells to become an osteoblast calcifying phenotype [18, 19, 41, 48, 49, 61–63]. If traditional risk factors are responsible for the development of valvular heart disease, then an oxidative stress mechanism is important for the development of a gradient in this niche.

Nitric oxide is important in terms of the mechanism in adult disease processes and also in the developmental abnormalities such as the bicuspid aortic valve phenotype in the eNOS null mouse [18, 64]. The proof of principle experiment to test the importance of eNOS enzymatic activity is an overexpression experiment to determine if eNOS is able to inhibit cell proliferation, an early cellular event in the development of aortic stenosis [40].

A recent study demonstrates the effects of lipids regulating the development of a “Wnt3a” gradient in the abnormal oxidative stress microenvironment [18]. If the presence of elevated LDL can increase Wnt3a secretion into the conditioned media or the microenvironment of the diseased aortic valve, this further contributes to the activation of the canonical Wnt pathway in the subendothelial space of the aortic valve. The stem cell niche is a unique model for the development of an oxidative stress secondary to hyperlipidemia communication within the aortic valve endothelium. The model proposed for a stem cell niche in calcific aortic valve disease in Fig. 1.2, provides the cellular architecture for the development of this disease process. This model does not take into account other cytokine/growth factor mediated mechanisms shown to also be important in this disease process [64].

As shown in Fig. 1.2, oxidative stress contributes to the release of Wnt3a into the subendothelial space to activate Lrp5/Frizzled receptor complex on the extracellular membrane of the myofibroblast. This trimeric complex then induces glycogen synthase kinase to be phosphorylated. This phosphorylation event causes β-catenin translocation to the nucleus. β-catenin acts as a coactivator of osteoblast specific transcription factor, Cbfa1, to induce mesenchymal osteoblastogenesis in the aortic valve myofibroblast cell.

Isolated Aortic Valve Endothelial Cells and Myofibroblast Cells by Light Microscopy

Figure 1.3 is the Light Microscopy of in vitro Aortic Valve Endothelial Cells and Myofibroblast Cells demonstrating the morphology of the cells isolated in the stem cell niche. Figure 1.3 is the light microscopy of the isolated cells from the aortic valve, including the top layer of cells, the endothelial cell, as shown in Fig. 1.3, Panel a. The lower layer of cells, the subendothelial cell, Fig. 1.3, Panel b, now entitled the myofibroblast cell. Figure 1.3, Panel c, is immunohistochemistry for alpha-actin stain to confirm the presence of actin filaments in the cell layer found in the valve fibrosa [45]. The techniques for isolation of these cell populations involves specific isolation techniques to clone populations of endothelial and vascular smooth muscles from the aorta, and myofibroblasts from the aortic valve, mitral valve, and pulmonary valve [47, 57–59].

In Vitro Model of Endothelial-Myofibroblast Cell-Cell Signaling

Figure 1.4 is a summary of these experimental results. Figure 1.4 demonstrates the isolation and characterization of the mitogenic protein from the conditioned media microenvironment. Endothelial cells were cultured as shown in Fig. 1.4, Panel a, which is a light microscopy photograph of aortic valve endothelial cells isolated from the aortic surface of the aortic valve. The media was obtained from the endothelial cells and then transferred directly to the myofibroblast cell to determine effects on cell proliferation. The results of the mitogen assays for fractions eluting from a DEAE- Sephadex column are shown in Fig. 1.4, Panel c. It can be seen that the mitogenic activity appeared as a single peak eluting at approximately 0.25 M NaCl. The material eluting from DEAE- Sephadex was then applied to Sephadex G-100; the results of mitogen assays on fractions eluting from such a gel

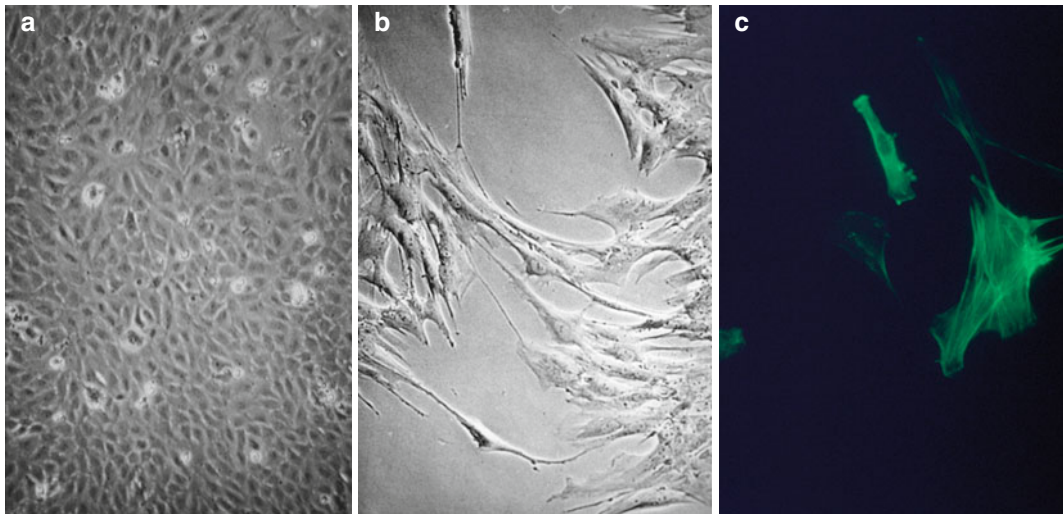

Fig. 1.3 Demonstrates the light microscopy of the In vitro cells isolated from the aortic valve endothelium, Panel (**a**) the aortic valve myofibroblast cell, Panel (**b**) and Alpha-Actin Stain of the myofibroblast cell, Panel (**c**)

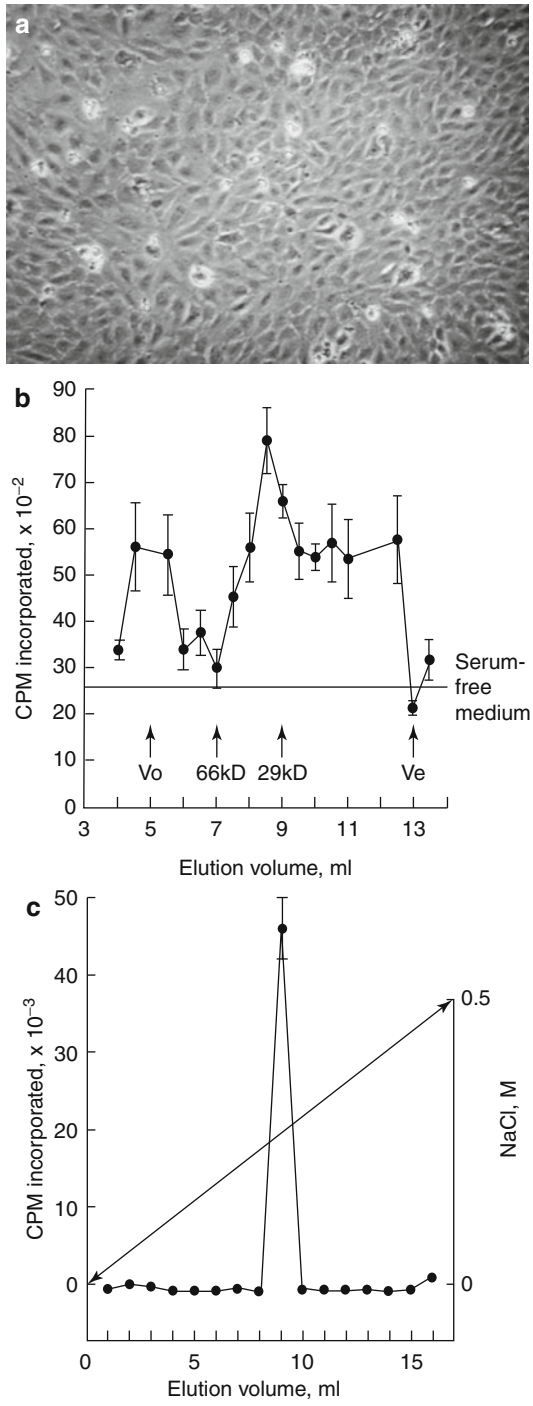

Fig. 1.4 Protein isolation and characterization of aortic valve endothelial cell conditioned media. Panel (**a**) Light microscopy for aortic valve endothelial cells. Panel (**b**) Cell proliferation for fractions eluting from a DEAE-Sephadex column. ($p<0.001$). Panel (**c**). Fractions from DEAE- Sephadex to characterize weight with Sephadex G-100. ($p<0.001$)

filtration column are shown in Fig. 1.4, Panel b. It can be seen that under these native, non-denaturing conditions the bulk of the mitogenic activity eluted as a peak corresponding to standard proteins of 30–40,000 molecular weight. This material lost all activity when heated to 100 °C for 5 min; disulfide bond reduction with dithiothreitol also abolished all mitogenic activity, and treatment with trypsin destroyed all activity, implicating a protein structure.

These data demonstrate. Importance of the first corollary for defining a tissue stem cell niche: the physical architecture necessary for the signaling mechanisms. The endothelial lining cells along the aortic surface of the aortic valve signal to the myofibroblast cells that are resident below the endothelial cells to activate the disease process [18, 46].

The Role of Endothelial Nitric Oxide Synthase in Aortic Valve Endothelial Cells

The second corollary for identifying a stem cell niche is to define the gradient responsible for the proliferation to differentiation process. To answer this question of the role of oxidative stress and nitric oxide in the aortic valve, in vitro experiments were performed to determine eNOS enzymatic and protein regulation in the presence of lipids and attenuation with Atorvastatin to confirm the importance of eNOS enzymatic function in vitro [18].

eNOS Expression and Functional Assays in Aortic Valve Endothelial Cells

Figure 1.5 demonstrates the eNOS regulation in the endothelial cells in the presence of lipids with and without Atorvastatin. A number of standard nitric oxide assays were performed to measure eNOS functional activity. There was an increase in nitrites with lipid treatments and attenuation with Atorvastatin. This increase in nitrite levels correlates with a decrease in the functional activity of the eNOS enzyme in the aortic valve

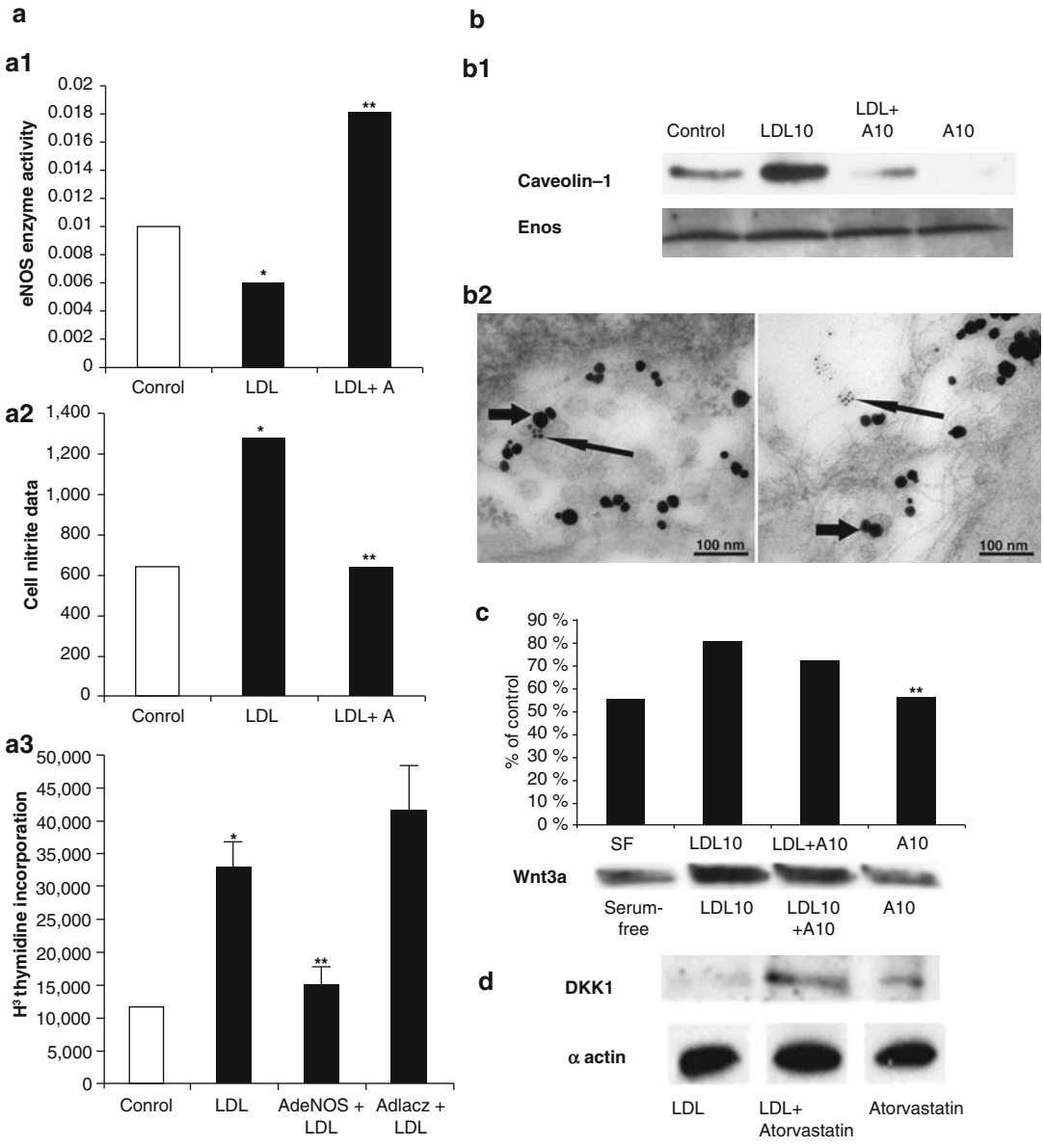

Fig. 1.5 Evidence for eNOS regulation and Wnt3a secretion from aortic valve endothelial cells. *$p<0.001$ for control compared to cholesterol, **$p<0.001$ for cholesterol compared to cholesterol + Atorvastatin. Panel (*a1)* Graph is the eNOS enzymatic activity in the presence of control conditioned media, LDL treated conditioned media decreasing the eNOS enzyme activity, and the LDL + Atorvastatin treatment improving the eNOS enzyme activity. Panel (*a2)* Cell Nitrite Data indicating the Nitrite levels increase with the LDL conditioned media. Panel (*a3)* . Cell Proliferation data as indicated by the LDL treated conditioned media, and the inhibition of myofibroblast cell proliferaiton data in the presend of adenoviral eNOS treatment. Panel (*b1)* Caveolin-1 and eNOS protein expression isolated from the lipid with and without atorvastatin treated cells as shown by Western Blot. Panel (*b2)* The large arrow points to the immunogold label. The large gold label points to the caveolin-1, and the small gold label points to the eNOS protein. Panel (**c**) Wnt3a Immunoprecipitate from Conditioned Media treated with LDL with and without Atorvastatin. Panel (**d**) Dkk1 protein expression from the myofibroblast cells treated with conditioned media with lipid and with and without atorvastatin treated cells as shown by Western Blot

endothelium [18]. The proof of principle experiment to test the importance of eNOS enzymatic activity is an overexpression experiment to determine if eNOS is able to inhibit cell proliferation, an early cellular event in the development of aortic stenosis [40]. Experiments were performed to overexpress eNOS to determine if eNOS overexpression in the aortic valve endothelial cells would regulate cell proliferation and found that eNOS overexpression reduced cell proliferation [18]. Caveolin-1 and eNOS expression confirmed the role of these structural proteins in the interaction with eNOS in the aortic valve similar to vasculature [65–69].

The regulatory mechanism of osteoblast differentiation from osteoblast progenitor cells into terminally differentiated cells is via a well-orchestrated and well-studied pathway which involves initial cellular proliferation events and then synthesis of bone matrix proteins, which requires the actions of specific paracrine/hormonal factors/cell signaling activation of the canonical Wnt pathway [10, 15, 16, 18, 45, 55, 70, 71]. The presence of variable depths of the COP cell in the calcific valve is consistent with the hypothesis that these cells can home to the diseased valve but are not responsible for the entire bone formation process. The native interstitial cells also have the potential to differentiate to bone in situ and contribute to the calcifying cells in the native valve. The contribution of these two cell types toward the development of calcification in the aortic valve requires further ongoing investigation for future translational implications.

Summary

This chapter demonstrates experimental methods to test the hypothesis that aortic valve stenosis develops secondary to stem cell niche mediated process. Figure 1.2 demonstrates the cell-cell signaling pathways necessary to fulfill the stem cell niche and to differentiate the myofibroblast cell to an osteogenic phenotype as described in Chap. 2. The two corollary requirements necessary for an adult stem cell niche is to first define the physical architecture of the stem-cell niche and second is to define the gradient of proliferation to differentiation within the tissue stem-cell niche. The aortic valve endothelial cell communicates with the myofibroblast cell to activate the myofibroblast to differentiate to form an osteoblast-like phenotype [4]. This concept is similar to the endothelial/mesenchymal transition critical in normal valve development [50].

References

1. Roberts WC, Ko JM. Frequency by decades of unicuspid, bicuspid, and tricuspid aortic valves in adults having isolated aortic valve replacement for aortic stenosis, with or without associated aortic regurgitation. Circulation. 2005;111:920–5.
2. O'Brien KD, Kuusisto J, Reichenbach DD, Ferguson M, Giachelli C, Alpers CE, Otto CM. Osteopontin is expressed in human aortic valvular lesions. Circulation. 1995;92:2163–8 [comment].
3. Mohler 3rd ER, Gannon F, Reynolds C, Zimmerman R, Keane MG, Kaplan FS. Bone formation and inflammation in cardiac valves. Circulation. 2001;103:1522–8.
4. Rajamannan NM, Subramaniam M, Rickard D, Stock SR, Donovan J, Springett M, Orszulak T, Fullerton DA, Tajik AJ, Bonow RO, Spelsberg T. Human aortic valve calcification is associated with an osteoblast phenotype. Circulation. 2003;107:2181–4.
5. Rajamannan NM, Subramaniam M, Springett M, Sebo TC, Niekrasz M, McConnell JP, Singh RJ, Stone NJ, Bonow RO, Spelsberg TC. Atorvastatin inhibits hypercholesterolemia-induced cellular proliferation and bone matrix production in the rabbit aortic valve. Circulation. 2002;105:2260–5.
6. Whittaker P, Boughner DR, Perkins DG, Canham PB. Quantitative structural analysis of collagen in chordae tendineae and its relation to floppy mitral valves and proteoglycan infiltration. Br Heart J. 1987;57:264–9.
7. Wooley CF, Baker PB, Kolibash AJ, Kilman JW, Sparks EA, Boudoulas H. The floppy, myxomatous mitral valve, mitral valve prolapse, and mitral regurgitation. Prog Cardiovasc Dis. 1991;33:397–433.
8. Grande-Allen KJ, Borowski AG, Troughton RW, Houghtaling PL, Dipaola NR, Moravec CS, Vesely I, Griffin BP. Apparently normal mitral valves in patients with heart failure demonstrate biochemical and structural derangements: an extracellular matrix and echocardiographic study. J Am Coll Cardiol. 2005;45:54–61 [see comment].
9. Grande-Allen KJ, Calabro A, Gupta V, Wight TN, Hascall VC, Vesely I. Glycosaminoglycans and proteoglycans in normal mitral valve leaflets and chordae: association with regions of tensile and compressive loading. Glycobiology. 2004;14:621–33.

10. Caira FC, Stock SR, Gleason TG, McGee EC, Huang J, Bonow RO, Spelsberg TC, McCarthy PM, Rahimtoola SH, Rajamannan NM. Human degenerative valve disease is associated with up-regulation of low-density lipoprotein receptor-related protein 5 receptor-mediated bone formation. J Am Coll Cardiol. 2006;47:1707–12.
11. Jian B, Jones PL, Li Q, Mohler 3rd ER, Schoen FJ, Levy RJ. Matrix metalloproteinase-2 is associated with tenascin-c in calcific aortic stenosis. Am J Pathol. 2001;159:321–7.
12. Mohler 3rd ER, Adam LP, McClelland P, Graham L, Hathaway DR. Detection of osteopontin in calcified human aortic valves. Arterioscler Thromb Vasc Biol. 1997;17:547–52.
13. Ducy P, Zhang R, Geoffroy V, Ridall AL, Karsenty G. Osf2/cbfa1: a transcriptional activator of osteoblast differentiation. Cell. 1997;89:747–54 [see comment].
14. Aubin JE, Liu F, Malaval L, Gupta AK. Osteoblast and chondroblast differentiation. Bone. 1995;17:77S–83.
15. Rajamannan NM. The role of lrp5/6 in cardiac valve disease: experimental hypercholesterolemia in the apoe-/- /lrp5-/- mice. J Cell Biochem. 2011;112:2987–91.
16. Rajamannan NM. The role of lrp5/6 in cardiac valve disease: Ldl-density-pressure theory. J Cell Biochem. 2011;112:2222–9.
17. Rajamannan NM. Bicuspid aortic valve disease: the role of oxidative stress in lrp5 bone formation. Cardiovasc Pathol. 2011;20:168–76.
18. Rajamannan NM. Oxidative-mechanical stress signals stem cell niche mediated lrp5 osteogenesis in enos(-/-) null mice. J Cell Biochem. 2012;113:1623–34.
19. Rajamannan NM, Subramaniam M, Caira F, Stock SR, Spelsberg TC. Atorvastatin inhibits hypercholesterolemia-induced calcification in the aortic valves via the lrp5 receptor pathway. Circulation. 2005;112:I229–34.
20. Little RD, Carulli JP, Del Mastro RG, Dupuis J, Osborne M, Folz C, Manning SP, Swain PM, Zhao SC, Eustace B, Lappe MM, Spitzer L, Zweier S, Braunschweiger K, Benchekroun Y, Hu X, Adair R, Chee L, FitzGerald MG, Tulig C, Caruso A, Tzellas N, Bawa A, Franklin B, McGuire S, Nogues X, Gong G, Allen KM, Anisowicz A, Morales AJ, Lomedico PT, Recker SM, Van Eerdewegh P, Recker RR, Johnson ML. A mutation in the ldl receptor-related protein 5 gene results in the autosomal dominant high-bone-mass trait. Am J Hum Genet. 2002;70:11–9.
21. Gong Y, Slee RB, Fukai N, Rawadi G, Roman-Roman S, Reginato AM, Wang H, Cundy T, Glorieux FH, Lev D, Zacharin M, Oexle K, Marcelino J, Suwairi W, Heeger S, Sabatakos G, Apte S, Adkins WN, Allgrove J, Arslan-Kirchner M, Batch JA, Beighton P, Black GC, Boles RG, Boon LM, Borrone C, Brunner HG, Carle GF, Dallapiccola B, De Paepe A, Floege B, Halfhide ML, Hall B, Hennekam RC, Hirose T, Jans A, Juppner H, Kim CA, Keppler-Noreuil K, Kohlschuetter A, LaCombe D, Lambert M, Lemyre E, Letteboer T, Peltonen L, Ramesar RS, Romanengo M, Somer H, Steichen-Gersdorf E, Steinmann B, Sullivan B, Superti-Furga A, Swoboda W, van den Boogaard MJ, Van Hul W, Vikkula M, Votruba M, Zabel B, Garcia T, Baron R, Olsen BR, Warman ML, Osteoporosis-Pseudoglioma Syndrome Collaborative G. Ldl receptor-related protein 5 (lrp5) affects bone accrual and eye development. Cell. 2001;107:513–23.
22. Willert K, Nusse R. Beta-catenin: a key mediator of wnt signaling. Curr Opin Genet Dev. 1998;8:95–102.
23. Behrens J, von Kries JP, Kuhl M, Bruhn L, Wedlich D, Grosschedl R, Birchmeier W. Functional interaction of beta-catenin with the transcription factor lef-1. Nature. 1996;382:638–42.
24. Huber O, Korn R, McLaughlin J, Ohsugi M, Herrmann BG, Kemler R. Nuclear localization of beta-catenin by interaction with transcription factor lef-1. Mech Dev. 1996;59:3–10.
25. Holmen SL, Salic A, Zylstra CR, Kirschner MW, Williams BO. A novel set of wnt-frizzled fusion proteins identifies receptor components that activate beta -catenin-dependent signaling. J Biol Chem. 2002;277:34727–35.
26. Caverzasio J. [wnt/lrp5, a new regulation osteoblastic pathway involved in reaching peak bone masses]. Rev Med Suisse Romande. 2004;124:81–2.
27. Kahler RA, Westendorf JJ. Lymphoid enhancer factor-1 and beta-catenin inhibit runx2-dependent transcriptional activation of the osteocalcin promoter. J Biol Chem. 2003;278:11937–44.
28. Smith E, Frenkel B. Glucocorticoids inhibit the transcriptional activity of lef/tcf in differentiating osteoblasts in a glycogen synthase kinase-3{beta}-dependent and -independent manner. J Biol Chem. 2005;280:2388–94.
29. Wang HY, Malbon CC. Wnt signaling, ca2+, and cyclic gmp: visualizing frizzled functions. Science. 2003;300:1529–30.
30. Gregory CA, Perry AS, Reyes E, Conley A, Gunn WG, Prockop DJ. Dkk-1-derived synthetic peptides and lithium chloride for the control and recovery of adult stem cells from bone marrow. J Biol Chem. 2005;280:2309–23.
31. Yano F, Kugimiya F, Ohba S, Ikeda T, Chikuda H, Ogasawara T, Ogata N, Takato T, Nakamura K, Kawaguchi H, Chung UI. The canonical wnt signaling pathway promotes chondrocyte differentiation in a sox9-dependent manner. Biochem Biophys Res Commun. 2005;333:1300–8.
32. Drolet MC, Arsenault M, Couet J. Experimental aortic valve stenosis in rabbits. J Am Coll Cardiol. 2003;41:1211–7.
33. Weiss RM, Ohashi M, Miller JD, Young SG, Heistad DD. Calcific aortic valve stenosis in old hypercholesterolemic mice. Circulation. 2006;114:2065–9.
34. Aikawa E, Nahrendorf M, Sosnovik D, Lok VM, Jaffer FA, Aikawa M, Weissleder R. Multimodality molecular imaging identifies proteolytic and osteogenic activities in early aortic valve disease. Circulation. 2007;115:377–86.
35. Rajamannan NM, Springett MJ, Pederson LG, Carmichael SW. Localization of caveolin 1 in aortic

valve endothelial cells using antigen retrieval. J Histochem Cytochem. 2002;50:617–28.
36. Rajamannan NM, Edwards WD, Spelsberg TC. Hypercholesterolemic aortic-valve disease. N Engl J Med. 2003;349:717–8.
37. Rajamannan NM, Subramaniam M, Stock SR, Stone NJ, Springett M, Ignatiev KI, McConnell JP, Singh RJ, Bonow RO, Spelsberg TC. Atorvastatin inhibits calcification and enhances nitric oxide synthase production in the hypercholesterolaemic aortic valve. Heart. 2005;91:806–10.
38. Makkena B, Salti H, Subramaniam M, Thennapan S, Bonow RH, Caira F, Bonow RO, Spelsberg TC, Rajamannan NM. Atorvastatin decreases cellular proliferation and bone matrix expression in the hypercholesterolemic mitral valve. J Am Coll Cardiol. 2005;45:631–3.
39. Ortlepp JR, Pillich M, Schmitz F, Mevissen V, Koos R, Weiss S, Stork L, Dronskowski R, Langebartels G, Autschbach R, Brandenburg V, Woodruff S, Kaden JJ, Hoffmann R. Lower serum calcium levels are associated with greater calcium hydroxyapatite deposition in native aortic valves of male patients with severe calcific aortic stenosis. J Heart Valve Dis. 2006;15:502–8.
40. Rajamannan NM, Sangiorgi G, Springett M, Arnold K, Mohacsi T, Spagnoli LG, Edwards WD, Tajik AJ, Schwartz RS. Experimental hypercholesterolemia induces apoptosis in the aortic valve. J Heart Valve Dis. 2001;10:371–4.
41. Shao JS, Cheng SL, Pingsterhaus JM, Charlton-Kachigian N, Loewy AP, Towler DA. Msx2 promotes cardiovascular calcification by activating paracrine wnt signals. J Clin Invest. 2005;115:1210–20.
42. Egan KP, Kim JH, Mohler 3rd ER, Pignolo RJ. Role for circulating osteogenic precursor cells in aortic valvular disease. Arterioscler Thromb Vasc Biol. 2011;31:2965–71.
43. Rajamannan NM. Calcific aortic valve disease: cellular origins of valve calcification. Arterioscler Thromb Vasc Biol. 2011;31:2777–8.
44. Tanaka K, Sata M, Fukuda D, Suematsu Y, Motomura N, Takamoto S, Hirata Y, Nagai R. Age-associated aortic stenosis in apolipoprotein e-deficient mice. J Am Coll Cardiol. 2005;46:134–41.
45. Rajamannan NM, Evans FJ, Aikawa E, Grande-Allen KJ, Demer LL, Heistad DD, Simmons CA, Masters KS, Mathieu P, O'Brien KD, Schoen FJ, Towler DA, Yoganathan AP, Otto CM. Calcific aortic valve disease: not simply a degenerative process: a review and agenda for research from the national heart and lung and blood institute aortic stenosis working group. Executive summary: Calcific aortic valve disease-2011 update. Circulation. 2011;124:1783–91.
46. Rajamannan NM, Helgeson SC, Johnson CM. Anionic growth factor activity from cardiac valve endothelial cells: partial purification and characterization. Clin Res. 1988:309A.
47. Johnson CM, Hanson MN, Helgeson SC. Porcine cardiac valvular subendothelial cells in culture: cell isolation and growth characteristics. J Mol Cell Cardiol. 1987;19:1185–93.
48. Mohler 3rd ER, Chawla MK, Chang AW, Vyavahare N, Levy RJ, Graham L, Gannon FH. Identification and characterization of calcifying valve cells from human and canine aortic valves. J Heart Valve Dis. 1999;8:254–60.
49. Osman L, Yacoub MH, Latif N, Amrani M, Chester AH. Role of human valve interstitial cells in valve calcification and their response to atorvastatin. Circulation. 2006;114:I547–52.
50. Paruchuri S, Yang JH, Aikawa E, Melero-Martin JM, Khan ZA, Loukogeorgakis S, Schoen FJ, Bischoff J. Human pulmonary valve progenitor cells exhibit endothelial/mesenchymal plasticity in response to vascular endothelial growth factor-a and transforming growth factor-beta2. Circ Res. 2006;99:861–9.
51. Hurlstone AF, Haramis AP, Wienholds E, Begthel H, Korving J, Van Eeden F, Cuppen E, Zivkovic D, Plasterk RH, Clevers H. The wnt/beta-catenin pathway regulates cardiac valve formation. Nature. 2003;425:633–7.
52. de Haan G, Dontje B, Nijhof W. Concepts of hemopoietic cell amplification. Synergy, redundancy and pleiotropy of cytokines affecting the regulation of erythropoiesis. Leuk Lymphoma. 1996;22:385–94.
53. Sciaudone M, Gazzerro E, Priest L, Delany AM, Canalis E. Notch 1 impairs osteoblastic cell differentiation. Endocrinology. 2003;144:5631–9.
54. Deregowski V, Gazzerro E, Priest L, Rydziel S, Canalis E. Notch 1 overexpression inhibits osteoblastogenesis by suppressing wnt/beta-catenin but not bone morphogenetic protein signaling. J Biol Chem. 2006;281:6203–10.
55. Rajamannan NM. Role of oxidative stress in calcific aortic valve disease: from bench to bedside – the role of a stem cell niche. In: Morales-Gonzalez J.A.Oxidative Stress and Chronic Degenerative Diseases - A Role for Antioxidants, InTech Publisher, 2013; Chapter 11, pp. 265–87.
56. Johnson CM, Fass DN. Porcine cardiac valvular endothelial cells in culture. A relative deficiency of fibronectin synthesis in vitro. Lab Invest. 1983; 49:589–98.
57. Johnson CM, Helgeson SC. Platelet adherence to cardiac and noncardiac endothelial cells in culture: lack of a prostacyclin effect. J Lab Clin Med. 1988;112: 372–9.
58. Johnson CM, Helgeson SC. Fibronectin biosynthesis and cell-surface expression by cardiac and non-cardiac endothelial cells. Am J Pathol. 1993;142:1401–8.
59. Johnson CM, Helgeson SC. Glycoproteins synthesized by cultured cardiac valve endothelial cells: unique absence of fibronectin production. Biochem Biophys Res Commun. 1988;153:46–50.
60. Tintut Y, Alfonso Z, Saini T, Radcliff K, Watson K, Bostrom K, Demer LL. Multilineage potential of cells from the artery wall. Circulation. 2003;108: 2505–10.
61. Wada T, McKee MD, Steitz S, Giachelli CM. Calcification of vascular smooth muscle cell cultures: inhibition by osteopontin. Circ Res. 1999;84:166–78.

62. Kirton JP, Crofts NJ, George SJ, Brennan K, Canfield AE. Wnt/beta-catenin signaling stimulates chondrogenic and inhibits adipogenic differentiation of pericytes: potential relevance to vascular disease? Circ Res. 2007;101:581–9.
63. Lee TC, Zhao YD, Courtman DW, Stewart DJ. Abnormal aortic valve development in mice lacking endothelial nitric oxide synthase. Circulation. 2000;101:2345–8.
64. O'Brien KD. Pathogenesis of calcific aortic valve disease: a disease process comes of age (and a good deal more). Arterioscler Thromb Vasc Biol. 2006; 26:1721–8.
65. d'Uscio LV, Smith LA, Katusic ZS. Differential effects of enos uncoupling on conduit and small arteries in gtp-cyclohydrolase i-deficient hph-1 mice. Am J Physiol Heart Circ Physiol. 2011;301: H2227–34.
66. Sato J, Nair K, Hiddinga J, Eberhardt NL, Fitzpatrick LA, Katusic ZS, O'Brien T. Enos gene transfer to vascular smooth muscle cells inhibits cell proliferation via upregulation of p27 and p21 and not apoptosis. Cardiovasc Res. 2000;47:697–706.
67. Shah V, Cao S, Hendrickson H, Yao J, Katusic ZS. Regulation of hepatic enos by caveolin and calmodulin after bile duct ligation in rats. Am J Physiol Gastrointest Liver Physiol. 2001;280:G1209–16.
68. Tsutsui M, Chen AF, O'Brien T, Crotty TB, Katusic ZS. Adventitial expression of recombinant enos gene restores no production in arteries without endothelium. Arterioscler Thromb Vasc Biol. 1998;18: 1231–41.
69. Tsutsui M, Onoue H, Iida Y, Smith L, O'Brien T, Katusic ZS. Effects of recombinant enos gene expression on reactivity of small cerebral arteries. Am J Physiol Heart Circ Physiol. 2000;278:H420–7.
70. Rajamannan NM. Mechanisms of aortic valve calcification: the ldl-density-radius theory a translation from cell signaling to physiology. Am J Physiol Heart Circ Physiol. 2010;298(1):H5–15.
71. Antonini-Canterin F, Moura LM, Enache R, Leiballi E, Pavan D, Piazza R, Popescu BA, Ginghina C, Nicolosi GL, Rajamannan NM. Effect of hydroxymethylglutaryl coenzyme-a reductase inhibitors on the long-term progression of rheumatic mitral valve disease. Circulation. 2010;121(19):2130–6.

2 In Vitro Cell Culture Model of Calcification: Molecular Regulation of Myofibroblast Differentiation to an Osteoblast Phenotype

Nalini M. Rajamannan, Muzaffer Cicek, John R. Hawse, Thomas C. Spelsberg, and Malayannan Subramaniam

Introduction

The presence of calcification in the aortic valve is responsible for important prognostic information regarding the natural history of this disease [1, 2]. Although calcification in aortic valves has been described in the literature for over 100 years, little is known about the synthesis of bone matrix proteins in the aortic valve. Studies evaluating aortic valve calcification have focused on the expression of osteopontin (OP) expression in the mineralization zones of heavily calcified aortic valves obtained at autopsy and surgery [3, 4]. Furthermore, studies in cardiovascular calcification demonstrate parallel histologic findings in the valve and the vasculature in regards to the cellular abnormalities involved in the calcification [5].

Vascular biologists [6], have demonstrated that lipids are important in the differentiation of vascular smooth muscle cells to calcifying cells. The field of valvular biology has also demonstrated that a similar phenotypic switch occurs in myofibroblasts isolated from the aortic valve [7–12]. Several lines of evidence indicate that osteoblasts, chondrocytes, and adipocytes are all derived from a common progenitor cell called an undifferentiated mesenchymal cell [13, 14]. The mineralized valve has been characterized as an osteoblast-like bone phenotype [11, 15].

Bone is the major component of the skeleton and is formed by two distinct process, intramembranous and endochondral. Intramembranous bone arises directly from mesenchymal cells condensing at ossification centers and transforming directly into osteoblasts. This form of ossification gives rise to the flat bones of the skull, parts of the clavicle, and the periosteal surface of long bones. Endochondral ossification differs from the intramembranous component in that is formed in the presence of a cartilaginous blastema. It is a complex, multistep process requiring the sequential formation and degradation of cartilaginous structures that serve as templates for the development of axial and appendicular bones. This formation of calcified bone on a cartilage scaffold occurs not only during skeletogenesis, but is an integral part of post-natal growth and fracture repair [16].

Valve Myofibroblast Differentiation to Bone: Cell Proliferation to Mineralization to Bone

Bone is a mineralized connective tissue, comprising an exquisite assembly of functionally distinct cell populations that are required to support the

N.M. Rajamannan, MD (✉) • M. Cicek • J.R. Hawse
T.C. Spelsberg, PhD, BA • M. Subramaniam
Division of Biochemistry and Molecular Biology,
Mayo Clinic, 200 First St SW,
Rochester, MN 55905, USA
e-mail: rajamannan.nalini@mayo.edu;
spelsberg.thomas@mayo.edu

N.M. Rajamannan (ed.), *Molecular Biology of Valvular Heart Disease*,
DOI 10.1007/978-1-4471-6350-3_2, © Springer-Verlag London 2014

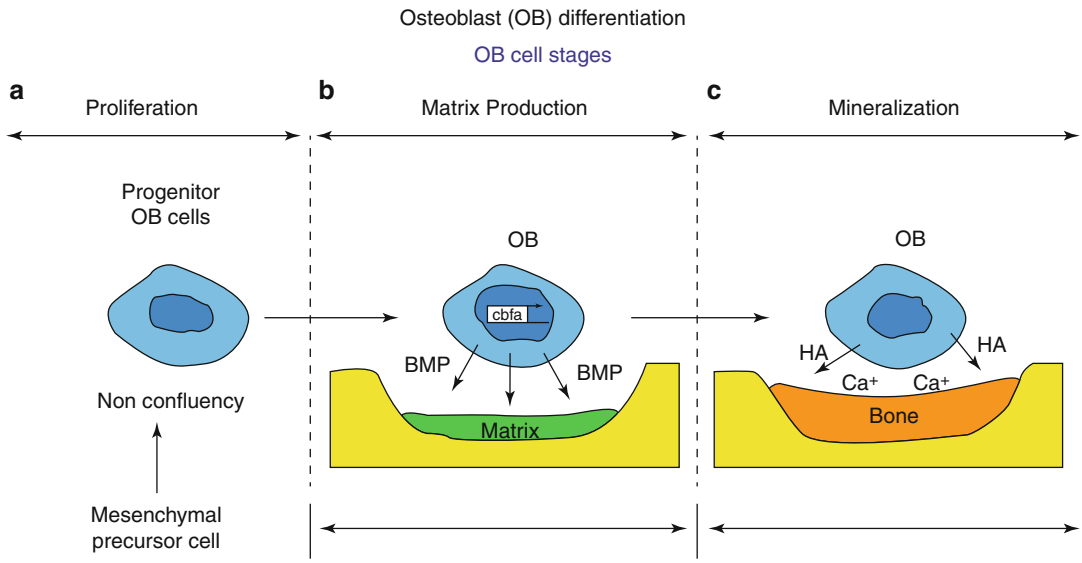

Fig. 2.1 Demonstrates the three phases for developing a porcine valvular fibroblast model system to follow the osteoblast (*OB*) differentiation and mineralization process, important in the phenotypic switch. (**a**) Stage one, cell proliferation stage. (**b**) Stage two, extracellular matrix synthesis. (**c**) Stage three, mineralization phase

structural integrity and remodeling of the skeleton. The bone forming OB cells are derived from mesenchymal precursor cells in the bone marrow stroma and periosteum, and have the capacity for extensive proliferation [17]. In cell culture, osteoblasts are morphologically indistinguishable from fibroblasts [18, 19]. Figure 2.1, Panel a, demonstrates the first stage of OB differentiation, which is the transition of the undifferentiated mesenchymal cells to OB progenitors [20]. Figure 2.1 Panel b, demonstrates the second stage is the maturation of osteoblast progenitors into functional OB cells, which produce collagen, osteocalcin, osteopontin, bone sialoprotein and high levels of alkaline phosphatase activity. Figure 2.1, Panel c, demonstrates the final stage of OB mineralization and binding of hydroxyapatite to the newly synthesized matrix in the tissues. The regulatory mechanism of osteoblast differentiation from OB progenitor cells into terminally differentiated cells that produce bone matrix proteins has been extensively studied and requires the actions of specific paracrine/hormonal factors [21]. Genes which code for the bone extracellular matrix proteins in OB cells include alkaline phosphatase (AP), osteopontin (OP), osteocalcin (OC), bone sialoprotein (BSP) and matrix Gla protein (MGP) [22]. Interestingly, Giachelli et al. have shown that OP may have an inhibitory role in mineralization in the vascular smooth muscle cells [23, 24]. This data supports a potential regulatory mechanism that these matrix proteins may play in the development of biomineralization. To date, many of these markers have been shown to be critical in the extracellular mineralization and bone formation developing in normal OB differentiation [19]. Recent descriptive studies from patient specimens have demonstrated the critical features of aortic valve calcification, including osteoblast expression, cell proliferation and atherosclerosis [3, 11, 12, 15]. These studies define the biochemical and histological characterization of these valve lesions. Furthermore, these studies have also shown that specific bone cell phenotypes are present in calcifying valve tissue from human specimens [25, 26]. Early studies in vascular smooth muscle cells demonstrate the ability of calcifying vascular cells to have the multipotential ability to differentiate to calcifying phenotypes [13]. The first description of a possible bone protein in the valve was the discovery of the expression of the bone matrix protein osteopontin in the diseased calcific aortic valves [3, 4]. This concept was confirmed once the molecular phenotype was published demonstrating the RNA

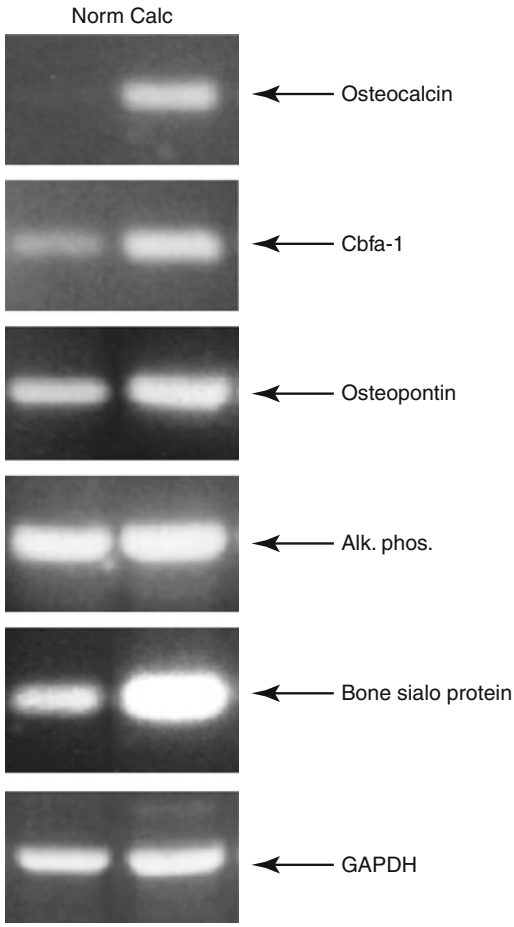

Fig. 2.2 RNA level for the activation of the osteoblast gene program in calcified human aortic valves from surgical valve replacement as compared to valve removed at the time of heart transplantation [11]

osteogenic regulation in the control versus the calcified valves from surgery explants [11]. Figure 2.2 demonstrates the first evidence at the RNA level for the activation of the osteoblast gene program in calcified human aortic valves from surgical valve replacement as compared to valve removed at the time of heart transplantation [11]. Increased gene expression of osteopontin, bone sialoprotein, and Cbfa1 (the osteoblast specific transcription factor) were all increased in the calcified aortic valves as compared to the control valves from heart transplantation. This data has provided the first molecular evidence that a parallel osteoblast gene program is important in the mineralizing phenotype found in calcified human aortic valves. The gene expression and the histomorphometric data that endochondral bone formation provide the foundation for an ossification phenotype. Osteoblast bone formation is a complex process involving multiple growth and differentiation cellular mechanisms. The presence of osteoblast bone formation in the aortic valve has provided the foundation for the hypothesis that the cells residing in the aortic valve have the potentiality to trans-differentiate into a bone forming cell, which over time mineralizes and expresses and ossification phenotype. There have been a number of studies that have identified the signaling pathways critical in the development of calcific aortic stenosis. A number of these signaling factors are similar to those found in vascular atherosclerosis and bone formation. Matrix MetalloProteinases (MMP) [27], Interleukin1 [28], Transforming Growth Factor-beta(TGF-beta), purine nucleotides [29, 30], RANK [31], osteoprotegrin(OPG) [31], and TNF alpha [32], have all been identified as signaling pathways important in the development of this disease process.

Cardiac Valve Cell Types: Valvular Interstitial Cells

VICs are abundant in all layers of the heart valves and are crucial to function. VICs synthesize VECM and express matrix degrading enzymes (including matrix metalloproteinases [MMPs] and their inhibitors [TIMPs]) that mediate and regulate remodeling of collagen and other matrix components. VICs comprise a diverse, dynamic, and highly plastic population of resident cells [33]. They modulate function among phenotypes in response to changes in stimulation by the mechanical environment or by certain chemicals, during valvular homeostasis, adaptation, and pathology. Adult heart valve VICs in-situ have characteristics of resting fibroblasts; they are quiescent, without synthetic or destructive activity for ECM. VICs are activated during intrauterine valvular maturation, by abrupt changes in the mechanical stress state of valves and in disease states, and VICs continuously repair a low level of injury to the VECM that occurs during

Table 2.1 In vitro valvular cell phenotypes

Cell type	Location	Function
Embryonic progenitor endothelial/mesenchymal cells	Embryonic cardiac cushions	Give rise to resident qVICs, possibly through an activated stage. EMT can be detected by the loss of endothelial and the gain of mesenchymal markers
qVICs	Heart valve leaflet	Maintain physiologic valve structure and function and inhibit angiogenesis in the leaflets
pVICs	Bone marrow, circulation, and/or heart valve leaflet	Enter valve or are resident in valve to provide aVICs to repair the heart valve, may be CD34-, CD133-, and/or S100-positive
aVICs	Heart valve leaflet	α-SMA-containing VICs with activated cellular repair processes including proliferation, migration, and matrix remodeling. Respond to valve injury attributable to pathological conditions and abnormal hemodynamic/mechanical forces
obVICs	Heart valve leaflet	Calcification, chondrogenesis, and osteogenesis in the heart valve. Secrete alkaline phosphatase, osteocalcin, osteopontin, bone sialoprotein

Valve myofibroblast cells undergo cell transitions in vitro, which can range form the embryonic precursor cell to the quiescent VIC, to the circulating bone marrow cells, the active VIC which is the early differentiating cell to the final bone forming cell which is the obVIC cell type. Used with permission Liu et al. [33]

physiological functional remodeling of AV tissue [34]. Table 2.1 demonstrates the phenotypic transitions of the VIC cells, which are critical for normal development, homeostasis, and function of the aortic valve, and likely mediate the development of valve calcification [33]. Once activated, VICs can differentiate into a variety of other cell types [35], including myofibroblasts and osteoblasts, although valve osteoblasts may respond to cellular signals differently than skeletal osteoblasts.

Establish an In Vitro Model of Aortic Valve Calcification

This cell culture model is currently being utilized in other laboratories [7, 36, 37]. We established this model in order to investigate the molecular mechanisms of calcification in the aortic valve. The myofibroblast cell is the suspected target for differentiation into OB like cells in the aortic valve. Therefore, determining the signaling pathways in this cell will help to define the changes found in the ex vivo calcified aortic valves and define future medical therapies for this disease. In vitro studies have been instrumental to determine the timing and phenotypic characterization of calcifying nodules using an in vitro cell culture model of porcine aortic valve cells. Chapter 1, describes the cell isolation technique for myofibroblast cells from porcine aortic valves.

Osteogenic Transcription Factor Expression in Calcified Aortic Valves

The evidence for osteoblastogeneis in aortic valve myofibroblast is dependent on defining the regulatory elements controlling osteoblast (OB) differentiation as in Fig. 2.2, which demonstrates the bone transcription factors upregulated in the calcified valves. The next step to study the osteogenic regulation of bone formation in the valve, Fig. 2.3, demonstrates the in vitro evidence for osteogensis in the myofibroblast cell.

Myofibroblast cells in culture were differentiated to osteoblast-like cells using osteogenic media. Figure 2.3 demonstrates the three phases for developing a porcine valvular fibroblast model system to follow the osteoblast (OB) differentiation and mineralization process, and determine the cell type responsible for the phenotypic switch as shown in the model for Fig. 2.1. Figure 2.3, Panel a, demonstrates the mRNA expression of the bone markers, osteopontin and type-I collagen in porcine valve fibroblast cells cultured for 2–20 days with dexamethasone and TGFbeta. The results indicate that the growth of

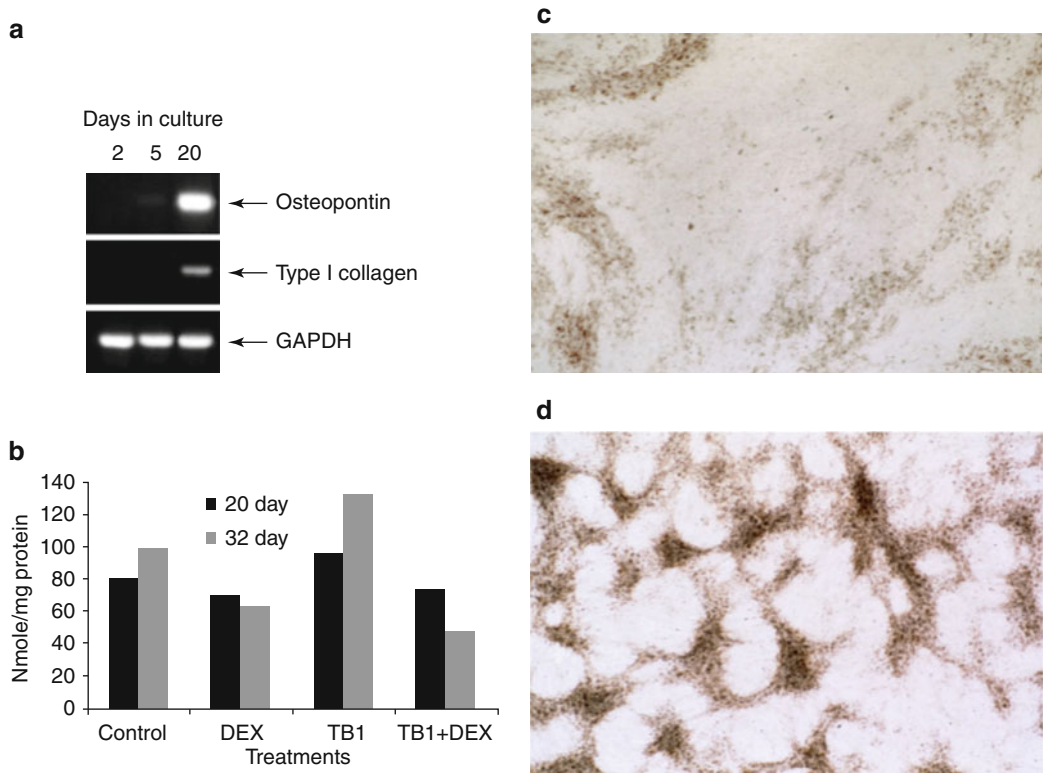

Fig. 2.3 Panel (**a**) Matrix gene expression in valve myofibroblast cells, Panel (**b**) Alkaline phosphatase assay in myofibroblast cells treated with dexamethasone and TGF beta, and Panel (**c**), is the Control experiment with the non-calcifying cells, (Negative Von Kossa stain), Panel (**d**), is the Calcifying cells treated with the osteogenic media (Positive Von kossa stain) after 6 weeks of treatment in vitro

these cells in culture for longer periods and under specified certain conditions induces expression of two important OB markers. Figure 2.3, Panel b, demonstrates the increase in myofibroblast synthesis of alkaline phosphatase after treatment with TGFbeta for 32 days. Figure 2.3, Panel d, Von Kossa staining of the valvular fibroblasts reveals nodule formation after treatment with dexamethasone and TGFbeta for 20 days whereas the control myofibroblast cells, Fig. 2.3, Panel c, received only 0.5 % media and no dex and no TGFbeta demonstrates no nodule formation. These results demonstrating that dexamethasone and TGFbeta are important in myofibroblast differentiation are also important agents in OB differentiation [38–40]. This data supports the feasibility of using an in vitro system to investigate and characterize potential signaling pathways. Also, the preliminary data supports the hypothesis that myofibroblasts can differentiate into an OB-like cell. An in vitro model system will be invaluable to determine the cellular mechanisms involved in the cellular differentiation/transformation and induction of the calcification process as well as determining the mechanism by which these cells undergo a phenotype switch from a valve myofibroblast cell to an OB-like cell.

The Role of the Stem Cell Niche: Myofibroblast Cell Differentiating to Osteogenic Bone

The next assay is to test the myofibroblast cell's ability to differentiate to mineralized bone via upregulation of the Lrp5 receptor. The concept of the cell-cell communication was the foundation

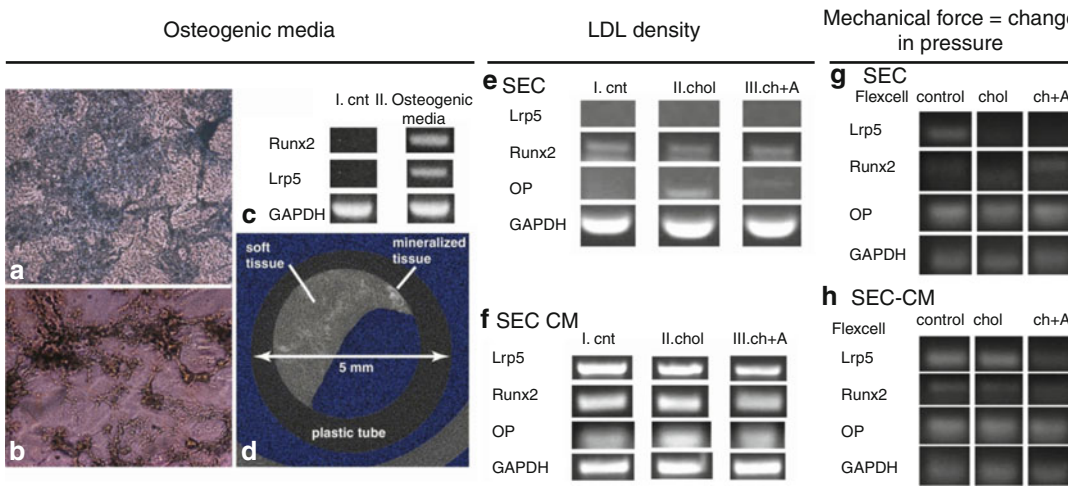

Fig. 2.4 Osteogenic mineralization assays in a stem cell niche. Panel (**a**) The myofibroblast cells stain for Alcian blue, indicating a cartilaginous phenotype treated with osteogenic media. Panel (**b**) The myofibroblast cells stain positive for Alizarin red, indicating an osteoblast phenotype treated with osteogenic media. Panel (**c**) RTPCR for Cbfa1 and Lrp5, in the myofibroblast cells treated with osteogenic media. Panel (**d**) MicroCT of the calcifying cells indicating mineralization present in the cells. Panel (**e**) RTPCR for Lrp5, Cbfa1 and osteopontin in the myofibroblast cells treated with directly with lipids with and without Atorvastatin. Panel (**f**) RTPCR for Lrp5, Cbfa1 and osteopontin in the myofibroblast cells treated with conditioned media from Endothelial cells with lipids with and without Atorvastatin. Panel (**g**) RTPCR for Lrp5, Cbfa1 and osteopontin in the myofibroblast cells treated with cyclic stretch and with lipids with and without Atorvastatin. Panel (**h**) RTPCR for Lrp5, Cbfa1 and osteopontin in the myofibroblast cells treated with cyclic stretch and conditioned media from Endothelial cells with lipids with and without Atorvastatin

for these sets of experiments to test the role of conditioned media released from the endothelial cell to initiate the myofibroblast differentiation. There are two necessary corollaries for this experiment: (1) cell-cell communication, (2) oxidative stress gradient in the presence of elevated LDL [41].

Myofibroblasts were treated with three different conditions to determine the microenvironment necessary to activate the Lrp5 pathway of bone formation. The initial set of conditions includes treatment of the myofibroblasts with osteogenic differentiating media. This osteogenic differentiation media provides the mineralizing microenvironment necessary for the calcification of bone mineralization [42]. The cells were treated with osteogenic media in Fig. 2.4, Panel a. Over time the myofibroblast cells stain positive for Alcian blue, indicating the transformation to a chondrocyte phenotype. After 6 weeks, the cells begin to mineralize and form bone as implicated with the positive stain for Alizarin read as shown in Fig. 2.4, Panel b. The microCT indicates mineralization in this in vitro model with upregulation of Runx2 and Lrp5 the key regulators of Wnt regulation of bone formation, Fig. 2.4, Panels c and d.

Next, the cells were treated with LDL, with and without Atorvastatin directly shown in Fig. 2.4, Panel e. When the cells were treated with lipids directly, there was no gene expression of the Lrp5 receptor and low level expression of Runx2 and osteopontin. Figure 2.4, Panel f, demonstrates the gene expression in myofibroblast cells treated with conditioned media from aortic valve endothelial cells. The conditioned media was produced in the presence of LDL, with and without Atorvastatin. The AEC conditioned media is required to upregulate the Lrp5 gene in this model of endothelial/mesenchmyal cross talk. The conditioned media from the endothelial cells treated with lipids induced the Lrp5 gene expression and mildly attenuated with Atorvastatin therapy. Figure 2.4, Panels g and h, demonstrates the final set of conditions, the response to mechanical force by measuring the Lrp5 expression in the myofibroblast cells

with cyclic stress. The Lrp5 is expressed after the application of the cyclic stretch, and is further increased with the application of the cyclic stretch and the Conditioned media treated cells. This data, in combination with previously published data [10, 43, 44], indicates that LDL and Pressure are both necessary for the upregulation of the Lrp5/Wnt3a pathway [45, 46].

Summary

The model proposed in the study as described in Fig. 2.2 provides the cellular architecture for the development of this disease process. The stem cell niche is a unique model for the development of an oxidative stress communication within the aortic valve endothelium. As shown in Fig. 2.2, oxidative stress contributes to the release of Wnt3a into the subendothelial space to activate Lrp5/Frizzled receptor complex on the extracellular membrane of the myofibroblast. This trimeric complex then induces glycogen synthase kinase to be phosphorylated. This phosphorylation event causes β-catenin translocation to the nucleus. β-catenin acts as a coactivator of osteoblast specific transcription factor Runx2 to induce mesenchymal osteoblastogenesis in the aortic valve myofibroblast cell.

References

1. Rajamannan NM, Evans FJ, Aikawa E, Grande-Allen KJ, Demer LL, Heistad DD, Simmons CA, Masters KS, Mathieu P, O'Brien KD, Schoen FJ, Towler DA, Yoganathan AP, Otto CM. Calcific aortic valve disease: not simply a degenerative process: A review and agenda for research from the National Heart and Lung and Blood Institute Aortic Stenosis Working Group. Circulation. 2011;124(16):1783–91.
2. Rosenhek R, Binder T, Porenta G, Lang I, Christ G, Schemper M, Maurer G, Baumgartner H. Predictors of outcome in severe, asymptomatic aortic stenosis. N Engl J Med. 2000;343:611–7.
3. O'Brien KD, Kuusisto J, Reichenbach DD, Ferguson M, Giachelli C, Alpers CE, Otto CM. Osteopontin is expressed in human aortic valvular lesions. Circulation. 1995;92:2163–8 [comment].
4. Mohler 3rd ER, Adam LP, McClelland P, Graham L, Hathaway DR. Detection of osteopontin in calcified human aortic valves. Arterioscler Thromb Vasc Biol. 1997;17:547–52.
5. Vattikuti R, Towler DA. Osteogenic regulation of vascular calcification: an early perspective. Am J Physiol Endocrinol Metab. 2004;286:E686–96.
6. Parhami F, Basseri B, Hwang J, Tintut Y, Demer LL. High-density lipoprotein regulates calcification of vascular cells. Circ Res. 2002;91:570–6.
7. Mohler 3rd ER, Chawla MK, Chang AW, Vyavahare N, Levy RJ, Graham L, Gannon FH. Identification and characterization of calcifying valve cells from human and canine aortic valves. J Heart Valve Dis. 1999;8:254–60.
8. Rajamannan NM. Calcific aortic valve disease: cellular origins of valve calcification. Arterioscler Thromb Vasc Biol. 2011;31:2777–8.
9. Rajamannan NM. Role of oxidative stress in calcific aortic valve disease: from bench to bedside. In: Morales-Gonzalez J.A.Oxidative Stress and Chronic Degenerative Diseases – A Role for Antioxidants, InTech Publisher, 2013; Chapter 11, pp. 265–87.
10. Rajamannan NM, Subramaniam M, Caira F, Stock SR, Spelsberg TC. Atorvastatin inhibits hypercholesterolemia-induced calcification in the aortic valves via the lrp5 receptor pathway. Circulation. 2005;112:I229–34.
11. Rajamannan NM, Subramaniam M, Rickard D, Stock SR, Donovan J, Springett M, Orszulak T, Fullerton DA, Tajik AJ, Bonow RO, Spelsberg T. Human aortic valve calcification is associated with an osteoblast phenotype. Circulation. 2003;107:2181–4.
12. Rajamannan NM, Subramaniam M, Springett M, Sebo TC, Niekrasz M, McConnell JP, Singh RJ, Stone NJ, Bonow RO, Spelsberg TC. Atorvastatin inhibits hypercholesterolemia-induced cellular proliferation and bone matrix production in the rabbit aortic valve. Circulation. 2002;105:2260–5.
13. Tintut Y, Alfonso Z, Saini T, Radcliff K, Watson K, Bostrom K, Demer LL. Multilineage potential of cells from the artery wall. Circulation. 2003;108:2505–10.
14. Rawadi G, Vayssiere B, Dunn F, Baron R, Roman-Roman S. Bmp-2 controls alkaline phosphatase expression and osteoblast mineralization by a wnt autocrine loop. J Bone Miner Res. 2003;18:1842–53.
15. Mohler 3rd ER, Gannon F, Reynolds C, Zimmerman R, Keane MG, Kaplan FS. Bone formation and inflammation in cardiac valves. Circulation. 2001;103:1522–8.
16. Bonner F, Farach-Carson MC. Bone formation. New York: Springer; Topics in Bone Biology. 2003. Vol 1. p. 1–15.
17. Bostrom K, Tintut Y, Kao SC, Stanford WP, Demer LL. Hoxb7 overexpression promotes differentiation of c3h10t1/2 cells to smooth muscle cells. J Cell Biochem. 2000;78:210–21.
18. Ducy P, Zhang R, Geoffroy V, Ridall AL, Karsenty G. Osf2/cbfa1: a transcriptional activator of osteoblast differentiation. Cell. 1997;89:747–54 [see comment].
19. Ducy P, Schinke T, Karsenty G. The osteoblast: a sophisticated fibroblast under central surveillance. Science. 2000;289:1501–4.

20. Waters KM, Rickard DJ, Riggs BL, Khosla S, Katzenellenbogen JA, Katzenellenbogen BS, Moore J, Spelsberg TC. Estrogen regulation of human osteoblast function is determined by the stage of differentiation and the estrogen receptor isoform. J Cell Biochem. 2001;83:448–62.
21. Aubin JE, Liu F, Malaval L, Gupta AK. Osteoblast and chondroblast differentiation. Bone. 1995;17:77S–83.
22. Young MF, Kerr JM, Ibaraki K, Heegaard AM, Robey PG. Structure, expression, and regulation of the major noncollagenous matrix proteins of bone. Clin Orthop Relat Res. 1992;281:275–94.
23. Speer MY, McKee MD, Guldberg RE, Liaw L, Yang HY, Tung E, Karsenty G, Giachelli CM. Inactivation of the osteopontin gene enhances vascular calcification of matrix gla protein-deficient mice: evidence for osteopontin as an inducible inhibitor of vascular calcification in vivo. J Exp Med. 2002;196:1047–55.
24. Steitz SA, Speer MY, McKee MD, Liaw L, Almeida M, Yang H, Giachelli CM. Osteopontin inhibits mineral deposition and promotes regression of ectopic calcification. Am J Pathol. 2002;161:2035–46.
25. Caira FC, Stock SR, Gleason TG, McGee EC, Huang J, Bonow RO, Spelsberg TC, McCarthy PM, Rahimtoola SH, Rajamannan NM. Human degenerative valve disease is associated with up-regulation of low-density lipoprotein receptor-related protein 5 receptor-mediated bone formation. J Am Coll Cardiol. 2006;47:1707–12.
26. Jian B, Jones PL, Li Q, Mohler 3rd ER, Schoen FJ, Levy RJ. Matrix metalloproteinase-2 is associated with tenascin-c in calcific aortic stenosis. Am J Pathol. 2001;159:321–7.
27. Kaden JJ, Vocke DC, Fischer CS, Grobholz R, Brueckmann M, Vahl CF, Hagl S, Haase KK, Dempfle CE, Borggrefe M. Expression and activity of matrix metalloproteinase-2 in calcific aortic stenosis. Z Kardiol. 2004;93:124–30.
28. Kaden JJ, Dempfle CE, Grobholz R, Tran HT, Kilic R, Sarikoc A, Brueckmann M, Vahl C, Hagl S, Haase KK, Borggrefe M. Interleukin-1 beta promotes matrix metalloproteinase expression and cell proliferation in calcific aortic valve stenosis. Atherosclerosis. 2003;170:205–11.
29. Osman L, Chester AH, Amrani M, Yacoub MH, Smolenski RT. A novel role of extracellular nucleotides in valve calcification: a potential target for atorvastatin. Circulation. 2006;114:I566–72.
30. Osman L, Amrani M, Isley C, Yacoub MH, Smolenski RT. Stimulatory effects of atorvastatin on extracellular nucleotide degradation in human endothelial cells. Nucleosides Nucleotides Nucleic Acids. 2006;25:1125–8.
31. Kaden JJ, Bickelhaupt S, Grobholz R, Haase KK, Sarikoc A, Kilic R, Brueckmann M, Lang S, Zahn I, Vahl C, Hagl S, Dempfle CE, Borggrefe M. Receptor activator of nuclear factor kappab ligand and osteoprotegerin regulate aortic valve calcification. J Mol Cell Cardiol. 2004;36:57–66.
32. Kaden JJ, Kilic R, Sarikoc A, Hagl S, Lang S, Hoffmann U, Brueckmann M, Borggrefe M. Tumor necrosis factor alpha promotes an osteoblast-like phenotype in human aortic valve myofibroblasts: a potential regulatory mechanism of valvular calcification. Int J Mol Med. 2005;16:869–72.
33. Liu AC, Joag VR, Gotlieb AI. The emerging role of valve interstitial cell phenotypes in regulating heart valve pathobiology. Am J Pathol. 2007;171:1407–18.
34. Aikawa E, Whittaker P, Farber M, Mendelson K, Padera RF, Aikawa M, Schoen FJ. Human semilunar cardiac valve remodeling by activated cells from fetus to adult: implications for postnatal adaptation, pathology, and tissue engineering. Circulation. 2006;113:1344–52.
35. Chen JH, Yip CY, Sone ED, Simmons CA. Identification and characterization of aortic valve mesenchymal progenitor cells with robust osteogenic calcification potential. Am J Pathol. 2009;174:1109–19.
36. Tintut Y, Parhami F, Bostrom K, Jackson SM, Demer LL. Camp stimulates osteoblast-like differentiation of calcifying vascular cells. Potential signaling pathway for vascular calcification. J Biol Chem. 1998;273:7547–53.
37. Johnson CM, Hanson MN, Helgeson SC. Porcine cardiac valvular subendothelial cells in culture: cell isolation and growth characteristics. J Mol Cell Cardiol. 1987;19:1185–93.
38. Selvamurugan N, Kwok S, Alliston T, Reiss M, Partridge NC. Transforming growth factor-beta 1 regulation of collagenase-3 expression in osteoblastic cells by cross-talk between the smad and mapk signaling pathways and their components, smad2 and runx2. J Biol Chem. 2004;279:19327–34.
39. Roelen BA, Dijke P. Controlling mesenchymal stem cell differentiation by tgfbeta family members. J Orthop Sci. 2003;8:740–8.
40. Chang W, Parra M, Ji C, Liu Y, Eickelberg O, McCarthy TL, Centrella M. Transcriptional and post-transcriptional regulation of transforming growth factor beta type ii receptor expression in osteoblasts. Gene. 2002;299:65–77.
41. Rajamannan NM. Oxidative-mechanical stress signals stem cell niche mediated lrp5 osteogenesis in enos(-/-) null mice. J Cell Biochem. 2012;113:1623–34.
42. Stringa E, Filanti C, Giunciuglio D, Albini A, Manduca P. Osteoblastic cells from rat long bone. I. Characterization of their differentiation in culture. Bone. 1995;16:663–70.
43. Shao JS, Cheng SL, Pingsterhaus JM, Charlton-Kachigian N, Loewy AP, Towler DA. Msx2 promotes cardiovascular calcification by activating paracrine wnt signals. J Clin Invest. 2005;115:1210–20.
44. Kirton JP, Crofts NJ, George SJ, Brennan K, Canfield AE. Wnt/beta-catenin signaling stimulates chondrogenic and inhibits adipogenic differentiation of pericytes: potential relevance to vascular disease? Circ Res. 2007;101:581–9.
45. Rajamannan NM. The role of lrp5/6 in cardiac valve disease: Ldl-density-pressure theory. J Cell Biochem. 2011;112(9):2222–9.
46. Rajamannan NM. The role of lrp5/6 in cardiac valve disease: experimental hypercholesterolemia in the apoe-/-/lrp5-/- mice. J Cell Biochem. 2011;112:2987–91.

3 Aortic Valve Apoptosis, Cell Proliferation and Atherosclerosis in Experimental Hypercholesterolemia

Mony Shuvy, Chaim Lotan, and Nalini M. Rajamannan

Introduction

Degenerative aortic valvular disease is a common medical condition. With the decline of acute rheumatic fever, aortic valvular dysfunction secondary to degeneration has become the most common indication for surgical valve replacement. The cost of this disease in morbidity, mortality and dollars is substantial. Despite the high prevalence of degenerative aortic stenosis, the cellular causes are virtually unknown. Recent analysis evaluating the risk factors leading to degenerative aortic valvular disease have found inciting factors similar to those of vascular atherosclerosis, such as smoking, male gender, hypertension, and elevated cholesterol levels [1].

The correlation between elevated serum cholesterol levels and cardiovascular disease has been known for more than 100 years. Prior to the advent of lipid-lowering therapies, aortic valvular stenosis occurred frequently in patients with familial hyperlipidemia. Patients with hyperlipidemia (homozygote type II pattern), have several features not found in the heterozygote patient, or in patients with other forms of hyperlipidemia [2]. In this form of degenerative aortic stenosis, the cusps are often thickened and relatively immobile. Histologic analysis has disclosed foam cells, cholesterol clefts, and calcific deposits within the leaflets. The occurrence of intracellular lipid and cholesterol clefts within the cusps is distinct and not seen in other forms of valvular aortic stenosis. It is now thought that lipid-laden foam cells found in the arterial wall in early atherosclerotic lesions are generated by a massive accumulation of cholesterol within macrophage cells. It is this early lesion in the intima of the vascular wall that leads to progression of atherosclerosis [3]. The histopathologic findings in aortic valvular disease are similar to those seen in atherosclerotic disease.

Several experimental studies have shown hypercholesterolemia in rabbits [4–6] eventually causes a lesion resembling early atherosclerosis. However, little is known how experimental hypercholesterolemia may cause similar morphologic aortic valve changes, or if this process is associated with early valvular degeneration.

This early study demonstrated that elevated cholesterol levels contribute to the early pathogenesis of aortic valvular disease, similar to atherosclerosis [7]. This model of experimental hypercholesterolemia helped to determine if valvular changes occur similar to those described in vascular atherosclerosis. Male New Zealand White Rabbits were randomly assigned to control or cholesterol-fed groups and lipid levels were measured. Terminal deoxynucleotidyl transferase (TdT)-mediated dUTP-biotin nick end-labeling assay was used to measure apoptosis.

M. Shuvy, MD • C. Lotan, MD, FACC, FESC
Division of Cardiology, Hadassah Hospital, Hadassah, Israel

N.M. Rajamannan, MD (✉)
Division of Biochemistry and Molecular Biology, Mayo Clinic, 200 First St SW, Rochester, MN 55905, USA
e-mail: rajamannan.nalini@mayo.edu

N.M. Rajamannan (ed.), *Molecular Biology of Valvular Heart Disease*,
DOI 10.1007/978-1-4471-6350-3_3, © Springer-Verlag London 2014

Transmission Electron Microscopy Analysis was performed to confirm apoptosis in the valves.

Apoptosis in Experimental Hypercholesterolemia Aortic Valves

Serum cholesterol levels and a total plasma cholesterol levels were significantly higher in the cholesterol-fed animals, compared to control animals (2,235 ± 162 mg/dL vs 39 ± 4 mg/dL, $p < 0.0005$). Similarly, HDL cholesterol and plasma triglyceride levels were higher in hypercholesterolemia animals compared to controls (35 ± 7 mg/dL vs 15 ± 1 mg/dL, $p < 0.04$) and 472 ± 3 mg/dl vs 13 ± 3 mg/dl ($p < 0.006$). Figure 3.1, Panel a, **normal aortic valve**, Panel b, **hypercholesterolemia aortic valve**. In the hypercholesterolemia animals, marked positive PCNA, positive staining cells were mainly detected in the plaque lesion on the endothelial surface of the valve. The Hematoxylin and eosin stain in Figure 3.2, Panel a, **normal, and** b, **hypercholesterolemia**, demonstrate the fatty streak type lesion typical of early atherosclerosis. Figure 3.3, Panel a **normal**, **and** b **hypercholesterolemia** demonstrates the PCNA staining of the valves with a marked increase in the cholesterol treated as compared to control.

In situ detection of apoptosis using TUNEL staining was positive in all hypercholesterolemia animals. The total density of TUNEL positive cells in hypercholesterolemia animals was 110.8 ± 15.0 cells/mm [2]. In contrast, TUNEL stain was not detected in any control aortic valve specimen, suggesting that this process may occur at a very limited rate or below the level of detection in normal valves. By transmission electron microscopy, aortic valves from control animals exhibited normal cellular architecture. Normal appearing cytoplasm and nuclei were present. Conversely, hypercholesterolemia aortic valves were infiltrated by multiple layers of subendothelial foam cells on the endocardial surface. In particular, the foam cells were embedded in a matrix composed of ground substance and elastin interspersed with diffuse cholesterol cleft deposition Fig. 3.3, Panel a **normal and** b **hypercholesterolemia**. Most of the TUNEL-positive cells demonstrated hyperchromatic and fragmented nuclei, characteristic morphological features of apoptosis. Cells with distinct morphologic features consistent with apoptosis such as nuclear condensation and fragmentation were detected in the subendothelial layers of the valve surface from hypercholesterolemia animals, but not in controls Fig. 3.3, Panel c **hypercholesterolemia**.

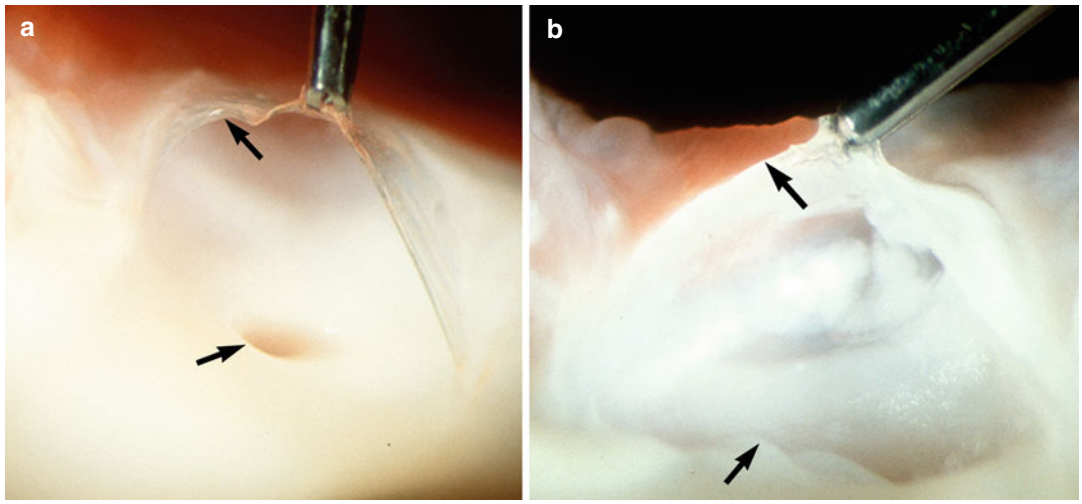

Fig. 3.1 (**a**) Gross picture of the normal control rabbit aortic valve. (**b**) Gross picture of the hypercholesterolemia rabbit aortic valve. *Upper arrow* in both figures points to the aortic valve leaflet and the *lower arrow* points to the coronary ostia

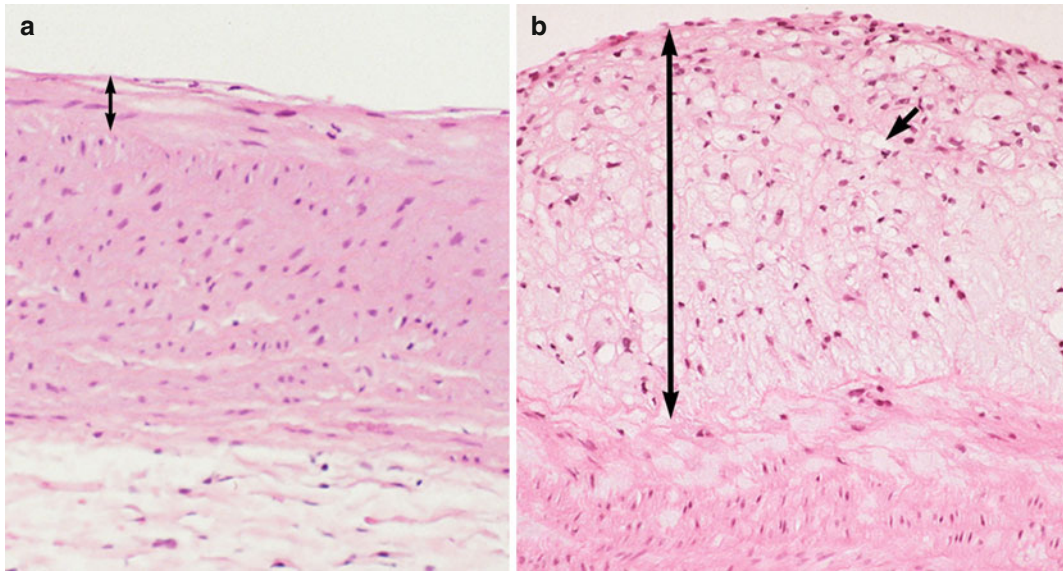

Fig. 3.2 (**a**) Hematoxylin and Eosin staining, normal control rabbit aortic valve, (**b**), hypercholesterolemia rabbit aortic valve. *Arrow point* to the surface of the valve. (**a**) no evidence of atherosclerosis, (**b**) *arrow* demonstrates the degree of atherosclerosis in the hypercholesterolemic rabbit aortic valve

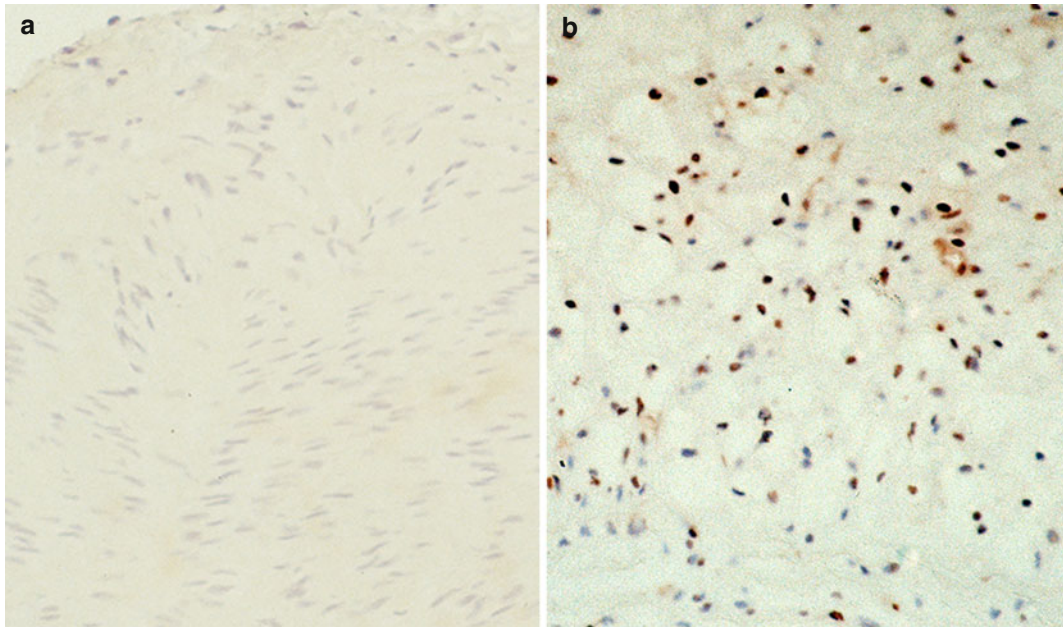

Fig. 3.3 Panel (**a**) normal, and (**b**) hypercholesterolemia demonstrates the PCNA staining

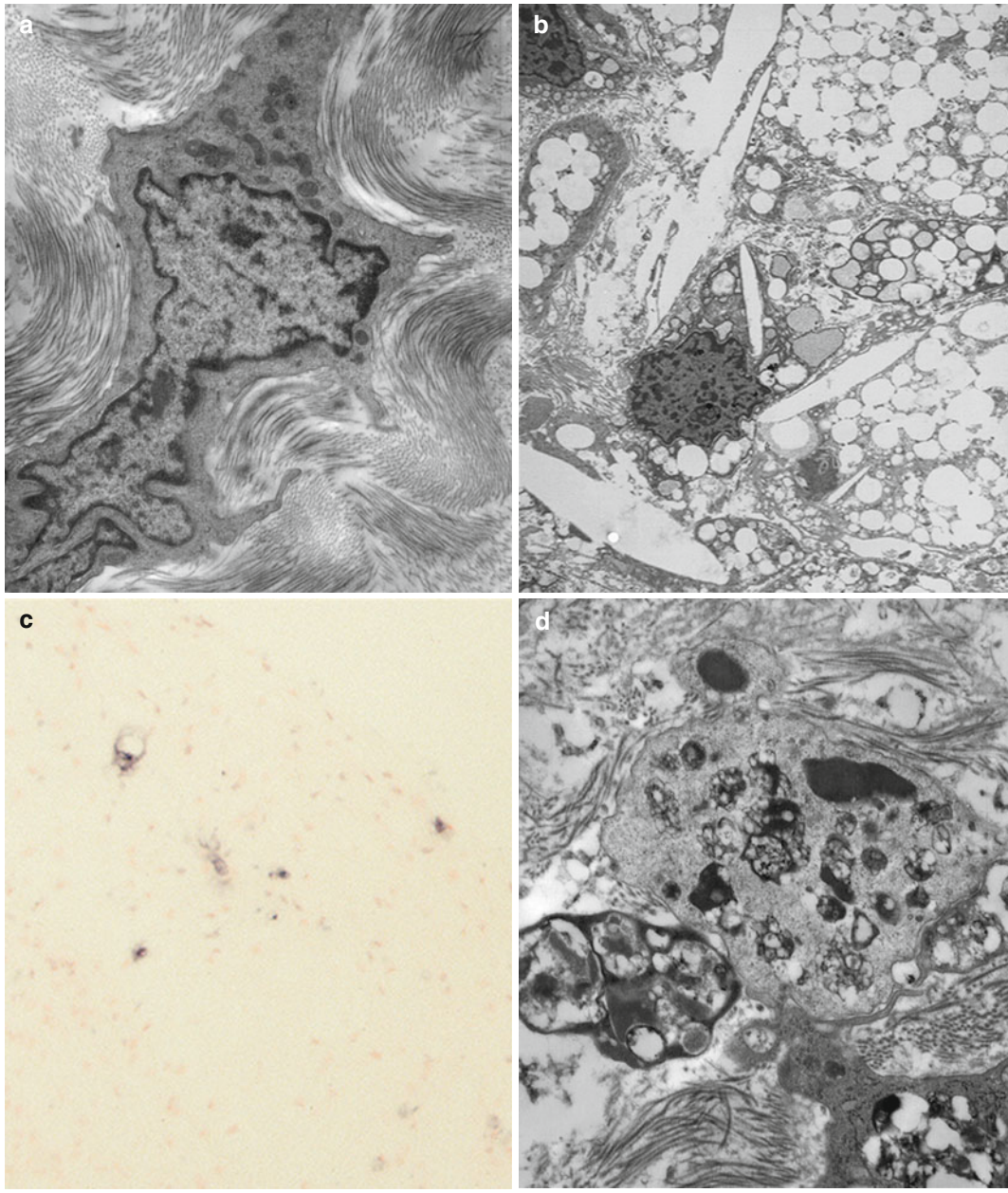

Fig. 3.4 Transmission electron microscopy. (**a**) Normal control rabbit aortic valve, (**b**), Hypercholesterolemia rabbit aortic valve demonstrating cholesterol cleft formation and foam cell formation, Immunostaining for TUNEL to demonstrate apoptosis. (**c**) TUNEL staining in the hypercholesterolemia aortic valve demonstrating positive staining by blue nuclei, Magnification × 50. (**d**) Hypercholesterolemia rabbit aortic valve demonstrating DNA condensation and nuclear fragmentation consistent with apoptosis. Magnification × 50 K

Summary

Calcific aortic valve disease and sclerosis occurs as the aortic valve ages. Recent epidemiological studies reveal the association of risk factors such as increased cholesterol, smoking, etc., in the development of progressive severe aortic valvular degeneration. Familial hypercholesterolemia is also a known risk factor for progressive atherosclerosis and aortic valvular disease. This model of experimental hypercholesterolemia revealed biochemical and morphologic evidence of atherosclerotic changes in the aortic valve similar to findings in early lesion of vascular atherosclerotic formation.

This study demonstrates that experimental hypercholesterolemia is associated with characteristic histomorphologic change in the rabbit aortic valve. In particular, there was marked endothelial cell disruption, foam cell infiltration and cholesterol cleft deposition on the valve surface of high-cholesterol fed animals. These fatty infiltrative changes are unique to the hypercholesterolemia animal model and has been well studied in the evolution of hypercholesterolemia vascular disease. Furthermore, these associations suggest that hypercholesterolemia may play a role in the development of early aortic valve tissue injury.

It is now well established that apoptosis, a form of programmed cell death, is a vital aspect of normal development. Yet, dysregulated apoptosis may have an important role in a variety of cardiovascular disorders. The TUNEL staining and TEM reveal that the values of hypercholesterolemia animals have a characteristic increase in apoptotic cells compared to controls. The role of apoptosis was further determined in a model of renal failure [8]. Apoptosis occurs mainly in the region of the hypercholesterolemia lesion of the endothelial surface of the aortic valve. Our data present a static view of an early valvular lesion at a single point in time, not an integrated picture over the life of the valve. In conclusion, our data suggests that programmed cell death is upregulated in the early phase of valvular lesions in the presence of hypercholesterolemia. These observations suggest that apoptosis may be an important, independent factor contributing to the pathological changes characteristic of advanced degenerative aortic valve disease, including generation of hypocellular regions of the valve. In the next chapter, the effect of long-term cholesterol diets on the aortic valve will demonstrate the mineralization process that ensues in the development of calcific aortic valve disease.

References

1. Stewart BF, Siscovick D, Lind BK, Gardin JM, Gottdiener JS, Smith VE, Kitzman DW, Otto CM. Clinical factors associated with calcific aortic valve disease. Cardiovascular health study. J Am Coll Cardiol. 1997;29:630–4.
2. Rajamannan NM, Edwards WD, Spelsberg TC. Hypercholesterolemic aortic-valve disease. N Engl J Med. 2003;349:717–8.
3. Daugherty A. Atherosclerosis: cell biology and lipoproteins. Curr Opin Lipidol. 2001;12:467–9.
4. Sarphie TG. A cytochemical study of the surface properties of aortic and mitral valve endothelium from hypercholesterolemic rabbits. Exp Mol Pathol. 1986;44:281–96.
5. Sarphie TG. Anionic surface properties of aortic and mitral valve endothelium from new zealand white rabbits. Am J Anat. 1985;174:145–60.
6. Sarphie TG. Surface responses of aortic valve endothelia from diet-induced, hypercholesterolemic rabbits. Atherosclerosis. 1985;54:283–99.
7. Rajamannan NM, Sangiorgi G, Springett M, Arnold K, Mohacsi T, Spagnoli LG, Edwards WD, Tajik AJ, Schwartz RS. Experimental hypercholesterolemia induces apoptosis in the aortic valve. J Heart Valve Dis. 2001;10:371–4.
8. Shuvy M, Abedat S, Beeri R, Valitsky M, Daher S, Kott-Gutkowski M, Gal-Moscovici A, Sosna J, Rajamannan NM, Lotan C. Raloxifene attenuates gas6 and apoptosis in experimental aortic valve disease in renal failure. Am J Physiol Heart Circ Physiol. 2011;300:H1829–40.

4 Experimental Model of Aortic Valve Calcification to Induce Osteoblast Differentiation

Nalini M. Rajamannan, Muzaffer Cicek, John R. Hawse, Thomas C. Spelsberg, and Malayannan Subramaniam

Introduction

Over the past 25 years, the development of an in vivo model to test for calcific aortic valve disease has been challenging. The understanding of the biology, imaging, and duration of exposure to risk factors have been the cornerstone for defining the different stages of osteoblast differentiation. The first experimental was a high cholesterol-diet rabbit model. The studies published demonstrated apoptosis [1], cell proliferation [2], and atherosclerosis [1, 3–6] along the aortic valve surface. These models all include short time diet experiments to define the early atherosclerotic findings in the valve. The next level of experimentation includes testing the diet for 6 months. This duration of diet provides the time necessary for the valve to mineralize and to calcify.

Prior to 2005, there were few established in vivo models of aortic valves to demonstrate osteoblastogeneis in the calcifying aortic valve. Studies in the bone field demonstrated that different mutations in Lrp5, an LDL receptor related protein, develop a high bone mass phenotype and an osteoporotic phenotype [7, 8]. An early study from Japan was the first to demonstrate that the Lrp5 receptor is upregulated in the thoracic aortas of hypercholesterolemia Watanabe rabbits [9].

The Lrp5 receptor is upregulated and binds to palmitoylated Wnt, which in turn actives beta-catenin accumulation in the cytoplasm. The increase in beta-catenin, eventually translocates to the nucleus via binding to nucleoporins [10] where it can interacts with LEF-1/TCFs in an inactive transcription complex [11, 12]. The Wnt/Lrp5/frizzled complex turns on downstream components such as Dishevelled (Dvl/Dsh) which leads to repression of the glycogen synthase kinase-3 (GSK3) [13]. Inhibition of GSK3 allows beta-catenin to accumulate in the nucleus, interacting with members of the LEF/TCF class of architectural HMG box of transcription factors, including Cbfa1 involved in cell differentiation and osteoblast activation [14–18]; and Sox 9, a HMG box transcription factor, is required for chondrocyte cell fate determination and marks early chondrocytic differentiation of mesenchymal progenitors [19]. This background outlines the potential for lipids in the regulation of aortic valve mineralization via the canonical Wnt pathway and upregulation of Lrp5/.

In Vivo Experimental Hypercholesterolemia Model

Forty-eight Watanabe Rabbits were fed a high cholesterol diet for 6 months. Immunohistochemistry, RTPCR, and light microscopy were performed

N.M. Rajamannan, MD (✉) • M. Cicek • J.R. Hawse
T.C. Spelsberg, Phd • M. Subramaniam
Division of Biochemistry and Molecular Biology,
Mayo Clinic, 200 First St SW,
Rochester, MN 55905, USA
e-mail: rajamannan.nalini@mayo.edu

N.M. Rajamannan (ed.), *Molecular Biology of Valvular Heart Disease*,
DOI 10.1007/978-1-4471-6350-3_4, © Springer-Verlag London 2014

to measure cell proliferation, extracellular matrix production and mineralization of the aortic valve.

Light Microscopy of the Aortic Valves

The hematoxylin and eosin, Masson trichrome, and EVG stained hypercholesterolemia aortic valves as shown in Fig. 4.1 a2, b2, c2 demonstrate an increase in leaflet thickness that begins at the base of the aortic valve leaflet and extends along the valve leaflet from the attachment to the aorta. There is a marked increase in cellularity and collagen staining in the blue Masson Trichrome and black staining elastin fibers in the EVG stain throughout the leaflet lesion. The aortic valve surface from control animals appeared normal, thin, and intact, with

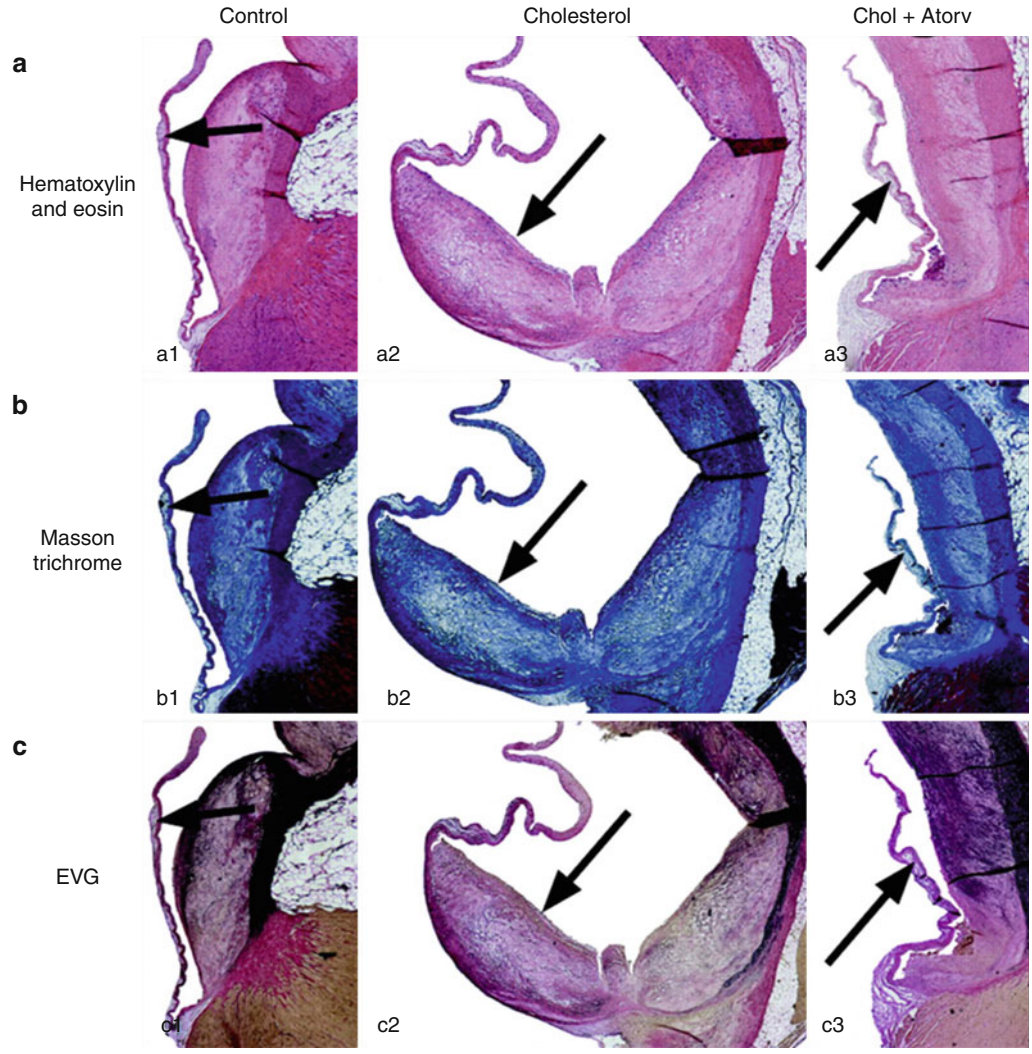

Fig. 4.1 Light microscopy of rabbit aortic valves and aorta. *Left column*, control diet; *middle column*, cholesterol diet; *right column*, cholesterol diet plus atorvastatin. In each panel, the aortic valve leaflet is positioned on the *left*, with the aorta on the *right*. *Arrow points* to aortic valve in each figure. All frames 12.5× magnification. (**a**) Hematoxylin and eosin stain. (**b**) Masson trichrome stain. (**c**) Elastin Van Geison stain

a smooth endothelial cell layer covering the entire surface and a thin collagen layer in the spongiosa of the valve (Fig. 4.1 a1, b1, c1). Abnormal leaflet thicknesses did not develop when cholesterol-fed rabbits received atorvastatin (Fig. 4.1 a3, b3, and c3).

Proliferation Marker and Lrp5 Expression

Figure 4.2a demonstrates the alpha-actin staining cells within the valve leaflet. The control aortic valve in Fig. 4.2 a1 shows that there are few

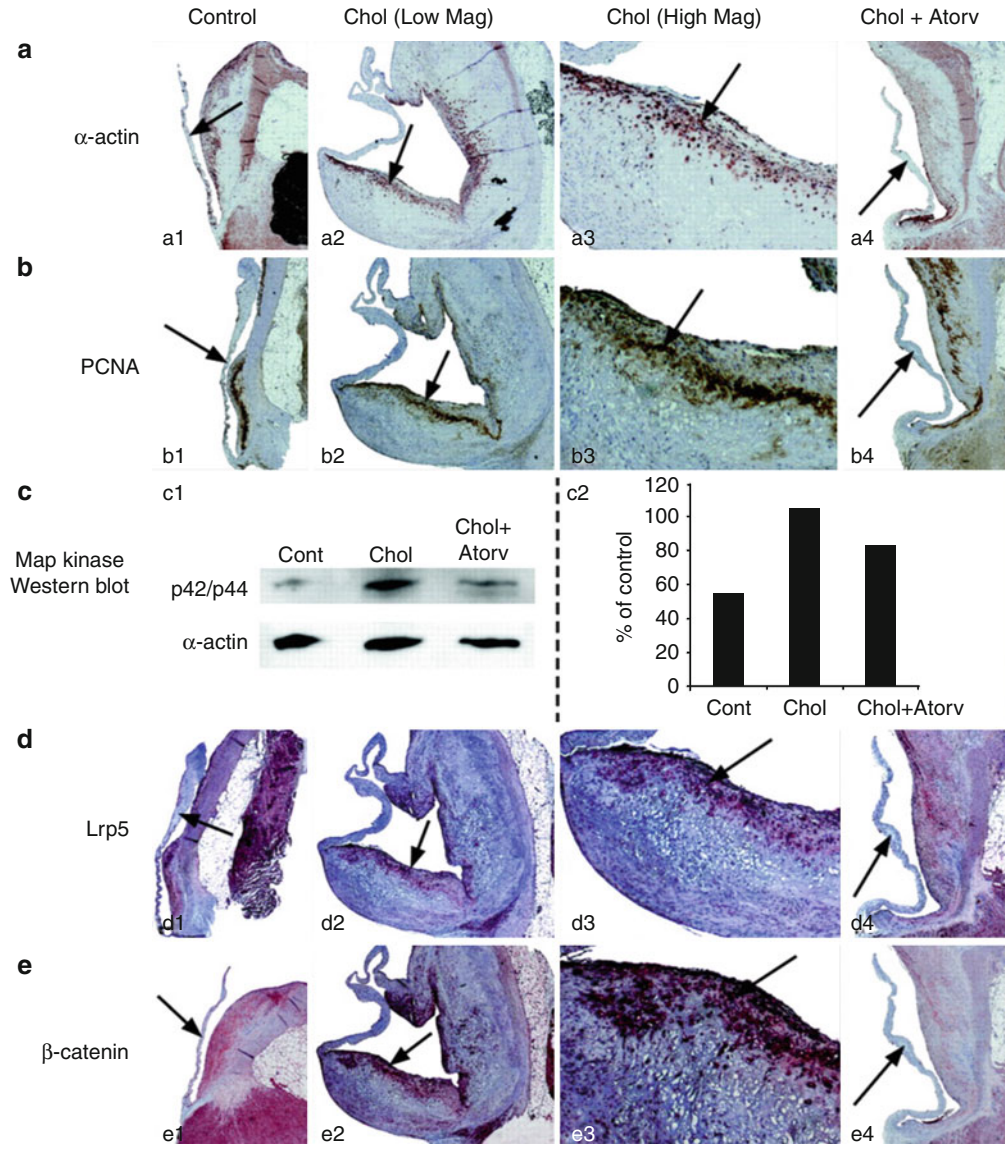

Fig. 4.2 Proliferation marker and Lrp5/β-catenin protein expression. *Left column*, control diet; *middle column*, cholesterol diet; *right column*, cholesterol diet plus atorvastatin. *Arrow points* to aortic valve in each figure. (**a**) α-actin immunostain. (**b**) PCNA immunostain. (**c**) p42/44 Western blot (1) and quantification (2). (**d**) Lrp5 receptor immunostain. (**e**) β-catenin immunostain

actin-positive cells within the control treated leaflets. Figure 4.2 a2, a3 of cholesterol treated leaflets show many actin-positive staining cells along the growing surface of the valve leaflet. Figure 4.2 a4 demonstrates few positive staining cells along the surface of the atorvastatin-treated valve leaflet. Figure 4.2b shows the results of the PCNA stain, which is a DNA polymerase upregulated during cell division. The control valve leaflet demonstrates few PCNA-positive staining cells (Fig. 4.2 b1). Figure 4.2 b2, b3 demonstrates positive staining PCNA in the same area as the actin-positive staining cells of the leaflets from the cholesterol-fed animals. Figure 4.2 b4 indicates that there are few PCNA staining-positive cells in the atorvastatin-treated valves. Figure 4.2c demonstrates the Western blot for the p42/44 expression in the valve leaflets from the different treatment arms, again indicating that protein expression increased in the cholesterol leaflets and decreased in the atorvastatin-treated leaflets. Figure 4.2d demonstrates the immunostain for the Lrp5 receptor. The Lrp5 receptor is present along the normal valve leaflet (Fig. 4.2 d1). There was a marked increased in the hypercholesterolemia valve leaflet (Fig. 4.2 d2, d3). Again, the Lrp5 receptors colocalize with the actin-positive cells along the proliferating edge of the valve leaflet. Figure 4.2 d4 demonstrates a decrease in the Lrp5 receptors in the valve leaflet. Figure 4.2e demonstrates the immunohistochemistry for beta-catenin in the valve leaflet. beta-catenin is a critical regulatory protein that, when activated, translocates to the nucleus to activate osteoblastogenesis. Beta-catenin is expressed in low levels in the control aortic valve, as shown in Fig. 4.2 e1. The hypercholesterolemia aortic valve leaflet has increased beta-catenin in the proliferating edge of the valve leaflet, as shown in Fig. 4.2 e2, e3. Atorvastatin decreased the beta-catenin expression in the leaflet (Fig. 4.2 e4).

Establishment of the Bone-Like Phenotype in the Calcified Aortic Valves

Light microscopy evaluating the osteopontin immunostain in the control aortic valves revealed a low level of osteopontin protein expression (Fig. 4.3 a1). Osteopontin is a glycosylated phosphoprotein that is important in mineralization. In the hypercholesterolemia valves, the osteopontin expression increased along the aortic valve leaflet edge and also in the center of valve, as shown in Fig. 4.3 a2, a3. The osteopontin protein expression was significantly decreased with the atorvastatin treatment, as shown in Fig. 4.3 a4. Osteopontin protein levels were measured in the valve leaflets as indicated in the Western blot data (Fig. 4.3 b1). The Western blot confirms that osteopontin protein concentration increased in the cholesterol-treated aortic valves and decreased in the atorvastatin-treated aortic valves. Micro-computed tomography of the aortic valves revealed the depth and extent of calcification in each nodule on the valve, as shown in Fig. 4.3c. Figure 4.3 c1 shows a typical 2-dimensional reconstructed slice of a control aortic valve, and Fig. 4.3 c2 shows a slice of a hypercholesterolemia aortic valve. The images indicate that mineral level is greatest at the outer edge of each nodule and decreases toward the center of the mineralized lesion, similar to what is seen in skeletal bone formation. Figure 4.3 c3 demonstrates a marked reduction in the amount of calcification present by microcomputed tomography.

Finally, we injected intravenous calcein to determine localization of in vivo new bone formation. Figure 4.3d shows the in vivo calcein label incorporation into the proliferating valve myofibroblast cells. In the control group, there was little calcein label in the valve leaflet (Fig. 4.3 d1). In the hypercholesterolemia valves, calcein colocalized to the proliferating valve leaflet edge, shown in Fig. 4.3 d2. The localization of calcein in the hypercholesterolemia aortic valves is parallel to the localization of the proliferating, actin-positive myofibroblast cells. There is a marked increase in the calcein label in the valve leaflets. The aortic valves in the atorvastatin-treated animals demonstrated no incorporation of calcein (Fig. 4.3 d3).

Figure 4.4 demonstrates the Lrp5/Wnt signaling pathway upregulated in the presence of bone formation in calcifying aortic valves.

Summary

Chronic exposure to experimental cholesterol diets over 6 months in the natural occurring LDLR null rabbit model demonstrates the development

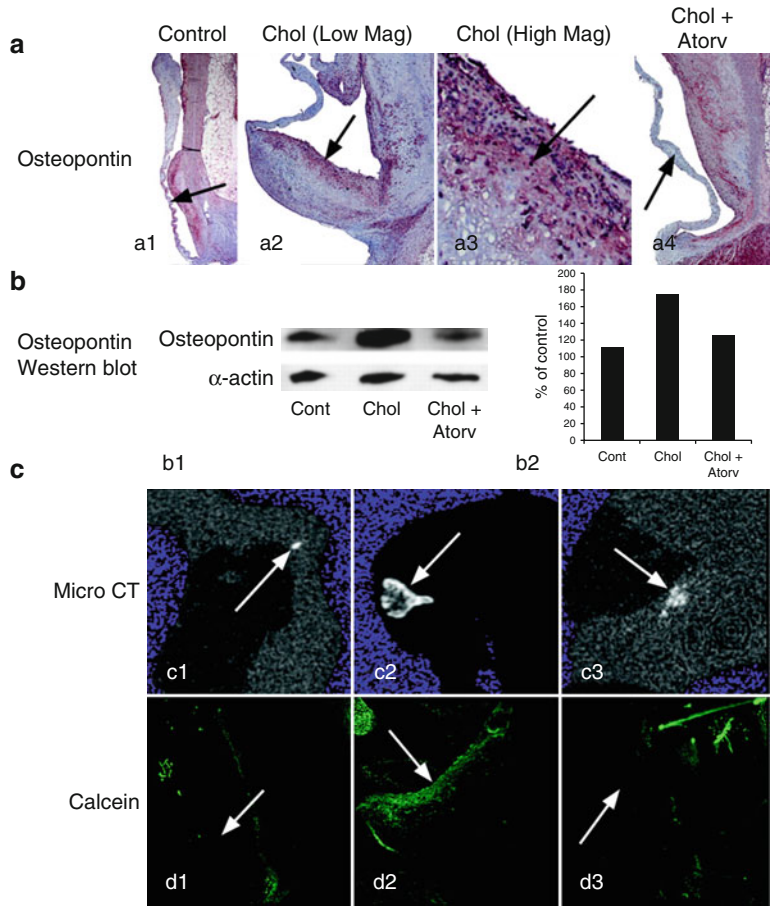

Fig. 4.3 Establishment of the bone-like phenotype in the calcified aortic valves. *Left column*, control diet; *middle column*, cholesterol diet; *right column*, cholesterol diet plus atorvastatin. (**a**) Osteopontin immunostain light microscopy; aortic valve on the left and aorta on the right. *Arrow points* to aortic valve in each figure. All frames 12.5× magnification. (**b**) Osteopontin Western blot and quantification. (**c**) Micro-computed tomography 2-dimensional reconstructed slices of each valve (3.4 mm horizontal field of view). (**d**) Confocal microscopy of the calcein labelling in the mineralizing valve

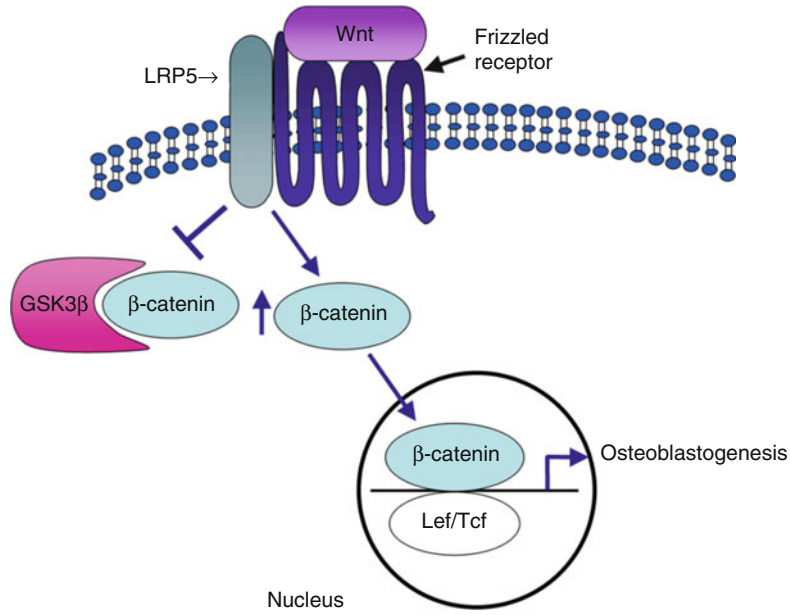

Fig. 4.4 Lrp5 pathway upregulated in the aortic valve during myofibroblast differentiation

of early mineralization and calcification in the aortic valve. This model after 2 months of cholesterol diet develops the classis fatty streak lesion as demonstrated in Chap. 3. The model after 3 months of cholesterol diet develops early calcification in the rabbit aortic valve [20]. The 6 month exposure was necessary to develop progressive valve lesions, complex mineralization, and bone formation as demonstrated by the calcein uptake in the valve. Our conclusions from this 6 months support the use of our rabbit model with a high cholesterol diet to induce Lrp5 expression in association with early calcification in the aortic valves of rabbits.

References

1. Rajamannan NM, Sangiorgi G, Springett M, Arnold K, Mohacsi T, Spagnoli LG, Edwards WD, Tajik AJ, Schwartz RS. Experimental hypercholesterolemia induces apoptosis in the aortic valve. J Heart Valve Dis. 2001;10:371–4.
2. Rajamannan NM, Subramaniam M, Springett M, Sebo TC, Niekrasz M, McConnell JP, Singh RJ, Stone NJ, Bonow RO, Spelsberg TC. Atorvastatin inhibits hypercholesterolemia-induced cellular proliferation and bone matrix production in the rabbit aortic valve. Circulation. 2002;105:2260–5.
3. Sarphie TG. Interactions of igg and beta-vldl with aortic valve endothelium from hypercholesterolemic rabbits. Atherosclerosis. 1987;68:199–212.
4. Sarphie TG. A cytochemical study of the surface properties of aortic and mitral valve endothelium from hypercholesterolemic rabbits. Exp Mol Pathol. 1986;44:281–96.
5. Sarphie TG. Anionic surface properties of aortic and mitral valve endothelium from New Zealand white rabbits. Am J Anat. 1985;174:145–60.
6. Sarphie TG. Surface responses of aortic valve endothelia from diet-induced, hypercholesterolemic rabbits. Atherosclerosis. 1985;54:283–99.
7. Gong Y, Slee RB, Fukai N, Rawadi G, Roman-Roman S, Reginato AM, Wang H, Cundy T, Glorieux FH, Lev D, Zacharin M, Oexle K, Marcelino J, Suwairi W, Heeger S, Sabatakos G, Apte S, Adkins WN, Allgrove J, Arslan-Kirchner M, Batch JA, Beighton P, Black GC, Boles RG, Boon LM, Borrone C, Brunner HG, Carle GF, Dallapiccola B, De Paepe A, Floege B, Halfhide ML, Hall B, Hennekam RC, Hirose T, Jans A, Juppner H, Kim CA, Keppler-Noreuil K, Kohlschuetter A, LaCombe D, Lambert M, Lemyre E, Letteboer T, Peltonen L, Ramesar RS, Romanengo M, Somer H, Steichen-Gersdorf E, Steinmann B, Sullivan B, Superti-Furga A, Swoboda W, van den Boogaard MJ, Van Hul W, Vikkula M, Votruba M, Zabel B, Garcia T, Baron R, Olsen BR, Warman ML, Osteoporosis-Pseudoglioma Syndrome Collaborative G. Ldl receptor-related protein 5 (lrp5) affects bone accrual and eye development. Cell. 2001;107:513–23.
8. Little RD, Carulli JP, Del Mastro RG, Dupuis J, Osborne M, Folz C, Manning SP, Swain PM, Zhao SC, Eustace B, Lappe MM, Spitzer L, Zweier S, Braunschweiger K, Benchekroun Y, Hu X, Adair R, Chee L, FitzGerald MG, Tulig C, Caruso A, Tzellas N, Bawa A, Franklin B, McGuire S, Nogues X, Gong G, Allen KM, Anisowicz A, Morales AJ, Lomedico PT, Recker SM, Van Eerdewegh P, Recker RR, Johnson ML. A mutation in the ldl receptor-related protein 5 gene results in the autosomal dominant high-bone-mass trait. Am J Hum Genet. 2002;70:11–9.
9. Kim DH, Inagaki Y, Suzuki T, Ioka RX, Yoshioka SZ, Magoori K, Kang MJ, Cho Y, Nakano AZ, Liu Q, Fujino T, Suzuki H, Sasano H, Yamamoto TT. A new low density lipoprotein receptor related protein, lrp5, is expressed in hepatocytes and adrenal cortex, and recognizes apolipoprotein e. J Biochem. 1998;124:1072–6.
10. Willert K, Nusse R. Beta-catenin: a key mediator of wnt signaling. Curr Opin Genet Dev. 1998;8:95–102.
11. Behrens J, von Kries JP, Kuhl M, Bruhn L, Wedlich D, Grosschedl R, Birchmeier W. Functional interaction of beta-catenin with the transcription factor lef-1. Nature. 1996;382:638–42.
12. Huber O, Korn R, McLaughlin J, Ohsugi M, Herrmann BG, Kemler R. Nuclear localization of beta-catenin by interaction with transcription factor lef-1. Mech Dev. 1996;59:3–10.
13. Holmen SL, Salic A, Zylstra CR, Kirschner MW, Williams BO. A novel set of wnt-frizzled fusion proteins identifies receptor components that activate beta-catenin-dependent signaling. J Biol Chem. 2002;277:34727–35.
14. Caverzasio J. [wnt/lrp5, a new regulation osteoblastic pathway involved in reaching peak bone masses]. Rev Med Suisse Romande. 2004;124:81–2.
15. Kahler RA, Westendorf JJ. Lymphoid enhancer factor-1 and beta-catenin inhibit runx2-dependent transcriptional activation of the osteocalcin promoter. J Biol Chem. 2003;278:11937–44.
16. Smith E, Frenkel B. Glucocorticoids inhibit the transcriptional activity of lef/tcf in differentiating osteoblasts in a glycogen synthase kinase-3{beta}-dependent and -independent manner. J Biol Chem. 2005;280:2388–94.
17. Wang HY, Malbon CC. Wnt signaling, ca2+, and cyclic gmp: visualizing frizzled functions. Science. 2003;300:1529–30.
18. Gregory CA, Perry AS, Reyes E, Conley A, Gunn WG, Prockop DJ. Dkk-1-derived synthetic peptides and lithium chloride for the control and recovery of adult stem cells from bone marrow. J Biol Chem. 2005;280:2309–23.

19. Yano F, Kugimiya F, Ohba S, Ikeda T, Chikuda H, Ogasawara T, Ogata N, Takato T, Nakamura K, Kawaguchi H, Chung UI. The canonical wnt signaling pathway promotes chondrocyte differentiation in a sox9-dependent manner. Biochem Biophys Res Commun. 2005;333:1300–8.

20. Rajamannan NM, Subramaniam M, Stock SR, Stone NJ, Springett M, Ignatiev KI, McConnell JP, Singh RJ, Bonow RO, Spelsberg TC. Atorvastatin inhibits calcification and enhances nitric oxide synthase production in the hypercholesterolaemic aortic valve. Heart. 2005;91:806–10.

5 Development of an Experimental Model of Mitral Valve Regurgitation via Hypertrophic Chondrocytes

Nalini M. Rajamannan, Jeff Park, and Francesco Antonini-Canterin

Introduction

Degenerative myxomatous mitral valve disease is the most common indication for surgical valve repair in the US and Europe [1, 2]. Degenerative myxomatous mitral valve disease is associated with mitral valve prolapse and abnormal movement of the leaflets into the left atrium during systole due to inadequate chordal support (elongation or rupture) and excessive valvular tissue [3]. There is a spectrum of pathologic changes found in the development of myxomatous mitral valve disease, which range from a marked increase in valve area and length to secondary ruptured chordae. Microscopically, the valves are myxomatous, with deposition of mucopolysaccahrides in a thickened spongiosa layer encroaching on the fibrosa layer [4]. Annular myxomatous changes may lead to dilation and calcification of the annulus. Previously, our laboratory has demonstrated that human myxomat mitral valve disease is associated with a chondrogenic phenotype [5].

N.M. Rajamannan, MD (✉) • J. Park, MD
Division of Biochemistry and Molecular Biology,
Mayo Clinic, 200 First St SW,
Rochester, MN 55905, USA
e-mail: rajamannan.nalini@mayo.edu;
jeff.park06@gmail.com

F. Antonini-Canterin, MD
Preventive and Rehabilitative Cardiology, Cardiologia
ARC, Azienda Ospedaliera "S. Maria degli Angeli",
Via montereale 24, Pordenone 33170, Italy
e-mail: antonini.canterin@gmail.com

Idiopathic calcification of the mitral annulus (MAC) is one of the most common cardiac abnormalities demonstrated at autopsy and is commonly associated with degenerative mitral valve disease. Epidemiologic studies have identified traditional cardiovascular risk factors, risk factors associated with the development of MAC and mitral valve disease, which include hypertension, hypercholesterolemia, smoking and male gender, and similarly to calcific aortic valve disease [6–34]. This lesion presents with various clinical presentations, including prolapse, retraction and redundancy of the leaflet. Although there is a spectrum of presentation of this valve lesion, over time it uniformly develops progressive regurgitation. An association between mitral valve calcification and atherosclerosis has been described; nevertheless, few experimental models have demonstrated these changes. Experimentally, we tested this hypothesis in an in vivo rabbit model of valvular heart disease, similar to previous studies examining the hypercholesterolemic aortic valve [35–37]. In a previous study, 2 months of experimental hypercholesterolemia, the mitral valve has an active cellular biology similar to the hypercholesterolemia aortic valve [37, 38]. This chapter outlines a model, which identifies whether a model of chronic experimental hypercholesterolemia would induce mitral regurgitation as defined by Transesophageal color Doppler echocardiography after 6 months, and whether Atorvastatin would alleviate the regurgitation in this animal model.

N.M. Rajamannan (ed.), *Molecular Biology of Valvular Heart Disease*,
DOI 10.1007/978-1-4471-6350-3_5, © Springer-Verlag London 2014

Low-density lipoprotein receptors (LDLR) are critical in the uptake, processing, and cellular metabolism of cholesterol. The LDL receptor-related protein 5 (LRP5), a receptor involved in canonical Wnt signaling, has been identified as an important receptor in the activation of skeletal bone formation and also implicated in cholesterol metabolism [39, 40]. In this current study, we studied the Watanabe rabbit, which harbors a naturally occurring genetic LDLR mutation, in order to determine the effect of experimental hypercholesterolemia with and without atorvastatin induces chondrogenesis in the mitral valve.

In Vivo Experimental Hypercholesterolemia Model

Watanabe Rabbits were fed a high cholesterol diet for 6 months. All the rabbits underwent transesophageal echocardiograms (TEE) using the Siemens AccuNav probe. Immunohistochemistry was performed.

Gross Photography of the Mitral Valves

Figure 5.1, shows the mitral valves from the rabbits on the three diet regimens. The control mitral valves in Fig. 5.1, Panel a, demonstrate a clear glistening leaflet. The cholesterol diet as shown in Fig. 5.1, Panel b, demonstrates the atherosclerotic lesion along the atrial surface of the mitral valve leaflet. There is a more advanced lesion, which starts along the mitral annulus and decreases in the amount of lesion toward the leaflet attachment along the chordae tendinae. Figure 5.1, Panel c, demonstrates attenuation in the atherosclerotic lesion with the Atorvastatin.

Transesophageal Echocardiography

Figure 5.2 demonstrates the color doppler for the Transesophageal echo (TEE) of mitral valves from the rabbits on the three diet regimens.

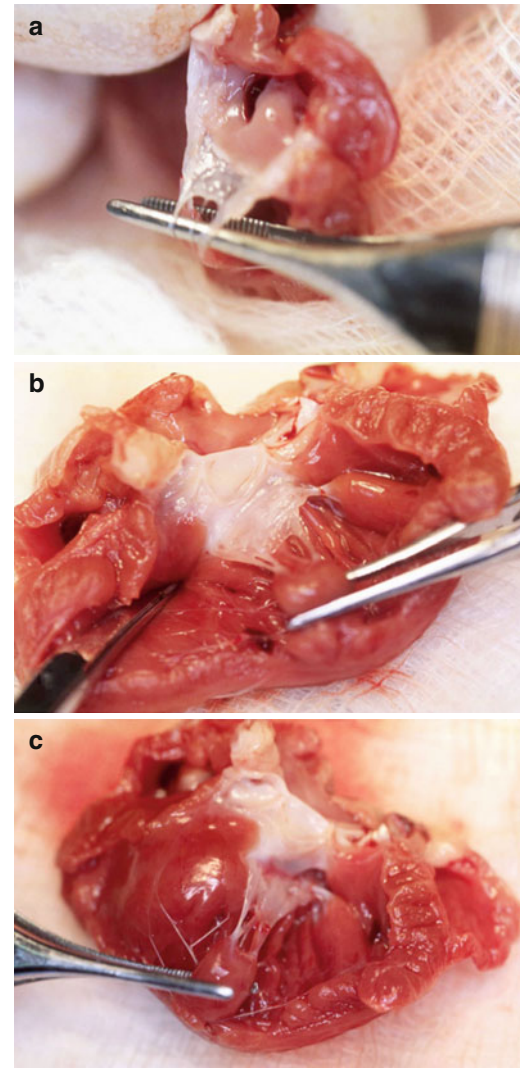

Fig. 5.1 Demonstrates the gross anatomy of the mitral valves from the rabbits on the three diet treatments. *Left column*, control diet; *middle column*, cholesterol diet; *right column*, cholesterol diet plus atorvastatin. (All frames 12.5× magnification). Panel (**a**) Control mitral valve. Panel (**b**) Cholesterol mitral valve. Panel (**c**) Cholesterol + Atorvastatin [42]

The TEE in Fig. 5.2, Panel a, demonstrates no evidence of regurgitation in the control diet. The TEE from the cholesterol diet is shown in Fig. 5.2, Panel b, which demonstrates multiple large jets of regurgitation. Figure 5.2, Panel c, demonstrates no evidence of regurgitation by color flow doppler evaluation.

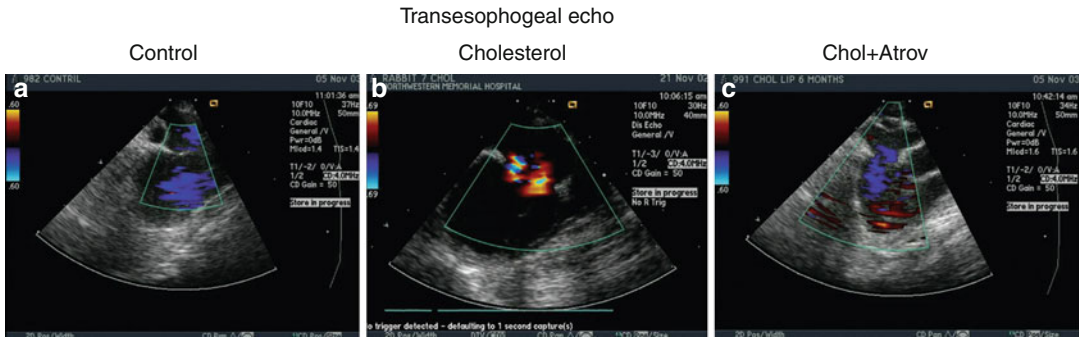

Fig. 5.2 Demonstrates the Transesophageal color flow Doppler echo of the mitral valves from the rabbits on the three diet treatments. *Left column*, control diet; *middle column*, cholesterol diet; *right column*, cholesterol diet plus atorvastatin [42]. Panel (**a**) Control mitral valve and heart. Panel (**b**) Cholesterol mitral valve and heart. Panel (**c**) Cholesterol + Atorvastatin mitral valve and heart

Establishment of the Chondrocyte-Like Phenotype in the Myxomatous Hypercholesterolemia Mitral Valves

Figure 5.3, Panels a–c, demonstrates the proliferating nuclear antigen staining cells, osteocalcin staining and the macrophage cells within the hypercholesterolemia mitral valve leaflet. Each hypercholesterolemia mitral valve was photographed at four different magnifications for each of the specific stains to demonstrate the coalescing chondrocyte-like cells developing within the atherosclerotic lesion. These cells express the markers secondary to atherosclerosis in addition to the markers of osteogenesis. The coalescing cells within the hypercholesterolemia mitral valve are consistent with the identification of expanding hypertrophic chondrocytes [42].

Summary

The naturally occurring LDLR defect in Watanabe rabbits provides a model system reflecting the symptoms observed in patients (FH) who have mutations in the LDLR [41]. In this study, we demonstrate that atherosclerosis and markers of cartilage formation are present in the cholesterol mitral valve leaflets with associated valve regurgitation. Treatment with atorvastatin also resulted in decreased regurgitation and leaflet thickening. The light microscopy demonstrates that cartilage formation is indicated by coalescing hypertrophic chondrocytes. Cartilage is a connective tissue, comprising an exquisite assembly of functionally distinct cell populations that are required to support the structural integrity in endochondral bone formation. This chapter confirms the presence of severe mitral regurgitation and cartilage formation associated with cellular proliferation in the hypercholesterolemia mitral valve. Together, this new observations in our in vivo models supports the hypothesis that degenerative valvular mitral regurgitation is the result of active cartilage formation in the mitral valve, which may be mediated through a process involving chondrocyte differentiation. Furthermore, statins inhibit this regurgitant process, likely by repressing the expression of genes essential for chondrocyte maturation.

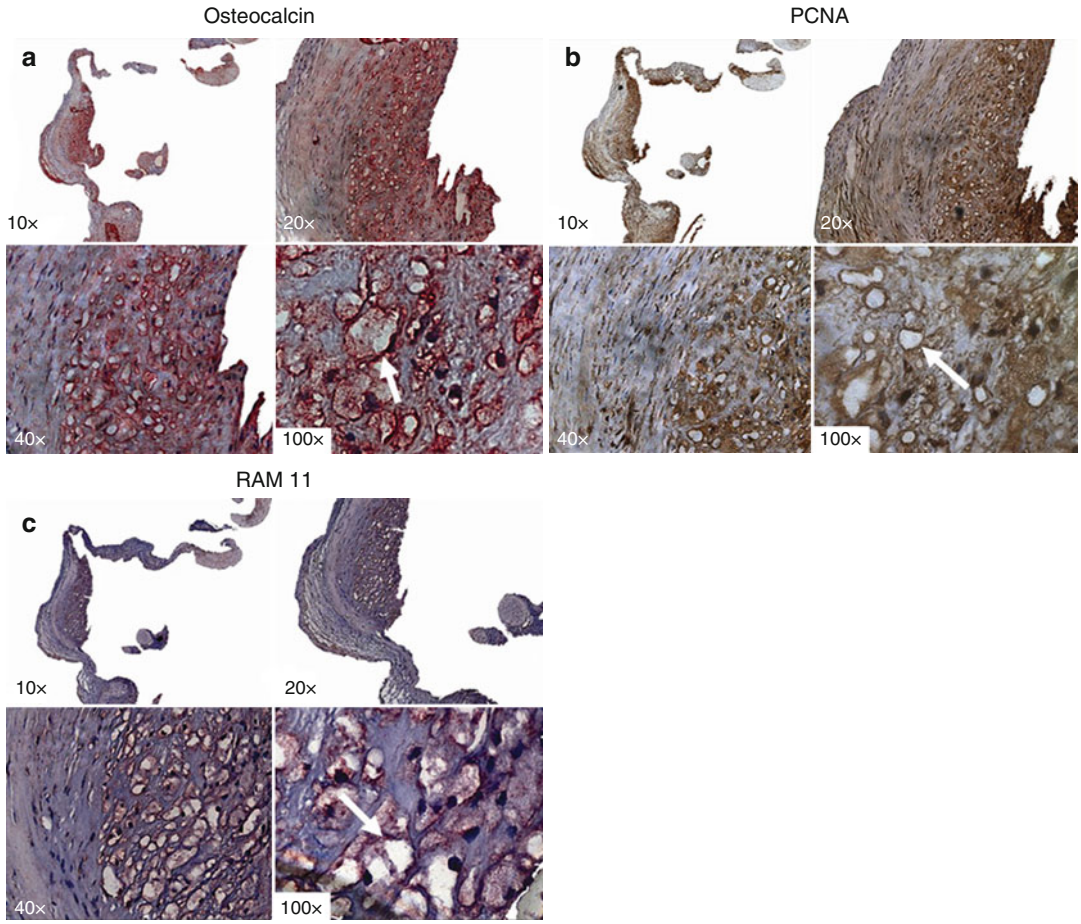

Fig. 5.3 Demonstrates the high power magnification of the hypercholesterolemic Mitral Valve demonstrating hypertrophic chondrocytes in the cholesterol mitral valve. Panel (**a**) Osteocalcin immunohistochemical stain. Panel (**b**) Proliferating cell nuclear antigen stain. Panel (**c**) RAM11 immunohistochemical stain [42]

References

1. Bonow RO, Carabello BA, Kanu C, de Leon Jr AC, Faxon DP, Freed MD, Gaasch WH, Lytle BW, Nishimura RA, O'Gara PT, O'Rourke RA, Otto CM, Shah PM, Shanewise JS, Smith Jr SC, Jacobs AK, Adams CD, Anderson JL, Antman EM, Fuster V, Halperin JL, Hiratzka LF, Hunt SA, Nishimura R, Page RL, Riegel B. Acc/aha 2006 guidelines for the management of patients with valvular heart disease: a report of the American College of Cardiology/American Heart Association Task Force on Practice Guidelines (writing committee to revise the 1998 Guidelines for the Management of Patients with Valvular Heart Disease): developed in Collaboration with the Society of Cardiovascular Anesthesiologists: endorsed by the Society for Cardiovascular Angiography and Interventions and the Society of Thoracic Surgeons. Circulation. 2006;114:e84–231.
2. Vahanian A, Baumgartner H, Bax J, Butchart E, Dion R, Filippatos G, Flachskampf F, Hall R, Iung B, Kasprzak J, Nataf P, Tornos P, Torracca L, Wenink A. Guidelines on the management of valvular heart disease: the task force on the management of valvular heart disease of the european society of cardiology. Eur Heart J. 2007;28:230–68.
3. Rahimtoola SH, Frye RL. Valvular heart disease. Circulation. 2000;102:IV24–33.
4. Grande-Allen KJ, Calabro A, Gupta V, Wight TN, Hascall VC, Vesely I. Glycosaminoglycans and proteoglycans in normal mitral valve leaflets and chordae: association with regions of tensile and compressive loading. Glycobiology. 2004;14:621–33.
5. Caira FC, Stock SR, Gleason TG, McGee EC, Huang J, Bonow RO, Spelsberg TC, McCarthy PM, Rahimtoola SH, Rajamannan NM. Human degenerative valve disease is associated with up-regulation of low-density lipoprotein receptor-related protein 5

receptor-mediated bone formation. J Am Coll Cardiol. 2006;47:1707–12.
6. Nair CK, Sudhakaran C, Aronow WS, Thomson W, Woodruff MP, Sketch MH. Clinical characteristics of patients younger than 60 years with mitral anular calcium: comparison with age- and sex-matched control subjects. Am J Cardiol. 1984;54:1286–7.
7. Aronow WS, Ahn C, Kronzon I. Association of mitral annular calcium with symptomatic peripheral arterial disease in older persons. Am J Cardiol. 2001;88:333–4.
8. Deutscher S, Rockette HE, Krishnaswami V. Diabetes and hypercholesterolemia among patients with calcific aortic stenosis. J Chronic Dis. 1984;37:407–15.
9. Hoagland PM, Cook EF, Flatley M, Walker C, Goldman L. Case-control analysis of risk factors for presence of aortic stenosis in adults (age 50 years or older). Am J Cardiol. 1985;55:744–7.
10. Aronow WS, Ahn C, Kronzon I, Goldman ME. Association of coronary risk factors and use of statins with progression of mild valvular aortic stenosis in older persons. Am J Cardiol. 2001;88:693–5.
11. Aronow WS, Schwartz KS, Koenigsberg M. Correlation of serum lipids, calcium, and phosphorus, diabetes mellitus and history of systemic hypertension with presence or absence of calcified or thickened aortic cusps or root in elderly patients. Am J Cardiol. 1987;59:998–9.
12. Mohler ER, Sheridan MJ, Nichols R, Harvey WP, Waller BF. Development and progression of aortic valve stenosis: atherosclerosis risk factors–a causal relationship? A clinical morphologic study. Clin Cardiol. 1991;14:995–9.
13. Lindroos M, Kupari M, Valvanne J, Strandberg T, Heikkila J, Tilvis R. Factors associated with calcific aortic valve degeneration in the elderly. Eur Heart J. 1994;15:865–70.
14. Boon A, Cheriex E, Lodder J, Kessels F. Cardiac valve calcification: characteristics of patients with calcification of the mitral annulus or aortic valve. Heart. 1997;78:472–4.
15. Chui MC, Newby DE, Panarelli M, Bloomfield P, Boon NA. Association between calcific aortic stenosis and hypercholesterolemia: is there a need for a randomized controlled trial of cholesterol-lowering therapy? Clin Cardiol. 2001;24:52–5.
16. Wilmshurst PT, Stevenson RN, Griffiths H, Lord JR. A case-control investigation of the relation between hyperlipidaemia and calcific aortic valve stenosis. Heart. 1997;78:475–9.
17. Chan KL, Ghani M, Woodend K, Burwash IG. Case-controlled study to assess risk factors for aortic stenosis in congenitally bicuspid aortic valve. Am J Cardiol. 2001;88:690–3.
18. Briand M, Lemieux I, Dumesnil JG, Mathieu P, Cartier A, Despres JP, Arsenault M, Couet J, Pibarot P. Metabolic syndrome negatively influences disease progression and prognosis in aortic stenosis. J Am Coll Cardiol. 2006;47:2229–36.
19. Palta S, Pai AM, Gill KS, Pai RG. New insights into the progression of aortic stenosis: implications for secondary prevention. Circulation. 2000;101:2497–502.
20. Peltier M, Trojette F, Sarano ME, Grigioni F, Slama MA, Tribouilloy CM. Relation between cardiovascular risk factors and nonrheumatic severe calcific aortic stenosis among patients with a three-cuspid aortic valve. Am J Cardiol. 2003;91:97–9.
21. Stewart BF, Siscovick D, Lind BK, Gardin JM, Gottdiener JS, Smith VE, Kitzman DW, Otto CM. Clinical factors associated with calcific aortic valve disease. Cardiovascular health study. J Am Coll Cardiol. 1997;29:630–4.
22. Otto CM, Lind BK, Kitzman DW, Gersh BJ, Siscovick DS. Association of aortic-valve sclerosis with cardiovascular mortality and morbidity in the elderly. N Engl J Med. 1999;341:142–7 [comment].
23. Faggiano P, Antonini-Canterin F, Baldessin F, Lorusso R, D'Aloia A, Cas LD. Epidemiology and cardiovascular risk factors of aortic stenosis. Cardiovasc Ultrasound. 2006;4:27.
24. Pohle K, Maffert R, Ropers D, Moshage W, Stilianakis N, Daniel WG, Achenbach S. Progression of aortic valve calcification: association with coronary atherosclerosis and cardiovascular risk factors. Circulation. 2001;104:1927–32.
25. Allison MA, Pavlinac P, Wright CM. The differential associations between hdl, non-hdl and total cholesterols and atherosclerotic calcium deposits in multiple vascular beds. Atherosclerosis. 2007;194:e87–94.
26. Anvari MS, Boroumand MA, karimi A, Alidoosti M, Yazdanifard P, Shirzad M, Abbasi SH, Soleymani A. Aortic and mitral valve atherosclerosis: predictive factors and associations with coronary atherosclerosis using gensini score. Arch Med Res. 2009;40:124–7.
27. Bai XJ, Liu Q, Han LL, Sun XF, Lin HL, Chen XM. Quantitative assessment of healthy people's cardiovascular aging and analysis of the relevant law: study in three cities in northern China. Zhonghua Yi Xue Za Zhi. 2007;87:2385–9.
28. Deluca G, Correale M, Ieva R, Del Salvatore B, Gramenzi S, Di Biase M. The incidence and clinical course of caseous calcification of the mitral annulus: a prospective echocardiographic study. J Am Soc Echocardiogr. 2008;21:828–33.
29. Fox CS, Larson MG, Vasan RS, Guo CY, Parise H, Levy D, Leip EP, O'Donnell CJ, D'Agostino Sr RB, Benjamin EJ. Cross-sectional association of kidney function with valvular and annular calcification: the Framingham heart study. J Am Soc Nephrol. 2006;17:521–7.
30. Ix JH, Chertow GM, Shlipak MG, Brandenburg VM, Ketteler M, Whooley MA. Association of fetuin-a with mitral annular calcification and aortic stenosis among persons with coronary heart disease: data from the heart and soul study. Circulation. 2007;115:2533–9.
31. Jassal DS, Tam JW, Bhagirath KM, Gaboury I, Sochowski RA, Dumesnil JG, Giannoccaro PJ, Jue J, Pandey AS, Joyner CD, Teo KK, Chan KL. Association of mitral annular calcification and aortic

valve morphology: a substudy of the aortic stenosis progression observation measuring effects of rosuvastatin (astronomer) study. Eur Heart J. 2008;29:1542–7.
32. Rahimtoola SH. The year in valvular heart disease. J Am Coll Cardiol. 2008;51:760–70.
33. Sharma R, Pellerin D, Gaze DC, Mehta RL, Gregson H, Streather CP, Collinson PO, Brecker SJ. Mitral annular calcification predicts mortality and coronary artery disease in end stage renal disease. Atherosclerosis. 2007;191:348–54.
34. Zapolski T, Wysokinski A, Przegalinski J, Wojcik J, Tomaszewski A, Drozd J, Madejczyk A, Pijanowski Z, Widomska-Czekajska T. Coronary atherosclerosis in patients with acquired valvular disease. Kardiol Pol. 2004;61:534–43; discussion 544–5.
35. Sarphie TG. A cytochemical study of the surface properties of aortic and mitral valve endothelium from hypercholesterolemic rabbits. Exp Mol Pathol. 1986;44:281–96.
36. Sarphie TG. Surface topography of mitral valve endothelium from diet-induced, hypercholesterolemic rabbits. Atherosclerosis. 1982;45:203–20.
37. Makkena B, Salti H, Subramaniam M, Thennapan S, Bonow RH, Caira F, Bonow RO, Spelsberg TC, Rajamannan NM. Atorvastatin decreases cellular proliferation and bone matrix expression in the hypercholesterolemic mitral valve. J Am Coll Cardiol. 2005;45:631–3.
38. Rajamannan NM, Subramaniam M, Springett M, Sebo TC, Niekrasz M, McConnell JP, Singh RJ, Stone NJ, Bonow RO, Spelsberg TC. Atorvastatin inhibits hypercholesterolemia-induced cellular proliferation and bone matrix production in the rabbit aortic valve. Circulation. 2002;105:2260–5.
39. Little RD, Carulli JP, Del Mastro RG, Dupuis J, Osborne M, Folz C, Manning SP, Swain PM, Zhao SC, Eustace B, Lappe MM, Spitzer L, Zweier S, Braunschweiger K, Benchekroun Y, Hu X, Adair R, Chee L, FitzGerald MG, Tulig C, Caruso A, Tzellas N, Bawa A, Franklin B, McGuire S, Nogues X, Gong G, Allen KM, Anisowicz A, Morales AJ, Lomedico PT, Recker SM, Van Eerdewegh P, Recker RR, Johnson ML. A mutation in the ldl receptor-related protein 5 gene results in the autosomal dominant high-bone-mass trait. Am J Hum Genet. 2002;70:11–9.
40. Gong Y, Slee RB, Fukai N, Rawadi G, Roman-Roman S, Reginato AM, Wang H, Cundy T, Glorieux FH, Lev D, Zacharin M, Oexle K, Marcelino J, Suwairi W, Heeger S, Sabatakos G, Apte S, Adkins WN, Allgrove J, Arslan-Kirchner M, Batch JA, Beighton P, Black GC, Boles RG, Boon LM, Borrone C, Brunner HG, Carle GF, Dallapiccola B, De Paepe A, Floege B, Halfhide ML, Hall B, Hennekam RC, Hirose T, Jans A, Juppner H, Kim CA, Keppler-Noreuil K, Kohlschuetter A, LaCombe D, Lambert M, Lemyre E, Letteboer T, Peltonen L, Ramesar RS, Romanengo M, Somer H, Steichen-Gersdorf E, Steinmann B, Sullivan B, Superti-Furga A, Swoboda W, van den Boogaard MJ, Van Hul W, Vikkula M, Votruba M, Zabel B, Garcia T, Baron R, Olsen BR, Warman ML, The Osteoporosis-Pseudoglioma Syndrome Collaborative G. Ldl receptor-related protein 5 (lrp5) affects bone accrual and eye development. Cell. 2001;107:513–23.
41. Aliev G, Burnstock G. Watanabe rabbits with heritable hypercholesterolaemia: a model of atherosclerosis. Histol Histopathol. 1998;13:797–817.
42. Rajamannan NM, Rosenhek RA, Rahimtoola S, Atorvastatin attenuates severe myxomatous mitral regurgitation via Lrp5/Sox9 formation, European Society of Cardiology, Abstract, European Heart Journal. 2009; 30 (Abstract Supplement), 997.

6 Testing Drug Eluting Paclitaxel Balloon Valvuloplasty in an Experimental Model of Aortic Stenosis

Konstantinos Spargias, Mariann Gyöngyösi, Rayyan Hemetsberger, Aniko Posa, Noemi Pavo, Imre J. Pavo, Kurt Huber, Zsolt Petrasi, Ors Petnehazy, Rembert Pogge von Strandmann, Jeffrey Park, Dietmar Glogar, Gerald Maurer, and Nalini M. Rajamannan

Introduction

Balloon aortic valvuloplasty (BAV) was introduced in 1986 as an alternative non- surgical therapeutic option in elderly and high-risk patients with aortic stenosis [1]. It generates small to moderate increase in the effective aortic valve area (AVA) and decline in the transvalvular pressure gradient (by average 50 %) which results in early symptomatic improvements in the majority of patients [2–5]. Nonetheless, clinical data demonstrates restenosis rates of the aortic valve occurring up to 83 % observed at 6 months and is almost universal within 1 year after the procedure [3, 6, 7]. Restenosis promptly revokes the improvement in symptoms and quality of life, which is so much valued especially in the elderly population with multiple comorbidities and limited life expectancy. The initial enthusiasm about BAV led to its more liberal use in high-risk patients but registry data indicated that it does not alter the natural history of aortic stenosis [8].

The advent of transcatheter aortic valve replacement (TAVR) in recent years is the main factor for the resurrection of a contemporary BAV [9]. Consequently, a decrease in the complication rates and improved outcomes with contemporary BAV has been demonstrated [10–12]. Although recent data from the medical treatment group in the PARTNERS trial, in which 83 % of the patients underwent BAV, showed lower event

K. Spargias, MD, PhD, FESC (✉)
Department of Transcatheter Heart Valves, Hygeia Hospital, 9 Erythrou Stavrou Street, 151 23 Athens, Greece
e-mail: spargias@hygeia.gr

M. Gyöngyösi, MD, PhD • R. Hemetsberger, MD
A. Posa, PhD • N. Pavo, MD, MSC • I.J. Pavo, MD
D. Glogar, MD • G. Maurer, MD
Department of Cardiology, Medical University of Vienna, Währinger Gürtel 18-20, Vienna A-1090, Austria
e-mail: mariann.gyongyosi@meduniwien.ac.at; rayyan.hemetsberger@joho-dortmund.de; posaaniko@hotmail.com; noemi.pavo@meduniwien.ac.at; imrus11@yahoo.de; d.glogar@aon.at; gerald.maurer@meduniwien.ac.at

K. Huber
3rd Department Medicine, Wilhelminen Hospital, Montleartstrasse 37, A-1170 Vienna, Austria
e-mail: kurt.huber@wienkav.at

Z. Petrasi, PhD • O. Petnehazy
Diagnostic Imaging and Radiation Oncology, University of Kaposvar, Guba S u. 40, Kaposvar, Somogy, H-7400, Hungary
e-mail: petrasi.zsolt@sic.ke.hu; petnehazy.ors@sic.ke.hu

R.P. von Strandmann, PhD
Department of Clinical, Eurocor GmbH, In den Dauen 6a, Bonn 53117, Germany
e-mail: pogge@eurocor.de

J. Park, MD • N.M. Rajamannan, MD
Division of Biochemistry and Molecular Biology, Mayo Clinic, 200 First St SW, Rochester, MN 55905, USA

N.M. Rajamannan (ed.), *Molecular Biology of Valvular Heart Disease*,
DOI 10.1007/978-1-4471-6350-3_6, © Springer-Verlag London 2014

rates in those who underwent BAV compared to those who did not, the outcomes in this group in general are unchanged [7]. Approximately 20–40 % of patients screened for TAVR, and turned down for various reasons are still subjected to BAV [13, 14]. Understanding the cellular events in an experimental model of aortic valve disease after BAV may further optimize this approach to provide translational experimental evidence towards this treatment modality in this patient population.

Restenosis following BAV has been attributed to elastic recoil and prolonged scaring of the valve leaflets with evidence of fusion of split commissures, myofibroblast cell proliferation [15], valve thickening and ossification [16–19]. Similar biological mechanisms have been found in coronary artery restenosis and the benefits of drug eluting stents in this disease mechanism has been critical in improving outcomes for this patient population [20, 21].

Several studies have demonstrated that the cellular mechanisms of calcific aortic valve disease in experimental rabbit model include: (1) atherosclerosis, (2) cell proliferation, (3) extracellular matrix production and (4) calcification via osteogenic mechanisms [22–24]. This chapter will demonstrate a parallel approach for calcific aortic valve disease (CAVD) to coronary stenosis by locally deliver drugs to inhibit the cellular proliferation and extracellular matrix production at valves with drug-eluting valvuloplasty balloons, a paclitaxel-eluting balloon, which can prevent restenosis in an experimental animal model of CAVD [25].

In Vivo Rabbit Model of Aortic Valve Disease

An experimental in vivo model of aortic valve stenosis in rabbits was used, and standard echo, cardiac cath imaging, MicroCT, and histology was performed to measure the effect of the drug-eluting balloo [15, 22–24, 29]. Baseline and post-BAV aortic stenosis severity as assessed by the invasive transvalvular gradient was similar in the groups (Table 6.1). One month after BAV, reduction in the aortic valve area resulted in a significant increase in the mean invasive pressure gradient in the plain-balloon group (from 1.5 ± 2.5 to 7.7 ± 7.7 mmHg, $p = 0.02$), and a non- significant increase in the paclitaxel-balloon group (from 1.5 ± 2.2 to 3.6 ± 3.7 mmHg, $p = 0.15$), as shown in Fig. 6.1, leading to a trend for less mean gradient at follow-up in the latter group (3.6 ± 3.7 vs. 7.7 ± 7.7 mmHg, $p = 0.08$). There was no difference in the primary end point of the study since reduction in the gradient based on the transvalvular gradients occurred in 64 % of the plain and 50 % of the paclitaxel-balloon treated animals. Baseline and post-BAV aortic stenosis severity, as assessed by several echocardiographic indices, were similar between the groups. However, 1 month after BAV, the AVA was significantly larger, while the SWL loss and the aortic valve resistance were significantly lower in the paclitaxel-BAV group (Table 6.1). Indices of left ventricular systolic performance such as fractional shortening (31.9 ± 4.7 vs. 37.3 ± 7.0 %, $p = 0.02$) and stroke volume (69 ± 7 vs. 74 ± 10 ml, $p = 0.14$) appeared improved in the paclitaxel-balloon compared to the plain-balloon group at follow-up.

Immunohistochemistry of the Coated Versus the Uncoated Aortic Valve

Pathology of the animals revealed severe calcified atherosclerosis of the aorta and large vessels, and thickened aortic valves with variable degree of calcification. Histology demonstrated a marked decrease in collagen trichrome stain and cell proliferation in the aortic valve leaflets in the paclitaxel-balloon group compared to the plain-balloon group as shown in Fig. 6.2, Panels a, b. Panel c on Fig. 6.2 demonstrates representative samples from the MicroCT analysis. The paclitaxel treated balloon substantially decreased the calcification response as compared to the uncoated balloon. This led to significantly smaller leaflet thickness in the paclitaxel-balloon compared

Table 6.1 Result summary

	Uncoated n = 14	Paclitaxel-coated n = 14	P value
Systolic BP Baseline (mm Hg)	75 ± 13	74 ± 10	0.81
Systolic BP Post-BAV (mm Hg)	86 ± 10	89 ± 10	0.97
Systolic BP Follow-up (mm Hg)	80 ± 13	93 ± 11	0.004
Pressure gradient[a] Baseline (mm Hg)	5.7 ± 4.6	7.0 ± 7.6	0.59
Pressure gradient[a] Post-BAV (mm Hg)	1.5 ± 2.5	1.5 ± 2.2	0.97
Pressure gradient[a] Follow-up (mm Hg)	7.7 ± 7.7	3.6 ± 17	0.08
Aortic valve area Baseline (cm^2)	0.63 ± 0.15	0.61 ± 0.23	0.42
Aortic valve area Post-BAV (cm^2)	0.62 ± 0.16	0.59 ± 0.18	0.57
Aortic valve area Follow-up (cm^2)	0.55 ± 0.22	0.91 ± 0.59	0.04
SWL Baseline (%)	6.9 ± 5.4	8.0 ± 8.0	0.66
SWL Post-BAV (%)	1.6 ± 2.4	1.6 ± 2.0	0.97
SWL Follow-up (%)	7.7 ± 7.7	3.45 ± 4.0	0.047
Aortic valve resistance Baseline (dynes/s/cm^5)	110 ± 37	130 ± 139	0.67
Aortic valve resistance Post-BAV(dynes/s/cm^5)	49 ± 64	49 ± 56	0.99
Aortic valve resistance Follow-up (dynes/s/cm^5)	177 ± 137	86 ± 71	0.039

BP blood pressure, *BAV* balloon aortic valvuloplasty, *SWL* stroke work loss
[a]Transvalvular pressure gradient measured invasively

to the plain-balloon group (0.60 ± 0.15 vs. 0.71 ± 0.17 mm, p = 0.03). A significant reduction in the mean PCNA stain grade in the paclitaxel-balloon group was observed (1.53 ± 0.04 vs. 2.24 ± 0.55, p = 0.049).

Summary

This chapter provides a novel approach to drug eluting balloon testing for aortic valve disease. An established experimental in vivo model of calcific aortic valve disease in rabbits to test the hypothesis that local drug delivery at the aortic valve tissues by means of a paclitaxel-eluting valvuloplasty balloon can modify the cellular events in aortic valve restenosis. The injury to the experimental atherosclerotic aortic valve caused by the balloon valvuloplasty initiates the process of restenosis that was directly and indirectly quantified and differences between the drug-eluting and plain balloon groups were measured. The results are all pointing towards the direction that restenosis was less evident in the valves dilated with the paclitaxel-eluting balloon. There was reduced extracellular matrix synthesis, cell proliferation and calcification in the paclitaxel-balloon treated leaflets that culminated in the following cellular and hemodynamic findings: (1) decreased leaflet thickness,

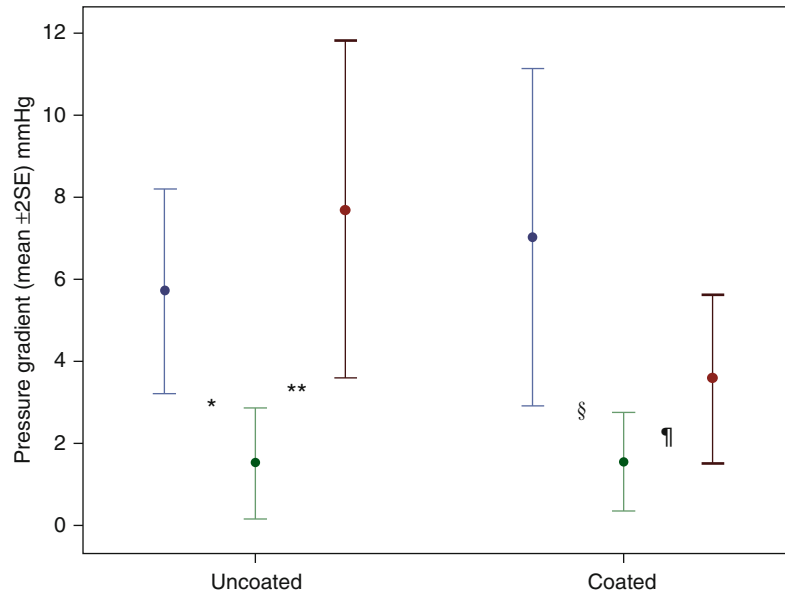

Fig. 6.1 Mean transvalvular pressure gradients. *Blue lines*: baseline, *green lines*: post-BAV, *brown lines*: follow-up. *0.01, **0.02, §0.004, 0.15

(2) larger AVA, (3) diminished SWL and (4) decreased aortic valve resistance. These observations suggest that local paclitaxel delivery attenuated the myofibroblast osteogenic differentiation driving the restenosis process and typically seen following BAV with a plain balloon [15, 23, 26–28, 30–33].

Paclitaxel is known to inhibit cell proliferation and cell activation in the dynamic process of aortic stenosis and restenosis such as macrophages, smooth muscle cells, fibroblasts, endothelial cells and T-lymphocytes [34–38]. Therefore, it is plausible that by its actions pacifies the cellular and molecular signaling processes that are accountable for restenosis as a response to the injury caused by valvuloplasty. The rabbits receiving the uncoated balloon developed accelerated calcification, and the rabbits receiving the paclitaxel balloon demonstrated a decrease in cell proliferation and also diminished calcification as measured by MicroCT. This effect is a direct attribute to the antiproliferative effects of the paclitaxel therapy.

The cellular mechanisms of aortic valve calcification and vascular calcification have been extensively studied over the past decade. The cellular mechanisms for this process have been identified as differentiation of the mesenchymal derived myofibroblast cell to an osteoblast like phenotype [23]. This process has been replicated in several studies in the field and continues to be the target for medical therapy to slow the progression of this disease process [31–33]. The inhibition of the differentiation process is a potential mechanism for the diminished cell proliferation and calcification in the aortic valves from the coated treatment. The study was designed to measure early markers of cellular markers in the rabbit model to determine if the delivery of the medication would have any effects on the valve tissue.

This chapter demonstrates that the use of a paclitaxel-eluting valvuloplasty balloon in an animal model of CAVD is associated with less evidence of restenosis as assessed by histology findings and echocardiographic and invasive aortic stenosis severity evaluations. Studies on prevention of restenosis with drug-eluting valvuloplasty balloons in high-risk patients with aortic stenosis not acceptable for surgical valve replacement or TAVR are justified to elucidate whether drug-eluting balloon valvuloplasty has future clinical value, especially in patients who are not candidates for surgery or TAVR due to co-morbidities, peripheral vascular disease and/or other significant illnesses.

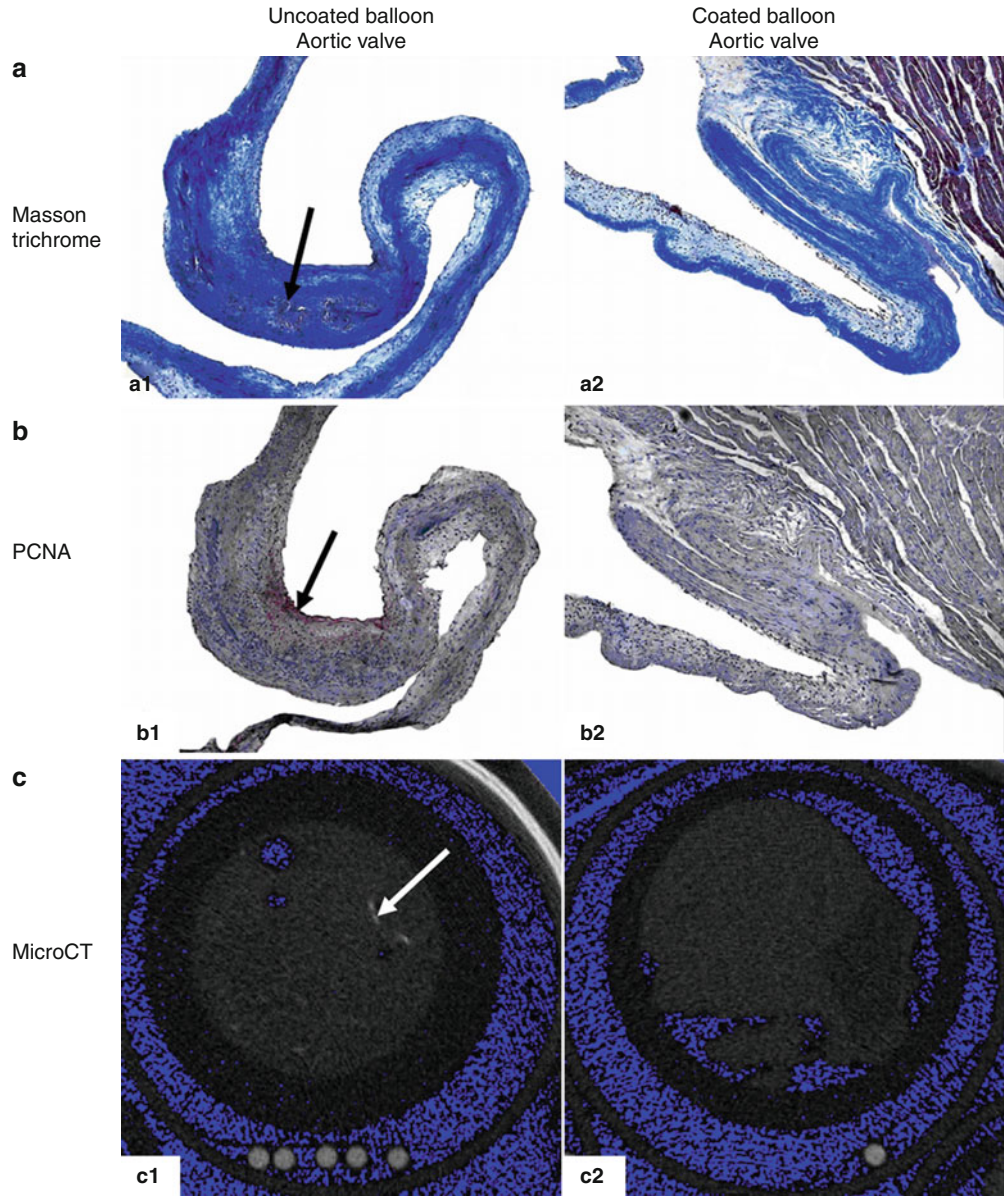

Fig. 6.2 Masson trichrome, proliferating cell nuclear antigen and MicroCT of the aortic valves from the coated versus uncoated balloon treatments. Panel (**a**) Masson trichrome stain, Panel (**b**) PCNA stain, Panel (**c**) MicroCT. *Arrows* point to areas of calcification in each figure

References

1. Cribier A, Savin T, Saoudi N, Rocha P, Berland J, Letac B. Percutaneous transluminal valvuloplasty of acquired aortic stenosis in elderly patients: an alternative to valve replacement. Lancet. 1986;11(1):63–7.
2. McKay RG, Safian RD, Lock JE, et al. Assessment of left ventricular and aortic valve function after aortic balloon valvuloplasty in adult patients with critical aortic stenosis. Circulation. 1987;75:192–203.
3. Harrison JK, Davidson CJ, Leithe ME, Kisslo KB, Skelton TN, Bashore TM. Serial left ventricular performance evaluated by cardiac catheterization before, immediately after and at 6 months after balloon aortic valvuloplasty. J Am Coll Cardiol. 1990;16:1351–8.
4. Dorros G, Lewin RF, Stertzer SH, et al. Percutaneous transluminal aortic valvuloplasty: the acute outcome

and follow-up of 149 patients who underwent the double balloon technique. Eur Heart J. 1990;11:429–40.
5. NHLBI Balloon Valvuloplasty Registry Participants. Percutaneous balloon aortic valvuloplasty. Acute and 30-day follow-up results from the NHLBI balloon valvuloplasty registry. Circulation. 1991;84:2383–97.
6. Otto CM, Mickel MC, Kennedy JW, et al. Three-year outcome after balloon aortic valvuloplasty: insights into prognosis of valvular aortic stenosis. Circulation. 1994;89:642–50.
7. Tuzcu EM. Clinical outcomes from "Standard Therapy" in the P AR TNER inoperable patients. In: Paper presented at: Transcatheter cardiovascular therapeutics 2010, Washington, DC, 24 Sept 2010.
8. Lieberman EB, Bashore TM, Hermiller JB, et al. Balloon aortic valvuloplasty in adults: failure of procedure to improve longterm survival. J Am Coll Cardiol. 1995;26:1522–8.
9. Hara H, Pedersen WR, Ladich E, et al. Percutaneous balloon aortic valvuloplasty revisited: time for a renaissance? Circulation. 2007;115:334–8.
10. Klein A, Lee K, Gera A, Ports TA, Michaels AD. Long-term mortality, cause of death, and temporal trends in complications after percutaneous aortic balloon valvuloplasty for calcific aortic stenosis. J Interv Cardiol. 2006;19:269–75.
11. Shareghi S, Rasouli L, Shavelle DM, Burstein S, Matthews RV. Current results of balloon aortic valvuloplasty in high-risk patients. J Invasive Cardiol. 2007;19:1–5.
12. Pedersen WR, Klaassen PJ, Boisjolie CR, et al. Feasibility of transcatheter intervention for severe aortic stenosis in patients 90 years of age: aortic valvuloplasty revisited. Catheter Cardiovasc Interv. 2007;70:149–54.
13. Descoutures F, Himbert D, Lepage L, et al. Contemporary surgical or percutaneous management of severe aortic stenosis in the elderly. Eur Heart J. 2008;29:1410–7.
14. Leon M. Lessons learned from the PARTNER experience in the United States. In: Paper presented at: Transcatheter valve therapies 2010, Seattle, 6–9 June 2010.
15. Rajamannan NM, Subramaniam M, Springett M, et al. Atorvastatin inhibits hypercholesterolemia-induced cellular proliferation and bone matrix production in the rabbit aortic valve. Circulation. 2002;105:2660–5.
16. Feldman T, Glagov S, Carroll JD. Restenosis following successful balloon valvuloplasty: bone formation in aortic valve leaflets. Cathet Cardiovasc Diagn. 1993;29:1–7.
17. Van Den Brand M, Essed CE, DiMario C, et al. Histological changes in the aortic valve after balloon dilatation: evidence for a delayed healing process. Br Heart J. 1992;67:445–9.
18. Waller BF, Dorros G, Lewin RF, King JF, McKay C, van Tassel JW. Catheter balloon valvuloplasty of stenotic aortic valves. Part II: Balloon valvuloplasty during life subsequent tissue examination. Clin Cardiol. 1991;14:924–30.
19. McKay RG, Safian RD, Lock JE, et al. Balloon dilatation of calcific aortic stenosis in elderly patients: postmortem, intraoperative, and percutaneous valvuloplasty studies. Circulation. 1986;74:119–25.
20. Moses JW, Leon MB, Popma JJ, SIRIUS Investigators, et al. Sirolimus-eluting stents versus standard stents in patients with stenosis in a native coronary artery. N Engl J Med. 2003;349:1315–23.
21. Stone GW, Ellis SG, Cox DA, TAXUS-IV Investigators, et al. A polymer-based, paclitaxel-eluting stent in patients with coronary artery disease. N Engl J Med. 2004;350:221–31.
22. Rajamannan NM, Subramaniam M, Caira F, Stock SR, Spelsberg TC. Atorvastatin inhibits hypercholesterolemia-induced calcification in the aortic valves via the Lrp5 receptor pathway. Circulation. 2005;112:I229–34.
23. Rajamannan NM, Subramaniam M, Rickard D, et al. Human aortic valve calcification is associated with an osteoblast phenotype. Circulation. 2003;107:2181–4.
24. Rajamannan NM, Subramaniam M, Stock SR, et al. Atorvastatin inhibits calcification and enhances nitric oxide synthase production in the hypercholesterolaemic aortic valve. Heart. 2005;91:806–10.
25. Spargias K, Milewski K, Debinski M, et al. Drug delivery at the aortic valve tissues of healthy domestic pigs with a paclitaxel-eluting valvuloplasty balloon. J Interv Cardiol. 2009;22:291–8.
26. Drolet MC, Arsenault M, Couet J. Experimental aortic valve stenosis in rabbits. J Am Coll Cardiol. 2003;41:1211–7.
27. Posa A, Hemetsberger R, Petnehazy O, et al. Attainment of local drug delivery with paclitaxel-eluting balloon in porcine coronary arteries. Coron Artery Dis. 2008;19:243–7.
28. Baumgartner H, Hung J, Bermejo J, EAE/ASE, et al. Echocardiographic assessment of valve stenosis: EAE/ASE recommendations for clinical practice. Eur J Echocardiogr. 2009;10:1–25.
29. Rajamannan NM, Nealis TB, Subramaniam M, et al. Calcified rheumatic valve neoangiogenesis is associated with vascular endothelial growth factor expression and osteoblast-like bone formation. Circulation. 2005;111:3296–301.
30. Rajamannan NM. Mechanisms of aortic valve calcification: the LDL-density-radius theory: a translation from cell signaling to physiology. Am J Physiol. 2010;298:H5–15.
31. Rajamannan NM, Edwards WD, Spelsberg TC. Hypercholesterolemic aortic-valve disease. N Engl J Med. 2003;349:717–8.
32. Rajamannan NM, Gersh B, Bonow RO. Calcific aortic stenosis: from bench to the bedside-emerging clinical and cellular concepts. Heart. 2003;89:801–5.
33. Rajamannan NM. Calcific aortic stenosis: lessons learned from experimental and clinical studies. Arterioscler Thromb Vasc Biol. 2009;29:162–8.

34. Ong AT, Serruys PW. Technology Insight: an overview of research in drug-eluting stents. Nat Clin Pract Cardiovasc Med. 2005;2:647–58.
35. Herdeg C, Oberhoff M, Baumbach A, et al. Local paclitaxel delivery for the prevention of restenosis: biological effects and efficacy in vivo. J Am Coll Cardiol. 2000;35:1969–76.
36. Sheikh SH, Mulchandani A. Continuous-flow fluoroimmunosensor for paclitaxel measurement. Biosens Bioelectron. 2001;16:647–52.
37. Axel DI, Kunert W, Goggelmann C, et al. Paclitaxel inhibits arterial smooth muscle cell proliferation and migration in vitro and in vivo using local drug delivery. Circulation. 1997;96:636–45.
38. Mullins DW, Koci MD, Burger CJ, Elgert KD. Interleukin-12 overcomes paclitaxel- mediated suppression of T -cell proliferation. Immunopharmacol Immunotoxicol. 1998;20:473–92.

Ex Vivo Model for Bioprosthetic Valve Calcification via Stem Cell Differentiation to Bone

7

Nalini M. Rajamannan

Introduction

Calcific aortic stenosis is the most common indication for surgical valve replacement in the United States and Europe [1]. Currently, mechanical versus bioprosthetic heart valves are the two options for valve replacement. The choice of valve depends on patient characteristics at the time of surgery [2]. Bioprosthetic heart valves have decreased risk of thrombosis, therefore decreasing the need for anticoagulation. It is estimated that 20–30 % of implanted bioprosthetic heart valves will have some degree of hemodynamic dysfunction at 10 years. For years, the mechanisms of valve degeneration were thought to be due to a passive process in which calcium sticks to the valve directly from the circulation. However, recent studies have demonstrated risk factors for bioprosthetic valve calcification that are similar to vascular atherosclerosis [3, 4]. Furthermore, recent pathologic studies [5] have clearly shown that an inflammatory reaction develops in these calcifying bioprosthesis, which includes lipid deposits, inflammatory cell infiltration, and bone matrix proteins expression.

This chapter demonstrates the cellular mechanisms that are responsible for bioprosthetic valve calcification that involve stem cells, which migrate to the bioprosthesis and initiate mesenchymal differentiation via upregulation of Cbfa1 [6, 7]. Human valves explanted from patients versus control bioprosthetic valves prior to implantation were evaluated for calcification and the prescience of mesenchymal cKit positive stem cells.

Calcified Bioprosthetic Explanted Aortic Valves from Humans and Control Non-Explanted Bioprosthetic Valves

Tissues were collected at the time of surgery. For controls, bioprosthetic bovine pericardial valves were tested. They were never implanted. Immunostaining of the bioprosthetic valves from the human study was performed to identify PCNA (proliferating cell nuclear antigen), osteopontin, and cKit marker to confirm cellular proliferation, bone matrix protein expression and mesenchymal stem cell marker. Figure 7.1, Panels a1, a2, demonstrates a control bioprosthetic pericardial valve prior to implantation in a patient or the subcutaneous experimental model. This photo was taken of the valve from the manufacturer prior to implant. Panel a1 is the ventricular surface, and Panel a2 is the aortic surface. Figure 7.1, Panel b, demonstrates the explanted bovine pericardial valve from a patient. Panel b1 is the ventricular surface, and Panel b2 is the aortic surface. Calcified lesions develop along both surfaces of the pericardial tissue valve. This is different from native calcific

N.M. Rajamannan, MD
Division of Biochemistry and Molecular Biology,
Mayo Clinic, 200 First St SW,
Rochester, MN 55905, USA
e-mail: rajamannan.nalini@mayo.edu

N.M. Rajamannan (ed.), *Molecular Biology of Valvular Heart Disease*,
DOI 10.1007/978-1-4471-6350-3_7, © Springer-Verlag London 2014

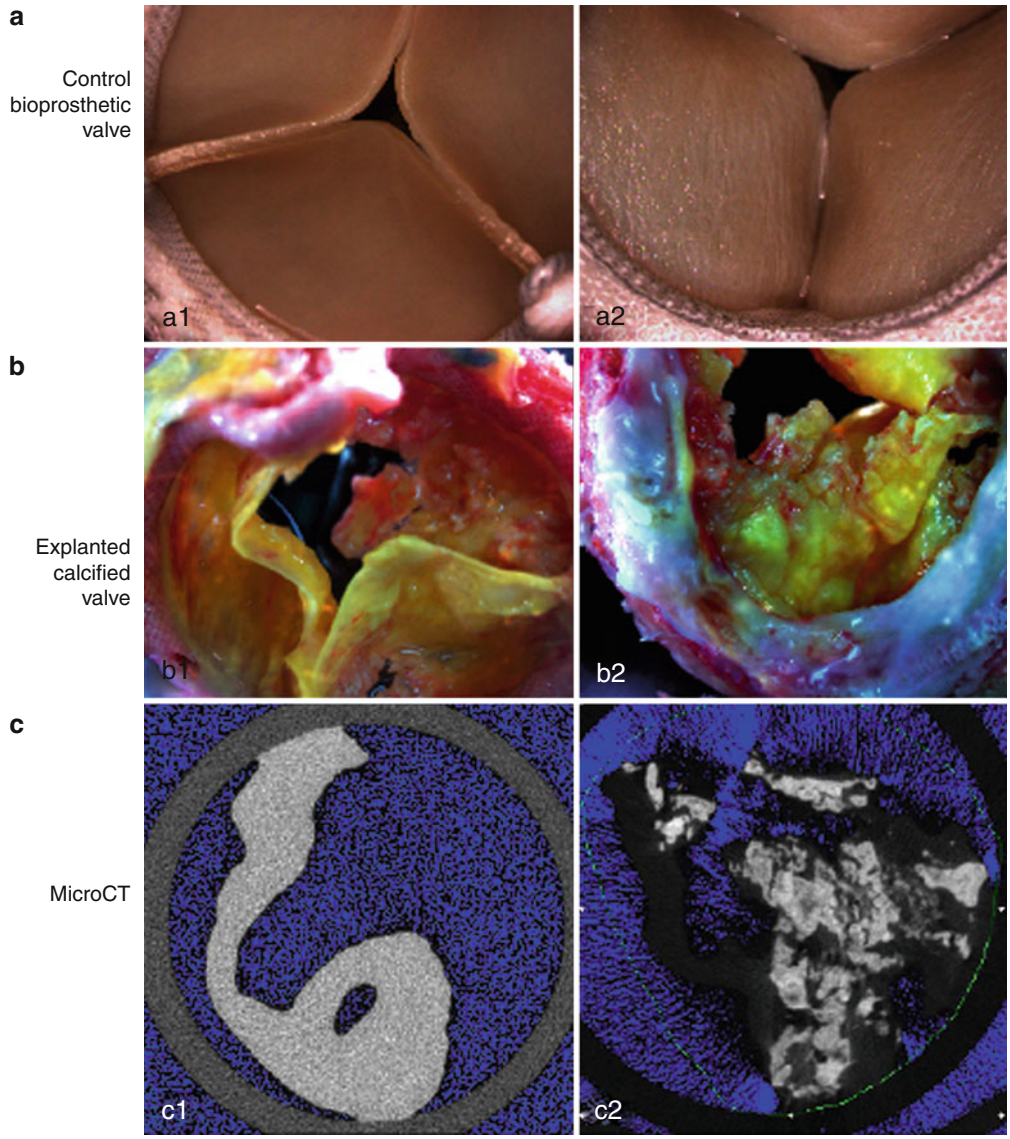

Fig. 7.1 Control bioprosthetic valve versus explanted bioprosthetic valve from humans. Panel (**a**) Control bioprosthetic valve. *a1* Ventricular surface, *a2* Aortic surface. Panel (**b**) Explanted calcified valve. *b1* Ventricular surface, *b2* Aortic surface. Panel (**c**) MicroCT of valves. *c1* Control valve, *c2*. Calcified explanted valve

aortic valve disease, in which the lesion only develops along the aortic surface of the valve leaflet [6, 8]. Figure 7.1, Panels c1, c2, demonstrates mineralized tissue by MicroCT in the control versus explanted pericardial valve leaflets. The explanted valve develops a large burden of calcification as indicated in the white areas of mineralization. The gray area is the non-mineralized tissue. The blue area is the background.

Immunostaining and RTPCR for the Explanted Bioprosthetic Valves from Humans

Figure 7.2 demonstrates the histology from the explanted valves from the patients. Figure 7.2, Panels a1, a2, is the Masson Trichrome stain from the control valve versus the explanted bioprosthetic valve, demonstrating an atherosclerotic

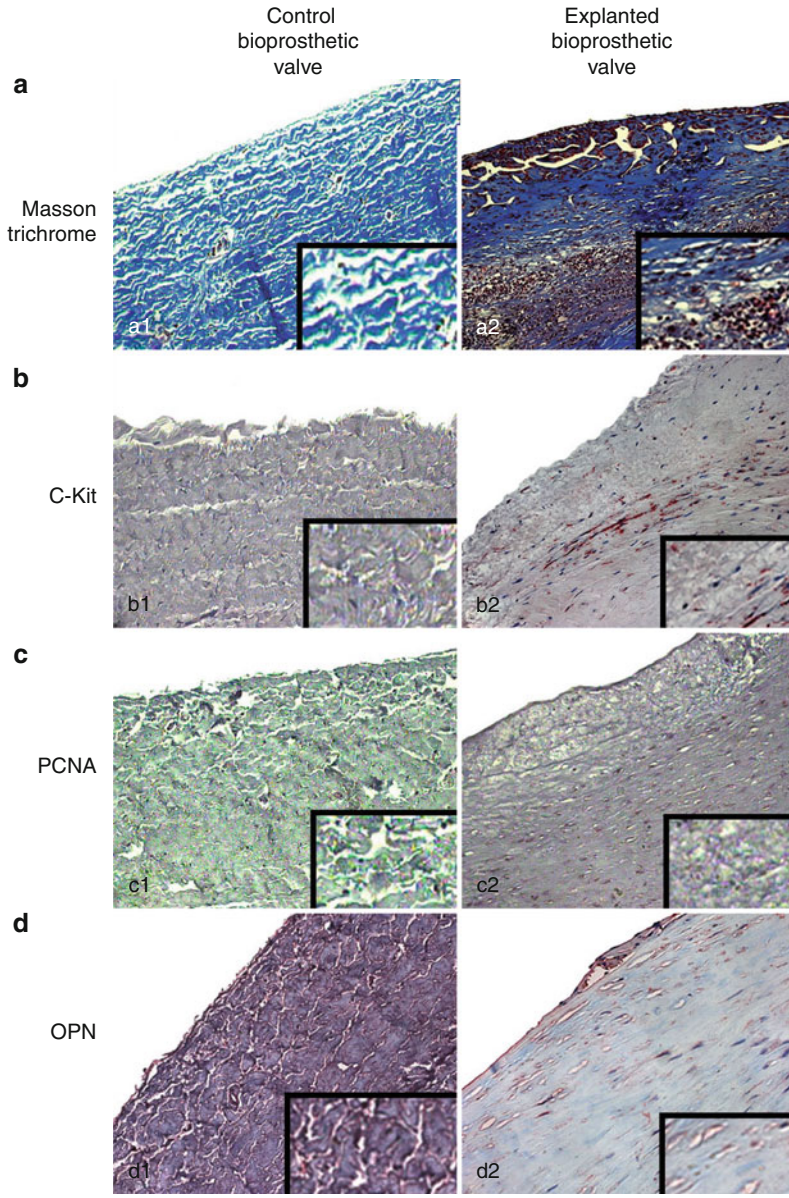

Fig. 7.2 Light microscopy of the control versus explanted bioprosthetic valves from humans. (All frames 20× magnification, with a 100× magnification in the right hand lower corner). Panel (**a**) Masson trichrome stain. Panel (**b**) cKit stain. Panel (**c**) Proliferating cell nuclear antigen stain. Panel (**d**) Osteopontin stain

type lesion along the surface of the explanted valve. Figure 7.2, Panels b1, b2, is the cKit immunohistochemistry for the control versus the explanted valve, which demonstrates cKit stain in the diseased valves. Figure 7.2, Panels c1, c2, is the PCNA stain, which demonstrates proliferating cells in the areas of PCNA positive stains. Finally, Fig. 7.2, Panels d1, d2, is the osteopontin stain, which is expressed in a low level in the control valve and is increased significantly in the diseased valve. Figure 7.3 demonstrates the gene expression for the control versus the explanted valves. As expected, there is no evidence of RNA present in the control pericardial valves that have not been implanted. The diseased valves demonstrate an increase in GAPDH(1139.71 ± 550.07), cKit(1639.25 ± 2226.07), Cbfa1(7030.19 ± 9179.96), and osteopontin(1549.01 ± 467.45) gene expression ($p < 0.001$). Figure 7.4 demonstrates the normal prosthetic valve implanted in the aortic position in the diagram of the heart.

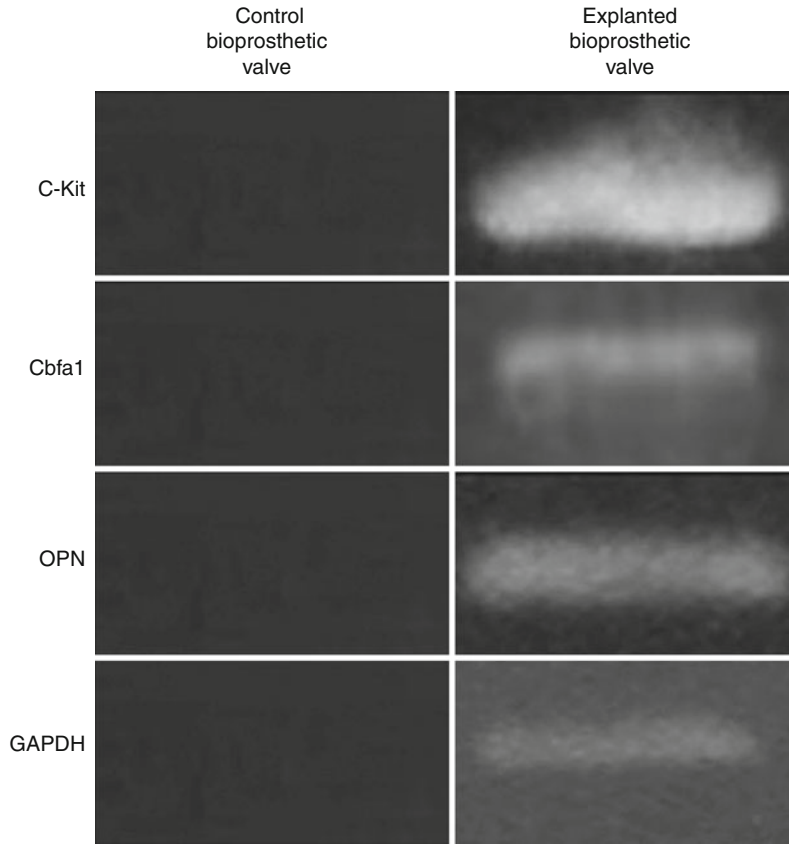

Fig. 7.3 Semi-quantitative RT-PCR in the control versus explanted bioprosthetic valves from humans. RT-PCR using the total RNA from the bioprosthetic valves for cKit (731 bp), Cbfa-1 (289 bp), Osteopontin (OP) (102 bp), and GAPDH (451 bp)

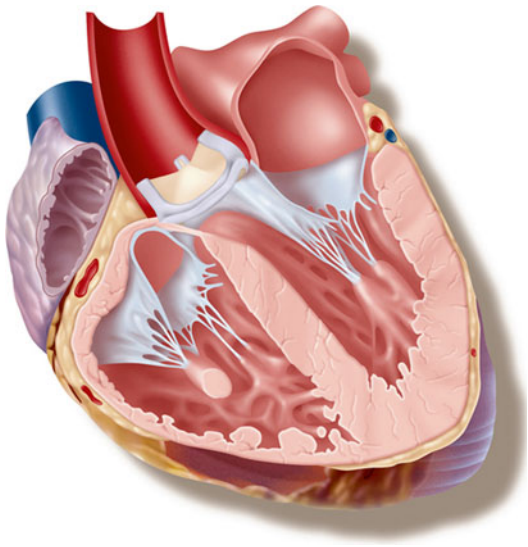

Fig. 7.4 Bioprosthetic valves implanted in the aortic position

Summary

The mechanism of bioprosthetic valve disease occurs secondary to cKit mesenchymal expression, and increase in Cbfa1 expression in human bioprosthetic porcine valves. It shows that cKit positive stem cells can migrate to implanted valves and induce Cbfa1 expression. Tanaka et al., [9] have demonstrated in native aortic valves in hypercholesterolemia mice that 10 % of cells are bone marrow derived cells which migrate to an atherosclerotic valve lesion. This model provides a foundation for the mechanism of a stem cell migrating to implanted bioprosthetic valves which can then differentiate to a bone forming cell, which is similar to that seen in native valve calcification [6, 7, 10].

Recent epidemiological studies have revealed that the risk factors for bioprosthetic valve

calcification, namely male gender, smoking, and elevated serum cholesterol, are similar to the risk factors associated with vascular atherosclerosis [5, 11–14]. The atherosclerotic calcified lesion in the bioprosthetic valves explanted from patients expressed the mesenchymal transcription factor that is characteristic of osteoblast differentiation (Cbfa1) and osteopontin in association with the mineralized tissue as demonstrated by MicroCT. Sox9 is a critical transcription factor in the early stage of mesenchymal cartilage differentiation in the osteogenic gene program. Cbfa-1 has all the attributes of a 'master gene' differentiation factor for the osteoblast lineage. During embryonic development, Cbfa-1 expression precedes osteoblast differentiation and is restricted to mesenchymal cells destined to become osteoblasts [15, 16]. In addition to its critical role in osteoblast commitment and differentiation, Cbfa-1 appears to control the rate of bone formation by differentiated osteoblasts [15]. Chapter 2 from this book demonstrates that the mechanism for calcific aortic stenosis present is a transformation of the aortic valve myofibroblasts to osteoblast-like cells or an invasion of osteoblast precursors [9], and this osteoblast phenotype may play a critical role in the subsequent process of valvular calcification similar to that of vascular calcification [17–19]. In conclusion, this chapter demonstrates human explanted bioprosthetic valves express cKit positive cells and have the potential to upregulate Cbfa1 and osteopontin which may be a critical in the mechanism of the progression of bioprosthetic valve calcification. These changes coincide with the changes found in the ex vivo explanted valves from humans as compared to control valves that have never been implanted.

References

1. Roberts WC, Ko JM. Frequency by decades of unicuspid, bicuspid, and tricuspid aortic valves in adults having isolated aortic valve replacement for aortic stenosis, with or without associated aortic regurgitation. Circulation. 2005;111:920–5.
2. Bonow RO, Carabello BA, Kanu C, de Leon Jr AC, Faxon DP, Freed MD, Gaasch WH, Lytle BW, Nishimura RA, O'Gara PT, O'Rourke RA, Otto CM, Shah PM, Shanewise JS, Smith Jr SC, Jacobs AK, Adams CD, Anderson JL, Antman EM, Fuster V, Halperin JL, Hiratzka LF, Hunt SA, Nishimura R, Page RL, Riegel B. ACC/AHA 2006 guidelines for the management of patients with valvular heart disease: a report of the American College of Cardiology/American Heart Association Task Force on Practice Guidelines (writing committee to revise the 1998 Guidelines for the Management of Patients With Valvular Heart Disease): developed in collaboration with the Society of Cardiovascular Anesthesiologists: endorsed by the Society for Cardiovascular Angiography and Interventions and the Society of Thoracic Surgeons. Circulation. 2006;114:e84–231.
3. Antonini-Canterin F, Zuppiroli A, Popescu BA, Granata G, Cervesato E, Piazza R, Pavan D, Nicolosi GL. Effect of statins on the progression of bioprosthetic aortic valve degeneration. Am J Cardiol. 2003;92(12):1479–82.
4. Briand M, Lemieux I, Dumesnil JG, Mathieu P, Cartier A, Despres JP, Arsenault M, Couet J, Pibarot P. Metabolic syndrome negatively influences disease progression and prognosis in aortic stenosis. J Am Coll Cardiol. 2006;47:2229–36.
5. Shetty R, Pepin A, Charest A, Perron J, Doyle D, Voisine P, Dagenais F, Pibarot P, Mathieu P. Expression of bone-regulatory proteins in human valve allografts. Heart. 2006;92:1303–8.
6. Rajamannan NM, Subramaniam M, Rickard D, Stock SR, Donovan J, Springett M, Orszulak T, Fullerton DA, Tajik AJ, Bonow RO, Spelsberg T. Human aortic valve calcification is associated with an osteoblast phenotype. Circulation. 2003;107:2181–4 [see comment].
7. Caira FC, Stock SR, Gleason TG, McGee EC, Huang J, Bonow RO, Spelsberg TC, McCarthy PM, Rahimtoola SH, Rajamannan NM. Human degenerative valve disease is associated with up-regulation of low-density lipoprotein receptor-related protein 5 receptor-mediated bone formation. J Am Coll Cardiol. 2006;47:1707–12.
8. O'Brien KD, Reichenbach DD, Marcovina SM, Kuusisto J, Alpers CE, Otto CM. Apolipoproteins b, (a), and e accumulate in the morphologically early lesion of 'degenerative' valvular aortic stenosis. Arterioscler Thromb Vasc Biol. 1996;16:523–32.
9. Tanaka K, Sata M, Fukuda D, Suematsu Y, Motomura N, Takamoto S, Hirata Y, Nagai R. Age-associated aortic stenosis in apolipoprotein e-deficient mice. J Am Coll Cardiol. 2005;46:134–41.
10. Rajamannan NM, Subramaniam M, Caira F, Stock SR, Spelsberg TC. Atorvastatin inhibits hypercholesterolemia-induced calcification in the aortic valves via the lrp5 receptor pathway. Circulation. 2005;112:I229–34.
11. Wilhelmi MH, Bara C, Kofidis T, Wilhelmi M, Pichlmaier M, Haverich A. Long-term cardiac allograft valves after heart transplant are functionally

and structurally preserved, in contrast to homografts and bioprostheses. J Heart Valve Dis. 2006;15:777–82.
12. Wilhelmi MH, Mertsching H, Wilhelmi M, Leyh R, Haverich A. Role of inflammation in allogeneic and xenogeneic heart valve degeneration: immunohistochemical evaluation of inflammatory endothelial cell activation. J Heart Valve Dis. 2003;12:520–6.
13. Skowasch D, Steinmetz M, Nickenig G, Bauriedel G. Is the degeneration of aortic valve bioprostheses similar to that of native aortic valves? Insights into valvular pathology. Expert Rev Med Devices. 2006;3:453–62.
14. Bottio T, Thiene G, Pettenazzo E, Ius P, Bortolotti U, Rizzoli G, Valfre C, Casarotto D, Valente M. Hancock ii bioprosthesis: a glance at the microscope in mid-long-term explants. J Thorac Cardiovasc Surg. 2003;126:99–105.
15. Ducy P, Zhang R, Geoffroy V, Ridall AL, Karsenty G. Osf2/cbfa1: A transcriptional activator of osteoblast differentiation. Cell. 1997;89:747–54 [see comment].
16. Deng ZL, Sharff KA, Tang N, Song WX, Luo J, Luo X, Chen J, Bennett E, Reid R, Manning D, Xue A, Montag AG, Luu HH, Haydon RC, He TC. Regulation of osteogenic differentiation during skeletal development. Front Biosci. 2008;13:2001–21.
17. Tintut Y, Alfonso Z, Saini T, Radcliff K, Watson K, Bostrom K, Demer LL. Multilineage potential of cells from the artery wall. Circulation. 2003;108:2505–10.
18. Kirton JP, Crofts NJ, George SJ, Brennan K, Canfield AE. Wnt/beta-catenin signaling stimulates chondrogenic and inhibits adipogenic differentiation of pericytes: potential relevance to vascular disease? Circ Res. 2007;101:581–9.
19. Shao JS, Cheng SL, Pingsterhaus JM, Charlton-Kachigian N, Loewy AP, Towler DA. Msx2 promotes cardiovascular calcification by activating paracrine wnt signals. J Clin Invest. 2005;115:1210–20.

8 Experimental Hypercholesterolemia in Genetic ApoE$^{-/-}$/Lrp5$^{-/-}$ Mice: Proof of Principle

Nalini M. Rajamannan

Introduction

The low-density protein-related receptor 5 and 6 (Lrp5 and Lrp6) genes were cloned in 1998 based on their homology with the low-density lipoprotein receptor (LDLR) [1–4]. Mutations in either LRP5 or LRP6, proteins have caused a number of disease processed in the field of bone [5, 6], and have been associated with cardiovascular disease [4, 7–9]. There are several experimental models and clinical studies which demonstrate that cholesterol induces calcification in the aortic valves [10–13].

The LDL-Density-Pressure theory [14] combines the structure, function analysis of these co-receptors with the results from the genetic studies to provide a unique hypothesis for the role of these receptors in the heart. This chapter provides the genetic mouse evidence to demonstrate that in the presence of experimental hypercholesterolemia, Lrp5/6 receptors, Runx2 genes are up-regulated in the presence of cholesterol and mediate calcification by MicroCT analysis. ApoE$^{-/-}$/Lrp5$^{-/-}$ experimental hypercholesterolemia mouse model, provides the foundation for the proof of principle for the role of Lrp5 in valve calcification.

N.M. Rajamannan, MD
Division of Biochemistry and Molecular Biology,
Mayo Clinic, 200 First St SW,
Rochester, MN 55905, USA
e-mail: rajamannan.nalini@mayo.edu

Histology and MicroCT

The proof of principle for the hypothesis tests if Lrp5$^{-/-}$/ApoE$^{-/-}$:Lrp5$^{-/-}$/ApoE$^{-/-}$, mice develops atherosclerosis in the cholesterol valve inducing calcification via an increase in Lrp5/6 receptors. Figure 8.1, demonstrates the characterization of the aortic valve phenotype as defined by histology and MicroCT. In Figure 8.1, Panels a1, a2, b1, and b2 is the histology and MicroCT scan for the ApoE$^{-/-}$ aortic valve in the control and cholesterol demonstrating atherosclerosis and calcification in the cholesterol treated valves and no evidence of atherosclerosis and calcification in the controls. Figure 8.1, Panels c1, c2, d1, and d2 demonstrates that there is no atherosclerosis or calcification in the Lrp5$^{-/-}$ mice by MicroCT (Data not shown) MicroCT synchrotron scan. Figure 8.1, Panels e1, e2, f1, and f2 is the ApoE$^{-/-}$:Lrp5$^{-/-}$ histology and MicroCT for the aortic valves from these mice demonstrating a mild increase in calcification in the cholesterol treated valves but to a lesser degree than the ApoE$^{-/-}$ cholesterol treated valves in Figure. 8.1 Panel a2. Table 8.1, demonstrates the echocardiography, serum cholesterol and the gene expression for the valves. Table 8.1 includes the quantification of the gene expression for the ApoE$^{-/-}$ valves and the ApoE$^{-/-}$:Lrp5$^{-/-}$ valves the Lrp5$^{-/-}$ for Lrp5, Lrp6 and Runx2. The echocardiography demonstrated mild but not statistically significant increases in flow across the cholesterol treated valves. The MicroCT demonstrates calcification in the ApoE$^{-/-}$ to a greater extent than the ApoE$^{-/-}$:Lrp5$^{-/-}$.

N.M. Rajamannan (ed.), *Molecular Biology of Valvular Heart Disease*,
DOI 10.1007/978-1-4471-6350-3_8,

Discussion

The low density lipoprotein co-receptor Lrp5/6 is a member of the family of structurally closely related cell surface low density lipoprotein receptors that have diverse biological functions in different organs, tissues and cell types which are important in development and disease mechanisms. The most prominent role in this evolutionary ancient family is cholesterol homeostasis. The LRP5 pathway regulates bone formation in different diseases of bone [5, 15]. The discovery of the LRP5 receptor in the gain of function [15] and loss of function [5] mutations in the development of bone diseases, resulted in a number of studies which have shown that activation

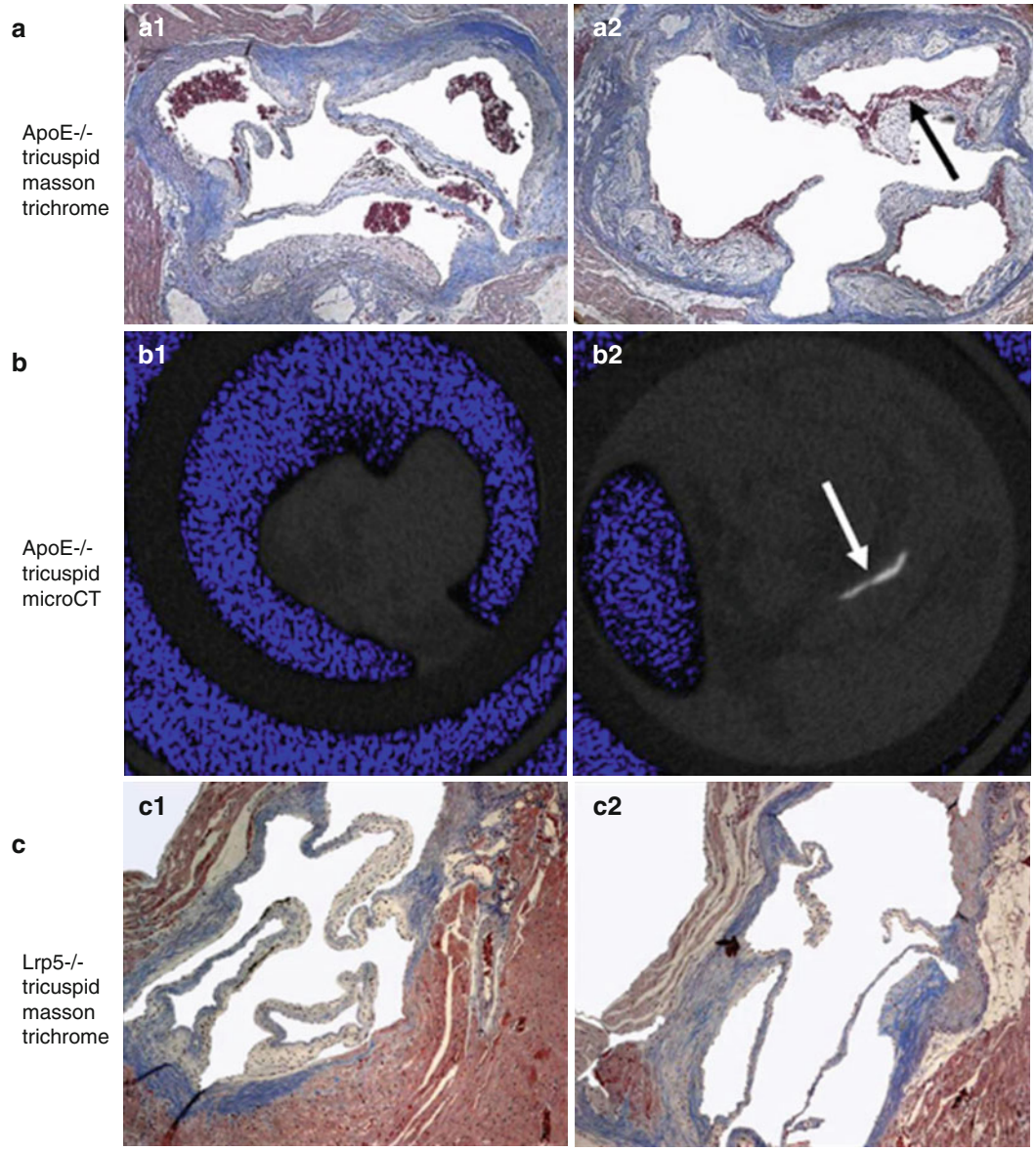

Fig. 8.1 Experimental hypercholesterolemia genetic mouse model: control versus cholesterol diet. Panel (**a**, **b**) $ApoE^{-/-}$ (**a**) Masson trichrome (**b**) MicroCT. Panel (**c**, **d**) $Lrp5^{-/-}$ (**c**) Masson trichrome (**d**) Synchrotron MicroCT. Panel (**e**, **f**): $ApoE^{-/-}$:$Lrp5^{-/-}$ (**e**) Masson trichrome (**f**) MicroCT. *Arrows* point to areas of calcification

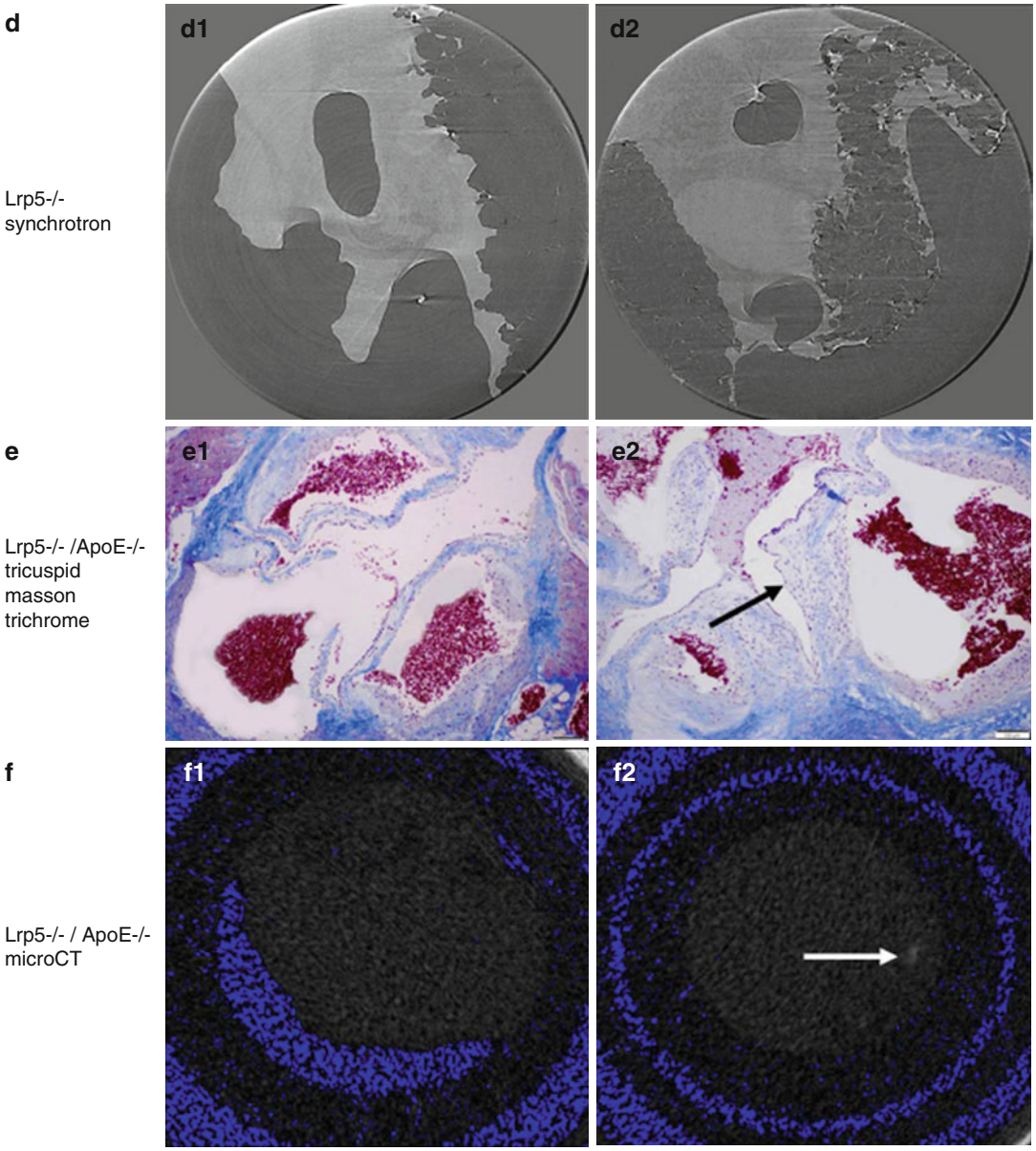

Fig. 8.1 (continued)

of the canonical Wnt pathway is important in osteoblastogenesis [7, 16–18]. Three studies to date have confirmed the regulation of the LRP5/Wnt pathway for cardiovascular calcification in vivo and ex vivo [8, 9, 19]. Lrp5 has been shown to have an effect on bone mass via the mechanostat effect on regulating bone formation. The findings in the human of the high bone mass gain of function mutation [6], led to a series of discoveries that Lrp5 regulates bone mass via the mechanical force effect on the receptor [20–22], Lrp6 also regulates bone but has been found to have a low bone mass effect in patients in which a putative partial loss-of-function mutation in LRP6 was identified to early cardiovascular-related death associated with increased plasma LDL, triglycerides, hypertension, diabetes and osteoporosis [23]. This chapter summarizes the

Table 8.1 Quantification of the echocardiography, serum cholesterol levels and the gene expression for Lrp5, Lrp6 and Runx2 in the ApoE$^{-/-}$ valves and ApoE$^{-/-}$:Lrp5$^{-/-}$ valves: Lrp5 and Runx2 is upregulated in the ApoE$^{-/-}$ valves, Lrp6 and Runx2 is upregulated in the ApoE$^{-/-}$:Lrp5$^{-/-}$ valves, no Runx 2 or Lrp6 was present in the Lrp5$^{-/-}$ valves

	Control	Cholesterol
ApoE$^{-/-}$		
A. Echocardiographic		
Peak jet velocity	1.6 ± 0.1	1.7 ± 0.2
Ejection fraction (%)	59 ± 7	55 ± 8*
B. Cholesterol serum level	540 ± 63.9	1,761 ± 510.4*
C. Gene expression		
Lrp5	0.34	2.38*
Runx2	0.05	0.86*
Lrp6	–	–
Lrp5$^{-/-}$		
A. Echocardiographic		
Peak jet velocity	1.5 ± 0.082	1.6 ± 0.141
Ejection fraction (%)	56 ± 8.29	49.0 ± 4.08*
B. Cholesterol	90.5 ± 28.8	304.7 ± 78.4*
C. Gene expression		
Lrp5	0.11	0.14
Runx2	0.43	0.90*
Lrp6	1.10	1.75*
ApoE$^{-/-}$ Lrp5$^{-/-}$		
A. Echocardiographic		
Peak jet velocity	1.8 ± 0.32	2.0 ± 0.40
Ejection fraction (%)	50.1 ± 9.57	42.5 ± 1.24*
B. Cholesterol	694.5 ± 70.9	1,063.6 ± 620.0
C. Gene expression		
Lrp5	–	–
Runx2	0.80	1.36*
Lrp6	0.97	1.13

– not performed
*$p < 0.05$ Cholesterol compared to control

role of genetic mice to demonstrate that experimental cholesterol diets can upregulate Lrp5 and Lrp6 with varying degrees of calcification. The ApoE$^{-/-}$ demonstrated marked increase in the calcification, which is consistent with the lipid and pressure effect of Lrp5 on the aortic valves. The Lrp5$^{-/-}$ had no calcification in the valves. The Lrp5$^{-/-}$ single gene KO demonstrates the role of Lrp5 for calcification and the ApoE$^{-/-}$ single gene knockout to demonstrate the role cholesterol to activate the Lrp5/6 receptors. The double knockout mice ApoE$^{-/-}$:Lrp5$^{-/-}$ were tested to show that in the elevated lipids secondary to the lack of the ApoE receptor as compared to the Lrp5$^{-/-}$ mice caused some mild calcification via the upregulation of the Lrp6 gene expression in the mice.

The right-sided valves in all of the specific mice did not develop any calcification, which further demonstrates the role of the higher pressures in the left side of the heart to activate the Lrp5/6 receptor in the valve. LRP5 binds apoE-containing lipoproteins in vitro, and is widely expressed in many tissues including hepatocytes, adrenal gland and pancreas [4]. The production of mice lacking LRP5 revealed that LRP5 deficiency led to increased plasma cholesterol levels in mice fed a high-fat diet, secondary to decreased hepatic clearance of chylomicron remnants and also marked impaired glucose tolerance [7]. In the LRP5 mice that were not fed the high cholesterol diet, the mice did not develop high cholesterol levels [24]. The investigators went on to define the role of LRP5 in the lipoprotein metabolism by developing a double knockout mouse for ApoE:LRP5. They found that the double KO mouse had approx 60 % higher cholesterol levels

compared with the age matched apoE knockout mice. High performance liquid chromatography analysis of plasma lipoproteins revealed that no difference in the apoproteins, but the cholesterol levels in the very low density and low density lipoprotein fractions, were markedly increased in the apoE:Lrp5 double KO mice. There was threefold increase in the atherosclerosis indicating that the Lrp5 mediates both apoE-dependent and apoE-independent catabolism of lipoproteins. In this current study, the serum cholesterol levels demonstrated a marked increase in the cholesterol in both of the ApoE$^{-/-}$ and the ApoE:Lrp5 double KO mice further confirming the association of elevated cholesterol and the mineralization process. In 1994, studies demonstrated that the plasma cholesterol levels in the double KO mice lacking both ApoE and LDLR, were not significantly different from the levels in the ApoE knockout mice [25]. This chapter sets the foundation to confirm the hypothesis published in the LDL-Density-Pressure theory [10] to indicate a biologic-hemodynamic foundation for the mechanism of Lrp5/6 activation in the heart.

References

1. Dong Y, Lathrop W, Weaver D, Qiu Q, Cini J, Bertolini D, Chen D. Molecular cloning and characterization of lr3, a novel ldl receptor family protein with mitogenic activity. Biochem Biophys Res Commun. 1998;251:784–90.
2. Brown SD, Twells RC, Hey PJ, Cox RD, Levy ER, Soderman AR, Metzker ML, Caskey CT, Todd JA, Hess JF. Isolation and characterization of lrp6, a novel member of the low density lipoprotein receptor gene family. Biochem Biophys Res Commun. 1998;248:879–88.
3. Hey PJ, Twells RC, Phillips MS, Yusuke N, Brown SD, Kawaguchi Y, Cox R, Guochun X, Dugan V, Hammond H, Metzker ML, Todd JA, Hess JF. Cloning of a novel member of the low-density lipoprotein receptor family. Gene. 1998;216:103–11.
4. Kim DH, Inagaki Y, Suzuki T, Ioka RX, Yoshioka SZ, Magoori K, Kang MJ, Cho Y, Nakano AZ, Liu Q, Fujino T, Suzuki H, Sasano H, Yamamoto TT. A new low density lipoprotein receptor related protein, lrp5, is expressed in hepatocytes and adrenal cortex, and recognizes apolipoprotein e. J Biochem. 1998;124:1072–6.
5. Gong Y, Slee RB, Fukai N, Rawadi G, Roman-Roman S, Reginato AM, Wang H, Cundy T, Glorieux FH, Lev D, Zacharin M, Oexle K, Marcelino J, Suwairi W, Heeger S, Sabatakos G, Apte S, Adkins WN, Allgrove J, Arslan-Kirchner M, Batch JA, Beighton P, Black GC, Boles RG, Boon LM, Borrone C, Brunner HG, Carle GF, Dallapiccola B, De Paepe A, Floege B, Halfhide ML, Hall B, Hennekam RC, Hirose T, Jans A, Juppner H, Kim CA, Keppler-Noreuil K, Kohlschuetter A, LaCombe D, Lambert M, Lemyre E, Letteboer T, Peltonen L, Ramesar RS, Romanengo M, Somer H, Steichen-Gersdorf E, Steinmann B, Sullivan B, Superti-Furga A, Swoboda W, van den Boogaard MJ, Van Hul W, Vikkula M, Votruba M, Zabel B, Garcia T, Baron R, Olsen BR, Warman ML, Osteoporosis-Pseudoglioma Syndrome Collaborative G. Ldl receptor-related protein 5 (lrp5) affects bone accrual and eye development. Cell. 2001;107:513–23.
6. Little RD, Carulli JP, Del Mastro RG, Dupuis J, Osborne M, Folz C, Manning SP, Swain PM, Zhao SC, Eustace B, Lappe MM, Spitzer L, Zweier S, Braunschweiger K, Benchekroun Y, Hu X, Adair R, Chee L, FitzGerald MG, Tulig C, Caruso A, Tzellas N, Bawa A, Franklin B, McGuire S, Nogues X, Gong G, Allen KM, Anisowicz A, Morales AJ, Lomedico PT, Recker SM, Van Eerdewegh P, Recker RR, Johnson ML. A mutation in the ldl receptor-related protein 5 gene results in the autosomal dominant high-bone-mass trait. Am J Hum Genet. 2002;70:11–9.
7. Fujino T, Asaba H, Kang MJ, Ikeda Y, Sone H, Takada S, Kim DH, Ioka RX, Ono M, Tomoyori H, Okubo M, Murase T, Kamataki A, Yamamoto J, Magoori K, Takahashi S, Miyamoto Y, Oishi H, Nose M, Okazaki M, Usui S, Imaizumi K, Yanagisawa M, Sakai J, Yamamoto TT. Low-density lipoprotein receptor-related protein 5 (lrp5) is essential for normal cholesterol metabolism and glucose-induced insulin secretion. Proc Natl Acad Sci U S A. 2003;100:229–34.
8. Rajamannan NM, Subramaniam M, Caira F, Stock SR, Spelsberg TC. Atorvastatin inhibits hypercholesterolemia-induced calcification in the aortic valves via the lrp5 receptor pathway. Circulation. 2005;112:I229–34.
9. Caira FC, Stock SR, Gleason TG, McGee EC, Huang J, Bonow RO, Spelsberg TC, McCarthy PM, Rahimtoola SH, Rajamannan NM. Human degenerative valve disease is associated with up-regulation of low-density lipoprotein receptor-related protein 5 receptor-mediated bone formation. J Am Coll Cardiol. 2006;47:1707–12.
10. Rajamannan NM, Subramaniam M, Springett M, Sebo TC, Niekrasz M, McConnell JP, Singh RJ, Stone NJ, Bonow RO, Spelsberg TC. Atorvastatin inhibits hypercholesterolemia-induced cellular proliferation and bone matrix production in the rabbit aortic valve. Circulation. 2002;105:2260–5.
11. Rajamannan NM, Subramaniam M, Stock SR, Stone NJ, Springett M, Ignatiev KI, McConnell JP, Singh RJ, Bonow RO, Spelsberg TC. Atorvastatin inhibits calcification and enhances nitric oxide synthase production in the hypercholesterolaemic aortic valve. Heart. 2005;91:806–10.

12. Adler Y, Fink N, Spector D, Wiser I, Sagie A. Mitral annulus calcification–a window to diffuse atherosclerosis of the vascular system. Atherosclerosis. 2001;155:1–8.
13. Rajamannan NM, Subramaniam M, Rickard D, Stock SR, Donovan J, Springett M, Orszulak T, Fullerton DA, Tajik AJ, Bonow RO, Spelsberg T. Human aortic valve calcification is associated with an osteoblast phenotype. Circulation. 2003;107:2181–4.
14. Rajamannan NM. The role of lrp5/6 in cardiac valve disease: Ldl-density-pressure theory. J Cell Biochem. 2011;112(9):2222–9.
15. Boyden LM, Mao J, Belsky J, Mitzner L, Farhi A, Mitnick MA, Wu D, Insogna K, Lifton RP. High bone density due to a mutation in ldl-receptor-related protein 5. N Engl J Med. 2002;346:1513–21.
16. Babij P, Zhao W, Small C, Kharode Y, Yaworsky PJ, Bouxsein ML, Reddy PS, Bodine PV, Robinson JA, Bhat B, Marzolf J, Moran RA, Bex F. High bone mass in mice expressing a mutant lrp5 gene. J Bone Miner Res. 2003;18:960–74.
17. Westendorf JJ, Kahler RA, Schroeder TM. Wnt signaling in osteoblasts and bone diseases. Gene. 2004;341:19–39.
18. Holmen SL, Giambernardi TA, Zylstra CR, Buckner-Berghuis BD, Resau JH, Hess JF, Glatt V, Bouxsein ML, Ai M, Warman ML, Williams BO. Decreased bmd and limb deformities in mice carrying mutations in both lrp5 and lrp6. J Bone Miner Res. 2004;19:2033–40.
19. Shao JS, Cheng SL, Pingsterhaus JM, Charlton-Kachigian N, Loewy AP, Towler DA. Msx2 promotes cardiovascular calcification by activating paracrine wnt signals. J Clin Invest. 2005;115:1210–20.
20. Akhter MP, Wells DJ, Short SJ, Cullen DM, Johnson ML, Haynatzki GR, Babij P, Allen KM, Yaworsky PJ, Bex F, Recker RR. Bone biomechanical properties in lrp5 mutant mice. Bone. 2004;35:162–9.
21. Johnson ML, Harnish K, Nusse R, Van Hul W. Lrp5 and wnt signaling: a union made for bone. J Bone Miner Res. 2004;19:1749–57.
22. Johnson ML, Summerfield DT. Parameters of lrp5 from a structural and molecular perspective. Crit Rev Eukaryot Gene Expr. 2005;15:229–42.
23. Mani A, Radhakrishnan J, Wang H, Mani A, Mani MA, Nelson-Williams C, Carew KS, Mane S, Najmabadi H, Wu D, Lifton RP. Lrp6 mutation in a family with early coronary disease and metabolic risk factors. Science (New York, NY). 2007;315:1278–82.
24. Magoori K, Kang MJ, Ito MR, Kakuuchi H, Ioka RX, Kamataki A, Kim DH, Asaba H, Iwasaki S, Takei YA, Sasaki M, Usui S, Okazaki M, Takahashi S, Ono M, Nose M, Sakai J, Fujino T, Yamamoto TT. Severe hypercholesterolemia, impaired fat tolerance, and advanced atherosclerosis in mice lacking both low density lipoprotein receptor-related protein 5 and apolipoprotein e. J Biol Chem. 2003;278:11331–6.
25. Ishibashi S, Goldstein JL, Brown MS, Herz J, Burns DK. Massive xanthomatosis and atherosclerosis in cholesterol-fed low density lipoprotein receptor-negative mice. J Clin Invest. 1994;93:1885–93.

Wnt3a-Lrp5 mediated Bicuspid Aortic Valve Disease

9

Nalini M. Rajamannan

Introduction

Calcific Aortic Valve Disease is the most common indication for surgical valve replacement. For years this disease was thought to be a passive degenerative phenomenon. However, the cellular mechanisms involving this disease process are emerging. There are two forms of calcific aortic valve disease, tricuspid aortic valve disease and bicuspid aortic valve disease. Bicuspid aortic valve (BAV) is the most common congenital cardiac anomaly, having a prevalence of 0.9–1.37 % in the general population [1]. Bicuspid aortic valve disease occurs more frequently in patients who are undergoing surgical valve replacement. Understanding of the cellular mechanisms of aortic valve lesions will present future understanding to target pathways to slow disease progression. Currently, there are three fundamental cellular mechanisms defined in the development of aortic valve disease: (1) oxidative stress via traditional cardiovascular risk factors [2–10], (2) cellular proliferation [11], and (3) osteoblastogenesis in the end stage disease process [12, 13]. This chapter will characterize the phenotype of the bicuspid aortic valve model.

N.M. Rajamannan, MD
Division of Biochemistry and Molecular Biology,
Mayo Clinic, 200 First St SW, Rochester,
MN 55905, USA
e-mail: rajamannan.nalini@mayo.edu

eNOS$^{-/-}$ Mouse Model of Bicuspid vs. Tricuspid Aortic Valve Disease

The eNOS null mouse model, provides the perfect model to study the progression of tricuspid versus bicuspid aortic valve disease. Lee et al., demonstrated that bicuspid valves develop in 25 % of this mouse population develop bicuspid aortic valves, thus providing a natural model to compare the bicuspid versus tricuspid phenotype.

eNOS$^{-/-}$ mice were treated with high cholesterol diets to determine if the bicuspid would progress faster than the tricuspid aortic valves. MicroCT, Bone Tag injection, immunohistochemistry and RTPCR were assessed in addition to non-invasive imagine to determine the progression of the valve disease in the mice.

In Vivo Mouse Model of Calcific Aortic Valve Disease

To understand if eNOS$^{-/-}$ mice with the BAV phenotype, develops accelerated stenosis earlier than tricuspid aortic valves via the Lrp5 pathway activation, eNOS$^{-/-}$ mice were given a cholesterol diet versus cholesterol and atorvastatin. The Visual Sonics mouse echocardiography machine was used to screen for the BAV phenotype. Echocardiography hemodynamics was also performed to determine the timing of stenosis in bicuspid vs. tricuspid aortic valves eNOS$^{-/-}$ mice on different diets. Figure 9.1 demonstrates the characterization of the eNOS phenotype as defined

N.M. Rajamannan (ed.), *Molecular Biology of Valvular Heart Disease*,
DOI 10.1007/978-1-4471-6350-3_9, © Springer-Verlag London 2014

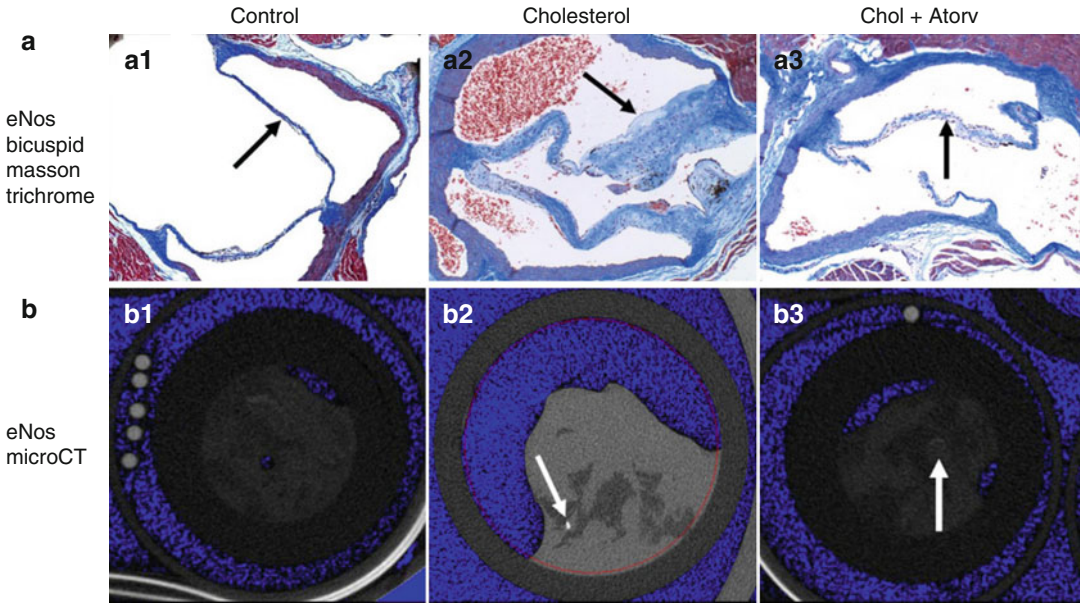

Fig. 9.1 Histology of the aortic valves from the eNOS$^{-/-}$ bicuspid mice. Panel (**a**) Masson trichrome stain of the eNOS$^{-/-}$ aortic valves on the control, *a1*, Cholesterol *a2*, and the Cholesterol + Atorvastatin diets *a3*. Panel (**b**) MicroCT of the of eNOS$^{-/-}$ aortic valves on the control *b1*, Cholesterol *b2* and the Cholesterol + Atorvastatin Diets *b3*. *Arrows* in *a2* and *b2* demonstrate atherosclerosis and calcification in the bicuspid leaflet. *Arrows* in *a3* and *b3* demonstrate no evidence of atherosclerosis in the valve leaflet and minimal calcification in the leaflet

by histology, and echocardiography. In Fig. 9.1, Panel a is the histology for BAV, Fig. 9.1, Panel b is the microCT for the eNOS$^{-/-}$ mice hearts on the different diets. The bicuspid valves developed tiny areas of mineralization as indicated by the arrows.

Figure 9.2, demonstrates the characterization of the eNOS phenotype as defined by Li-Cor near infrared imaging and RTPCR of the bicuspid aortic valves and the femurs of the eNOS null mice on the different diets. In Fig. 9.2, Panel a is the infrared imaging of the whole mouse 48 h after injection with the bone tag. Imaging of the whole mouse demonstrated the highest concentration of the Bone Tag in the cholesterol diet mouse with less in the Atorvastatin and minimal in the control mice as shown by the green fluorescence. The red area in the image in the control mouse GI tract is the chlorophyll in the chow diet, which is part of the background that appears red with the NIR imaging. The Bone Tag (Green dye) shows up in the bones of the mice and any other areas of the mouse that is undergoing incorporation of the bone tag. Since the ribs and sternum, block the heart and therefore, do not allow for optimal in vivo imaging of the hearts. Individual organs were dissected including the hearts and femurs from the mice to image the tissues ex vivo.

The hearts in Fig. 9.2, Panel b1, injected with the bone tag are in the top row. The control (Carboxylate) probe injected hearts are in the bottom row. The Pearl Imager then quantifies the amount of Bone Tag uptake into areas of active osteogenesis. The cholesterol hearts increased in the amount of bone tag uptake as compared to the control and Atorvastatin. The femurs in Fig. 9.2, Panel c1, injected with the bone tag are in the top row. The control probe injected femurs are in the bottom row. The cholesterol femurs demonstrate increase in active bone formation as compared to the control and the atorvastatin.

Figure 9.2, Panels b2, c2, is the semi-quantitative RTPCR from the BAV and femurs respectively. In the BAV as shown in There was no change in the TAV obtained from the eNOS$^{-/-}$ null mice from the different diets in terms of histology, RTCPR gene expression, and echocardiographic data. The gene expression for the femurs as shown in Fig. 9.2, Panel c2, demonstrated that Runx2, Lrp5, and Wnt3a increased in the cholesterol group and attenuation with atorvastatin.

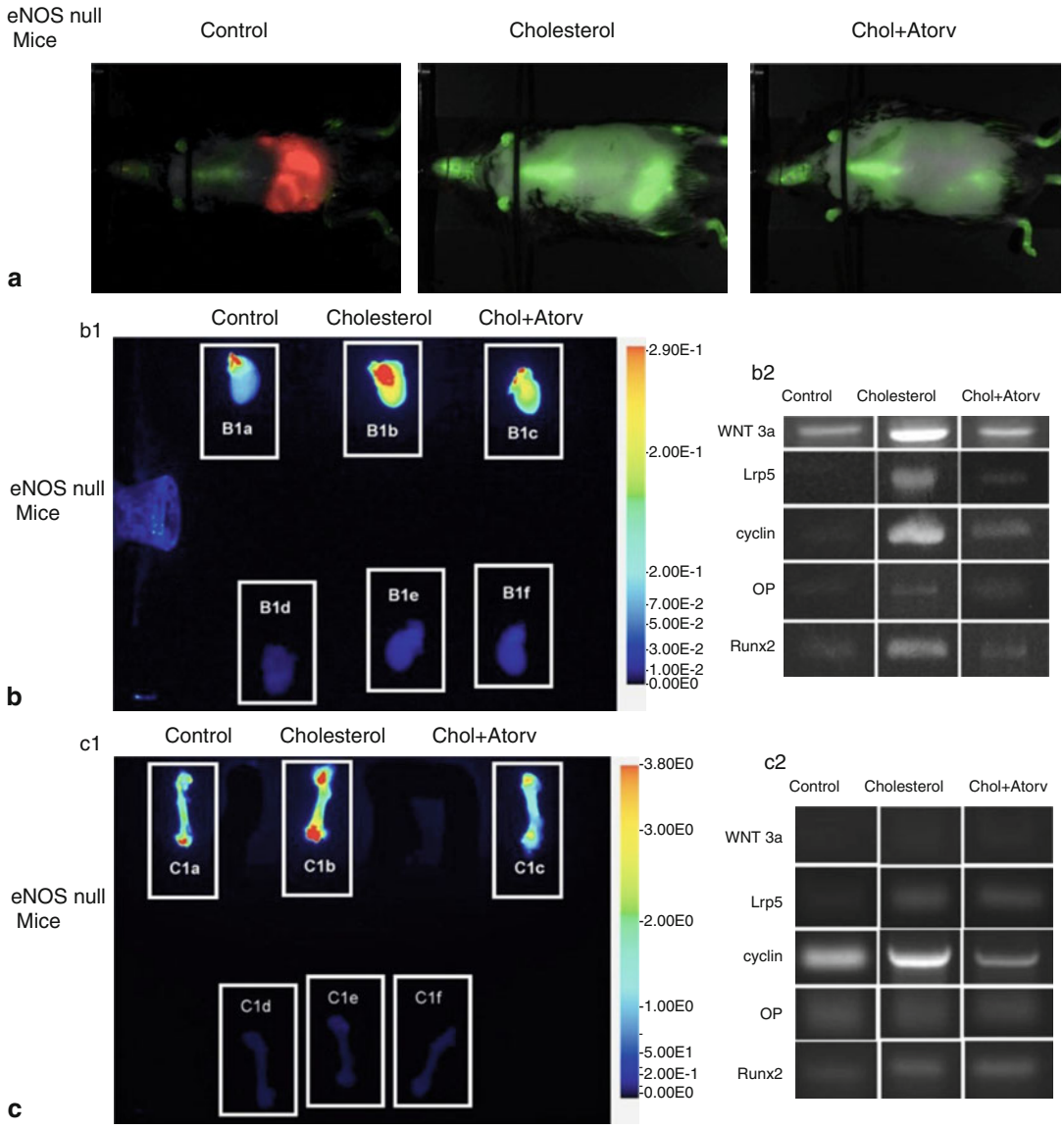

Fig. 9.2 Characterization of the Bicuspid Aortic valve and femurs in eNOS null mice by licor infrared imaging. *Left column*, control diet; *middle column*, cholesterol diet; *right column*, cholesterol diet plus atorvastatin. In each panel, the aortic valve leaflet is in the center. (All frames 20× magnification) *p < 0.001 for control compared to cholesterol, **p < 0.001 for cholesterol compared to cholesterol + Atorvastatin. Panel (**a**) Infrared imaging of the entire mouse on each diet. Panel (*b1*) Infrared imaging of the bicuspid hearts, Panel (*b2*), RTPCR on the aortic valves for Wnt3a, Lrp5, Cyclin1, OP, Runx2, GAPDH. Panel (*c1*) Infrared imaging of the bicuspid hearts, Panel (*c2*) RTPCR on the femurs for Wnt3a, Lrp5, Cyclin1, OP, Runx2, GAPDH

Summary

This chapter demonstrates that in the presence of oxidative stress environment and abnormal mechanical forces the aortic valve develops a mineralizing phenotype via the Lrp5/Wnt3a signaling pathway. For years, CAVD was thought to be due to a degenerative process but recent Working Group by NHLBI, has concluded based on the scientific progress in the field, that the

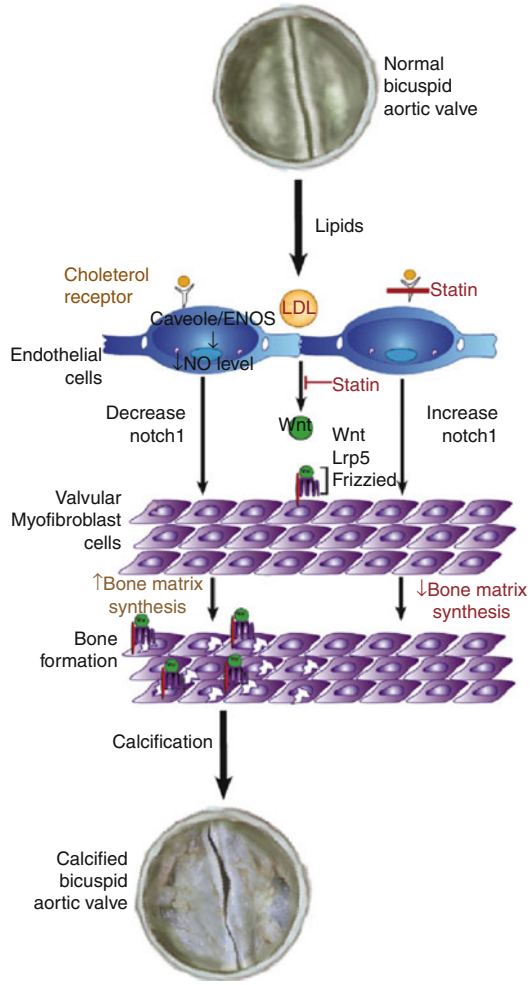

Fig. 9.3 Demonstrates that in the presence of lipids activates Lrp5 and Wnt signaling in the aortic valve cell layers to form bone in the valve leaflet

biology is an active process [14]. The implications that this model demonstrates the risk factor hypothesis for the development of aortic valve disease, and the role of mechanical force is an important mechanism of the Lrp5 receptor and the accelerated progression of bicuspid aortic valve disease over tricuspid aortic valve disease. Figure 9.3, demonstrates the cellular signaling important in the development of bicuspid aortic valve disease.

References

1. Roberts WC, Ko JM. Frequency by decades of unicuspid, bicuspid, and tricuspid aortic valves in adults having isolated aortic valve replacement for aortic stenosis, with or without associated aortic regurgitation. Circulation. 2005;111:920–5.
2. Drolet MC, Arsenault M, Couet J. Experimental aortic valve stenosis in rabbits. J Am Coll Cardiol. 2003;41:1211–7.
3. Rajamannan NM, Subramaniam M, Caira F, Stock SR, Spelsberg TC. Atorvastatin inhibits hypercholesterolemia-induced calcification in the aortic valves via the lrp5 receptor pathway. Circulation. 2005;112:I229–34.
4. Rajamannan NM, Subramaniam M, Springett M, Sebo TC, Niekrasz M, McConnell JP, Singh RJ, Stone NJ, Bonow RO, Spelsberg TC. Atorvastatin inhibits hypercholesterolemia-induced cellular proliferation and bone matrix production in the rabbit aortic valve. Circulation. 2002;105:2260–5.
5. Weiss RM, Ohashi M, Miller JD, Young SG, Heistad DD. Calcific aortic valve stenosis in old hypercholesterolemic mice. Circulation. 2006;114:2065–9.
6. Aikawa E, Nahrendorf M, Sosnovik D, Lok VM, Jaffer FA, Aikawa M, Weissleder R. Multimodality molecular imaging identifies proteolytic and osteogenic activities in early aortic valve disease. Circulation. 2007;115:377–86.
7. Rajamannan NM, Springett MJ, Pederson LG, Carmichael SW. Localization of caveolin 1 in aortic valve endothelial cells using antigen retrieval. J Histochem Cytochem. 2002;50:617–28.
8. Rajamannan NM, Edwards WD, Spelsberg TC. Hypercholesterolemic aortic-valve disease. N Engl J Med. 2003;349:717–8.
9. Rajamannan NM, Subramaniam M, Stock SR, Stone NJ, Springett M, Ignatiev KI, McConnell JP, Singh RJ, Bonow RO, Spelsberg TC. Atorvastatin inhibits calcification and enhances nitric oxide synthase production in the hypercholesterolaemic aortic valve. Heart. 2005;91:806–10.
10. Makkena B, Salti H, Subramaniam M, Thennapan S, Bonow RH, Caira F, Bonow RO, Spelsberg TC, Rajamannan NM. Atorvastatin decreases cellular proliferation and bone matrix expression in the hypercholesterolemic mitral valve. J Am Coll Cardiol. 2005;45:631–3.
11. Rajamannan NM, Sangiorgi G, Springett M, Arnold K, Mohacsi T, Spagnoli LG, Edwards WD, Tajik AJ, Schwartz RS. Experimental hypercholesterolemia induces apoptosis in the aortic valve. J Heart Valve Dis. 2001;10:371–4.
12. Rajamannan NM, Subramaniam M, Rickard D, Stock SR, Donovan J, Springett M, Orszulak T, Fullerton

DA, Tajik AJ, Bonow RO, Spelsberg T. Human aortic valve calcification is associated with an osteoblast phenotype. Circulation. 2003;107:2181–4.
13. Mohler 3rd ER, Gannon F, Reynolds C, Zimmerman R, Keane MG, Kaplan FS. Bone formation and inflammation in cardiac valves. Circulation. 2001;103:1522–8.
14. Rajamannan NM, Evans FJ, Aikawa E, Grande-Allen KJ, Demer LL, Heistad DD, Simmons CA, Masters KS, Mathieu P, O'Brien KD, Schoen FJ, Towler DA, Yoganathan AP, Otto CM. Calcific aortic valve disease: not simply a degenerative process: a review and agenda for research from the national heart and lung and blood institute aortic stenosis working group. Executive summary: Calcific aortic valve disease-2011 update. Circulation. 2011;124:1783–91.

Mouse Models of Calcific Aortic Valve Disease

10

Bin Zhang, Grace Casaclang-Verzosa, and Jordan D. Miller

The hallmarks of advanced calcific aortic valve stenosis include massive accumulation of amorphous or bone-like calcium and the excessive production and accrual of collagen and extracellular matrix proteins. These histopathological changes are frequently associated with increases in valvular lipid deposition, inflammatory cell infiltrate, pro-inflammatory cytokine elaboration, and matrix metalloproteinase expression. In the search for key mechanisms underlying the calcification and fibrosis that drive progression of valvular stenosis, animal models have played an integral role. To date, mouse models of hypercholesterolemia have been the predominant model of choice [1–4].

The remainder of this chapter will provide an overview of currently used mouse models of disease, a brief review of methods for assessing valve function in mice, molecular contributors to valvular calcification that have been elucidated from mouse models, and potential future directions for research in the field.

B. Zhang, MD • G. Casaclang-Verzosa, MD
Department of Surgery, Mayo Clinic, Rochester, MN, USA

J.D. Miller, PhD (✉)
Department of Surgery, Mayo Clinic, Rochester, MN, USA

Department of Physiology and Biomedical Engineering, Mayo Clinic, 200 First St. SW, Rochester, MN 55905, USA
e-mail: miller.jordan@mayo.edu

Mouse Models of Aortic Valve Disease

The Value of Single Mutation Mice

Mice with a single genetic mutation that prevents clearance of lipids from the circulation (e.g., low density lipoprotein receptor deficient mice, $ldlr^{-/-}$, or apolipoprotein E-deficient mice, $apoE^{-/-}$) have played major roles in advancing our understanding of mechanisms that contribute to atherosclerosis in the vasculature [5, 6]. Over the past decade, a number of investigators have examined histopathological and functional changes that occur with prolonged hypercholesterolemia in $ldlr^{-/-}$ and $apoE^{-/-}$ mice. Importantly, when fed a high fat or high cholesterol diet, both of these strains appear to develop significant valvular calcification which appears to be due in part to activation of osteogenic signaling in valve interstitial cells, which is also associated with significant increases in valvular fibrosis [3, 4]. It is critical to note, however, that the preponderance of studies conducted to date have not reported the presence of hemodynamically significant aortic valve stenosis in these mouse strains (i.e., reductions in valve area that are sufficient to elicit ventricular hypertrophy and/or cardiac failure). Thus, these models are likely to serve as useful platforms to understand mechanisms that contribute to activation of osteogenic and a phenotype of aortic valve sclerosis (i.e., stiffening of the valve without reductions in valve area), but are not likely to serve as a useful platform for screening of

N.M. Rajamannan (ed.), *Molecular Biology of Valvular Heart Disease*,
DOI 10.1007/978-1-4471-6350-3_10,

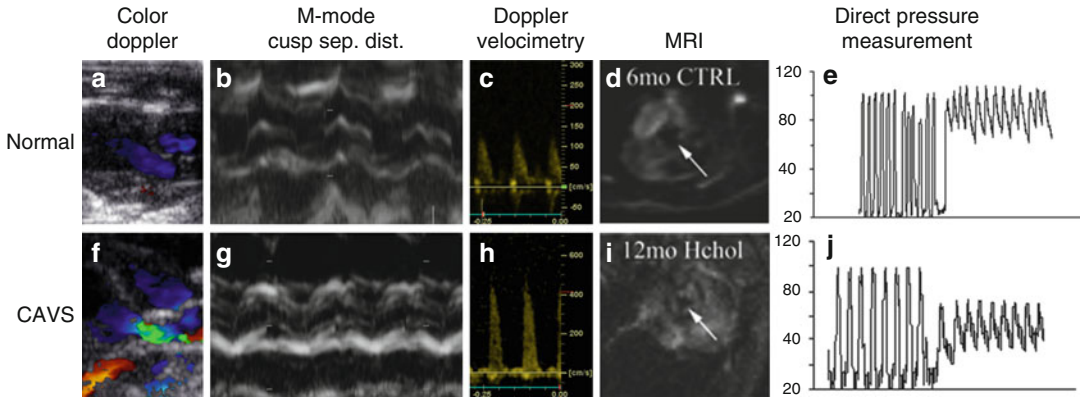

Fig. 10.1 Common methods used to measure aortic valve function in mice (Adapted from Miller et al. [3]) *Upper panels* (**a**–**e**) depict data derived from normal, healthy mice, and *lower panels* (**f**–**j**) depict data from mice with severe calcific aortic valve stenosis. In healthy mice, the absence of aliasing (i.e., green) in the color Doppler signal (Panel **a**) indicates that flow across the aortic valve is laminar during systole. M-Mode imaging across the aortic valve allows for assessment of cusp separation distance with high spatial and temporal resolution (Panel **b**). Doppler velocimetry across the normal valve also suggests that valve function is relatively normal, as peak transvalvular velocity is <1.5 m/s (Panel **c**). MRI imaging of the mouse aortic valve allows for evaluation of aortic valve orifice area without making assumptions regarding aortic valve orifice geometry (Panel **d**; *arrows* point to valve orifice). Similarly, direct measurements of transvalvular pressure using a Millar catheter demonstrate a negligible systolic pressure gradient across the aortic valve (pullback method from the ventricle to the aorta, Panel **e**). Note that in CAVS mice, the irregular shape of the aortic valve and turbulent/irregular flow pattern result in significant aliasing in the color Doppler signal (Panel **f**). Furthermore, reductions in cusp separation distance (*arrows*, Panel **g**) are associated with increases in peak transvalvular velocity (Panel **h**) as long as left ventricular function is maintained. Reductions in aortic valve orifice area can be clearly visualized using MRI imaging in mice with severe stenosis (Panel **i**). Note that non-invasive measurements of the aortic valve are strongly associated with increases in the systolic transvalvular pressure gradient measured directly using a Millar catheter (pullback method from the ventricle to the aorta)

treatments aimed at ameliorating the functional consequences of severe valvular calcification evident in humans calcific aortic valve stenosis. As other chapters in this book cover information gleaned from these models in detail, the remainder of this chapter will focus primarily on mouse models that aim to induce valvular stenosis through the combination of multiple genetic mutations.

The Value of "Complex" Mouse Models of Hyperlipidemia

In 2006, Weiss et al. identified a unique hypercholesterolemic mouse model that developed hemodynamically significant aortic valve stenosis [5]. Of particular interest was that these mice were ldlr-deficient, but also had a hit-and-run mutation in the apolipoprotein B100 gene that prevented its splicing to apoB48. Approximately 30 % of the ldlr-deficient, apoB100-only mice (or $ldlr^{-/-}$/$apoB^{100/100}$ mice) developed hemodynamically-significant aortic valve stenosis (as evaluated by echocardiography and direct measurement of transvalvular gradients), and this percentage could be dramatically increased to >80 % by placing mice on a Western-type diet for 12 months [4, 5, 7]. Importantly, this model also captured many of the osteogenic signaling pathways that were activated in humans with severe CAVD. Thus, this model provides a unique platform on which to test therapeutic interventions aimed at slowing the functional consequences of massive calcium and extracellular matrix accumulation evident in humans with end-stage CAVD.

Molecular Signaling Underlying Calcification in Valve Disease

Importantly, both of the above-mentioned mouse models of valve calcification provide model systems which allow for mechanistic interrogation

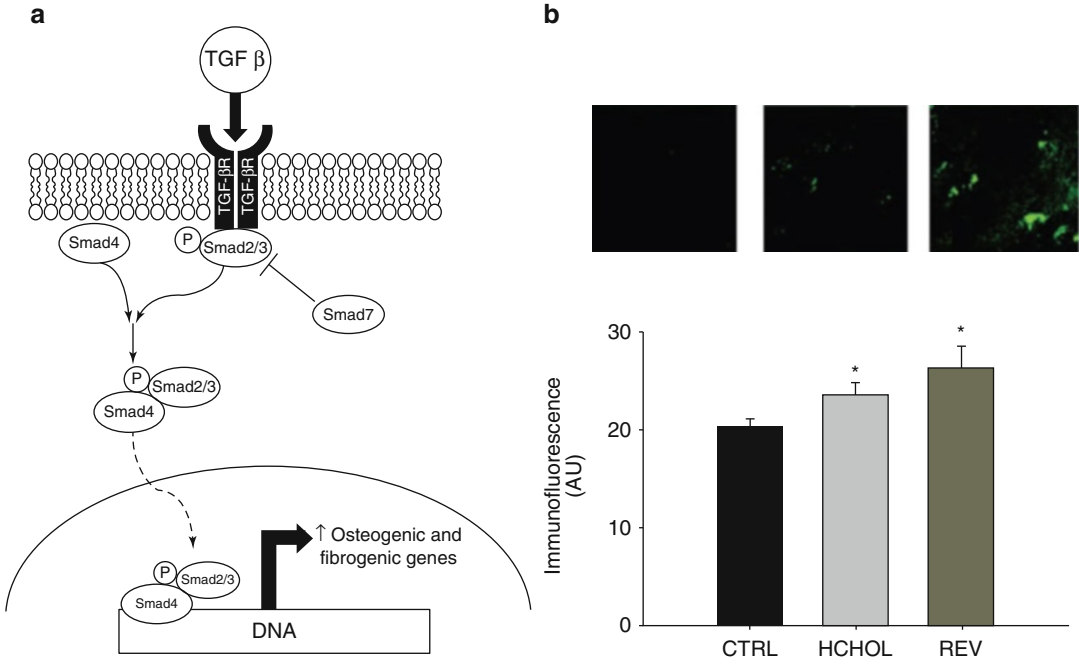

Fig. 10.2 Role of TGFβ signaling in calcific aortic valve disease. Panel (**a**) depicts the canonical TGFβ signaling cascade. Key events include phosphorylation of smad2 or smad3, resulting in nuclear translocation of the smad2/3-smad4 complex, allowing for increased expression of fibrogenic and osteogenic genes. Panel (**b**) depicts changes in p-smad2 levels following reduction of lipid levels with a genetic switch in ldlr-deficient, apoB100-only mice with severe CAVD (Taken from Miller et al. [7]). Note that p-smad2 levels are significantly increased in mice with severe CAVD, but are not reduced by lipid lowering

of pathways that contribute to initiation and progression of aortic valve calcification and fibrosis. The ensuing sections will highlight several of the key signaling cascades that have been characterized in these mouse strains, key considerations that must be taken into account when evaluating changes in aortic valve function in rodents over time, and briefly discuss future areas of investigation.

Osteogenic Signaling

Bone Morphogenetic Protein (BMP) Signaling

Numerous studies have shown that bone morphogenetic protein signaling is increased in humans and animals with end-stage CAVD, including increases in ligand elaboration, smad1/5/8 phosphorylation, and increased expression of BMP target genes [8–13]. There are three lines of evidence supporting a major role of BMP signaling in valve calcification. First, increases in smad1/5/8 phosphorolyation precede calcification in hyperlipidemic mice, suggesting that osteogenic activation does not occur as a local epiphenomenon/secondary to calcium deposition [7]. Second, treatment of cells with inhibitors of BMP signaling (e.g., Noggin) attenuates osteogenic differentiation and mineralization in vitro [14]. Finally, and perhaps most compellingly, smad6-deficient mice develop significant valvular calcification, suggesting that de-repression of BMP signaling is sufficient to drive overt cardiovascular calcification in vivo [15–17].

Wnt/β-Catenin Signaling

Wnt/β-Catenin signaling plays a major role in osteogenic differentiation in orthotopic bone, and emerging evidence suggests that this signaling pathway is activated in humans and animals with calcified aortic valves [18–24]. More specifically, increases in Wnt ligands (e.g., Wnt3a) and consequent nuclear localization of the β-catenin complex drive osteogenic gene expression both in vitro and in vivo. Interestingly, induction of canonical

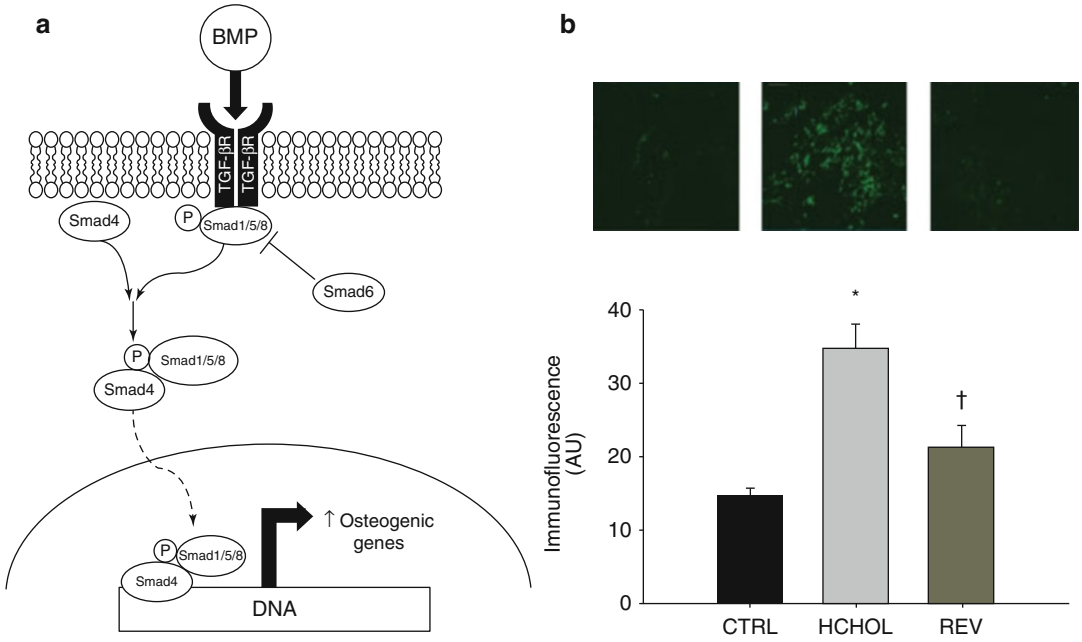

Fig. 10.3 Role of BMP signaling in calcific aortic valve disease. Panel (**a**) depicts the canonical BMP signaling cascade. Key events include phosphorylation of Smad1/5/8, resulting in nuclear translocation of the Smad1/5/8-Smad4 complex and subsequent expression of osteogenic genes. Panel (**b**) depicts changes in p-Smad1/5/8 levels following reduction of lipid levels with a genetic switch in ldlr-deficient, apoB100-only mice with severe CAVD (Taken from Miller et al. [7]). Note that p-Smad1/5/8 levels are substantially increased in mice with severe CAVD, and are dramatically decreased following reduction of blood lipids

Wnt/β-catenin signaling can occur through receptor transactivation (i.e., receptor activation in the absence of changes in Wnt ligand) by increases in TGFβ signaling, although it is unclear whether this phenomenon occurs in vivo [25].

Transforming Growth Factor-β (TGF-β) Signaling

There are abundant data demonstrating activation of canonical TGF-β signaling in humans and mice with various stages of aortic valve calcification, including increases in TGF-β1 ligand, smad2/3 phosphorylation, and smad2 target gene activation [4, 7, 26–28]. Treatment of cultured aortic valve interstitial cells with exogenous TGF-β1 results in calcified nodule formation, suggesting that activation of this pathway may be an independent driver of calcification in the valve [27, 29]. Importantly, this phenomenon can be inhibited by caspase inhibition, suggesting that induction of apoptosis is a key mechanism contributing to TGF-β1-induced interstitial cell calcification [29]. Whether experimentally reducing TGF-β1 levels in vivo slows progression of CAVD in experimental models of valve disease remains unclear.

Non-osteogenic Calcification

While the past two decades contain a large amount of data suggesting that "active", bone-like processes can contribute to valve calcification, the contribution of non-osteogenic processes may have an equal or greater contribution in some patient populations and/or animal models [3, 30]. To date, two major processes may contribute to non-osteogenic calcification in the valve: those that relate to cell death, and those that related to reductions in molecules that clear ectopic calcium.

Valve Calcification Related to Cell Death

Cell death may play a pivotal role in driving "non-osteogenic" calcium accumulation through increasing cellular debris and/or inorganic

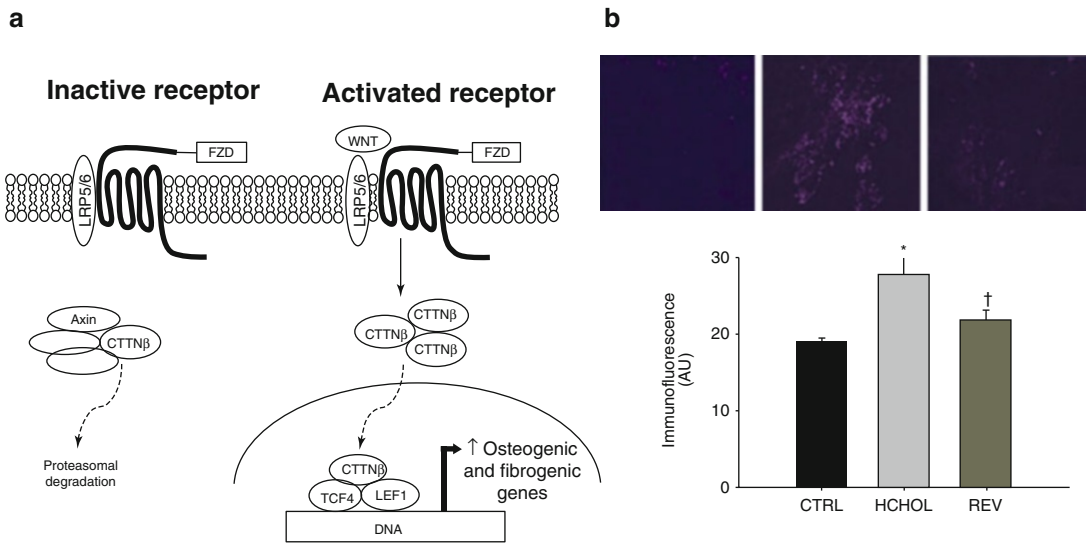

Fig. 10.4 Role of Wnt/β-catenin signaling in calcific aortic valve disease. Panel (**a**) depicts the canonical Wnt/β-catenin signaling cascade. When the LRP5/6-frizzled receptor complex is not activated by Wnt ligand, β-catenin is targeted for proteasomal degradation by an Axin-containing protein complex. The presence of Wnt ligand results in disruption of the degradation complex, which allows for nuclear translocation of β-catenin (CTTNβ), functional interaction of β-catenin with other nuclear co-factors (e.g., TCF/LEF), and subsequent induction of osteogenic and fibrogenic gene expression. Panel (**b**) depicts changes in β-catenin levels following reduction of lipid levels with a genetic switch in ldlr-deficient, apoB100-only mice with severe CAVD (Taken from Miller et al. [7]). Note that the intensity and nuclear localization of β-catenin is dramatically increased in mice with severe CAVD, and is markedly decreased following reduction of lipid levels

phosphate levels in interstitial cell microenvironments in the aortic valve. Apoptosis, or programmed cell death, often occurs as a result of caspase activation and—as noted above—can drive cellular calcification in vitro [31–34]. In contrast, necrosis involves cell death secondary to factors external to the cell (e.g., secondary to mechanical forces or immune-related mechanisms [35]). The role of cellular necrosis in CAVD in vivo and in vitro remains poorly understood.

Valve Calcification Related to Reductions in Fetuin-A

Fetuin-A is a glycoprotein constitutively secreted from the liver, and functionally serves to prevent the accumulation of calcification at ectopic sites [36–38]. The fact that the fetuin-A-deficient mouse develops massive calcification in soft tissues throughout the body suggests that "tonic" clearance of calcium is an important protective mechanism against valvular calcification [39]. Perhaps not surprisingly, apolipoprotein E-deficient mice crossed with fetuin-A-deficient mice also have dramatic increases in intimal plaque calcification [40]. Importantly, degradation of Fetuin-A by matrix metalloproteinases also promotes calcium deposition [41], suggesting that local injury and matrix remodeling may be key permissive events allowing local calcium accrual in the valve.

Methods for Imaging and Evaluation of Aortic Valve Function

Multiple methods of cardiac imaging have been developed over the years for the visualization and assessment of cardiac function in experimental animals. These include, echocardiography [4–6, 42, 43], micro CT [44], PET scan [45] and MRI [4, 46, 47]. While each modality has its strengths and limitations, echocardiography has emerged as the most validated means of exploring cardiac and valvular phenotypes in mice, thereby greatly contributing to the understanding of cardiovascular diseases [3]. With the advent of increasingly

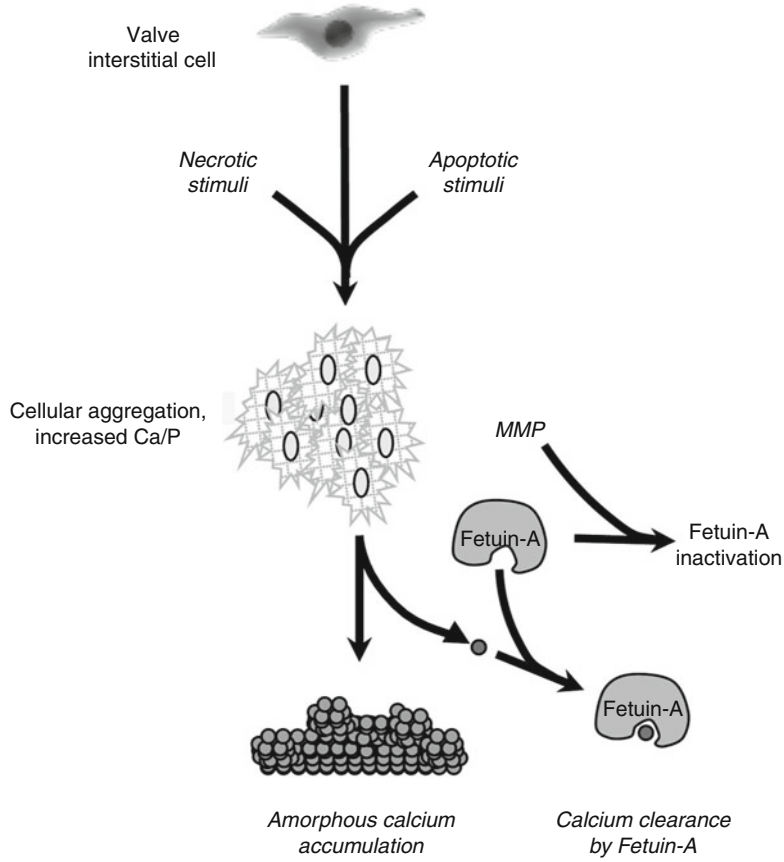

Fig. 10.5 Potential mechanisms contributing to non-osteogenic calcification in calcific aortic valve disease (Adapted from Miller et al. [3]). Necrotic or apoptotic stimuli result in cell death via fundamentally distinct mechanisms, but both paths are likely to induce cellular aggregation and in increased calcium and inorganic phosphate in microenvironments in the valvular interstitial space. Fetuin-A is a major protein responsible for clearance of excess calcium at ectopic sites of calcification. Inactivation of Fetuin-A by matrix metalloproteinases (*MMP*), however, may enable the accumulation of amorphous calcium (i.e., calcium deposition that does not have a bone-like ultrastructure) in the aortic valve

higher frequency probes, the anatomy of the mouse heart and valves can be seen with remarkable detail.

Echocardiographic evaluation of valvular function in the mouse is particularly challenging because of its small size, rapid heart rate and orientation. Furthermore, care must be taken to control the heart rate (>500 beats/min), body temperature (37 °C) and the level of anesthesia to prevent cardiodepression and maintain normal physiologic conditions [3]. The reduction in heart rate in animal models may yield better temporal and spatial resolution for improved image visualization and measurement of valve movement, but such conditions can also dramatically alter the relationship between variables such as peak transvalvular velocity and valve cusp separation distance (see below). As such, cardiac function should be accurately measured and compared when comparing the effectiveness of a genetic or pharmacological intervention [3]. The presence and severity of LV hypertrophy and systolic dysfunction can also be ascertained rapidly and reproducibly in mice in longitudinal studies [48–54], and can serve as a useful index of the hemodynamic consequences of reductions in aortic valve orifice area.

M-Mode, Two-Dimension, and Doppler Echocardiography

M-Mode Echocardiography

Two-dimensional echocardiography is a powerful technique for characterization of not only aortic valve function but also its impact on left ventricular structure and function in mice. The greatest advantages of M-mode echocardiography relate to the superior spatial and temporal resolution available throughout the cardiac cycle at high heart rates [3]. Images can be readily obtained from parasternal and long axis views,

and do not require coregistration with a Doppler line of interpretation. Recent work from our group and others suggest that aortic valve cusp separation correlates well with invasive hemodynamic measurements of aortic valve function and peak transvalvular velocity when aortic valve regurgitation is not evident [55], and facilitate longitudinal studies of progression/regression of aortic valve disease in mice [3, 4, 7]. Importantly, the variance of valve orifice dimensions is relatively low, achieving statistical power in between-groups comparisons with manageable sample sizes. Furthermore, M-mode derived orifice dimensions and by extrapolated valve area, are not appreciably affected by LV contraction or the presence of valvular regurgitation [3, 5, 43].

Perhaps the greatest disadvantage of M-mode echocardiographic techniques relates from the reliance on a unidimensional measurement to portray valve function [3]. In the presence of eccentric valvular remodeling (e.g., partial or complete cusp fusion), M-mode methods are susceptible to both under- and over-estimation of the severity of valve dysfunction [3]. Thus, confirmation with at least one additional parameter of valvular function (e.g., Doppler velocity, two-dimensional imaging, MRI, or direct catheterization) is important to ensure accurate assessment of valve function [3, 55].

Two-Dimensional Imaging

Two-dimensional imaging of the aortic valve in the short axis and long-axis views allow for real-time visualization of valvular motion as well as echogenic characteristics of the valve [3–7, 55, 56]. Correlation of M-mode cusp separation distance with two-dimensional images of the aortic valve (e.g., visualization of valve orifice area during systole) is important to confirm the true phenotypic characteristics of the valve [3, 55]. Great technological advancements will be required to apply three-dimensional echocardiography to the evaluation of valve structure and function in mice.

Doppler Velocity

Continuous- and pulse-wave Doppler evaluation of blood velocities are useful estimation of trans-valvular pressure gradients and valve areas in mice, especially when combined with two-dimensional or M-mode characterization of aortic valve function [3]. Doppler echocardiography, however, has several significant disadvantages. First, there is a wide range in normal transvalular velocities reflecting inherent technical limitation of Doppler echocardiography [43]. Second, it is not always possible to register the line of Doppler interrogation in a position that is parallel to the direction of blood flow, which can result in underestimation of valve gradients [3]. Third, the region of interrogation needs to be small enough to avoid contamination of velocity profiles by adjacent tissue motion, but large enough to capture a "true" peak velocity within the lumen of the vessel [3]. Finally, Doppler velocities can be affected by factors other than effective orifice area, such as changes in left ventricular contractility [3]. Furthermore, valvular regurgitation can artificially increase transvalvular gradients secondary to a "hyperdynamic" cardiac phenotype (e.g., increased stroke volume/contractility) even in the absence of aortic valve stenosis. Collectively, Doppler velocity alone should not be used as evidence of aortic valve stenosis in any species.

Magnetic Resonance Imaging

High-resolution cardiac magnetic resonance imaging (CMR) has evolved into one of the major non-invasive tools to study the cardiac and valvular function in healthy and diseased mice [3, 4]. CMR planimetry of the aortic valve orifice area can be performed with high sensitivity and specificity for the detection of aortic valve stenosis, and importantly, does not depend on acoustic windows essential for high-quality echocardiography [3, 4]. Furthermore, it provides additional information regarding global and regional left ventricular function, and can accurately define left ventricular hypertrophy, an integral feature of significant aortic stenosis [57].

The advantages of MRI are balanced by distinct disadvantages. While the availability of high-resolution systems (e.g., >7 T) and system programming expertise (for cardiac and

respiratory gating in mice) limit the application of this approach at many institutions perhaps the greatest limitation of this approach relates to the relatively long imaging times required for high-quality imaging (>20 min per study) [58]. Thus, CMR imaging requires deep sedation or general anesthesia, which places mice with severe aortic valve disease at a higher mortality risk due to cardiodepression [58, 59].

Invasive Hemodynamic Techniques

In clinical studies of valvular and left ventricular function, invasive hemodynamic techniques have been used as a "gold standard" [60]. In mice, microtransducer-tipped catheters provide high-fidelity assessments, by virtue of sampling rates on the order of 1,000 Hz. The small caliber, e.g., 1.4Fr (Millar, Houston, TX), allows retrograde introduction into the left ventricle via the carotid artery [5, 61]. Advantages of invasive techniques include precise ascertainment of transvalvular gradients, and left ventricular systolic and diastolic function [62]. As is the case in the clinical setting, invasive hemodynamic techniques in mice can serve as a validation standard for more convenient noninvasive methods [5, 61].

Disadvantages of invasive methods include blood loss (due to carotid arterial access), as well as inducing substantial damage to aortic valve endothelial and interstitial cells with the passage of the catheter through the valve orifice (i.e., initiation of a molecular "damage response"), thus rendering longitudinal studies very difficult and unlikely. General anesthesia can result in cardiac depression, especially in mice with severe aortic valve disease, resulting in discordance of findings obtained by invasive studies and those acquired by echocardiography in minimally sedated mice [5, 61].

Summary of Findings from Studies of Aortic Valve Function in Mice

In adult C57BL/6 J mice, the systolic aortic valve dimension is approximately 1.2 mm [5, 43]. Assuming that the orifice is roughly circular, anatomic estimates of normal adult aortic valve area from various strains of mice are about 0.8–1.3 mm^2. Estimates of normal aortic valve area are somewhat higher ($\approx 1.60\ mm^2$) when Doppler methods are used.

Normal peak systolic velocity of blood flow across the aortic valve in mice is <1.8 m/s [6, 43, 61], predicting peak transvalvular gradients of <10 mmHg, findings corroborated by invasive hemodynamic studies [5, 61]. Reduction of systolic aortic valve dimension by >50 %, corresponding to reduction of valve area by >75 %, is sufficient to induce hemodynamically important transvalvular pressure gradients of >50 mmHg, a finding that recapitulates seminal findings in humans with aortic valve disease [5].

Potential Therapeutic Targets in CAVD

Now that we have identified several key mechanisms contributing to initiation and progression of CAVD (i.e., osteogenic and non-osteogenic calcification) as well as methods used to measure valve function (echocardiography, MRI, and invasive techniques), we will now discuss potential therapeutic interventions that have been tested (or are currently being tested) in mouse models of valve disease. Importantly, these interventions will be discussed largely in the context of the pathobiological processes they are likely to impact.

Reducing Blood Lipids

Hypercholesterolemia is a powerful activator of osteogenic signaling in experimental animal models of CAVD. Reducing blood lipids in mice in early stages of valve disease results in attenuation of osteogenic and fibrogenic signaling, and importantly, halts progression of valvular dysfunction. Reducing blood lipids in advanced stages of valve disease can also reduce osteogenic signaling, but fails to reduce fibrogenic signaling or reverse valvular dysfunction [4, 7, 63]. Importantly, this latter finding is consistent

with recent clinical trials in humans, where initiation of lipid lowering with statins in advanced stages of CAVD failed to improve aortic valve function [4, 7]. Future trials aimed at initiating lipid lowering in earlier stages of valve disease, specific patient subsets with severe hypercholesterolemia, or targeting specific lipoproteins (e.g., lipoprotein (a)) may demonstrate a more beneficial therapeutic effect.

Reactive Oxygen Species

Reactive oxygen species are known to be upregulated in valves from humans with end-stage CAVD as well as mice with early- and late-stage CAVD [64, 65]. Recent work from Liberman et al. suggested that reducing oxidative stress with α-lipoic acid can attenuate valvular calcification in rabbits [65]. Interestingly, treatment of rabbits with tempol (a superoxide dismutase "mimetic") accelerated development of valve calcification, suggesting that different reactive oxygen species (e.g., superoxide versus hydrogen peroxide) can differentially impact valve calcification and progression of aortic valve stenosis, making harnessing of antioxidant treatments challenging [65, 66]. Additional investigation in this area examining the effects of different sources of reactive oxygen species as well as the effects of different antioxidants (through both genetic and pharmacological means) is an exciting and important area of research.

Hypertension and the Renin-Angiotensin System

Overt hypertension is a risk factor for development of CAVD, and is likely to exert its effects on the aortic valve through a direct mechanical effect on the valve (i.e., increased stress during systole and diastole due to increased pressure) [67–69]. Evidence for this effect comes from Merryman and colleagues, who demonstrated that aortic valve calcification can be accelerated by mechanical strain placed aortic valve interstitial cells [70].

Hypertension due to hyperactivation of the renin-angiotensin system, however, can exert direct biological effects on the valve as well. More specifically, angiotensin II—originating from circulating levels or from local inflammatory cells in the valve—can contribute to increases in oxidative stress, inflammation, and endothelial disruption in experimental animal models [67–69]. Future investigation aimed at understanding the effects of angiotensin-converting enzyme and/or AT1 receptor blockade on valve function in appropriate mouse models will lay key groundwork for future trials in this area [71, 72].

Nitric Oxide Signaling

Nitric oxide bioavailability is known to play a major protective effect in atherosclerosis [73–76], but its role in the regulation of aortic valve calcification is much more poorly understood. There is a substantial amount of evidence suggesting that nitric oxide signaling is reduced in CAVD, due to a combination of reduced nitric oxide synthase enzyme as well as increased "uncoupling" of nitric oxide synthases (i.e., generation of superoxide instead of nitric oxide) [77–79]. Furthermore, inhibition of nitric oxide signaling in vitro accelerates calcification of aortic valve interstitial cells [23, 80]. As such, identifying key cofactors and/or post-translational modifications to nitric oxide synthase that improve its activity is likely to lead to novel treatments that slow progression of valve calcification and dysfunction in CAVD.

Inflammation

Valves from patients with end-stage CAVD have massive infiltration of inflammatory cells, and cellular inflammation co-localizes with increased expression of osteogenic markers in animal models of cardiovascular calcification [81–89]. Emerging evidence suggests that neutralization of tumor necrosis factor alpha may attenuate vascular calcification in hyperlipidemic mice, but it will be essential to determine whether a similar

phenomenon occurs in calcifying aortic valves, as well as if such anti-inflammatory interventions reduce valvular dysfunction in advanced stages of CAVD [90–93].

Peroxisome Proliferator-Activator γ (PPARγ) Activation

Recent work from several groups suggests that long-term treatment with PPARγ activators such as pioglitazone may attenuate aortic valve dysfunction in experimental animal models [94, 95]. The mechanism for this effect is likely twofold. First, PPARγ agonists are known to reduce inflammation, which may indirectly reduce osteogenic differentiation of aortic valve interstitial cells [56, 96]. Second, PPARγ agonists promote the differentiation of cells to an adipocyte-like phenotype versus an osteoblast-like phenotype, which is likely to directly prevent osteogenic differentiation of interstitial cells [94, 95]. Importantly, the latter effect also occurs in bone, suggesting that low, anti-inflammatory doses of PPARγ may be the only viable clinical treatment given the observation that many patients with CAVD also have reduced bone mineral density and/or osteoporosis, and further inhibition of osteogenesis at orthotopic sites of calcification would be likely to increase fracture/fall risk [94].

Receptor Activator of NFκB Ligand (RANKL) Signaling

Recent work suggests that chronic administration of osteoprotegerin (which inhibits RANKL signaling) can inhibit vascular and valvular calcification in hypercholesterolemic mice [97, 98]. Importantly, long-term osteoprotegerin treatment was developed for treatment of osteoporosis, suggesting that RANKL differentially impacts calcification at ectopic and orthotopic sites of calcification [99, 100].

Altering Osteogenic Signaling

Recent observations suggest that lipid lowering in advanced stages of valve disease reduces osteogenic signaling, reduces valvular calcium, but does not reduce established aortic valve dysfunction [4, 7]. Importantly, reducing lipid levels does not reduce TGF-β signaling or fibrosis in the aortic valve, suggesting that excessive extracellular matrix deposition (and perhaps ECM cross-linking) may be a major contributor to valvular dysfunction in late stages of valve disease, and importantly, is likely to be a major biological factor to overcome should treatments that regress calcification show clinical efficacy [63, 101–103].

Summary

Collectively, mice harboring single or multiple genetic mutations can be used as experimental platforms to gain insight into the pathobiology of calcific aortic valve disease, as well as pre-clinical testing of pharmacological agents aimed at reducing osteogenic calcification, non-osteogenic calcification, or fibrosis in the aortic valve. While single mutation mice (e.g., apoE$^{-/-}$) [6, 104] may provide a platform that allows for characterization of changes in ectopic osteogenesis, multiple mutation mice (e.g., ldlr$^{-/-}$/apoB$^{100/100}$) will likely be required if overt valvular dysfunction/stenosis is a primary outcome variable [4, 7, 97]. By carefully characterizing changes in valvular and ventricular function using well-established, non-invasive imaging techniques, we anticipate the upcoming years will yield numerous insights and novel pharmacological candidates for mitigation of valve calcification and fibrosis in humans.

Acknowledgements This work was supported by funding from the National Institutes of Health (HL111121 and TR000954 to JDM), the Mayo Clinic Center for Regenerative Medicine, and the Mayo Clinic Kogod Center on Aging.

References

1. Faber M, Bette M, Preuss MA, Pulmanausahakul R, Rehnelt J, Schnell MJ, Dietzschold B, Weihe E. Overexpression of tumor necrosis factor alpha by a recombinant rabies virus attenuates replication in neurons and prevents lethal infection in mice. J Virol. 2005;79:15405–16.

2. Freeman RV, Otto CM. Spectrum of calcific aortic valve disease: Pathogenesis, disease progression, and treatment strategies. Circulation. 2005; 111:3316–26.
3. Miller JD, Weiss RM, Heistad DD. Calcific aortic valve stenosis: methods, models, and mechanisms. Circ Res. 2011;108:1392–412.
4. Miller JD, Weiss RM, Serrano KM, Brooks 2nd RM, Berry CJ, Zimmerman K, Young SG, Heistad DD. Lowering plasma cholesterol levels halts progression of aortic valve disease in mice. Circulation. 2009;119:2693–701.
5. Weiss RM, Ohashi M, Miller JD, Young SG, Heistad DD. Calcific aortic valve stenosis in old hypercholesterolemic mice. Circulation. 2006;114:2065–9.
6. Tanaka K, Sata M, Fukuda D, Suematsu Y, Motomura N, Takamoto S, Hirata Y, Nagai R. Age-associated aortic stenosis in apolipoprotein e-deficient mice. J Am Coll Cardiol. 2005;46:134–41.
7. Miller JD, Weiss RM, Serrano KM, Castaneda LE, Brooks RM, Zimmerman K, Heistad DD. Evidence for active regulation of pro-osteogenic signaling in advanced aortic valve disease. Arterioscler Thromb Vasc Biol. 2010;30:2482–6.
8. Edep ME, Shirani J, Wolf P, Brown DL. Matrix metalloproteinase expression in nonrheumatic aortic stenosis. Cardiovasc Pathol. 2000;9:281–6.
9. Ankeny RF, Thourani VH, Weiss D, Vega JD, Taylor WR, Nerem RM, Jo H. Preferential activation of smad1/5/8 on the fibrosa endothelium in calcified human aortic valves–association with low bmp antagonists and smad6. PLoS One. 2011;6:e20969.
10. Seya K, Yu Z, Kanemaru K, Daitoku K, Akemoto Y, Shibuya H, Fukuda I, Okumura K, Motomura S, Furukawa K. Contribution of bone morphogenetic protein-2 to aortic valve calcification in aged rat. J Pharmacol Sci. 2011;115:8–14.
11. Yanagawa B, Lovren F, Pan Y, Garg V, Quan A, Tang G, Singh KK, Shukla PC, Kalra NP, Peterson MD, Verma S. Mirna-141 is a novel regulator of bmp-2-mediated calcification in aortic stenosis. J Thorac Cardiovasc Surg. 2012;144:256–62.
12. Nagy JT, Foris G, Fulop Jr T, Paragh G, Plotnikoff NP. Activation of the lipoxygenase pathway in the methionine enkephalin induced respiratory burst in human polymorphonuclear leukocytes. Life Sci. 1988;42:2299–306.
13. Yu Z, Seya K, Daitoku K, Motomura S, Fukuda I, Furukawa K. Tumor necrosis factor-alpha accelerates the calcification of human aortic valve interstitial cells obtained from patients with calcific aortic valve stenosis via the bmp2-dlx5 pathway. J Pharmacol Exp Ther. 2011;337:16–23.
14. Chen C, Uludag H, Wang Z, Jiang H. Noggin suppression decreases bmp-2-induced osteogenesis of human bone marrow-derived mesenchymal stem cells in vitro. J Cell Biochem. 2012;113:3672–80.
15. Massague J, Wotton D. Transcriptional control by the tgf-beta/smad signaling system. EMBO J. 2000;19:1745–54.
16. Heldin CH, Miyazono K, ten Dijke P. Tgf-beta signalling from cell membrane to nucleus through smad proteins. Nature. 1997;390:465–71.
17. Galvin KM, Donovan MJ, Lynch CA, Meyer RI, Paul RJ, Lorenz JN, Fairchild-Huntress V, Dixon KL, Dunmore JH, Gimbrone Jr MA, Falb D, Huszar D. A role for smad6 in development and homeostasis of the cardiovascular system. Nat Genet. 2000;24:171–4.
18. Clevers H. Wnt/beta-catenin signaling in development and disease. Cell. 2006;127:469–80.
19. Logan CY, Nusse R. The wnt signaling pathway in development and disease. Annu Rev Cell Dev Biol. 2004;20:781–810.
20. Caira FC, Stock SR, Gleason TG, McGee EC, Huang J, Bonow RO, Spelsberg TC, McCarthy PM, Rahimtoola SH, Rajamannan NM. Human degenerative valve disease is associated with up-regulation of low-density lipoprotein receptor-related protein 5 receptor-mediated bone formation. J Am Coll Cardiol. 2006;47:1707–12.
21. Rajamannan NM. The role of lrp5/6 in cardiac valve disease: experimental hypercholesterolemia in the apoe-/-/lrp5-/- mice. J Cell Biochem. 2011;112: 2987–91.
22. Rajamannan NM. The role of lrp5/6 in cardiac valve disease: Ldl-density-pressure theory. J Cell Biochem. 2011;112:2222–9.
23. Rajamannan NM. Oxidative-mechanical stress signals stem cell niche mediated lrp5 osteogenesis in enos(-/-) null mice. J Cell Biochem. 2012;113:1623–34.
24. Rajamannan NM, Subramaniam M, Caira F, Stock SR, Spelsberg TC. Atorvastatin inhibits hypercholesterolemia-induced calcification in the aortic valves via the lrp5 receptor pathway. Circulation. 2005;112:I229–34.
25. Chen JH, Chen WL, Sider KL, Yip CY, Simmons CA. Beta-catenin mediates mechanically regulated, transforming growth factor-beta1-induced myofibroblast differentiation of aortic valve interstitial cells. Arterioscler Thromb Vasc Biol. 2011;31:590–7.
26. Yip CY, Chen JH, Zhao R, Simmons CA. Calcification by valve interstitial cells is regulated by the stiffness of the extracellular matrix. Arterioscler Thromb Vasc Biol. 2009;29:936–42.
27. Clark-Greuel JN, Connolly JM, Sorichillo E, Narula NR, Rapoport HS, Mohler 3rd ER, Gorman 3rd JH, Gorman RC, Levy RJ. Transforming growth factor-beta1 mechanisms in aortic valve calcification: increased alkaline phosphatase and related events. Ann Thorac Surg. 2007;83:946–53.
28. Jian B, Narula N, Li QY, Mohler 3rd ER, Levy RJ. Progression of aortic valve stenosis: Tgf-beta1 is present in calcified aortic valve cusps and promotes aortic valve interstitial cell calcification via apoptosis. Ann Thorac Surg. 2003;75:457–65; discussion 465–6.
29. Cushing MC, Liao JT, Anseth KS. Activation of valvular interstitial cells is mediated by transforming growth factor-beta1 interactions with matrix molecules. Matrix Biol. 2005;24:428–37.

30. Mohler 3rd ER, Gannon F, Reynolds C, Zimmerman R, Keane MG, Kaplan FS. Bone formation and inflammation in cardiac valves. Circulation. 2001;103:1522–8.
31. Fiers W, Beyaert R, Declercq W, Vandenabeele P. More than one way to die: apoptosis, necrosis and reactive oxygen damage. Oncogene. 1999;18:7719–30.
32. Kanduc D, Mittelman A, Serpico R, Sinigaglia E, Sinha AA, Natale C, Santacroce R, Di Corcia MG, Lucchese A, Dini L, Pani P, Santacroce S, Simone S, Bucci R, Farber E. Cell death: apoptosis versus necrosis (review). Int J Oncol. 2002;21:165–70.
33. Rajamannan NM, Sangiorgi G, Springett M, Arnold K, Mohacsi T, Spagnoli LG, Edwards WD, Tajik AJ, Schwartz RS. Experimental hypercholesterolemia induces apoptosis in the aortic valve. J Heart Valve Dis. 2001;10:371–4.
34. Shuvy M, Abedat S, Beeri R, Valitsky M, Daher S, Kott-Gutkowski M, Gal-Moscovici A, Sosna J, Rajamannan NM, Lotan C. Raloxifene attenuates gas6 and apoptosis in experimental aortic valve disease in renal failure. Am J Physiol Heart Circ Physiol. 2011;300:H1829–40.
35. Bonfoco E, Krainc D, Ankarcrona M, Nicotera P, Lipton SA. Apoptosis and necrosis: two distinct events induced, respectively, by mild and intense insults with n-methyl-d-aspartate or nitric oxide/superoxide in cortical cell cultures. Proc Natl Acad Sci U S A. 1995;92:7162–6.
36. Mori K, Emoto M, Inaba M. Fetuin-a and the cardiovascular system. Adv Clin Chem. 2012;56:175–95.
37. Mori K, Emoto M, Inaba M. Fetuin-a: a multifunctional protein. Recent Patent Endocr Metab Immune Drug Discov. 2011;5:124–46.
38. Jahnen-Dechent W, Heiss A, Schafer C, Ketteler M. Fetuin-a regulation of calcified matrix metabolism. Circ Res. 2011;108:1494–509.
39. Schafer C, Heiss A, Schwarz A, Westenfeld R, Ketteler M, Floege J, Muller-Esterl W, Schinke T, Jahnen-Dechent W. The serum protein alpha 2-heremans-schmid glycoprotein/fetuin-a is a systemically acting inhibitor of ectopic calcification. J Clin Invest. 2003;112:357–66.
40. Westenfeld R, Schafer C, Kruger T, Haarmann C, Schurgers LJ, Reutelingsperger C, Ivanovski O, Drueke T, Massy ZA, Ketteler M, Floege J, Jahnen-Dechent W. Fetuin-a protects against atherosclerotic calcification in ckd. J Am Soc Nephrol. 2009;20:1264–74.
41. Schure R, Costa KD, Rezaei R, Lee W, Laschinger C, Tenenbaum HC, McCulloch CA. Impact of matrix metalloproteinases on inhibition of mineralization by fetuin. J Periodontal Res. 2013;48:357–66.
42. Chen G, Li Y, Tian J, Zhang L, Jean-Charles P, Gobara N, Nan C, Jin JP, Huang XP. Application of echocardiography on transgenic mice with cardiomyopathies. Biochem Res Int. 2012;2012:715197.
43. Hinton Jr RB, Alfieri CM, Witt SA, Glascock BJ, Khoury PR, Benson DW, Yutzey KE. Mouse heart valve structure and function: echocardiographic and morphometric analyses from the fetus through the aged adult. Am J Physiol Heart Circ Physiol. 2008;294:H2480–8.
44. Budoff MJ, Takasu J, Katz R, Mao S, Shavelle DM, O'Brien KD, Blumenthal RS, Carr JJ, Kronmal R. Reproducibility of ct measurements of aortic valve calcification, mitral annulus calcification, and aortic wall calcification in the multi-ethnic study of atherosclerosis. Acad Radiol. 2006;13:166–72.
45. Kudo T, Fukuchi K, Annala AJ, Chatziioannou AF, Allada V, Dahlbom M, Tai YC, Inubushi M, Huang SC, Cherry SR, Phelps ME, Schelbert HR. Noninvasive measurement of myocardial activity concentrations and perfusion defect sizes in rats with a new small-animal positron emission tomograph. Circulation. 2002;106:118–23.
46. Schlosser T, Malyar N, Jochims M, Breuckmann F, Hunold P, Bruder O, Erbel R, Barkhausen J. Quantification of aortic valve stenosis in mri-comparison of steady-state free precession and fast low-angle shot sequences. Eur Radiol. 2007;17:1284–90.
47. Urboniene D, Haber I, Fang YH, Thenappan T, Archer SL. Validation of high-resolution echocardiography and magnetic resonance imaging vs. High-fidelity catheterization in experimental pulmonary hypertension. Am J Physiol Lung Cell Mol Physiol. 2010;299:L401–12.
48. Patten RD, Aronovitz MJ, Bridgman P, Pandian NG. Use of pulse wave and color flow doppler echocardiography in mouse models of human disease. J Am Soc Echocardiogr. 2002;15:708–14.
49. Pollick C, Hale SL, Kloner RA. Echocardiographic and cardiac doppler assessment of mice. J Am Soc Echocardiogr. 1995;8:602–10.
50. Ram R, Mickelsen DM, Theodoropoulos C, Blaxall BC. New approaches in small animal echocardiography: imaging the sounds of silence. Am J Physiol Heart Circ Physiol. 2011;301:H1765–80.
51. Roosens B, Bala G, Droogmans S, Van Camp G, Breyne J, Cosyns B. Animal models of organic heart valve disease. Int J Cardiol. 2013;165:398–409.
52. Rottman JN, Ni G, Brown M. Echocardiographic evaluation of ventricular function in mice. Echocardiography. 2007;24:83–9.
53. Rottman JN, Ni G, Khoo M, Wang Z, Zhang W, Anderson ME, Madu EC. Temporal changes in ventricular function assessed echocardiographically in conscious and anesthetized mice. J Am Soc Echocardiogr. 2003;16:1150–7.
54. Yang XP, Liu YH, Rhaleb NE, Kurihara N, Kim HE, Carretero OA. Echocardiographic assessment of cardiac function in conscious and anesthetized mice. Am J Physiol. 1999;277:H1967–74.
55. Weiss RM, Miller JD, Heistad DD. Fibrocalcific aortic valve disease: opportunity to understand disease mechanisms using mouse models. Circ Res. 2013;113:209–22.
56. Chu Y, Lund DD, Weiss RM, Brooks RM, Doshi H, Hajj GP, Sigmund CD, Heistad DD. Pioglitazone attenuates valvular calcification induced by hypercholesterolemia. Arterioscler Thromb Vasc Biol. 2013;33:523–32.

57. Kupfahl C, Honold M, Meinhardt G, Vogelsberg H, Wagner A, Mahrholdt H, Sechtem U. Evaluation of aortic stenosis by cardiovascular magnetic resonance imaging: comparison with established routine clinical techniques. Heart. 2004;90:893–901.
58. Berry CJ, Thedens DR, Light-McGroary K, Miller JD, Kutschke W, Zimmerman KA, Weiss RM. Effects of deep sedation or general anesthesia on cardiac function in mice undergoing cardiovascular magnetic resonance. J Cardiovasc Magn Reson. 2009;11:16.
59. Berry CJ, Miller JD, McGroary K, Thedens DR, Young SG, Heistad DD, Weiss RM. Biventricular adaptation to volume overload in mice with aortic regurgitation. J Cardiovasc Magn Reson. 2009;11:27.
60. Bonow RO, Carabello BA, Chatterjee K, de Leon Jr AC, Faxon DP, Freed MD, Gaasch WH, Lytle BW, Nishimura RA, O'Gara PT, O'Rourke RA, Otto CM, Shah PM, Shanewise JS. 2008 Focused update incorporated into the acc/aha 2006 guidelines for the management of patients with valvular heart disease: a report of the American College of Cardiology/American Heart Association Task Force on Practice Guidelines (Writing Committee to revise the 1998 guidelines for the management of patients with valvular heart disease): Endorsed by the Society of Cardiovascular Anesthesiologists, Society for Cardiovascular Angiography and Interventions, and Society of Thoracic Surgeons. Circulation. 2008;118:e523–661.
61. Barrick CJ, Roberts RB, Rojas M, Rajamannan NM, Suitt CB, O'Brien KD, Smyth SS, Threadgill DW. Reduced egfr causes abnormal valvular differentiation leading to calcific aortic stenosis and left ventricular hypertrophy in c57bl/6j but not 129 s1/svimj mice. Am J Physiol Heart Circ Physiol. 2009;297:H65–75.
62. Hanada K, Vermeij M, Garinis GA, de Waard MC, Kunen MG, Myers L, Maas A, Duncker DJ, Meijers C, Dietz HC, Kanaar R, Essers J. Perturbations of vascular homeostasis and aortic valve abnormalities in fibulin-4 deficient mice. Circ Res. 2007;100:738–46.
63. Moura LM, Ramos SF, Zamorano JL, Barros IM, Azevedo LF, Rocha-Goncalves F, Rajamannan NM. Rosuvastatin affecting aortic valve endothelium to slow the progression of aortic stenosis. J Am Coll Cardiol. 2007;49:554–61.
64. Miller JD, Chu Y, Brooks RM, Richenbacher WE, Pena-Silva R, Heistad DD. Dysregulation of antioxidant mechanisms contributes to increased oxidative stress in calcific aortic valvular stenosis in humans. J Am Coll Cardiol. 2008;52:843–50.
65. Liberman M, Bassi E, Martinatti MK, Lario FC, Wosniak Jr J, Pomerantzeff PM, Laurindo FR. Oxidant generation predominates around calcifying foci and enhances progression of aortic valve calcification. Arterioscler Thromb Vasc Biol. 2008;28:463–70.
66. Yang H, Roberts LJ, Shi MJ, Zhou LC, Ballard BR, Richardson A, Guo ZM. Retardation of atherosclerosis by overexpression of catalase or both cu/zn-superoxide dismutase and catalase in mice lacking apolipoprotein e. Circ Res. 2004;95:1075–81.
67. Nguyen Dinh Cat A, Touyz RM. A new look at the renin-angiotensin system–focusing on the vascular system. Peptides. 2011;32:2141–50.
68. Durante A, Peretto G, Laricchia A, Ancona F, Spartera M, Mangieri A, Cianflone D. Role of the renin-angiotensin-aldosterone system in the pathogenesis of atherosclerosis. Curr Pharm Des. 2012;18:981–1004.
69. Helske S, Lindstedt KA, Laine M, Mayranpaa M, Werkkala K, Lommi J, Turto H, Kupari M, Kovanen PT. Induction of local angiotensin ii-producing systems in stenotic aortic valves. J Am Coll Cardiol. 2004;44:1859–66.
70. Merryman WD, Schoen FJ. Mechanisms of calcification in aortic valve disease: role of mechanokinetics and mechanodynamics. Curr Cardiol Rep. 2013;15:355.
71. O'Brien KD, Probstfield JL, Caulfield MT, Nasir K, Takasu J, Shavelle DM, Wu AH, Zhao XQ, Budoff MJ. Angiotensin-converting enzyme inhibitors and change in aortic valve calcium. Arch Intern Med. 2005;165:858–62.
72. Arishiro K, Hoshiga M, Negoro N, Jin D, Takai S, Miyazaki M, Ishihara T, Hanafusa T. Angiotensin receptor-1 blocker inhibits atherosclerotic changes and endothelial disruption of the aortic valve in hypercholesterolemic rabbits. J Am Coll Cardiol. 2007;49:1482–9.
73. Anderson TJ. Nitric oxide, atherosclerosis and the clinical relevance of endothelial dysfunction. Heart Fail Rev. 2003;8:71–86.
74. Shimokawa H. Primary endothelial dysfunction: atherosclerosis. J Mol Cell Cardiol. 1999;31:23–37.
75. Channon KM, Qian H, George SE. Nitric oxide synthase in atherosclerosis and vascular injury: insights from experimental gene therapy. Arterioscler Thromb Vasc Biol. 2000;20:1873–81.
76. Ozaki M, Kawashima S, Yamashita T, Hirase T, Namiki M, Inoue N, Hirata K, Yasui H, Sakurai H, Yoshida Y, Masada M, Yokoyama M. Overexpression of endothelial nitric oxide synthase accelerates atherosclerotic lesion formation in apoe-deficient mice. J Clin Invest. 2002;110:331–40.
77. Rajamannan NM, Subramaniam M, Stock SR, Stone NJ, Springett M, Ignatiev KI, McConnell JP, Singh RJ, Bonow RO, Spelsberg TC. Atorvastatin inhibits calcification and enhances nitric oxide synthase production in the hypercholesterolaemic aortic valve. Heart. 2005;91:806–10.
78. Aicher D, Urbich C, Zeiher A, Dimmeler S, Schafers HJ. Endothelial nitric oxide synthase in bicuspid aortic valve disease. Ann Thorac Surg. 2007;83:1290–4.
79. McNeill E, Channon KM. The role of tetrahydrobiopterin in inflammation and cardiovascular disease. Thromb Haemost. 2012;108:832–9.
80. Kennedy JA, Hua X, Mishra K, Murphy GA, Rosenkranz AC, Horowitz JD. Inhibition of calcifying nodule formation in cultured porcine aortic valve cells by nitric oxide donors. Eur J Pharmacol. 2009;602:28–35.
81. Mehrabian M, Demer LL, Lusis AJ. Differential accumulation of intimal monocyte-macrophages relative

to lipoproteins and lipofuscin corresponds to hemodynamic forces on cardiac valves in mice. Arterioscler Thromb. 1991;11:947–57.
82. Kupreishvili K, Baidoshvili A, ter Weeme M, Huybregts MA, Krijnen PA, Van Hinsbergh VW, Stooker W, Eijsman L, Niessen HW. Degeneration and atherosclerosis inducing increased deposition of type IIA secretory phospholipase A2, C-reactive protein and complement in aortic valves cause neutrophilic granulocyte influx. J Heart Valve Dis. 2011;20:29–36.
83. ter Weeme M, Vonk AB, Kupreishvili K, van Ham M, Zeerleder S, Wouters D, Stooker W, Eijsman L, Van Hinsbergh VW, Krijnen PA, Niessen HW. Activated complement is more extensively present in diseased aortic valves than naturally occurring complement inhibitors: a sign of ongoing inflammation. Eur J Clin Invest. 2010;40:4–10.
84. Shuvy M, Ben Ya'acov A, Zolotarov L, Lotan C, Ilan Y. Beta glycosphingolipids suppress rank expression and inhibit natural killer t cell and cd8+ accumulation in alleviating aortic valve calcification. Int J Immunopathol Pharmacol. 2009;22:911–8.
85. Isoda K, Matsuki T, Kondo H, Iwakura Y, Ohsuzu F. Deficiency of interleukin-1 receptor antagonist induces aortic valve disease in balb/c mice. Arterioscler Thromb Vasc Biol. 2010;30:708–15.
86. Cote N, Mahmut A, Bosse Y, Couture C, Page S, Trahan S, Boulanger MC, Fournier D, Pibarot P, Mathieu P. Inflammation is associated with the remodeling of calcific aortic valve disease. Inflammation. 2013;36:573–81.
87. Lommi JI, Kovanen PT, Jauhiainen M, Lee-Rueckert M, Kupari M, Helske S. High-density lipoproteins (HDL) are present in stenotic aortic valves and may interfere with the mechanisms of valvular calcification. Atherosclerosis. 2011;219:538–44.
88. Mohty D, Pibarot P, Despres JP, Cote C, Arsenault B, Cartier A, Cosnay P, Couture C, Mathieu P. Association between plasma LDL particle size, valvular accumulation of oxidized LDL, and inflammation in patients with aortic stenosis. Arterioscler Thromb Vasc Biol. 2008;28:187–93.
89. Kapadia SR, Yakoob K, Nader S, Thomas JD, Mann DL, Griffin BP. Elevated circulating levels of serum tumor necrosis factor-alpha in patients with hemodynamically significant pressure and volume overload. J Am Coll Cardiol. 2000;36:208–12.
90. Olson EN. Things are developing in cardiology. Circ Res. 1997;80:604–6.
91. Csiszar A, Ungvari Z. Endothelial dysfunction and vascular inflammation in type 2 diabetes: interaction of age/rage and tnf-alpha signaling. Am J Physiol Heart Circ Physiol. 2008;295:H475–6.
92. Warnock JN, Nanduri B, Pregonero Gamez CA, Tang J, Koback D, Muir WM, Burgess SC. Gene profiling of aortic valve interstitial cells under elevated pressure conditions: modulation of inflammatory gene networks. Int J Inflamm. 2011;2011:176412.
93. Lai CF, Shao JS, Behrmann A, Krchma K, Cheng SL, Towler DA. Tnfr1-activated reactive oxidative species signals up-regulate osteogenic msx2 programs in aortic myofibroblasts. Endocrinology. 2012;153:3897–910.
94. Kawai M, Sousa KM, MacDougald OA, Rosen CJ. The many facets of ppargamma: novel insights for the skeleton. Am J Physiol Endocrinol Metab. 2010;299:E3–9.
95. Takada I, Kouzmenko AP, Kato S. Wnt and ppargamma signaling in osteoblastogenesis and adipogenesis. Nat Rev Rheumatol. 2009;5:442–7.
96. Li F, Cai Z, Chen F, Shi X, Zhang Q, Chen S, Shi J, Wang DW, Dong N. Pioglitazone attenuates progression of aortic valve calcification via down-regulating receptor for advanced glycation end products. Basic Res Cardiol. 2012;107:306.
97. Weiss RM, Lund DD, Chu Y, Brooks RM, Zimmerman KA, El Accaoui R, Davis MK, Hajj GP, Zimmerman MB, Heistad DD. Osteoprotegerin inhibits aortic valve calcification and preserves valve function in hypercholesterolemic mice. PLoS One. 2013;8:e65201.
98. Kaden JJ, Bickelhaupt S, Grobholz R, Haase KK, Sarikoc A, Kilic R, Brueckmann M, Lang S, Zahn I, Vahl C, Hagl S, Dempfle CE, Borggrefe M. Receptor activator of nuclear factor kappab ligand and osteoprotegerin regulate aortic valve calcification. J Mol Cell Cardiol. 2004;36:57–66.
99. Olesen M, Skov V, Mechta M, Mumm BH, Rasmussen LM. No influence of opg and its ligands, rankl and trail, on proliferation and regulation of the calcification process in primary human vascular smooth muscle cells. Mol Cell Endocrinol. 2012;362:149–56.
100. Atkins GJ, Welldon KJ, Halbout P, Findlay DM. Strontium ranelate treatment of human primary osteoblasts promotes an osteocyte-like phenotype while eliciting an osteoprotegerin response. Osteoporos Int. 2009;20:653–64.
101. Chan KL, Teo K, Dumesnil JG, Ni A, Tam J. Effect of lipid lowering with rosuvastatin on progression of aortic stenosis: results of the aortic stenosis progression observation: measuring effects of rosuvastatin (astronomer) trial. Circulation. 2010;121:306–14.
102. Cowell SJ, Newby DE, Prescott RJ, Bloomfield P, Reid J, Northridge DB, Boon NA. A randomized trial of intensive lipid-lowering therapy in calcific aortic stenosis. N Engl J Med. 2005;352:2389–97.
103. Rossebo AB, Pedersen TR, Boman K, Brudi P, Chambers JB, Egstrup K, Gerdts E, Gohlke-Barwolf C, Holme I, Kesaniemi YA, Malbecq W, Nienaber CA, Ray S, Skjaerpe T, Wachtell K, Willenheimer R. Intensive lipid lowering with simvastatin and ezetimibe in aortic stenosis. N Engl J Med. 2008;359:1343–56.
104. Aikawa E, Nahrendorf M, Sosnovik D, Lok VM, Jaffer FA, Aikawa M, Weissleder R. Multimodality molecular imaging identifies proteolytic and osteogenic activities in early aortic valve disease. Circulation. 2007;115:377–86.

11 Hemodynamic Mechanisms of Bicuspid Aortic Valve Calcification and Aortopathy

Philippe Sucosky

Introduction

The Aortic Valve-Ascending Aorta Complex

The bicuspid aortic valve (BAV) is the most common congenital valvular defect and is present in 2–3 % of the general population [29, 75, 87]. It is characterized by the presence of two leaflets of unequal size (resulting from the fusion of two of the three leaflets) and a fibrous raphe at the location of congenital fusion [13, 54]. The most prevalent type-I morphology [80] features a relatively normal non-coronary leaflet, three sinuses and one raphe joining two underdeveloped coronary leaflets [21, 89]. Besides those differences, BAV leaflets exhibit the same typical tri-layered structure as normal tricuspid aortic valve (TAV) leaflets. The ventricularis faces the left ventricle and consists of elastin fibers intertwined with radially-oriented collagen fibers. The fibrosa faces the aorta and also consists of elastin and collagen fibers but oriented along the circumferential direction. Between those two layers, the spongiosa, which consists essentially of glycosaminoglycan (GAG), is presumed to play the role of a lubricating layer allowing the fibrosa and ventricularis to slide and deform relative to each other. The valvular cell population consists of endothelial cells (VECs) lining the outermost layer of the ventricularis and fibrosa and interstitial cells (VICs), which include fibroblasts, myofibroblasts and smooth muscle cells (SMCs). Downstream of the valve is the ascending aorta (AA) that stems from the sinotubular junction and extends to the aortic arch. The proximal AA is a curved arterial segment consisting of three layers. The intima lines the inner surface of the lumen and consists of a monolayer of endothelial cells (ECs). The media, which consists of SMCs and connective tissue, regulates the contractility of the vessel wall. Lastly, the adventitia lines the outer surface of the artery and consists primarily of connective tissue.

P. Sucosky, PhD
Department of Aerospace and Mechanical Engineering, Eck Institute for Global Health, University of Notre Dame, 143 Multidisciplinary Research Building, Notre Dame, IN 46556-5637, USA
e-mail: philippe.sucosky@nd.edu

BAV Complications

Calcific Aortic Valve Disease

Despite its limited prevalence, the BAV malformation has emerged as the first indication for surgical valve replacement and as a major risk factor for calcific aortic valve disease (CAVD) [46, 76, 87]. This condition covers a spectrum of disease from initial changes in the cell biology of the valve leaflets, through early calcification, tissue remodeling and aortic sclerosis, to outflow obstruction and aortic stenosis [63, 67, 71]. The later stages are characterized by fibrotic thickening of the leaflets and side-specific formation of calcium nodules near the fibrosa [68]. Recent

N.M. Rajamannan (ed.), *Molecular Biology of Valvular Heart Disease*,
DOI 10.1007/978-1-4471-6350-3_11,

studies have evidenced the multi-faceted aspect of CAVD, which involves actively regulated processes including inflammation [63, 65, 68], osteogenesis [50, 66, 73], apoptosis [15, 85] and necrosis [36, 90]. Valvular inflammation, which is the hallmark of the early stage of CAVD, has been linked to the activation of the leaflet endothelium via enhanced expression of cell adhesion molecules [2, 25, 26, 55]. Elevated expressions of pro-inflammatory cytokines such as bone morphogenic proteins (BMPs) [35, 52] and transforming growth factor-β1 (TGF-β1) [15, 34] have also been observed in early calcific lesions, demonstrating the key role played by paracrine signaling in CAVD development. Downstream of those events, the VICs switch from a quiescent fibroblastic phenotype to an activated myofibroblastic phenotype expressing α-smooth muscle actin (α-SMA) or to an osteoblastic phenotype marked by runt-related transcription factor 2 (Runx2) [1, 48, 53, 86]. Those activated phenotypes result in the progressive loss of valvular homeostasis caused by the increased imbalance between matrix metalloproteinases (MMPs) and their tissue inhibitors (TIMPs) [22, 37], and the upregulation of cathepsins [5, 27, 70]. The ultimate end-point of the disease, which consists of the formation of calcific lesions, is associated with an upregulation of BMPs [47, 48, 51, 64].

Aortic Dilation

The BAV anatomy is also associated with a spectrum of secondary aortopathies, such as aortic dilation and subsequent dissection [11, 33, 38, 49, 62]. Acute aortic dissection occurs five to ten times more frequently and at an earlier age in BAV patients than in TAV patients [18, 33, 74, 87]. The dilation and thinning of the AA downstream of a BAV, which is the precursor event to dissection, is marked by structural wall abnormalities including SMC apoptosis and depletion, elastic fiber degeneration and abnormal ECM remodeling [84], which localize primarily to the convexity of the aortic wall [16, 17]. The degenerative remodeling of the aortic wall has been associated with the upregulation of the matrix metalloproteinases MMP-2 and MMP-9 [12, 20, 32, 57], two proteolytic enzymes that degrade collagen, elastin and fibronectin, and the downregulation of fibrillin-1 [20, 57], a fundamental protein component of the aortic media that links elastin to SMCs and is essential for the formation of elastic fibers. Fibrillin-1 depletion causes the loss of connectivity between SMCs and microfibrils, which results in decreased tissue elasticity, SMC apoptosis and MMP activation [20].

Hemodynamic Theory of BAV Disease

Mechano-Potential Etiology of BAV Disease

Valvular tissue interacts with its surrounding mechanical environment to drive critical cell-ECM processes [4, 39, 69]. As compared to stretch and pressure which propagate throughout the leaflet and stimulate both VECs and VICs, fluid shear stress (FSS) is an interfacial stress sensed primarily by VECs. Recent studies have evidenced the existence of an intricate communication network between the two cell types in the TAV, as illustrated by the change in valvular matrix stiffness in response to humoral endothelial stimulation [19], the modulation of valvular remodeling by FSS magnitude [69], and the upregulation of pro-inflammatory cytokines in the leaflet interstitium following endothelial exposure to abnormal FSS [28, 82]. Those observations suggest the ability of FSS to alter VIC phenotype and the potential of the abnormal BAV flow to trigger early CAVD pathogenesis. Similarly, given the particular sensitivity of the arterial wall to its surrounding hemodynamics [40–42, 44, 45, 59, 60] and the capability of hemodynamic stress alterations to mediate vascular remodeling, the apparent correlation between the asymmetric wall dilation and the asymmetric flow patterns in BAV AAs [16, 17] supports a hemodynamic etiology by which BAV flow abnormalities and associated FSS could trigger molecular pathways leading to the progressive weakening of the aortic wall [7, 10, 24]. The hemodynamic theory of BAV calcification and aortopathy can be illustrated as an irreversible feedback loop in which the abnormal BAV anatomy would subject the leaflets and the wall

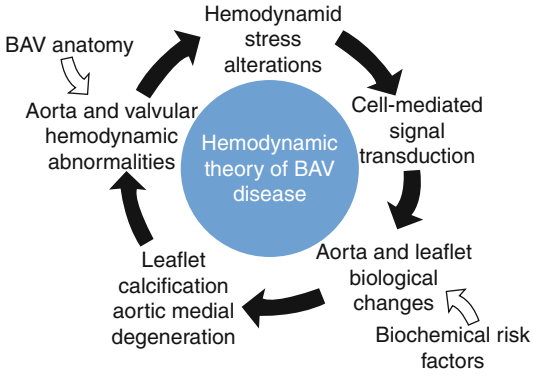

Fig. 11.1 Hemodynamic theory of BAV disease

of the ascending aorta to local FSS alterations (Fig. 11.1). Those alterations could be sensed by the endothelial cells lining the leaflets and the aortic wall and then transduced into different biological responses that would lead ultimately to the formation of calcific lesions on the leaflets or to the progressive degeneration of the aortic media. The resulting stiffening of the BAV leaflets and dilation of the proximal AA would lead in turn to further structural and hemodynamic alterations, which would amplify the cycle. While this etiology is supported by an increasing number of studies, its rigorous assessment requires the investigation of the potential cause-and-effect relationships between the local hemodynamics of BAV leaflets and the aortic wall and the local biology.

Ex Vivo Assessment

The evidence of contrasted hemodynamic environments on TAV and BAV leaflets and in TAV and BAV AAs has provided a rationale for mechanobiological studies investigating the effects of both environments on tissue biology. Historically, those studies have put more emphasis on the biological description of mechano-sensitive processes in simplified biological models (e.g., genes, cells) than on the implementation of realistic mechanical stimuli due to the limited knowledge of the native valvular mechanical environment and the challenge to replicate it on intact tissue in the laboratory setting. Although cell and gene studies have generated invaluable data on the isolated response of each cell type to various biochemical and mechanical factors, they do not account for the higher-level response resulting from the native cell-cell and cell-ECM interactions. In light of the recommendations made by the NIH working group on aortic stenosis [72], the assessment of the hemodynamic theory of BAV disease requires a thorough knowledge of the hemodynamic abnormalities generated by the BAV anatomy and the rigorous investigation of the cause-and-effects relationships between the local tissue hemodynamics and the local biological response. Those requirements can be satisfied through the implementation of an integrative approach combining state-of-the-art flow diagnostic techniques and innovative tissue conditioning methods. Anchored between the in vivo approach conducted in the native environment and the in vitro approach implemented in the laboratory with a simplified biological model, the ex vivo strategy, which maintains the native tissue architecture and mechanical environment in the laboratory, offers a higher level of fidelity to native processes and generates data that can be directly translated to the clinical disease. This approach has been implemented to validate the potential involvement of hemodynamic stresses in the pathogenesis of BAV calcification and aortic dilation. The overall strategy consists of: (1) the development of realistic computational models and flow diagnostic techniques to characterize the degree of hemodynamic abnormality on BAV leaflets and in BAV ascending aortas; (2) the design of sophisticated bioreactors to replicate those hemodynamic environments in the laboratory; and (3) the implementation of biological techniques to assess the biological changes experienced by normal valvular or aortic tissue subjected to native BAV hemodynamic abnormalities.

BAV Hemodynamics

Valvular Hemodynamic Abnormalities

Global Valvular Flow Characteristics

Echocardiography initially revealed that the BAV orifice presents an elliptical shape, an intrinsic

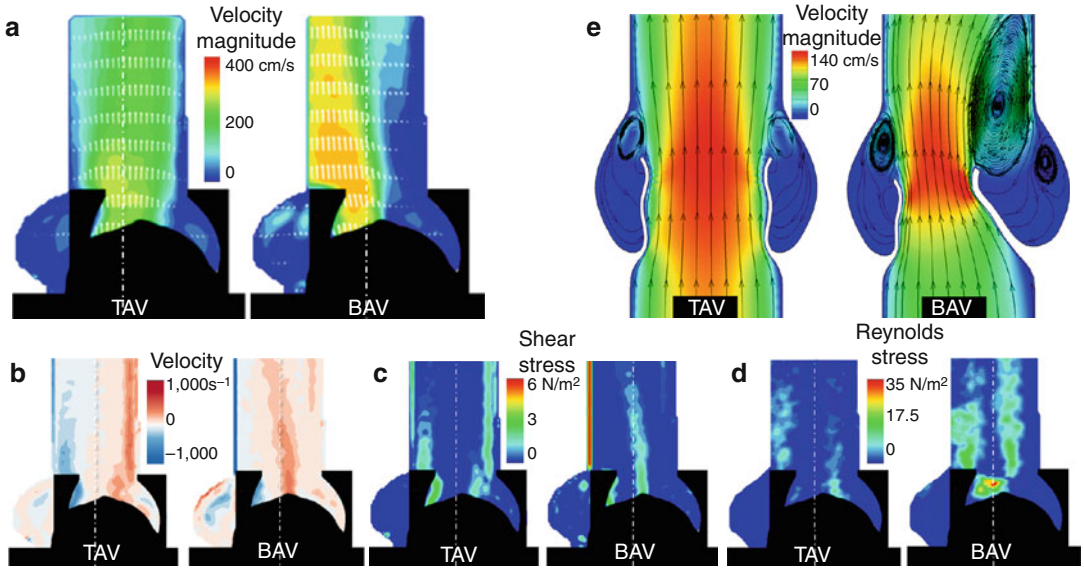

Fig. 11.2 Experimental and computational characterizations of TAV and BAV flow: (**a**) peak-systolic flow velocity, (**b**) vorticity, (**c**) viscous shear stress and (**d**) Reynolds stress fields measured using PIV, and (**e**) peak-systolic flow velocity field computed using FSI modeling

degree of stenosis, an eccentric systolic jet and abnormal downstream helical flow patterns [23, 56]. During the acceleration phase, the pressure gradient imposed across the valve produces a forward flow which contributes to the opening of the leaflets. Regardless of the anatomy, the flow downstream of the leaflets is divided into two regions: (1) a jet originating from the valvular orifice; and (2) a recirculation region marked by the presence of vortices located between the leaflet fibrosa and the wall of the aortic sinus.

The emergence of a hemodynamic theory of BAV calcification has motivated the investigation of BAV hemodynamics at higher resolutions using experimental and computational approaches to understand the flow through the valve and its contribution to the mechanisms of valvular heart disease. Particle-image velocimetry has been implemented to compare the flow, energy loss and valvular performance through a TAV and a BAV over a range of flow rates spanning the cardiac cycle [79]. The TAV was based on a native porcine valve while the type-I BAV anatomy was generated by suturing the two coronary leaflets of a porcine TAV. The measurements confirmed the existence of the same two flow regions and valve orifice shapes as those previously described by echocardiography. The analysis of the velocity fields also demonstrated an average BAV jet skewness of 4.4° over the range of flow rates tested, which contrasted with the average 1.9° skewness exhibited by the TAV jet. The higher maximum jet velocity observed downstream of the BAV (3.3 m/s) relative to the TAV (2.8 m/s) at 20 L/min suggested an intrinsic degree of stenosis in the BAV anatomy (Fig. 11.2a). High vorticity levels were detected in the shear layers extending from the tip of the leaflets, where the flow separates (Fig. 11.2b). As compared to the shear layers produced in the wake of the TAV, which remained essentially symmetric and parallel to the valve axis, the BAV shear layers exhibited the same skewness as the jet, which resulted in an asymmetric vorticity distribution characterized by high magnitude near the non-coronary leaflet and low magnitude near the fused leaflet. The particular skewness of the BAV jet was shown to force the shear layer extending from the non-coronary leaflet to roll up into the non-coronary sinus, which could adversely affect the closure of that leaflet during diastole. Regardless of the valve anatomy, the maximum viscous shear

stress was detected near the flow separation point at the tip of the leaflets (Fig. 11.2c). However, the measurements indicated important differences in shear stress magnitude with the TAV generating a maximum in-plane viscous shear stress of 20 dyn/cm^2 and the BAV 25 dyn/cm^2 immediately downstream of the leaflet tip. The BAV was also shown to generate a higher degree of turbulence, as indicated by the 62 % increase in maximum Reynolds stress relative to the TAV (Fig. 11.2d). Despite its intrinsic degree of stenosis marked by a 18 % increase in maximum jet velocity and 7 % decrease in effective orifice area (EOA) relative to the TAV at the maximum flow rate, the BAV was shown to generate only a 3 % increase in energy loss (EL) relative to the TAV and its average energy loss index (ELI, 2.10 cm^2/m^2) remained above the clinical threshold characterizing severe aortic stenosis (1.35 cm^2/m^2). This experimental study demonstrated the dependence of valvular hemodynamics on valvular anatomy but suggested importantly the ability of the BAV to function as a normal valve despite its intrinsic degree of stenosis.

Hemodynamic differences between the TAV and BAV have also been investigated computationally. In a recent study, fluid-structure interaction (FSI) models were developed to characterize the flow, leaflet dynamics and regional leaflet FSS in idealized TAV and type-I BAV anatomies [14]. The two-dimensional (2D) models captured the flow characteristics observed experimentally. The flow simulations indicated the existence of a jet aligned along the centerline of the aorta in the TAV and a jet slightly skewed toward the non-coronary leaflet in the BAV (Fig. 11.2e). Additionally, under a similar pressure gradient, the predicted TAV orifice was wider than the BAV orifice, regardless of the degree of BAV asymmetry. The high spatial resolution offered by the computational models permitted to characterize features of the vorticity field not captured experimentally. At peak systole, the 2D TAV geometry was shown to generate two symmetric vortices partially located in the aortic sinus between the tip of the leaflets and the sinotubular junction. In contrast, the type-I BAV generated two asymmetric vortices, with the vortex extending from the fused leaflet exhibiting a larger circulation than that extending from the non-coronary leaflet. In addition, the BAV generated a third vortex behind the fused leaflet. Those important differences in vorticity dynamics may explain the lower hemodynamic performance of the BAV relative to the TAV.

Valvular FSS Characteristics

The regional FSS distribution on the surface of the valve leaflets is an important indicator of how blood flow interacts with the valve. The FSI models described above were used to quantify the local FSS experienced on both sides of TAV and type-I BAV leaflets in the base, belly and tip regions of each leaflet (Fig. 11.3). The maximum FSS predicted near the tip of the TAV, non-coronary BAV and fused BAV leaflets was 71, 56 and 71 dyn/cm^2, respectively. The inspection of the FSS variations predicted on the three leaflet types (i.e., TAV leaflets, fused and non-coronary BAV leaflets) confirmed the existence of a mostly unidirectional (i.e., positive) FSS on the ventricularis and a bidirectional (i.e., alternatively positive and negative) FSS on the fibrosa. The comparison of the results obtained in the three regions (i.e., tip, belly and base) of one particular leaflet also indicated significant spatial variations in FSS magnitude and pulsatility along the ventricularis and fibrosa. In addition, the asymmetry of the BAV anatomy resulted in a higher degree of FSS fluctuations on the fibrosa of the non-coronary leaflet than on the fibrosa of the fused leaflet. Those observations were supported by the quantitative analysis of the local oscillatory shear index (OSI) and temporal shear magnitude (TSM). Regardless of the valve anatomy, the leaflet ventricularis was shown to consistently experience a more pulsatile FSS (leaflet-average OSI < 0.08) than the fibrosa (leaflet-average OSI > 0.13). The TSM predictions also evidenced strong differences in FSS magnitude between the ventricularis and fibrosa of each leaflet. Regardless of the leaflet anatomy, the FSS magnitude predicted along the ventricularis (leaflet-average TSM > 6.70 dyn/cm^2) was consistently higher than that computed along the fibrosa (leaflet-average TSM < 1.34 dyn/cm^2). An interesting characteristic was the strong site-specific

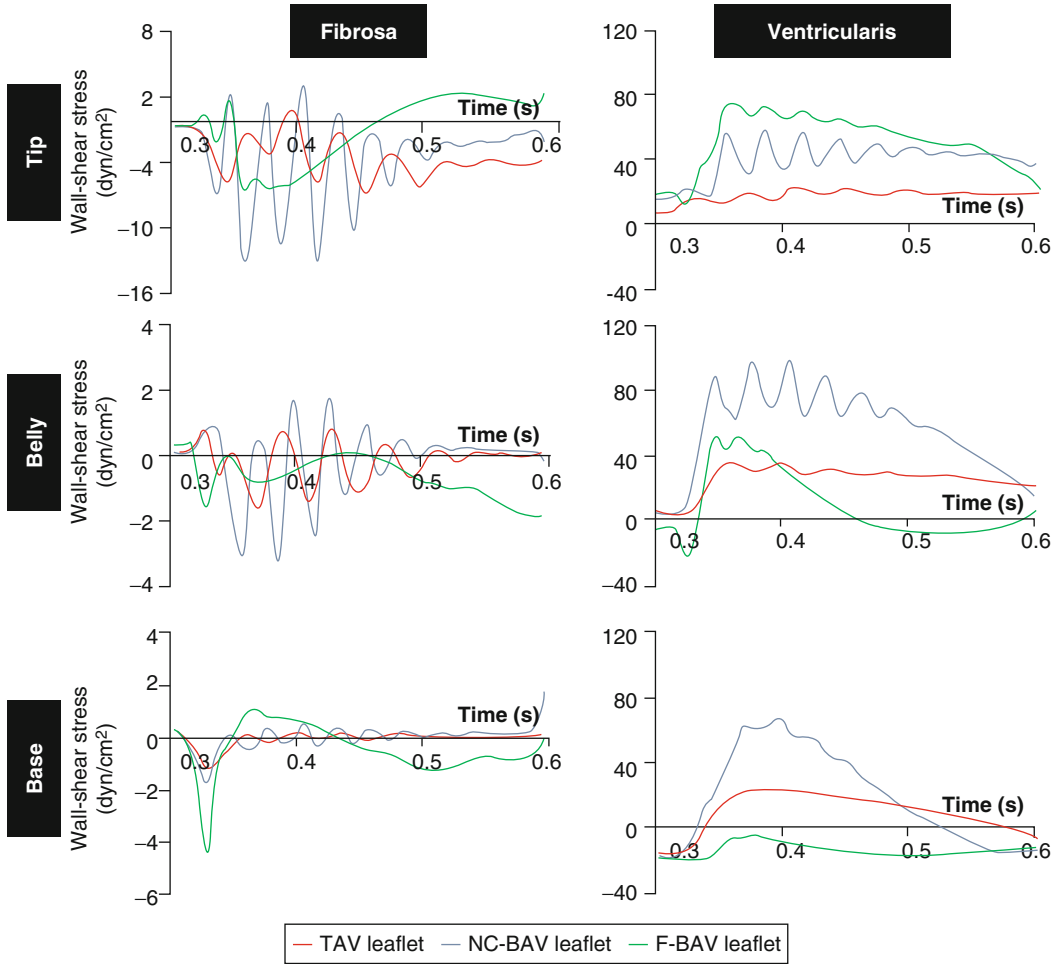

Fig. 11.3 FSI predictions of the temporal FSS variations in the base, belly and tip of TAV and type-I BAV leaflets (*NC* non-coronary leaflet, *F* fused leaflet)

nature of the fibrosa FSS. The OSI computed on the TAV leaflet fibrosa decreased from the base (OSI = 0.19) to the tip (OSI = 0.01) of the leaflets, suggesting the attenuation of the oscillatory nature of the waveform along this path. Conversely, the calculation of the regional TSM indicated an increase in FSS magnitude along the same path (from 0.07 dyn/cm^2 at the base to 1.68 dyn/cm^2 at the tip). A similar trend was observed along the fibrosa of the non-coronary BAV leaflet. In contrast, the regional FSS experienced by the fused BAV leaflet fibrosa was characterized by pulsatility in the base and belly regions (OSI = 0.21 and 0.01, respectively) and oscillation in the tip region (OSI = 0.38), moderate magnitude in the base and belly regions (TSM = 0.43 and 0.41 dyn/cm^2, respectively) and high magnitude in the tip region (TSM = 1.34 dyn/cm^2). Those observations confirmed the existence of complex cause-and-effect relationships between anatomical leaflet abnormalities and FSS abnormalities.

BAV Aorta Hemodynamic Abnormalities

Global BAV Aorta Flow Characteristics

Phase contrast-magnetic resonance imaging (PC-MRI) studies have demonstrated the existence of an abnormal right-handed helical flow in

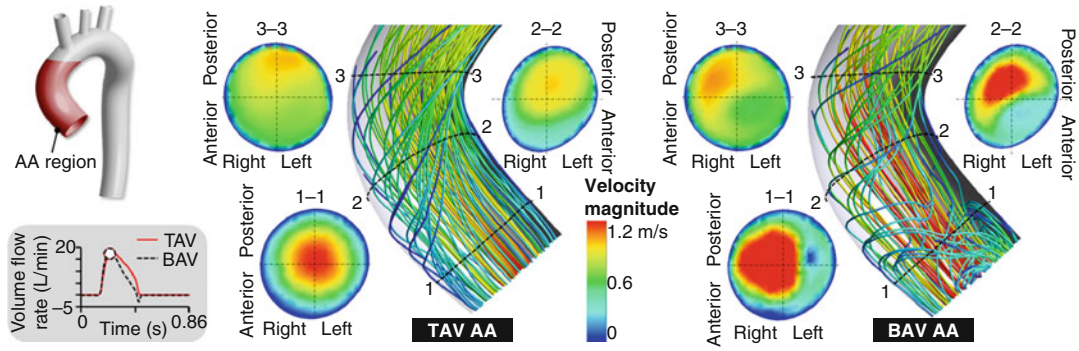

Fig. 11.4 Snapshots of the peak-systolic velocity and streamline fields in the TAV AA and BAV AA predicted by FSI

the AA of BAV patients characterized by higher rotationality, systolic flow angle and FSS than in TAV patients [6, 10]. Echocardiographic studies have revealed higher peak systolic flow velocities and FSS in the vicinity of the anterolateral region of the AA (region most prone to dilation) in BAV patients than in TAV patients [9]. In vitro flow measurements using particle image velocimetry (PIV) on tissue TAV and BAV models have confirmed those in vivo observations and have demonstrated the existence of a skewed BAV systolic jet and the generation of a strong vortex in the non-coronary leaflet sinus [77, 79].

The flow in the BAV AA was recently quantified using FSI modeling [3]. A realistic three-dimensional (3D) human AA anatomy extending from the sinotubular junction to a portion of the descending aorta and including the proximal segments of the braciocephalic, left common carotid and left subclavian arteries was reconstructed from computed tomography images. The aortic wall was modeled as a linear elastic and isotropic material, while blood was approximated as a Newtonian fluid. The boundary conditions imposed at the four outlets consisted of physiologic pressure waveforms, while the 3D pulsatile TAV and type-I BAV velocity profiles prescribed at the inlet of the model were generated by extrapolating the 2D velocity profiles predicted by the previously described FSI valve models. The model was used to predict the time-varying flow velocity and streamline fields produced in the two anatomies during an entire cardiac cycle. The flow characteristics predicted in the TAV and BAV AAs exhibited strong differences, which were first observed at peak systole (Fig. 11.4) and persisted throughout the deceleration phase. Consistent with previous phase-contrast magnetic resonance imaging (PC-MRI) measurements [30, 31], the flow in the TAV AA was shown to follow a smooth trajectory essentially parallel to the aortic wall, without any significant secondary flow effects. In contrast, the eccentricity of the BAV orifice jet gave rise to helical flow structures that originated in the proximal section of the AA and propagated downstream. The model also predicted the existence of a systolic retrograde flow near the BAV sinotubular junction, i.e., a phenomenon already reported in vivo [6, 30].

BAV Aorta FSS Characteristics

The same FSI model was used to quantify the FSS environments generated in the TAV AA and type-I BAV AA (Fig. 11.5a). The analysis of the spatial FSS distributions in the TAV AA and BAV AA revealed the impact of the flow abnormalities described above on the viscous force experienced by the aortic wall. While the TAV AA and BAV AA regional FSS remained essentially similar during the acceleration phase, the BAV jet skewness exposed the proximal section of the AA to higher FSS magnitudes than the TAV at peak systole. In contrast, consistent with previous PC-MRI flow measurements [8], the FSS environments generated by the TAV and BAV in the distal region of the AA were essentially similar. The most substantial FSS differences were predicted during the deceleration phase, where the decrease in flow momentum produced an overall

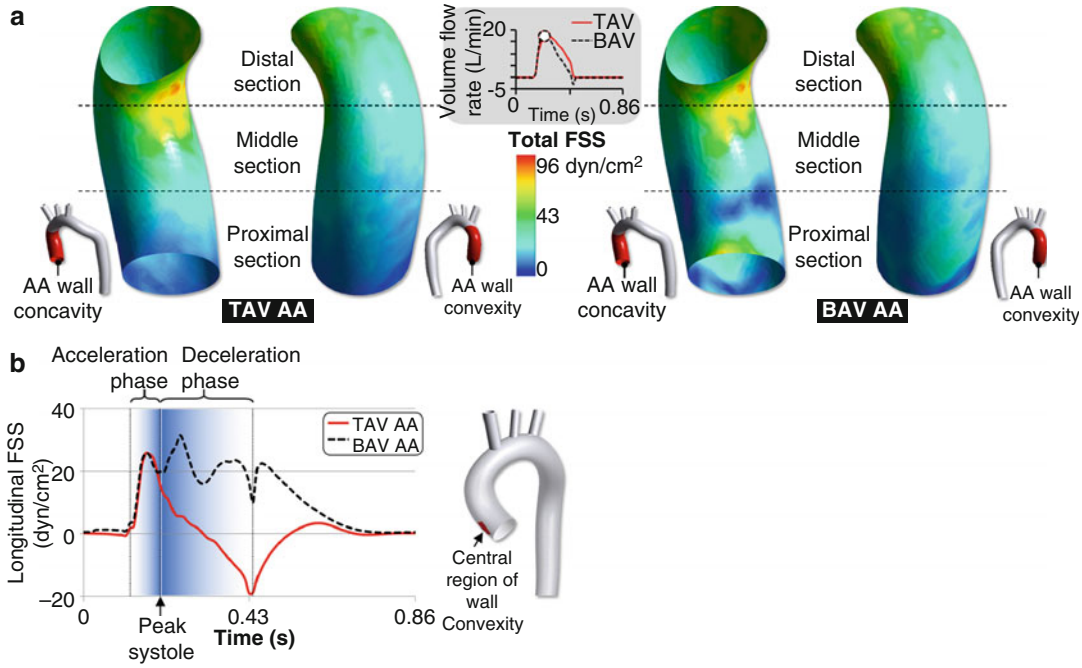

Fig. 11.5 Computational characterization of the FSS distributions in the TAV AA and BAV AA: (**a**) peak-systolic regional FSS distributions on the concavity (*left*) and convexity (*right*) of the TAV AA and BAV AA, and (**b**) temporal variations of the longitudinal FSS predicted at the center of the TAV AA and BAV AA convexity over one cardiac cycle

decrease in FSS in the TAV AA, while the widespread flow abnormalities in the BAV AA further increased the high FSS levels predicted at peak systole. The FSI model was also used to compare the temporal variations of the longitudinal FSS (i.e., FSS component acting in the direction of the main flow) at the center of the TAV and BAV AA wall convexity (Fig. 11.5b). The results suggested the existence of a unidirectional FSS ranging between 0.3 and 31.5 dyn/cm^2 on the BAV aortic wall and a bidirectional FSS on the TAV aortic wall ranging between −19.0 and +25.8 dyn/cm^2. During the acceleration phase ($0.12<t<0.20$ s), both waveforms were shown to be essentially similar in direction and magnitude. At peak systole ($t=0.20$ s), the BAV AA convexity was subjected to a higher longitudinal FSS (19.9 dyn/cm^2) than its TAV counterpart (15.0 dyn/cm^2). The deceleration phase ($0.20<t<0.44$ s) was associated with marked differences in FSS directionality and magnitude between the two anatomies. The longitudinal FSS in the convexity of the TAV AA decreased progressively, changed sign during the deceleration phase ($t=0.32$ s) and attained its minimum level (−19 dyn/cm^2) at the end of the deceleration phase. During the same phase, the longitudinal FSS in the convexity of the BAV AA remained positive and oscillated around its peak-systolic level. Despite its lower transvalvular flow rate, the BAV subjected the AA convexity to much higher TSM and peak FSS levels than the TAV (133 and 22 % increase, respectively). The OSI predictions confirmed the bidirectional and oscillatory nature of the longitudinal FSS in the TAV AA convexity (OSI = 0.42) and the perfectly unidirectional and pulsatile FSS (OSI = 0.00) in the BAV AA convexity. Lastly, the average longitudinal FSS predicted in the region of impingement of the valvular jet on the AA wall, which was 11.4 dyn/cm^2 in the BAV AA and 4.9 dyn/cm^2 in the TAV AA, agreed with previous PC-MRI measurements suggesting FSS of the order of 9 ± 3 and 4 ± 3 dyn/cm^2, respectively, over the same regions [8]. Those computational results

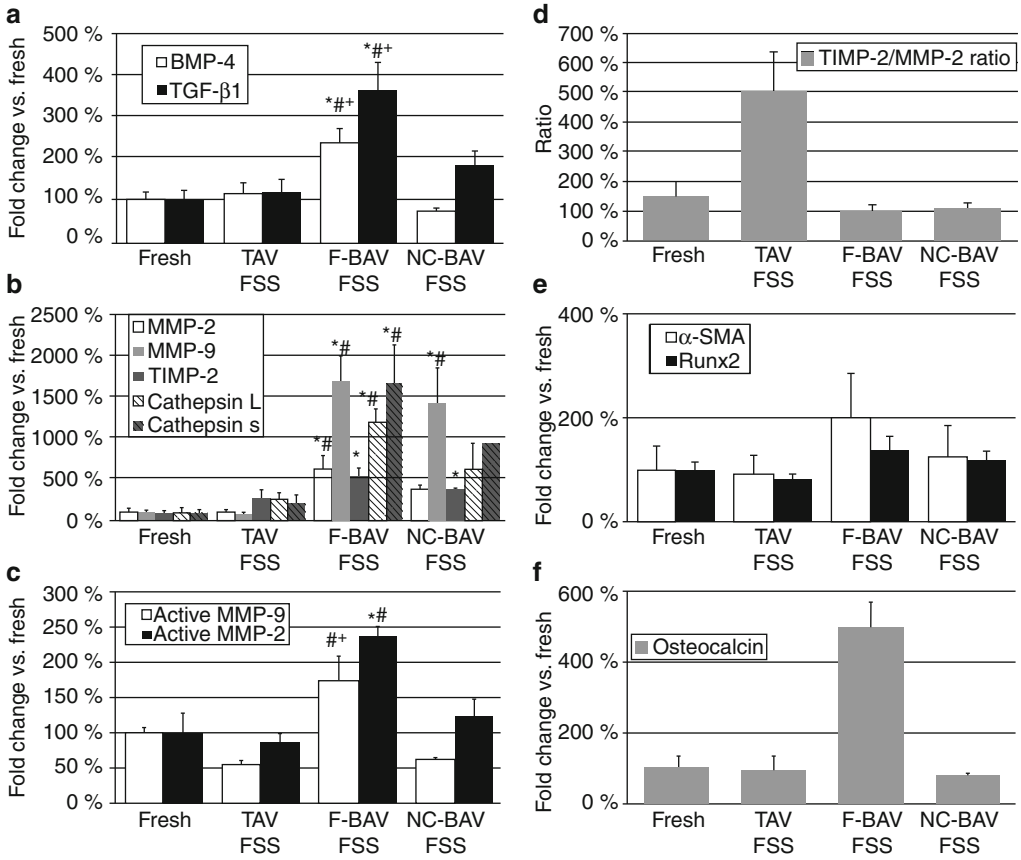

Fig. 11.6 Effects of TAV and BAV leaflet FSS on porcine leaflet pathogenesis: (**a**) BMP-4 and TGF-β1 expression, (**b**) MMP-2, MMP-9, TIMP-2, cathepsin L and cathepsin S expression, (**c**) MMP-2 and MMP-9 gelatinase activity, (**d**) TIMP-2/MMP-2 ratio, (**e**) α-SMA and Runx2 expression, and (**f**) osteocalcin expression (*NC* non-coronary leaflet, *F* fused leaflet, * $p<0.05$ vs. fresh control, # $p<0.05$ vs. TAV FSS, + $p<0.05$ vs. NC-BAV FSS, $N=3$)

confirmed the intrinsic degree of hemodynamic abnormality of the BAV AA and re-emphasized the possibility of a flow mechanism of BAV secondary aortopathy.

Hemodynamic Mechanisms of BAV Disease

Role of Hemodynamic Stresses in Calcific BAV Disease

The acute effects of native BAV FSS abnormalities on CAVD pathogenesis have been isolated ex vivo [83]. Porcine aortic valve leaflets were subjected to the native FSS predicted via FSI modeling on the surface of TAV leaflets and fused and non-coronary type-I BAV leaflets for 48 h in a double-sided shear stress bioreactor. Immunostaining, immunoblotting and zymography were performed to characterize endothelial activation, pro-inflammatory paracrine signaling, extracellular matrix remodeling and markers involved in valvular interstitial cell activation and osteogenesis (Fig. 11.6). The main contribution of this study was the demonstration of the key role played by BAV hemodynamic stress abnormalities in the initiation and progression of CAVD. While TAV and non-coronary BAV leaflet FSS essentially maintained valvular homeostasis, fused BAV leaflet FSS promoted fibrosa endothelial activation, paracrine signaling (2.4-fold and 3.7-fold increase in BMP-4 and TGF-β1, respectively, relative to fresh controls), catabolic

enzyme secretion (6.3-fold, 16.8-fold, 11.7-fold, 16.7-fold and 5.5-fold increase in MMP-2, MMP-9, cathepsin L, cathepsin S and TIMP-2, respectively) and activity (1.7-fold and 2.4-fold increase in MMP-2 and MMP-9 activity, respectively), and bone matrix synthesis (5-fold increase in osteocalcin). In contrast, BAV FSS did not significantly affect α-SMA and Runx2 expressions and TIMP/MMP ratio. Another important finding was the side-specific expression of cell-adhesion molecules on the fibrosa following leaflet exposure to BAV FSS abnormalities. This result was consistent with the previously established existence of pro- and anti-inflammatory VEC phenotypes on the leaflet fibrosa and ventricularis, respectively, which contribute to the specific vulnerability of the leaflet fibrosa to calcification [81]. In addition to this side-specificity, the study indicated that FSS-induced endothelial activation was leaflet-specific in the BAV and occurred primarily on the fused leaflet. The ex vivo results also provided further insights into the role played by VECs and VICs in FSS mechanotransduction. As compared to stretch and pressure, which propagate throughout the leaflet and stimulate both VECs and VICs, FSS is an interfacial stress sensed primarily by VECs. Interestingly, while BAV FSS abnormalities were shown to upregulate cell-adhesion molecule expression in VECs lining the leaflet fibrosa, all other downstream effects (i.e., cytokine expression, ECM remodeling, osteogenesis) are VIC-specific processes. This suggests that VECs are able not only to sense FSS abnormalities but also to transduce those signals deeper in the tissue by altering VIC function. Although the mode of communication between the two cell types remains largely unknown, the increased BMP-4 and TGF-β1 expressions detected in response to BAV FSS abnormalities provided further evidence of the involvement of paracrine signaling in VEC-VIC communication and its role in the transduction of FSS abnormalities into a pathological response.

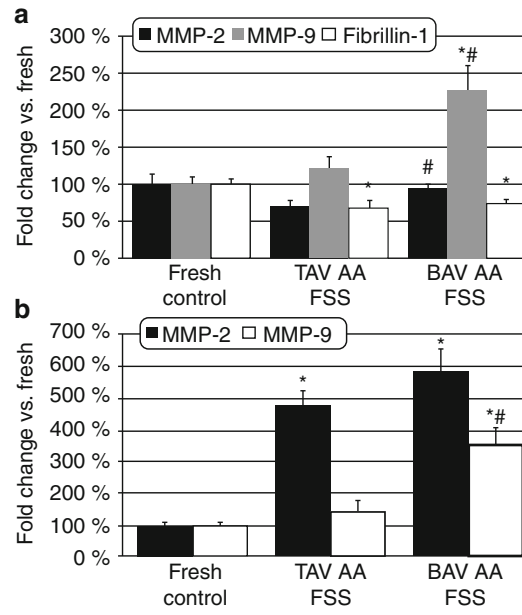

Fig. 11.7 Effects of TAV and BAV AA FSS on porcine aortic medial remodeling: (**a**) MMP-2, MMP-9 and fibrillin-1 expression (* $p<0.05$ vs. fresh control, # $p<0.05$ vs. TAV AA FSS), and (**b**) MMP-2 and MMP-9 gelatinase activity (* $p<0.01$ vs. fresh control, # $p<0.02$ vs. TAV AA FSS, $N=3$)

Role of Hemodynamic Stresses in BAV Ascending Aortic Dilation

Another ex vivo study isolated the contribution of BAV hemodynamic abnormalities on AA remodeling by subjecting porcine aortic tissue specimens to the local FSS environment predicted via FSI modeling downstream of the TAV or a type-I BAV [3]. The biological response was investigated via immunostaining, immunoblotting and zymography. The key contribution of this study was the demonstration of the capability of BAV hemodynamics alone to trigger vascular remodeling events involved in the early stage of aortic dilation. In the absence of any underlying congenital or biological wall abnormality, the exposure of normal porcine ascending aortic tissue to BAV AA FSS resulted in significant increases in MMP-2 and MMP-9 expressions (1.3-fold and 1.9-fold, respectively; $p<0.05$) relative to tissue conditioned under TAV AA FSS (Fig. 11.7). Increased expression of matrix-degrading proteins has already been observed in dilated aortas [12, 32, 43, 57, 88] and has been correlated with previous reports of medial degeneration in BAV AAs [20, 61, 78]. In addition, while MMP-2 activity was upregulated under BAV AA FSS, MMP-9 activity remained

essentially similar to that measured under TAV AA FSS. Similar trends have been reported in BAV AAs, which exhibited a two-fold increase in MMP-2 activity but no change in MMP-9 activity relative to TAV AAs [20]. Those results can be put in perspective of previous studies that have evidenced the preferential expression of matrix proteins and abnormal cytoskeletal rearrangement on the convexity of dilated BAV AAs, which seem to correlate with the established asymmetric stress distribution [16, 17, 58]. The differential ECM protein expression measured in the ex vivo study on the convexity of non-dilated AAs in response to TAV and BAV flow and the asymmetric ECM degradation observed on the convexity and concavity of dilated BAV AAs could stem from the same driving mechanism involving the particular sensitivity of vascular tissue to FSS magnitude and directional characteristics. In addition, the implementation of an ex vivo approach, which permitted to maintain the native interplay between ECs, SMCs and the ECM, provided important insights into the involvement of EC-SMC communication pathways in the transduction of BAV hemodynamic abnormalities into a pathological response. In fact, regardless of the mechanical treatment, MMP expression was only detected in the SMC-populated medial layer. Given that FSS is an interfacial stress sensed primarily by ECs, this result suggested that FSS disturbances generated by the BAV may act directly on the lipid bilayer of the AA wall and activate structures capable of transducing those mechanical abnormalities into downstream biochemical signals altering SMC function.

Conclusion

Those studies provide compelling support to the hemodynamic theory of BAV disease and suggest the unique capability of BAV hemodynamic stress abnormalities to trigger early CAVD pathogenesis and aortic medial degeneration in the absence of any underlying genetic defect. Experimental and computational flow diagnostic techniques have provided new insights into the impact of valvular anatomical defects on the hemodynamic stresses experienced by the leaflet and the ascending aortic wall. The implementation of sophisticated bioreactors capable of exposing normal tissue to those native hemodynamic abnormalities in the laboratory setting have demonstrated the sensitivity of valvular and vascular tissue to FSS abnormalities and suggested a direct correlation between the local degree of FSS abnormality and the severity of the pathological response. Mechanobiological studies harnessing the power of computational flow models, tissue culture systems and biological assays may provide a new way to elucidate the pathogenesis of BAV disease, slow down the progression of BAV complications by manipulating mechanosensitive molecules and use hemodynamic stresses as predictors of BAV disease progression in patient-specific anatomies.

Acknowledgments Those studies were supported in part by a National Science Foundation faculty early CAREER grant CMMI-1148558, an American Heart Association scientist development grant 11SDG7600103 and Faculty Seed Funds from the College of Engineering at the University of Notre Dame.

References

1. Aikawa E, Nahrendorf M, Sosnovik D, et al. Multimodality molecular imaging identifies proteolytic and osteogenic activities in early aortic valve disease. Circulation. 2007;115:377–86. doi:10.1161/CIRCULATIONAHA.106.654913.
2. Aikawa E, Whittaker P, Farber M, et al. Human semilunar cardiac valve remodeling by activated cells from fetus to adult: implications for postnatal adaptation, pathology, and tissue engineering. Circulation. 2006;113:1344–52. doi:10.1161/CIRCULATIONAHA.105.591768.
3. Atkins SK, Cao K, Rajamannan NM, Sucosky P. Bicuspid aortic valve hemodynamics induces abnormal medial remodeling in the convexity of porcine ascending aortas. Biomech Model Mechanobiol. 2014 (under review)
4. Balachandran K, Konduri S, Sucosky P, et al. An ex vivo study of the biological properties of porcine aortic valves in response to circumferential cyclic stretch. Ann Biomed Eng. 2006;34:1655–65. doi:10.1007/s10439-006-9167-8.
5. Balachandran K, Sucosky P, Jo H, Yoganathan AP. Elevated cyclic stretch alters matrix remodeling in aortic valve cusps – implications for degenerative aortic valve disease? Am J Physiol Heart Circ Physiol. 2009;296:H756–64. doi:10.1152/ajpheart.00900.2008.
6. Barker AJ, Lanning C, Shandas R. Quantification of hemodynamic wall shear stress in patients with

bicuspid aortic valve using phase-contrast MRI. Ann Biomed Eng. 2010;38:788–800. doi:10.1007/s10439-009-9854-3.
7. Barker AJ, Markl M. The role of hemodynamics in bicuspid aortic valve disease. Eur J Cardiothorac Surg. 2011;39:805–6. doi:10.1016/j.ejcts.2011.01.006.
8. Barker AJ, Markl M, Bürk J, et al. Bicuspid aortic valve is associated with altered wall shear stress in the ascending aorta. Circ Cardiovasc Imaging. 2012;5:457–66. doi:10.1161/CIRCIMAGING.112.973370.
9. Bauer M, Siniawski H, Pasic M, et al. Different hemodynamic stress of the ascending aorta wall in patients with bicuspid and tricuspid aortic valve. J Card Surg. 2006;21:218–20. doi:10.1111/j.1540-8191.2006.00219.x.
10. Bissell MM, Hess AT, Biasiolli L, et al. Aortic dilation in bicuspid aortic valve disease: flow pattern is a major contributor and differs with valve fusion type. Circ Cardiovasc Imaging. 2013;6:499–507. doi:10.1161/CIRCIMAGING.113.000528.
11. Bonderman D, Gharehbaghi-Schnell E, Wollenek G, et al. Mechanisms underlying aortic dilatation in congenital aortic valve malformation. Circulation. 1999;99:2138–43.
12. Boyum J, Fellinger EK, Schmoker JD, et al. Matrix metalloproteinase activity in thoracic aortic aneurysms associated with bicuspid and tricuspid aortic valves. J Thorac Cardiovasc Surg. 2004;127:686–91. doi:10.1016/j.jtcvs.2003.11.049.
13. Braverman AC, Guven H, Beardslee MA, et al. The bicuspid aortic valve. Curr Probl Cardiol. 2005;30:470–522. doi:10.1016/j.cpcardiol.2005.06.002.
14. Chandra S, Rajamannan NM, Sucosky P. Computational assessment of bicuspid aortic valve wall-shear stress: implications for calcific aortic valve disease. Biomech Model Mechanobiol. 2012;11:1085–96. doi:10.1007/s10237-012-0375-x.
15. Clark-Greuel JN, Connolly JM, Sorichillo E, et al. Transforming growth factor-beta1 mechanisms in aortic valve calcification: increased alkaline phosphatase and related events. Ann Thorac Surg. 2007;83:946–53. doi:10.1016/j.athoracsur.2006.10.026.
16. Della Corte A, Quarto C, Bancone C, et al. Spatiotemporal patterns of smooth muscle cell changes in ascending aortic dilatation with bicuspid and tricuspid aortic valve stenosis: focus on cell-matrix signaling. J Thorac Cardiovasc Surg. 2008;135:8–18. doi:10.1016/j.jtcvs.2007.09.009.
17. Cotrufo M, Della Corte A, De Santo LS, et al. Different patterns of extracellular matrix protein expression in the convexity and the concavity of the dilated aorta with bicuspid aortic valve: preliminary results. J Thorac Cardiovasc Surg. 2005;130:504–11. doi:10.1016/j.jtcvs.2005.01.016.
18. Edwards WD, Leaf DS, Edwards JE. Dissecting aortic aneurysm associated with congenital bicuspid aortic valve. Circulation. 1978;57:1022–5.
19. El-Hamamsy I, Balachandran K, Yacoub MH, et al. Endothelium-dependent regulation of the mechanical properties of aortic valve cusps. J Am Coll Cardiol. 2009;53:1448–55. doi:10.1016/j.jacc.2008.11.056.
20. Fedak PWM, de Sa MPL, Verma S, et al. Vascular matrix remodeling in patients with bicuspid aortic valve malformations: implications for aortic dilatation. J Thorac Cardiovasc Surg. 2003;126:797–806. doi:10.1016/S0022-5223(03)00398-2.
21. Fernandes SM, Sanders SP, Khairy P, et al. Morphology of bicuspid aortic valve in children and adolescents. J Am Coll Cardiol. 2004;44:1648–51. doi:10.1016/j.jacc.2004.05.063.
22. Fondard O, Detaint D, Iung B, et al. Extracellular matrix remodelling in human aortic valve disease: the role of matrix metalloproteinases and their tissue inhibitors. Eur Heart J. 2005;26:1333–41. doi:10.1093/eurheartj/ehi248.
23. Fowles RE, Martin RP, Abrams JM, et al. Two-dimensional echocardiographic features of bicuspid aortic valve. Chest. 1979;75:434–40.
24. Girdauskas E, Borger MA, Secknus MA, et al. Is aortopathy in bicuspid aortic valve disease a congenital defect or a result of abnormal hemodynamics? A critical reappraisal of a one-sided argument. Eur J Cardiothorac Surg. 2011;39:809–14. doi:10.1016/j.ejcts.2011.01.001.
25. Goldbarg SH, Elmariah S, Miller MA, Fuster V. Insights into degenerative aortic valve disease. J Am Coll Cardiol. 2007;50:1205–13. doi:10.1016/j.jacc.2007.06.024.
26. Hakuno D, Kimura N, Yoshioka M, Fukuda K. Molecular mechanisms underlying the onset of degenerative aortic valve disease. J Mol Med (Berl). 2009;87:17–24. doi:10.1007/s00109-008-0400-9.
27. Helske S, Syvaranta S, Lindstedt KA, et al. Increased expression of elastolytic cathepsins S, K, and V and their inhibitor cystatin C in stenotic aortic valves. Arterioscler Thromb Vasc Biol. 2006;26:1791–8. doi:10.1161/01.ATV.0000228824.01604.63.
28. Hoehn D, Sun L, Sucosky P. Role of pathologic shear stress alterations in aortic valve endothelial activation. Cardiovasc Eng Technol. 2010;1:165–78. doi:10.1007/s13239-010-0015-5.
29. Hoffman JI, Kaplan S. The incidence of congenital heart disease. J Am Coll Cardiol. 2002;39:1890–900. doi:10.1016/S0735-1097(02)01886-7.
30. Hope MD, Hope TA, Meadows AK, et al. Bicuspid aortic valve: four-dimensional MR evaluation of ascending aortic systolic flow patterns. Radiology. 2010;255:53–61. doi:10.1148/radiol.09091437.
31. Hope MD, Meadows AK, Hope TA, et al. Images in cardiovascular medicine. Evaluation of bicuspid aortic valve and aortic coarctation with 4D flow magnetic resonance imaging. Circulation. 2008;117:2818–9. doi:10.1161/CIRCULATIONAHA.107.760124.
32. Ikonomidis JS, Jones JA, Barbour JR, et al. Expression of matrix metalloproteinases and endogenous inhibitors within ascending aortic aneurysms of patients with bicuspid or tricuspid aortic valves. J Thorac Cardiovasc Surg. 2007;133:1028–36. doi:10.1016/j.jtcvs.2006.10.083.
33. Januzzi JL, Isselbacher EM, Fattori R, et al. Characterizing the young patient with aortic dissection: results from the International Registry of Aortic

Dissection (IRAD). J Am Coll Cardiol. 2004;43:665–9. doi:10.1016/j.jacc.2003.08.054.
34. Jian B, Narula N, Li QY, et al. Progression of aortic valve stenosis: TGF-beta1 is present in calcified aortic valve cusps and promotes aortic valve interstitial cell calcification via apoptosis. Ann Thorac Surg. 2003;75:456–7. doi:10.1016/S0003-4975(02)04312-6.
35. Kaden JJ, Bickelhaupt S, Grobholz R, et al. Expression of bone sialoprotein and bone morphogenetic protein-2 in calcific aortic stenosis. J Heart Valve Dis. 2004;13:560–6.
36. Kaden JJ, Kilic R, Sarikoc A, et al. Tumor necrosis factor alpha promotes an osteoblast-like phenotype in human aortic valve myofibroblasts: a potential regulatory mechanism of valvular calcification. Int J Mol Med. 2005;16:869–72.
37. Kaden JJ, Vocke DC, Fischer CS, et al. Expression and activity of matrix metalloproteinase-2 in calcific aortic stenosis. Z Kardiol. 2004;93:124–30. doi:10.1007/s00392-004-1021-0.
38. Khoo C, Cheung C, Jue J. Patterns of aortic dilatation in bicuspid aortic valve-associated aortopathy. J Am Soc Echocardiogr. 2013;26:600–5. doi:10.1016/j.echo.2013.02.017.
39. Konduri S, Xing Y, Warnock JN, et al. Normal physiological conditions maintain the biological characteristics of porcine aortic heart valves: an ex vivo organ culture study. Ann Biomed Eng. 2005;33:1158–66.
40. Lehoux S, Castier Y, Tedgui A. Molecular mechanisms of the vascular responses to haemodynamic forces. J Intern Med. 2006;259:381–92. doi:10.1111/j.1365-2796.2006.01624.x.
41. Lehoux S, Tedgui A. Cellular mechanics and gene expression in blood vessels. J Biomech. 2003;36:631–43. doi:10.1016/S0021-9290(02)00441-4.
42. Lehoux S, Tedgui A. Signal transduction of mechanical stresses in the vascular wall. Hypertension. 1998;32:338–45. doi:10.1161/01.HYP.32.2.338.
43. LeMaire SA, Wang X, Wilks JA, et al. Matrix metalloproteinases in ascending aortic aneurysms: bicuspid versus trileaflet aortic valves. J Surg Res. 2005;123:40–8. doi:10.1016/j.jss.2004.06.007.
44. Levesque MJ, Liepsch D, Moravec S, Nerem RM. Correlation of endothelial cell shape and wall shear stress in a stenosed dog aorta. Arteriosclerosis. 1986;6:220–9.
45. Levesque MJ, Nerem RM. Shear stress effects on endothelial cell monolayer cultures. In: Dean RC and Nerem RM (eds) Bioprocess Eng Colloq. ASME, New York, p 47–50.
46. Lewin MB, Otto CM. The bicuspid aortic valve: adverse outcomes from infancy to old age. Circulation. 2005;111:832–4. doi:10.1161/01.CIR.0000157137.59691.0B.
47. Lian JB, Gundberg CM. Osteocalcin. Biochemical considerations and clinical applications. Clin Orthop Relat Res. 1988;226:267–91.
48. Liu AC, Joag VR, Gotlieb AI. The emerging role of valve interstitial cell phenotypes in regulating heart valve pathobiology. Am J Pathol. 2007;171:1407–18. doi:10.2353/ajpath.2007.070251.
49. McKusick VA. Association of congenital bicuspid aortic valve and erdheim's cystic medial necrosis. Lancet. 1972;1:1026–7.
50. Miller JD, Weiss RM, Heistad DD. Calcific aortic valve stenosis: methods, models, and mechanisms. Circ Res. 2011;108:1392–412. doi:10.1161/CIRCRESAHA.110.234138.
51. Mohler 3rd ER, Adam LP, McClelland P, et al. Detection of osteopontin in calcified human aortic valves. Arterioscler Thromb Vasc Biol. 1997;17:547–52. doi:10.1161/01.ATV.17.3.547.
52. Mohler 3rd ER, Gannon F, Reynolds C, et al. Bone formation and inflammation in cardiac valves. Circulation. 2001;103:1522–8.
53. Monzack EL, Masters KS. Can valvular interstitial cells become true osteoblasts? A side-by-side comparison. J Heart Valve Dis. 2011;20:449–63.
54. De Mozzi P, Longo UG, Galanti G, Maffulli N. Bicuspid aortic valve: a literature review and its impact on sport activity. Br Med Bull. 2008;85:63–85. doi:10.1093/bmb/ldn002.
55. Muller AM, Cronen C, Kupferwasser LI. Expression of endothelial cell adhesion molecules on heart valves: up-regulation in degeneration as well as acute endocarditis. J Pathol. 2000;191:54–60. doi:10.1002/(SICI)1096-9896(200005)191:1<54::AID-PATH568>3.0.CO;2-Y.
56. Nanda NC, Gramiak R, Manning J, et al. Echocardiographic recognition of the congenital bicuspid aortic valve. Circulation. 1974;49:870–5.
57. Nataatmadja M, West M, West J, et al. Abnormal extracellular matrix protein transport associated with increased apoptosis of vascular smooth muscle cells in marfan syndrome and bicuspid aortic valve thoracic aortic aneurysm. Circulation. 2003;108(Suppl):II329–34. doi:10.1161/01.cir.0000087660.82721.15.
58. Nathan DP, Xu C, Plappert T, et al. Increased ascending aortic wall stress in patients with bicuspid aortic valves. Ann Thorac Surg. 2011;92:1384–9. doi:10.1016/j.athoracsur.2011.04.118.
59. Nerem RM. Hemodynamics and the vascular endothelium. ASME J Biomech Eng. 1993;115:510. doi:10.1115/1.2895532.
60. Nerem RM, Alexander RW, Chappell DC, et al. The study of the influence of flow on vascular endothelial biology. Am J Med Sci. 1998;316:169–75.
61. Niwa K, Perloff JK, Bhuta SM, et al. Structural abnormalities of great arterial walls in congenital heart disease: light and electron microscopic analyses. Circulation. 2001;103:393–400. doi:10.1161/01.CIR.103.3.393.
62. Nkomo VT, Enriquez-Sarano M, Ammash NM, et al. Bicuspid aortic valve associated with aortic dilatation: a community-based study. Arterioscler Thromb Vasc Biol. 2003;23:351–6. doi:10.1161/01.ATV.0000055441.28842.0A.
63. O'Brien KD. Pathogenesis of calcific aortic valve disease: a disease process comes of age (and a good deal more). Arterioscler Thromb Vasc Biol. 2006;26:1721–8. doi:10.1161/01.ATV.0000227513.13697.ac.

64. O'Brien KD, Kuusisto J, Reichenbach DD, et al. Osteopontin is expressed in human aortic valvular lesions. Circulation. 1995;92:2163–8. doi:10.1161/01.CIR.92.8.216.
65. Olsson M, Dalsgaard CJ, Haegerstrand A, et al. Accumulation of T lymphocytes and expression of interleukin-2 receptors in nonrheumatic stenotic aortic valves. J Am Coll Cardiol. 1994;23:1162–70. doi:10.1016/0735-1097(94)90606-8.
66. Osman L, Yacoub MH, Latif N, et al. Role of human valve interstitial cells in valve calcification and their response to atorvastatin. Circulation. 2006;114:I547–52. doi:10.1161/CIRCULATIONAHA.105.001115. 114/1_suppl/I-547 [pii].
67. Otto CM. Valvular heart disease. 2nd ed. Philadelphia: Saunders; 2004. p. 598.
68. Otto CM, Kuusisto J, Reichenbach DD. Characterization of the early lesion of "degenerative" valvular aortic stenosis. Histological and immunohistochemical studies. Circulation. 1994;90:844–53. doi:10.1161/01.CIR.90.2.844.
69. Platt MO, Xing Y, Jo H, Yoganathan AP. Cyclic pressure and shear stress regulate matrix metalloproteinases and cathepsin activity in porcine aortic valves. J Heart Valve Dis. 2006;15:622–9.
70. Rabkin E, Aikawa M, Stone J, et al. Activated interstitial myofibroblasts express catabolic enzymes and mediate matrix remodeling in myxomatous heart valves. Circulation. 2000;104:2525–32. doi:10.1161/hc4601.099489.
71. Rajamannan NM. Calcific aortic stenosis: lessons learned from experimental and clinical studies. Arterioscler Thromb Vasc Biol. 2009;29:162–8. doi:10.1161/ATVBAHA.107.156752.
72. Rajamannan NM, Evans FJ, Aikawa E, et al. Calcific aortic valve disease: not simply a degenerative process: a review and agenda for research from the National Heart and Lung and Blood Institute Aortic Stenosis Working Group. Executive summary: calcific aortic valve disease-2011 update. Circulation. 2011;124:1783–91. doi:10.1161/CIRCULATIONAHA.110.006767.
73. Rajamannan NM, Subramaniam M, Rickard D, et al. Human aortic valve calcification is associated with an osteoblast phenotype. Circulation. 2003;107:2181–4. doi:10.1161/01.CIR.0000070591.21548.69. 01.CIR.0000070591.21548.69 [pii].
74. Roberts CS, Roberts WC. Dissection of the aorta associated with congenital malformation of the aortic valve. J Am Coll Cardiol. 1991;17:712–6.
75. Roberts WC. The congenitally bicuspid aortic valve. A study of 85 autopsy cases. Am J Cardiol. 1970;26:72–83. doi:10.1016/0002-9149(70)90761-7.
76. Roberts WC, Ko JM. Frequency by decades of unicuspid, bicuspid, and tricuspid aortic valves in adults having isolated aortic valve replacement for aortic stenosis, with or without associated aortic regurgitation. Circulation. 2005;111:920–5. doi:10.1161/01.CIR.0000155623.48408.C5.
77. Saikrishnan N, Yap C-H, Milligan NC, et al. In vitro characterization of bicuspid aortic valve hemodynamics using particle image velocimetry. Ann Biomed Eng. 2012;40:1760–75. doi:10.1007/s10439-012-0527-2.
78. Schmid F-X, Bielenberg K, Schneider A, et al. Ascending aortic aneurysm associated with bicuspid and tricuspid aortic valve: involvement and clinical relevance of smooth muscle cell apoptosis and expression of cell death-initiating proteins. Eur J Cardiothorac Surg. 2003;23:537–43. doi:10.1016/S1010-7940(02)00833-3.
79. Seaman C, Akingba AG, Sucosky P. Steady flow hemodynamic and energy loss measurements in normal and simulated calcified tricuspid and bicuspid aortic valves. J Biomech Eng. 2014. doi:10.1115/1.4026575
80. Sievers HH, Schmidtke C. A classification system for the bicuspid aortic valve from 304 surgical specimens. J Thorac Cardiovasc Surg. 2007;133:1226–33. doi:10.1016/j.jtcvs.2007.01.039.
81. Simmons CA, Grant GR, Manduchi E, Davies PF. Spatial heterogeneity of endothelial phenotypes correlates with side-specific vulnerability to calcification in normal porcine aortic valves. Circ Res. 2005;96:792–9. doi:10.1161/01.RES.0000161998.92009.64.
82. Sucosky P, Balachandran K, Elhammali A, et al. Altered shear stress stimulates upregulation of endothelial VCAM-1 and ICAM-1 in a BMP-4- and TGF-beta1-dependent pathway. Arterioscler Thromb Vasc Biol. 2009;29:254–60. doi:10.1161/ATVBAHA.108.176347.
83. Sun L, Chandra S, Sucosky P. Ex vivo evidence for the contribution of hemodynamic shear stress abnormalities to the early pathogenesis of calcific bicuspid aortic valve disease. PLoS One. 2012;7:e48843. doi:10.1371/journal.pone.0048843.
84. Tadros TM, Klein MD, Shapira OM. Ascending aortic dilatation associated with bicuspid aortic valve: pathophysiology, molecular biology, and clinical implications. Circulation. 2009;119:880–90. doi:10.1161/CIRCULATIONAHA.108.795401.
85. Tanaka K, Sata M, Fukuda D, et al. Age-associated aortic stenosis in apolipoprotein E-deficient mice. J Am Coll Cardiol. 2005;46:134–41. doi:10.1016/j.jacc.2005.03.058.
86. Taylor PM, Batten P, Brand NJ, et al. The cardiac valve interstitial cell. Int J Biochem Cell Biol. 2003;35:113–8.
87. Ward C. Clinical significance of the bicuspid aortic valve. Heart. 2000;83:81–5. doi:10.1136/heart.83.1.81.
88. Wilton E, Bland M, Thompson M, Jahangiri M. Matrix metalloproteinase expression in the ascending aorta and aortic valve. Interact Cardiovasc Thorac Surg. 2008;7:37–40. doi:10.1510/icvts.2007.163311.
89. Yener N, Oktar GL, Erer D, et al. Bicuspid aortic valve. Ann Thorac Cardiovasc Surg. 2002;8:264–7.
90. Yip CY, Chen JH, Zhao R, Simmons CA. Calcification by valve interstitial cells is regulated by the stiffness of the extracellular matrix. Arterioscler Thromb Vasc Biol. 2009;29:936–42. doi:10.1161/ATVBAHA.108.182394.

12 Bioreactor and Biomaterial Platforms for Investigation of Mitral Valve Biomechanics and Mechanobiology

Patrick S. Connell, Varun K. Krishnamurthy, and K. Jane Grande-Allen

Introduction and Chapter Overview

Understanding the biomechanics of mitral valves (MVs) has significance for both surgical treatment and regenerative medicine. The biomechanics and mechanobiology of MVs is influenced by their complex anatomy, together with their extracellular matrix (ECM) composition and organization. Valve cells are mechanoresponsive, both to the hemodynamically active environment which the valve tissue is constantly exposed, as well as the altered hemodynamics of valve disease. This chapter will discuss the various tissue and cell level culture techniques and biomechanical approaches to date for examining MV biomechanics and mechanobiology, as well as directions for future studies.

Anatomy, Composition and Environment Impact Biomechanics

MVs are complex biomechanical gates that facilitate unidirectional blood flow from the left atrium to left ventricle; this action is performed about three billion times in an average human lifespan. Anatomically, the MV consists of two unequally sized primary leaflets (anterior, posterior) and numerous chordae tendineae [17, 51]. The upper ends of the chordae tendineae attach either underneath the leaflet (basal, strut) or at the leaflet free edge (marginal), and the lower ends insert in the papillary muscles. Normal MV mechanical function involves coordinated motion of the leaflets and chordae as guided by blood flow, ventricular and atrial pressures, and contraction of the ventricle, papillary muscles, and annulus (leaflet attachment region). Other surrounding anatomic structures such as the aortic valve, the coronary sinus, and the circumflex coronary artery are also crucial for determining regional biomechanical loading.

Similar to aortic valves, normal MV leaflets have three well-defined tissue layers: ventricularis/fibrosa, spongiosa and atrialis [55]. The fibrosa comprises densely packed and microscopically crimped collagen fibers arranged parallel to the free edge of the leaflet; this layer confers durability to the valve. The centrally located spongiosa is rich in chondroitin sulfate proteoglycans that provide a compressible ECM as they have a cushioning and shear absorbing function. The atrialis contains lamellar collagen and elastin sheets, which contribute to leaflet recoil during unloading [57]. Valve interstitial cells (VICs) are the predominant cell type in MVs, and are fibroblast-like, phenotypically plastic, and highly mechanosensitive [43]. Valve endothelial cells (VECs) form a blood-contacting layer surrounding the interior MV tissue.

The complex heterogeneity in terms of anatomy, valve cell phenotypes, and ECM

P.S. Connell, BS • V.K. Krishnamurthy, PhD
K.J. Grande-Allen, PhD (✉)
Department of Bioengineering, Rice University,
6500 Main St., MS 142, Houston, TX 77005, USA
e-mail: psc3@rice.edu; vkk1@rice.edu;
grande@rice.edu

N.M. Rajamannan (ed.), *Molecular Biology of Valvular Heart Disease*,
DOI 10.1007/978-1-4471-6350-3_12,

composition is associated with valve biomechanical behavior that is viscoelastic (anisotropic, non linear) with regional variations (free edge, belly, annulus) affecting the multi-scale function of the MV during normal and diseased states. These aspects will be dealt with in this chapter.

In Vitro Cell Culture and Substrate Manipulation

For the last few decades, the general paradigm for culturing heart valve cells in vitro has been to grow them in two-dimensional (2D) monolayers atop static substrates such as polystyrene, with few exceptions. Porcine valves, the widely used model of human valve disease, were used as early as the 1980s, when Johnson et al. successfully cultured porcine VICs and VECs in M199 media with serum supplementation [31]. While this study established the distinct VIC phenotypes in culture, these conditions did not include external mechanical stimulation and hence did not recapitulate in vivo loading conditions. A basic organ culture protocol was subsequently developed by Lester and colleagues to assess the wound healing capacity of VICs in porcine MV tissue. In that work, a wounding device was set up to exert the required tension (perpendicular to the direction of blood flow) on a segment of valve tissue secured with needles. After the wound was generated, scanning and transmission electron microscopy together with histology revealed VIC migration, multilayering, and orientation parallel to the wound edge, which suggested their involvement in tissue repair [38]. While it is unclear if the applied tension was comparable to the altered physiologic loading during MV disease, this and other similar organ culture studies do offer mechanistic insights into MV tissue repair and regeneration after mechanical fatigue [36–38]. Taken together, these early studies established the feasibility of performing mechanistic and mechanical studies on mitral VICs in basic 2D cultures.

Recently, it has been established that cells often exhibit unnatural behavior when they are removed from their native three dimensional (3D) tissue environment and confined to a monolayer. Hence, there is increasing interest in identifying both natural and synthetic matrices for 3D valve cell culture [63]. Among these, hydrogels prepared from either polyethylene glycol diacrylate (PEGDA) and/or alginate have been used successfully as scaffolds for 3D culture [5, 23]. Recent studies have investigated the development multi-layered hydrogel scaffolds designed to mimic the heterogeneity of the native valve, either through layering of collagen or PEGDA gels with different mechanical behavior [65] or heterogeneous 3D printing of synthetic scaffolds [23]. In the case of layering distinct collagen layers, two identical fibrous collagen scaffolds were decellularized and dried within a silicone mold prepared from native porcine valves. Subsequently, spongiosa scaffolds were prepared by decellurization of pulmonary arteries and treatment with elastase. These spongiosa scaffolds were then inserted between the fibrous collagen scaffolds and fused in place with a protein/aldehyde scaffold bio-adhesive. The final product was then repopulated with cells, mounted in a heart valve bioreactor, and subjected to cyclic mechanical stimulation in cell culture conditions. Micromechanical horizontal shearing of the completed scaffolds showed increased shearing between layers of the layered scaffold, although at lower angles than found in native valves. The layered collagen scaffolds supported in vitro cell repopulation, and bioreactor testing of the valves showed good leaflet opening and coaptation when closed [65]. In a different study, Tseng et al. employed a sandwich fabrication strategy to prepare a valve-inspired three-layered PEGDA-based scaffold in which the outer layers had stiffer material behavior and the inner layer had softer material behavior [64].

In the case of 3D printing of synthetic scaffolds, a PEGDA hydrogel supplemented with alginate has been printed using an extrusion/photocrosslinking method. A range of ratios of polymer to photoinitiator were used to achieve heterogeneous mechanical properties throughout the scaffold, with a resulting tenfold range in elastic modulus across the printed valve [23]. The 3D printed valves also demonstrated

good cell viability after scaffold population. In comparing these two methods of obtaining scaffold heterogeneity, the 3D printed valves have some distinct assets over the layered collagen valves. For one, printing allows for control of mechanical properties on a much smaller scale than does layering, due to the micro-scale resolution of 3D printers. Printing the scaffolds is also a faster process (about 45 min to print), and is more consistently reproducible. A comparison of the shearing properties of a 3D printed valve compared to those of the layered collagen valve would be valuable in order to understand further the differences between these two methods. It will also be interesting to observe the ongoing development of the 3D printer technology to determine whether the resolution of the printing approaches the scale of the ECM components. When considering how the valve cells behave in all of these 3D hydrogel methods as a whole, in contrast to how they behave in a 2D culture, the cells differentiated, proliferated, and migrated through the 3D scaffold gels and responded to added growth factors. Overall, these culture systems show promise for developing tissue engineered heart valves.

Mechanical factors impact various cell types, including valve cells, in fundamentally different ways, and can trigger specific changes similar to those stimulated by soluble ligands. The mechanically-dependent morphology and cytoskeletal structure of fibroblasts, endothelial cells, and neutrophils have been documented for cells cultured on surfaces with stiffness ranging from 2 to 55,000 Pa, and that have been laminated with fibronectin or collagen as adhesive ligand [69]. VICs are mechanosensitive, and their synthesis of ECM not only determines the material behavior of the valve but also provides an adhesive substrate for VICs. However, the interrelationship between substrate stiffness and VIC phenotype and synthetic properties has only been recently elucidated. Stephens et al. recently showed that the age-specific and valve-region-specific responses of VICs to different substrate stiffnesses link VIC phenotype to the leaflet regional matrix in which the VICs reside. In that work, stiffness values of the PEGDA hydrogels were varied by using different pre-polymerization weight ratios of PEG. Hydrogels of elastic modulus 34.5 and 323.3 kPa (5 and 15 % PEG w/v) were used as substrates for VICs from the mitral valve anterior and posterior leaflets from 6-week, 6-month, and 6-year-old pigs. This study demonstrated a range of cell activity for all three parameters considered, thus providing further rationale for investigating the role of substrate stiffness in VIC-driven remodeling of the ECM within diseased and tissue engineered valves [59].

Mitral VIC Contractility

VICs are contractile and believed to factor into mitral leaflet force generation [25], but the exact mechanisms for VICs in mitral leaflet force generation are only now being understood [60]. A study by Stephens et al. examined the effect of actin-mediated VIC force generation coupled to collagen via $\alpha_2\beta_1$ integrins for force generation in the mitral leaflet. Freshly excised porcine mitral leaflets were sutured to a strain-load device custom-built for use on a confocal microscope stage, which allowed for strain manipulation of the tissue (Fig. 12.1). High-magnification fluorescence and second harmonic generation-based imaging of the tissue revealed VIC cytoplasm tightly conforming to the collagen orientation, with actin aligned so that the VIC cytoplasmic processes appeared to wrap around the collagen fibers. Their results suggested that VIC-collagen coupling, mediated by $\alpha_2\beta_1$ integrins, is necessary for KCl-induced force generation in the mitral leaflet. This functional coupling between collagen and VICs via $\alpha_2\beta_1$ integrins may play a role for mitral valve function in vivo.

In addition, the finding that VICs express skeletal muscle cell markers such as myogenin and non-muscle myosin further supports the notion that valve cusps express the required machinery for contractile responses [7, 11]. Indeed, the ability of VICs to form a network in vitro is demonstrated by their ability to contract collagen gels in an efficient and unique manner [8, 21]. Given that VICs show both contractile properties (a smooth muscle cell-like characteristic) and

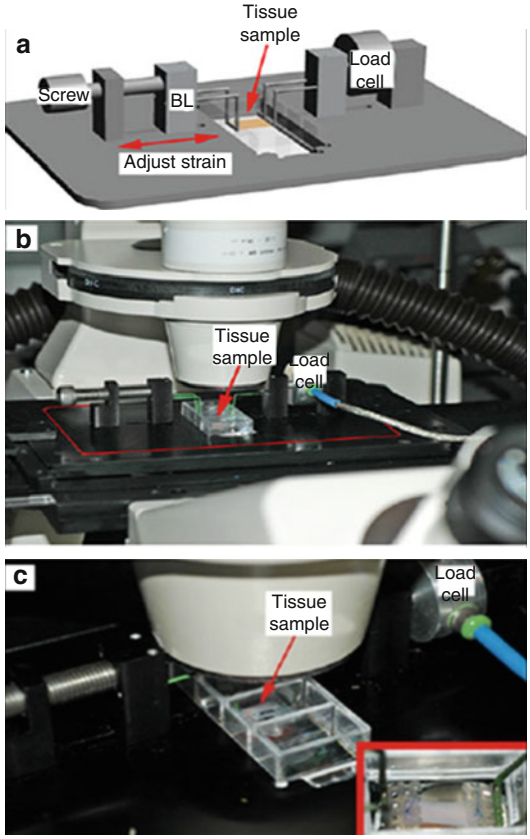

Fig. 12.1 Custom-built strain-load device. (**a**) Diagram illustrating strain-load device built to fit into a motorized confocal microscope stage. Adjustable screw is shown at left; this screw, coupled with a block (labeled "BL") that could freely slide in the cut-out channel, allowed manipulation of strain on tissue as indicated by *red arrow*. The chamber glass, which held the tissue sample in buffer, does not appear on this diagram. The chamber glass was held above objective by virtue of a small metal lip. Placement of tissue sample within the set-up is indicated by the beige rectangle and load cell is labeled. (**b**) Photo illustrating custom-built strain-load device shown in the schematic (a) set in place on confocal microscope stage. Edges of strain load device are outlined in red, tissue sample and load cell are labeled. Microscope objectives are located under the black stage (hidden from view) and microscope eye piece is evident in foreground of photo. Signal output from load cell is carried by silver cable to electronics not pictured. (**c**) Close-up photo of in situ strain-load device. Note valve tissue sutured to plastic mesh between green wire struts. Microscope objective can be seen beneath cover glass. Tissue sample and load cell are labeled. Inset: view of tissue sample from above (microscope head piece removed) demonstrating tissue sutured in place within the chamber. Microscope objective can be seen below (Adapted from Stephens et al. [60]. Copyright permission obtained from Springer for reprinting/reusing in book chapter)

synthesize matrix components (a fibroblast-like characteristic), VICs are well suited for studying their contraction and remodeling of collagen gels. The magnitude of this contraction was shown to be inversely proportional to the number of cells seeded into the gel, and it has been demonstrated that the VICs initially generate force within the collagen gels by spreading, elongating, and sending out extension processes.

Mitral Valve Tissue Biomechanics

The complex microstructure of the MV leaflets leads to a pronounced nonlinear anisotropic mechanical behavior [18, 19, 33, 39, 44, 60]. Both the anterior and posterior leaflets have a greater tensile elastic modulus and lower extensibility in the circumferential direction compared to the radial direction. Compared to the anterior leaflet, the posterior leaflet generally has greater extensibility and a lower elastic modulus, which might be due to the larger number of chordal attachments beneath the posterior leaflet, which provide it with additional mechanical support [44]. There is also a pronounced heterogeneity of mechanical behavior throughout individual leaflets [10, 56]; for example, the anterior leaflet clear zone has a circumferential elastic modulus that is 30–200 % higher than in the rough zone of the same leaflet [33, 60]. Mitral valve leaflets also show a rather unique combination of viscoelastic characteristics, being remarkably independent of strain rates [19], while exhibiting significant stress relaxation [18, 60], but showing negligible creep ex vivo [18] and in vivo [56]. Finally, the elastic modulus of the chordae tendinae is roughly an order of magnitude stiffer than for the mitral leaflets [16, 33].

An additional characteristic of the biomechanics of heart valve tissues, recently introduced by Stephens et al., was developed to assess the acuteness of the transition region in the stress-strain curve. This factor, the radius of transition curvature (RTC), is a measure of pre-transition and post-transition stiffness. In a study of the MVs from pig hearts, an age-dependent increase was observed for mitral valve tissue stiffness,

stress relaxation, and RTC, which was consistent with increases in collagen content, notably type III collagen [61, 62]. Further, mitral valves were stiffer than age-matched aortic valves in both the circumferential and radial directions, possibly due to the preponderance of the collagenous fibrosa layer in the mitral valve leaflets. ECM changes such as these may be traced to molecular events e.g., increased VIC activation in mitral valves compared to aortic valves, at advanced ages [62]. Regionally, the center of the MV anterior leaflet demonstrated higher circumferential stiffness, lower extensibility, and lower RTC compared with free edge of the anterior leaflet. In the radial direction, the MV strips had larger RTC than did those oriented in the circumferential direction.

Similar to porcine valves, mitral valves from mice have been reported to stiffen with age as a result of increased collagen fraction and alignment [15], as shown by continuous laser optical imaging and meso-scale uniaxial tissue stretching. In contrast, a micropipette aspiration based mechanical testing approach showed that aortic valve tissue from mice had compromised mechanical stiffness (more pronounced in the valve hinge region) at advanced ages due to a decrease in collagen/GAG fractional ratio [32]. Interestingly, another micromechanical analysis performed using atomic force microscopy indicated stiffening of aortic valve tissue with age, with focal collagen deposition in the leaflets [58]. While fibrotic disease states may manifest as different changes in ECM composition (more collagen or more GAG) [67], this distinguishing feature of age-induced, localized impairment of ECM maintenance in valves – and any differences between old aortic and mitral valves in general – has significant biomechanical implications and warrants further study. In the future, it will be important to consider a unified approach for measuring tissue biomechanical properties in the various heart valves of different animal models. In sum, age-related regional differences impact valve physiologic function, and information from studies such as these are useful in the context of tissue engineered valve design and understanding the mechanisms of MV disease.

Diseased Valve Biomechanics

The biomechanics of the MV are dramatically altered in disease conditions. Degenerative myxomatous mitral valve disease may lead to valve incompetence due to dilatation of the mitral annulus, an excess of valve tissue resulting in billowing floppy leaflets (usually more prominent in the posterior leaflet), or most commonly rupture of the chordae tendineae resulting in a flail leaflet [13]. Mechanically, the myxomatous leaflets are roughly one-third less stiff and twice as extensible as normal leaflets [1]. The chordae tendinae are even more mechanically compromised, being about two-thirds less stiff and 75 % less strong than normal chordae [2], thus enhancing the potential for chordal rupture.

During valve disease, cell-mediated matrix remodeling can lead to gross tissue biomechanical changes. For example, mitral valves from Marfan mutant (C1039G/+ Fbn1) mice demonstrated reduced tissue stiffness as early as 4 months of age, which was attributed to decreased connective tissue and elastin fractions, and a lower collagen/GAG fractional ratio [15]. Further, the analysis of the circularity and fiber alignment index (expressed as a function of stretch ratio) revealed decoupling of cellular deformation and fiber alignment from the tissue stretch in these Marfan mitral valves. This decoupling suggests an impairment of local cell sensitivity as well as abnormalities in integrin binding and traction force generation due to the Fbn1 deficiency.

Non-sterile In Vitro System for MV Function and Biomechanics

Non-sterile in vitro flow loop systems have generated a great deal of insight into the complexity of valve function and disease. Such systems have taken advantage of loosened restrictions on the design requirements that are needed for sterile culture by adding complex control of valve geometry and analysis capabilities. As non-sterile bioreactors are used for short-term studies as opposed to extended culture durations, these

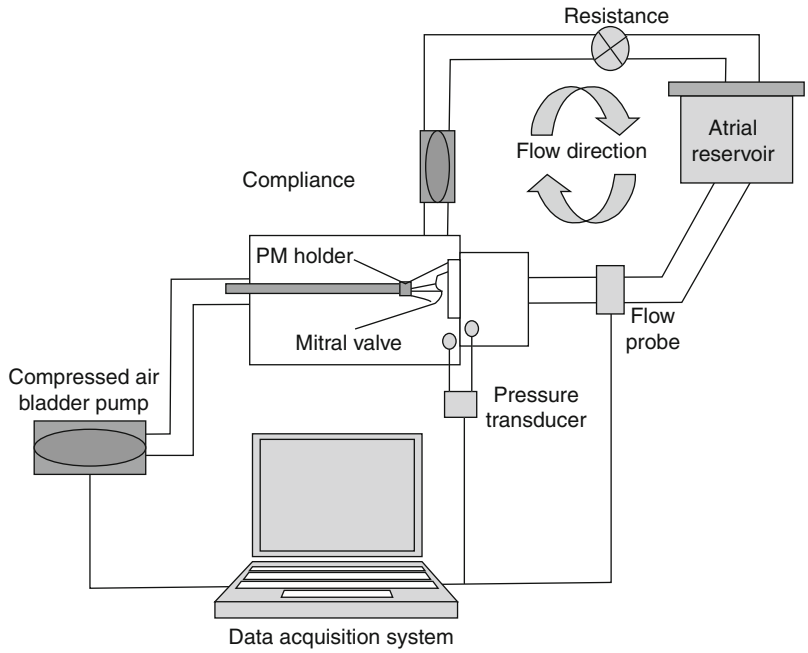

Fig. 12.2 Schematic of Georgia Tech Left Heart Simulator. This system, utilizing a compressed air pump, left ventricular chamber with papillary muscle holders, compliance chamber, variable resistance element, and reservoir, allows for the manipulation of flow and pressure values and valve geometry during a simulated cardiac cycle. Pressure transducers, flow probes, and imaging modalities allow for quantification of flow, pressure and valve movement throughout the cardiac cycle for better understanding of valve function and physiology (Adapted from Jimenez et al. [28]. Copyright permission obtained from Springer for reprinting/reusing in book chapter)

systems are not capable of in-depth investigation of underlying biological aspects of valve function. Instead, such studies concentrate on the mechanical and hemodynamic function of the mitral valve. Accordingly, these systems attempt to accurately reproduce the clinical environment of valve tissues. This includes considerations of pressure and flow waveforms throughout the cardiac cycle mimicking those experienced by natural valves, namely a low-pressure, high-volume filling diastole followed by a high-pressure systole that requires the mitral valve to prevent backflow under high stresses (when in non-diseased conditions). The ability to reproduce physiological heart rates and total flow volumes as well as appropriate dynamic pressure rates at the start and end of systole has also been considered. To accomplish these goals, these systems consist of a series of controls and adjustable elements including variable compliance, resistance, and reservoir components of the flow loop (Fig. 12.2). The flow and pressure inputs are then verified through a series of flow probes and pressure transducers placed throughout the system in critical areas [28]. The majority of work using these systems has been conducted or based on the work of Dr. Ajit Yoganathan using the Georgia Tech Left Heart Simulator.

In addition to generating an accurate reproduction of the hemodynamic environment, these systems allow for the manipulation of mitral valve geometry both in terms of annular size and shape as well as papillary muscle positioning. This control allows for investigation of the valvular geometry effects on valve function. In addition, the analysis tools used in conjunction with these systems enhance the types of data available to researchers. Such tools include visual or ultrasound tracking markers applied to valves to assess the strains experienced by the chordal and leaflet tissues throughout the cardiac cycle [26, 68]. In addition, force transducers have been placed in line with valve chordae to see how chordal forces change, either throughout the cardiac cycle [27]

or after altering valve geometry to mimic disease conditions [28, 29].

Using these systems and their ability to track and obtain high-resolution data resulting from directed manipulations of valve geometry, researchers can gain insight into valve function with fidelity not achievable during clinical or animal studies. Researchers have been able to investigate fundamental aspects of mitral valve function and mechanics, the importance of the shape of the annulus and leaflets, and the role that certain chordae perform in overall valve function throughout the cardiac cycle [9, 26, 47, 48, 50]. In addition, these systems have enabled numerous in-depth investigations of the mechanisms of mitral regurgitation, a common, varied, and clinically critical malfunctioning of the mitral valve. The resulting data have provided critical insight into what manipulations or malformations the valve can overcome without regurgitation and conversely what manipulations result in greater regurgitation volumes [22, 45, 46]. Such studies have found that a flexible mitral annulus increases forces on basal chordae and increased mitral regurgitation in the setting of dilated cardiomyopathy, that basal chordae are most sensitive to papillary muscle displacement, and that a saddle shape annulus more optimally balances the forces on the chordae to allow for better valve coaptation in the presence of papillary muscle displacement. Expanding upon the clinical relevance of such in vitro systems, multiple strategies to repair the mitral valve have been tested, validated or analyzed using these physiological flow loops [6, 12, 24, 30, 49, 53].

The newest generation of non-sterile systems has concentrated on expanding the range of imaging capabilities that can be employed to monitor valve function. By constructing these flow loops using materials compatible with echocardiography and magnetic resonance imaging technology, detailed characterization and visualization of tissue and fluid dynamics is possible within these bioreactor systems [41, 52]. In addition, by ensuring these systems are compatible with clinically relevant imaging modalities, investigators can be more confident in their comparisons to clinical findings in patients or in vivo models of valve mechanics and disease. These findings allow for in-depth analysis of the function of certain aspects of the mitral valve as well as deeper understanding of clinical phenomenon with a level of rigor only achievable in an in vitro system. The precise control features found in the in vitro systems can also be used to resolve controversies that arise using clinical measurement tools, especially in cases in which the unique geometry or complications of a given clinical situation casts doubt upon the validity of measurements from traditional imaging techniques such as Doppler echocardiography or cardiac MRI [42, 52].

As these systems continue to progress in complexity, imaging technologies used to analyze non-sterile flow loop systems have moved beyond the capabilities available to clinical practice. Recent studies have shown that higher resolution images can be obtained using flow loops that are compatible with micro-computed tomography (micro-CT) and digital particle image velocimetry (DPIV) [54]. With sufficiently high resolution, these in vitro flow loop models have the potential to establish, refine, or validate in situ models of valve function. In contrast to previous in vitro models, in which examining the impact of alterations in valve geometry required anatomic or mechanical changes that were large in scale, the improved resolution in these recently described systems could be used to assess the impact of smaller changes that are more representative of early disease progression [53, 54]. Examining the impact of such changes could provide clinical insight regarding controversial issues, such as the timing of intervention during the progression of valve disease or alternative novel therapy options. Additionally, the high fidelity of imaging of both tissue and flow that can be obtained in such systems should also promote more in-depth fundamental studies of how tissue and fluid mechanics impact overall valve function.

Despite their versatility and recent innovations, these non-sterile flow loops still have some important limitations to overcome. Currently, the main limitation is that no published loop has accurately reproduced the dynamic annular movement that occurs in clinical valves. An

innate limitation is that, since these loops are non-sterile, it is difficult to study the impact of biological and compositional changes on valve mechanics and function due to the challenge of obtaining fully intact diseased mitral valves from patients or animal models. The development of a source of diseased or disease-conditioned valves (such as from specialized animal models) that could be further investigated in these non-sterile flow loop systems could provide new information about how disease conditions affect the valve mechanics, function, and resulting hemodynamics, including mitral regurgitation.

Sterile Bioreactors: Models for Mitral Valve Biomechanics and Disease

Sterile bioreactor systems have a distinct advantage over non-sterile systems in their ability to incorporate and investigate the biological response to mechanical stimuli. As researchers look to gain insight into the factors that impact valve remodeling and how this might affect valve function and disease progression, design criteria for their systems must incorporate the desired balance between control of applied mechanical stimulation and the faithful replication of physiological function. Simpler bioreactor designs can offer more control over the selected manipulations being studied and greater ease in maintaining sterility within the system. However, simplicity can also lead to placing valve tissues in non-physiological environments, which can alter their typical, clinical response to mechanical stimuli.

The most simplified 3D culture systems harvest cells from valves (usually the valvular interstitial cells), place these cells in a known scaffold such as collagen or a synthetic polymer and stimulate these constructs using a stretch or flow mechanism [66]. By using precise numbers of cells within a well-defined substrate, researchers are controlling the biochemical signals the cells are receiving in addition to the mechanical stimulation. This approach also permits investigation of differences in extracellular matrix production as a result of varied experimental conditions without concern over inconsistencies in starting composition or intrinsic biochemical stimuli, allowing for higher fidelity studies [20]. By using simple flow or uniaxial or biaxial stretch, such systems can directly apply simple, measureable strain rates to their constructs, making it possible to correlate strain rates/magnitudes and changes in cell behavior. Using such a system, Gupta et al. found that chordal and leaflet valvular interstitial cells produce magnitudes of glycosaminoglycans in comparable proportions to the concentrations of glycosaminoglycans found in chordal and leaflet MV tissues. Waxman et al. determined that cyclic strain induced fibroblastic phenotypes in canine valvular interstitial cells. This simple design has similarly been used on strips of mitral leaflet tissue. These systems hold the same advantages as the uniaxial stretch scaffold systems, only they utilize the native tissue structure to provide the cells their natural extracellular matrix environment throughout the study [34, 35].

The next stage of sterile bioreactor incorporates multiple stimuli into their design while attempting to still balance relative simplicity and small size. The native mitral valve not only experiences tensile forces throughout the cardiac cycle, but also compression, bending, and shear forces due to flow. One example of such as system is the rotating "splashing" bioreactor system reported by Barzilla et al. [4]. In this system, a portion of the mitral valve is suspended within a chamber partially filled with media and then the chamber is rotated so that the change in orientation results in the culture media splashing across the valve, simulating some degree of tension, compression and shear upon the valve segment (although physiological flows and pressures are not obtained). This type of system is able to apply multiple types of stimuli to the valve simultaneously, and while it does not have the control of the directly applied strain systems and does not apply physiological loads, it still provides a platform by which the effect of these different stimuli on valve cell activation and valve compositional remodeling can be explored [3]. Using such a system, Barzilla et al. were able to reproduce the serotonergic plaques formed atop valves as a result of valve exposure to norfenfluramine,

and were able to gain insight into the underlying mechanism of this drug-induced valvulopathy.

The last category of sterile bioreactors is physiological flow loops. This type of bioreactor is a closed system that includes a mock left ventricle with attached pump, tubing, a compliance chamber, and a reservoir chamber to produce physiological or pseudo-physiological flow and pressure acting upon an intact mitral valve. These systems may closely resemble non-sterile flow loop systems, but are often simplified with fewer active mechanical parts in order to allow for easy assembly of a fully closed, sterile system with filtered air exchange. Although these systems may lack the resolution of control of previously discussed parameters such as strain rate, they do provide the valves with simulated native valve hemodynamics that allow for valve culture over multiple week periods so that the biological response to geometry and hemodynamic variations can be explored [14]. These systems also lack the full physiological response that would be present in an animal model, but do provide benefits in terms of reducing cost and allowing control of geometric and hemodynamic parameters within the system. Taken together, these systems would allow for the direct cause and effect comparison of very specific manipulations to be explored with a high enough number of valves to obtain high-powered studies of even subtle remodeling responses.

A system closely related to the physiological flow loops is the Miniature Tissue Culture System described by Lieber et al. This unique design takes advantage of flow loop principles and the physiology of a full intact murine left ventricle to allow for the culture of mitral valves in their native ventricular environment (Fig. 12.3). Given the genetic manipulation and viral targeting currently available throughout mouse lines, the use

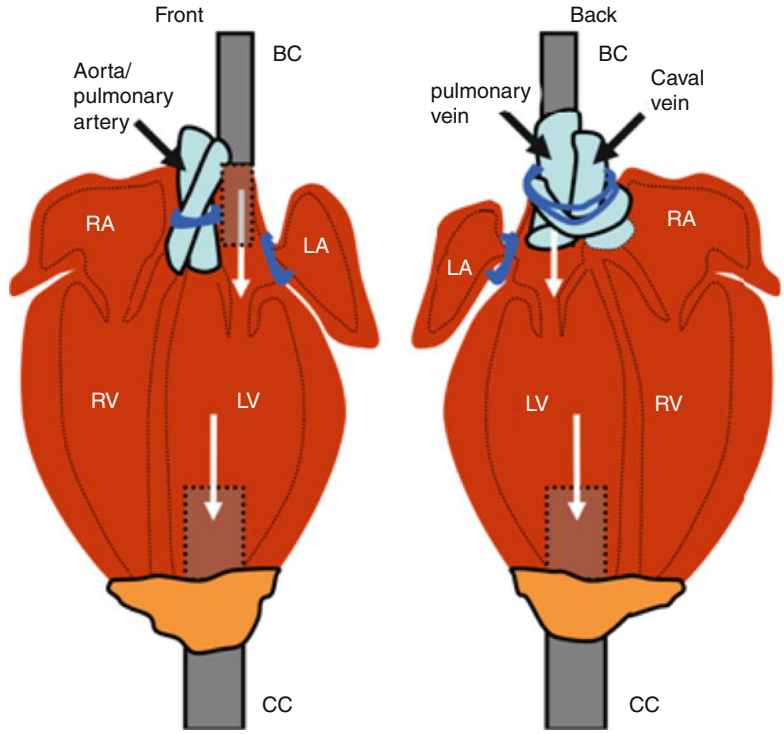

Fig. 12.3 Schematic of Miniature Tissue Culture System. This system allows for the culture of a mouse left ventricle, including intact mitral valve, with user controlled flow and pressure using a cannulation system. In this system a ball cannula (*BC*) is inserted through the pulmonary vein into the left atrium (*LA*) and secured in place above the level of the mitral valve. A cylinder cannula (*CC*) is then inserted through an opening cut into the apex of the left ventricle (*LV*) and secured using cyanoacrylate. The pulmonary artery, aorta, and left atrial appendage are ligated to prevent leakage. As a result of this ligation, the right atria (*RA*) and right ventricle (*RV*) are excluded from the flow of this system (Adapted from Lieber et al. [40]. Copyright permission obtained from Springer for reprinting/reusing in book chapter)

of this system to investigate murine hearts offers tremendous potential to explore the genetic components of heart and valve disease [40].

One disadvantage of these full, sterile, physiological flow loop systems is that the requirements of sterile culture often make imaging the active valve difficult or impossible, depending on the modality being used. Therefore, one area for improvement of such systems would be design advancements that would allow for the same imaging protocols as used in the non-sterile loops or for the ability to transfer valves (while maintaining their accurate attachment characteristics) into non-sterile systems that have state of the art imaging capabilities. Using this tandem approach, investigators could better characterize the hemodynamic conditions being experienced by the valve as well as measure the valve dynamics throughout the simulated cardiac cycle.

Summary

Although the mechanobiology of the mitral valve has not received as much attention as that of the aortic valve, there is a growing effort to develop in vitro tools to investigate the relationships between the distinctive and varied ECM composition of the mitral valve, the interstitial cells located throughout the MV, and their mechanical environment. These studies utilize a wide range of approaches employing native or synthetic hydrogel platforms, native valve tissues, and/or simple through complex bioreactor systems to transmit adhesive or applied strains to the valve cells. These systems and platforms can be used in studies of biomechanics or mechanobiology as a function of mechanical stimulation only, or applied in combination with chemical stimuli such as pharmacological agents or growth factors, and have provided great insight into the biomechanics and mechanisms of MV function, remodeling, and disease. In the future, it seems likely that sterile bioreactor systems will be designed with more hybrid functionality, such as integration of imaging modules to monitor MV function during culture, to take advantage of the versatility offered by non-sterile bioreactors for the MV. Further characterization of the MV of common animal models, and their comparison with human valves, will allow the development of a wealth of in vitro models for MV disease. These approaches will also be valuable in developing future culture and scaffold systems for the purpose of generating tissue engineered mitral valves. All of these potential research directions will be essential in the future as we strive to elucidate the critical steps in the development of mitral valve disease as targets for new treatment strategies.

References

1. Barber JE, Kasper FK, Ratliff NB, Cosgrove DM, Griffin BP, Vesely I. Mechanical properties of myxomatous mitral valves. J Thorac Cardiovasc Surg. 2001;122:955–62.
2. Barber JE, Ratliff NB, Cosgrove DM, Griffin BP, Vesely I. Myxomatous mitral valve chordae. I: mechanical properties. J Heart Valve Dis. 2001;10:320–4.
3. Barzilla JE, Acevedo FE, Grande-Allen KJ. Organ culture as a tool to identify early mechanisms of serotonergic valve disease. J Heart Valve Dis. 2010;19:626–35.
4. Barzilla JE, McKenney AS, Cowan AE, Durst CA, Grande-Allen KJ. Design and validation of a novel splashing bioreactor system for use in mitral valve organ culture. Ann Biomed Eng. 2010;38:3280–94.
5. Benton J, Fairbanks B, Anseth K. Characterization of valvular interstitial cell function in three dimensional matrix metalloproteinase degradable peg hydrogels. Biomaterials. 2009;30:6593–603.
6. Bhattacharya S, He Z. Annulus tension of the prolapsed mitral valve corrected by edge-to-edge repair. J Biomech. 2012;45:562–8.
7. Brand NJ, Roy A, Hoare G, Chester A, Yacoub MH. Cultured interstitial cells from human heart valves express both specific skeletal muscle and non-muscle markers. Int J Biochem Cell Biol. 2006;38:30–42.
8. Butcher JT, Penrod AM, García AJ, Nerem RM. Unique morphology and focal adhesion development of valvular endothelial cells in static and fluid flow environments. Arterioscler Thromb Vasc Biol. 2004;24:1429–34.
9. Chen L, May-Newman K. Effect of strut chordae transection on mitral valve leaflet biomechanics. Ann Biomed Eng. 2006;34:917–26.
10. Chen L, McCulloch AD, May-Newman K. Nonhomogeneous deformation in the anterior leaflet of the mitral valve. Ann Biomed Eng. 2004;32:1599–606.
11. Chester AH, Taylor PM. Molecular and functional characteristics of heart-valve interstitial cells. Philos Trans R Soc Lond B Biol Sci. 2007;362:1437–43.
12. Croft LR, Jimenez JH, Gorman RC, Gorman JH, Yoganathan AP. Efficacy of the edge-to-edge repair in

the setting of a dilated ventricle: an in vitro study. Ann Thorac Surg. 2007;84:1578–84.
13. Fornes P, Heudes D, Fuzellier JF, Tixier D, Bruneval P, Carpentier A. Correlation between clinical and histologic patterns of degenerative mitral valve insufficiency: a histomorphometric study of 130 excised segments. Cardiovasc Pathol. 1999;8:81–92.
14. Gheewala N, Grande-Allen KJ. Design and mechanical evaluation of a physiological mitral valve organ culture system. Cardiovasc Eng Technol. 2010;1:123–31.
15. Gould RA, Sinha R, Aziz H, Rouf R, Dietz HC, Judge DP, Butcher J. Multi-scale biomechanical remodeling in aging and genetic mutant murine mitral valve leaflets: insights into Marfan syndrome. PLoS One. 2012;7:e44639.
16. Grande-Allen KJ, Barber JE, Klatka KM, Houghtaling PL, Vesely I, Moravec CS, McCarthy PM. Mitral valve stiffening in end-stage heart failure: evidence of an organic contribution to functional mitral regurgitation. J Thorac Cardiovasc Surg. 2005;130:783–90.
17. Grande-Allen KJ, Liao J. The heterogeneous biomechanics and mechanobiology of the mitral valve: implications for tissue engineering. Curr Cardiol Rep. 2011;13:113–20.
18. Grashow JS, Sacks MS, Liao J, Yoganathan AP. Planar biaxial creep and stress relaxation of the mitral valve anterior leaflet. Ann Biomed Eng. 2006;34:1509–18.
19. Grashow JS, Yoganathan AP, Sacks MS. Biaixal stress-stretch behavior of the mitral valve anterior leaflet at physiologic strain rates. Ann Biomed Eng. 2006;34:315–25.
20. Gupta V, Grande-Allen KJ. Effects of static and cyclic loading in regulating extracellular matrix synthesis by cardiovascular cells. Cardiovasc Res. 2006;72:375–83.
21. Gupta V, Werdenberg JA, Blevins TL, Grande-Allen KJ. Synthesis of glycosaminoglycans in differently loaded regions of collagen gels seeded with valvular interstitial cells. Tissue Eng. 2007;13:41–9.
22. He S, Fontaine AA, Schwammenthal E, Yoganathan AP, Levine RA. Integrated mechanism for functional mitral regurgitation. Circulation. 1997;96:1826.
23. Hockaday LA, Kang KH, Colangelo NW, Bonassar LJ, Malone E, Wu J, Chu CC, Lipson H, Duan B, Cheung PYC, Girardi LN, Butcher JT. Rapid 3d printing of anatomically accurate and mechanically heterogeneous aortic valve hydrogel scaffolds. Biofabrication. 2012;4:035005.
24. Hu Y, Shi L, Parameswaran S. Left ventricular vortex under mitral valve edge-to-edge repair. Cardiovasc Eng Technol. 2010;1:235–43.
25. Itoh A, Krishnamurthy G, Swanson JC, Ennis DB, Bothe W, Kuhl E, Karlsson M, Davis LR, Miller DC, Ingels NB. Active stiffening of mitral valve leaflets in the beating heart. Am J Physiol Heart Circ Physiol. 2009;296:H1766–73.
26. Jimenez JH, Liou SW, Padala M, He Z, Sacks M, Gorman RC, Gorman JH, Yoganathan AP. A saddle-shaped annulus reduces systolic strain on the central region of the mitral valve anterior leaflet. J Thorac Cardiovasc Surg. 2007;134:1562–8.
27. Jimenez JH, Soerensen DD, He Z, He S, Yoganathan AP. Effects of a saddle shaped annulus on mitral valve function and chordal force distribution: an in vitro study. Ann Biomed Eng. 2003;31:1171–81.
28. Jimenez JH, Soerensen DD, He Z, Ritchie J, Yoganathan AP. Mitral valve function and chordal force distribution using a flexible annulus model: an in vitro study. Ann Biomed Eng. 2005;33:557–66.
29. Jimenez JH, Soerensen DD, He Z, Ritchie J, Yoganathan AP. Effects of papillary muscle position on chordal force distribution: an in-vitro study. J Heart Valve Dis. 2005;14:295–302.
30. Jimenez JH, Forbess J, Croft LR, Small L, He Z, Yoganathan AP. Effects of annular size, transmitral pressure, and mitral flow rate on the edge-to-edge repair: an in vitro study. Ann Thorac Surg. 2006;82:1362–8.
31. Johnson CM, Hanson MN, Helgeson SC. Porcine cardiac valvular subendothelial cells in culture: cell isolation and growth characteristics. J Mol Cell Cardiol. 1987;19:1185–93.
32. Krishnamurthy VK, Guilak F, Narmoneva DA, Hinton RB. Regional structure-function relationships in mouse aortic valve tissue. J Biomech. 2011;44:77–83.
33. Kunzelman KS, Cochran RP. Stress/strain characteristics of porcine mitral valve tissue: parallel versus perpendicular collagen orientation. J Card Surg. 1992;7:71–8.
34. Lacerda CMR, Kisiday J, Johnson B, Orton EC. Local serotonin mediates cyclic strain-induced phenotype transformation, matrix degradation, and glycosaminoglycan synthesis in cultured sheep mitral valves. Am J Physiol Heart Circ Physiol. 2012;302:H1983–90.
35. Lacerda CMR, Maclea HB, Kisiday JD, Orton EC. Static and cyclic tensile strain induce myxomatous effector proteins and serotonin in canine mitral valves. J Vet Cardiol. 2012;14:223–30.
36. Lester WM. Interstitial cells from the atrial and ventricular sides of the bovine mitral valve respond differently to denuding endocardial injury. In Vitro Cell Dev Biol. 1993;29:41–50.
37. Lester WM, Damji AA, Tanaka M, Gedeon I. Bovine mitral valve organ culture: role of interstitial cells in repair of valvular injury. J Mol Cell Cardiol. 1992;24:43–53.
38. Lester WM, Gotlieb AI. In vitro repair of the wounded porcine mitral valve. Circ Res. 1988;62:833–45.
39. Liao J, Yang L, Grashow J, Sacks MS. The relation between collagen fibril kinematics and mechanical properties in the mitral valve anterior leaflet. J Biomech Eng. 2007;129:78–87.
40. Lieber SC, Kruithof BPT, Aubry N, Vatner SF, Gaussin V. Design of a miniature tissue culture system to culture mouse heart valves. Ann Biomed Eng. 2010;38:674–82.
41. Little SH, Igo SR, Pirat B, McCulloch M, Hartley CJ, Nosé Y, Zoghbi WA. In vitro validation of real-time three-dimensional color Doppler echocardiography for direct measurement of proximal isovelocity surface area in mitral regurgitation. Am J Cardiol. 2007;99:1440–7.

42. Little SH, Pirat B, Kumar R, Igo SR, McCulloch M, Hartley CJ, Xu J, Zoghbi WA. Three-dimensional color Doppler echocardiography for direct measurement of vena contracta area in mitral regurgitation: in vitro validation and clinical experience. JACC Cardiovasc Imaging. 2008;1:695–704.
43. Liu AC, Joag VR, Gotlieb AI. The emerging role of valve interstitial cell phenotypes in regulating heart valve pathobiology. Am J Pathol. 2007;171:1407–18.
44. May-Newman K, Yin FC. Biaxial mechanical behavior of excised porcine mitral valve leaflets. Am J Physiol. 1995;269:H1319–27.
45. Nielsen SL, Nygaard H, Fontaine AA, Hasenkam JM, He S, Andersen NT, Yoganathan AP. Chordal force distribution determines systolic mitral leaflet configuration and severity of functional mitral regurgitation. J Am Coll Cardiol. 1999;33:843–53.
46. Nielsen SL, Nygaard H, Mandrup L, Fontaine AA, Hasenkam JM, He S, Yoganathan AP. Mechanism of incomplete mitral leaflet coaptation—interaction of chordal restraint and changes in mitral leaflet coaptation geometry. J Biomech Eng. 2002;124:596.
47. Padala M, Gyoneva L, Yoganathan AP. Effect of anterior strut chordal transection on the force distribution on the marginal chordae of the mitral valve. J Thorac Cardiovasc Surg. 2012;144:624–33.
48. Padala M, Hutchison RA, Croft LR, Jimenez JH, Gorman RC, Gorman JH, Sacks MS, Yoganathan AP. Saddle shape of the mitral annulus reduces systolic strains on the p2 segment of the posterior mitral leaflet. Ann Thorac Surg. 2009;88:1499–504.
49. Padala M, Powell SN, Croft LR, Thourani VH, Yoganathan AP, Adams DH. Mitral valve hemodynamics after repair of acute posterior leaflet prolapse: quadrangular resection versus triangular resection versus neochordoplasty. J Thorac Cardiovasc Surg. 2009;138:309–15.
50. Padala M, Sacks MS, Liou SW, Balachandran K, He Z, Yoganathan AP. Mechanics of the mitral valve strut chordae insertion region. J Biomech Eng. 2010;132:081004.
51. Perloff JK, Roberts WC. The mitral apparatus: functional anatomy of mitral regurgitation. Circulation. 1972;46:227–39.
52. Quaini A, Canic S, Guidoboni G, Glowinski R, Igo SR, Hartley CJ, Zoghbi WA, Little SH. A three-dimensional computational fluid dynamics model of regurgitant mitral valve flow: validation against in vitro standards and 3d color Doppler methods. Cardiovasc Eng Technol. 2011;2:77–89.
53. Rabbah J-P, Chism B, Siefert A, Saikrishnan N, Veledar E, Thourani VH, Yoganathan AP. Effects of targeted papillary muscle relocation on mitral leaflet tenting and coaptation. Ann Thorac Surg. 2013;95:621–8.
54. Rabbah J-P, Saikrishnan N, Yoganathan AP. A novel left heart simulator for the multi-modality characterization of native mitral valve geometry and fluid mechanics. Ann Biomed Eng. 2013;41:305–15.
55. Rabkin E, Aikawa M, Stone JR, Fukumoto Y, Libby P, Schoen FJ. Activated interstitial myofibroblasts express catabolic enzymes and mediate matrix remodeling in myxomatous heart valves. Circulation. 2001;104:2525–32.
56. Sacks MS, Enomoto Y, Graybill JR, Merryman WD, Zeeshan A, Yoganathan AP, Levy RJ, Gorman RC, Gorman JH. In-vivo dynamic deformation of the mitral valve anterior leaflet. Ann Thorac Surg. 2006;82:1369–77.
57. Schoen FJ. Evolving concepts of cardiac valve dynamics: the continuum of development, functional structure, pathobiology, and tissue engineering. Circulation. 2008;118:1864–80.
58. Sewell-Loftin M-K, Brown CB, Baldwin HS, Merryman WD. A novel technique for quantifying mouse heart valve leaflet stiffness with atomic force microscopy. J Heart Valve Dis. 2012;21:513–20.
59. Stephens E, Durst C, West J, Grande-Allen K. Mitral valvular interstitial cell responses to substrate stiffness depend on age and anatomic region. Acta Biomater. 2011;7:75–82.
60. Stephens EH, Durst CA, Swanson JC, Grande-Allen KJ, Ingels NB, Miller DC. Functional coupling of valvular interstitial cells and collagen via α2β1 integrins in the mitral leaflet. Cell Mol Bioeng. 2010;3:428–37.
61. Stephens EH, Grande-Allen KJ. Age-related changes in collagen synthesis and turnover in porcine heart valves. J Heart Valve Dis. 2007;16:672–82.
62. Stephens EH, de Jonge N, McNeill MP, Durst CA, Grande-Allen KJ. Age-related changes in material behavior of porcine mitral and aortic valves and correlation to matrix composition. Tissue Eng Part A. 2010;16:867–78.
63. Tibbitt MW, Anseth KS. Hydrogels as extracellular matrix mimics for 3d cell culture. Biotechnol Bioeng. 2009;103:655–63.
64. Tseng H, Balaoing LR, Grigoryan B, Raphael RM, Killian TC, Souza GR, Grande-Allen KJ. A three-dimensional co-culture model of the aortic valve using magnetic levitation. Acta Biomater. 2013;10:173–82.
65. Tedder ME, Simionescu A, Chen J, Liao J, Simionescu DT (2011) Assembly and testing of stem cell-seeded layered collagen constructs for heart valve tissue engineering. Tissue Eng Part A 17:25–36.
66. Waxman A, Kornreich B. Interactions between tgfβ1 and cyclic strain in modulation of myofibroblastic differentiation of canine mitral valve interstitial cells in 3d culture. J Vet Cardiol. 2012;14:211–21.
67. Wynn TA. Common and unique mechanisms regulate fibrosis in various fibroproliferative diseases. J Clin Invest. 2007;117:524–9.
68. Yap CH, Kim H-S, Balachandran K, Weiler M, Haj-Ali R, Yoganathan AP. Dynamic deformation characteristics of porcine aortic valve leaflet under normal and hypertensive conditions. Am J Physiol Heart Circ Physiol. 2010;298:H395–405.
69. Yeung T, Georges PC, Flanagan LA, Marg B, Ortiz M, Funaki M, Zahir N, Ming W, Weaver V, Janmey PA. Effects of substrate stiffness on cell morphology, cytoskeletal structure, and adhesion. Cell Motil Cytoskeleton. 2005;60:24–34.

13 Identification of Early Pathological Events in Calcific Aortic Valve Disease by Molecular Imaging

Eduardo Martínez-Martínez and Elena Aikawa

Introduction

The aberrant mineralization of soft tissues (i.e., ectopic calcification) recently has been associated with various chronic and degenerative conditions in humans. Cardiovascular tissue, particularly vasculature and valves, are among the peripheral tissues affected by the pathological deposition of calcium phosphate in connective tissue [1]. Although whether ectopic calcification originates from the same causes in different soft tissues is still unclear, the mineralization process seems to be triggered by chronic inflammatory conditions. This relationship has been especially demonstrated in the cardiovascular system, where macrophage infiltration and subsequent release of proteolytic enzymes and cytokines precedes the transformation of vascular smooth muscle cells and valve interstitial cells (VICs) into osteoblast-like cells. Over the last two decades, cardiovascular calcification has gradually gained the attention of more research groups with the acknowledgement that calcification constitutes an independent risk factor for cardiovascular morbidity and mortality [2–7]. Moreover, the prevalence of arterial calcification and calcific aortic valve disease (CAVD) is expected to increase, due to aging worldwide population. An estimated 2.1 million patients in Europe and 3.5 million patients in North America will suffer from severe CAVD by 2025 and 2050, respectively [8]. Therefore, a better understanding of the mechanisms underlying the initiation of CAVD will lead to the development of novel diagnostic and therapeutic methods to improve patients' quality of life.

Common epidemiological risk factors such as age, hypercholesterolemia, metabolic syndrome, chronic renal disease, and diabetes mellitus have been identified for atherosclerosis and CAVD [5, 9, 10]. Nevertheless, different molecular mechanisms may participate in arterial and aortic valve calcification, as suggested by the lack of benefit of statin therapy on the reduction of valve calcification [11, 12]. Indeed, we now recognize that aortic valve calcification represents a late stage of a progressive disease that alters the anatomy and functionality of the aortic valve [13, 14]. In a healthy valve, a layer of endothelium encloses three distinguishable layers of connective tissue: fibrosa, spongiosa, and ventricularis. Heart valve disease begins with microstructural changes involving a degenerative remodeling of the fibrosa layer. This stage of the disease, characterized by a mild thickening of the valve without overt changes on blood outflow from the left ventricle, is known as aortic sclerosis. A subset of patients develops aortic stenosis, characterized by the presence of macroscopically calcific lesions and limited motion of the valve leaflets. Stiffening of the aortic valve results in major

E. Martínez-Martínez • E. Aikawa, MD, PhD (✉)
Division of Cardiovascular Medicine,
Center for Excellence in Vascular Biology,
Brigham and Women's Hospital,
Harvard Medical School, 77 Avenue Louis Pasteur,
NRB-741, Boston, MA 02115, USA
e-mail: eaikawa@partners.org

N.M. Rajamannan (ed.), *Molecular Biology of Valvular Heart Disease*,
DOI 10.1007/978-1-4471-6350-3_13,

hemodynamic changes and remodeling of the left ventricle that can lead to fatal myocardial infarction in these patients [14].

Currently, the only available treatment options for aortic stenosis are surgical or transcatheter valve replacements [15]. But these interventions are intended for the end stage of the disease, and generally result in a poor prognosis. Furthermore, pharmacological therapies—including statins, mineralocorticoid receptor antagonists, and bisphosphonates—have not been effective in clinical practice [12, 16–18]. Two interrelated challenges thus need to be addressed by CAVD investigators. First, we must identify molecular targets to stop the progression of CAVD at different stages of the disease; and second, we should endeavor to generate new non-invasive methods of diagnosis that allow the visualization and quantification of early events of CAVD. The technology available in current clinical practice, such as intravascular ultrasonography (IVUS), transthoracic echocardiography (TTE), computed tomography (CT), or magnetic resonance imaging (MRI), fails to detect microcalcifications and to measure other key cellular events that are crucial to detect before valve damage is irreversible.

Molecular imaging, an emerging modality, can be used to visualize molecular processes in vivo [19, 20]. This approach has been extremely useful in several biomedical areas, including cardiovascular research. The design of fluorescent probes to target specific molecules or to monitor certain enzyme activity have helped researchers to understand biological processes simultaneously in real time at cellular and molecular levels. This chapter aims to provide a review of the imaging studies that have been crucial to our understanding of the early stages of CAVD, and to give an overview of the most recent advancements with potential to be translated to the clinic.

Imaging of Aortic Valve Disease

The notion that inflammation plays a fundamental role in the development of cardiovascular calcification is quite recent [13, 14]. To a large extent, studies using fluorescence-based imaging techniques support the paradigm that an identifiable sequence of cellular events triggers cardiovascular calcification [21–24]. The most frequent imaging modalities used for this purpose are fluorescence reflectance imaging (FRI) and intravital confocal microscopy (IVM). These platforms offer great versatility, as two or more fluorochromes can be employed in the same experiment to visualize two different biological processes simultaneously. The macroscopic resolution of FRI makes this platform ideal for imaging entire organs, while IVM is more suitable for obtaining information at the microscopic level. Both imaging systems have been used complementarily with a variety of targeted and activatable imaging agents. The targeted agents consist of an affinity ligand (antibody or small molecule) conjugated to a fluorochrome or magnetic compound [25–27]. The activatable agents must be chemically modified, commonly by an enzyme, in order to emit fluorescence. For in vivo applications, the near-infrared region of the light spectrum (600–900 nm) is preferred over visible or infrared light. The use of near-infrared fluorescence (NIRF) probes enables imaging from deeper regions of the tissue, avoids photon absorption, and increases the signal-to-noise ratio. Through the imaging of a battery of NIRF agents, we have been able to monitor over time the main cellular events leading to valve calcification: (1) endothelial activation, (2) macrophage infiltration, (3) extracellular matrix degradation, and (4) osteogenic activity in the aortic valves of hypercholesterolemic apolipoprotein E–deficient ($apoE^{-/-}$) mice [21–24].

Monitoring of Endothelial Activation and Inflammation In Vivo

In response to atherogenic factors, endothelial cells express a variety of adhesion and chemotactic molecules that initiate a local inflammatory response [28–31]. Furthermore, the expression of vascular cell adhesion molecule-1 (VCAM-1), intercellular adhesion molecule-1 (ICAM-1), and E-selectin increases in the valvular endothelium

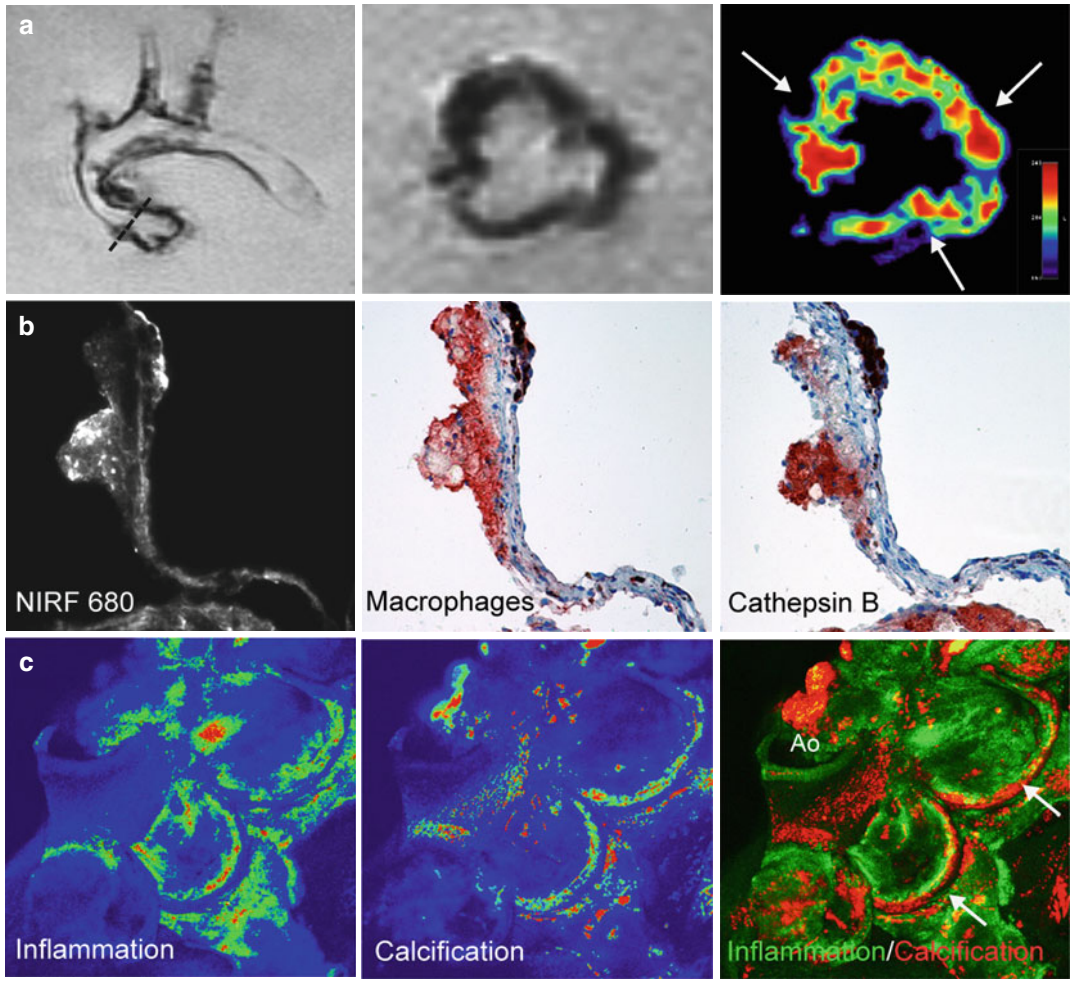

Fig. 13.1 Visualization of early events of aortic valve calcification through molecular imaging. (**a**), Endothelial cell activation occurs in the commissures of diseased aortic valves. (*Left*) Ex vivo MRI showing the long-axis view of the aortic arch and root. *Dotted line* depicts slice position of short-axis view (*middle*). Dark areas in the middle panel denotes where the nanoparticles were taken up by endothelial cells. (*Right*) Color-coded signal intensities of short-axis view show focused uptake of molecular agent in commissures (*arrows*). (**b**), NIRF microscopy with a protease-activatable agent for cathepsin activity (*left*). Immunochemistry colocalized NIRF signals with macrophages (Mac3) expressing cathepsin B. (**c**), In the aortic valve of atherogenic mice, the inflammatory activity correlates with osteogenesis as visualized by ex vivo IVM. (*Left*) Macrophage accumulation measured by accumulation of magnetofluorescent nanoparticles. (*Middle*) Bisphosphonate-imaging agent binds to nanomolar concentrations of hydroxyapatite to detects osteogenic activity. Molecular imaging allow inflammatory and osteogenic activities colocalized in the areas of highest mechanical stress at the aortic valve attachment (*arrows*) (Adapted from Aikawa et al. [21–23])

of diseased valves [31, 32]. Thus, adhesion molecules also may reflect an injury response of valvular endothelial cells. In support of this possibility, we found by MRI and NIRF microscopy that VCAM-1 is mainly distributed in the aortic valve leaflet near the region known as the commissure [23] (Fig. 13.1). This region is where the valve leaflet is attached to the aortic root, and is subjected to the greatest amount of mechanical stress during the cardiac cycle [33]. Interestingly, endothelial activation reflected by the expression of VCAM-1 has been found in an ex vivo model that recreates shear stress of the bicuspid aortic valve [34].

Through the use of magnetofluorescent nanoparticles, it was possible to determine that macrophages accumulate in regions of the leaflet that present endothelial cell activation [22, 23]. The NIRF signal from the nanoparticles was mainly located in the thickened regions of the valve containing abundant Mac3 immunoreactive cells. This finding suggested that macrophages are involved in the remodeling of the extracellular matrix (ECM) of the valve. Remarkably, the presence of macrophages determines how rapidly the aortic stenosis progresses [35]. Another consequence of macrophage accumulation is that the released cytokines, such as TGF-β, IL-1β, and TNF-α, induce the activation of VICs into myofibroblasts [36–38]. In our experiments, we have noticed a close spatial relationship between these cell types that needs further investigation. In this context, a pathological interaction between macrophages and VICs may lead to thickening and dysfunction of the valve through an aberrant remodeling of its architecture. A consideration about the interpretation of imaging experiments with polysaccharide-coated magnetic nanoparticles should be noted: a recent study found that valvular myofibroblasts also can uptake magnetonanoparticles, opening the possibility that to some extent, other cell types could accumulate these nanoparticles [39]. This finding is especially important considering that the immune infiltrate in CAVD also includes lymphocytes, plasma cells, and mast cells [40–43]. We therefore must generate cell-specific imaging agents to achieve better insight into the functions of different types of immune cells. Experiments with new imaging agents will help to determine if the timing and presence of a particular immune cell type associate with the progression and severity of calcification.

Extracellular Matrix Remodeling Promotes Valve Calcification

The release of matrix-degrading proteinases has been proposed as a mechanism to explain the pathobiology of CAVD [44–46]. Valvular myofibroblasts and macrophages synthesize matrix metalloproteinases (MMPs; e.g., collagenase-1/MMP-1, collagenase-3/MMP-13, gelatinase-A/MMP-2, and gelatinase-B/MMP-9) and cysteine endoproteases (cathepsins B, K, and S) [47–50]. Using hypercholesterolemic ApoE$^{-/-}$ mice, we have shown that regions of the aortic valve enriched with valvular myofibroblasts and macrophages displayed activity of cathpesins B and K, as well as MMP-2 and MMP-9 [21, 23]. The implications of collagen and elastin degradation are not only structural, but also functional. ECM composition has been proposed to modulate VIC calcification and proliferation [51–53]. A reduction in the number of interaction sites with ECM or by-products of ECM degradation may facilitate VIC transdifferentiation into an osteoblastic-like phenotype. In agreement with this notion, we found that cathepsin S activity accelerates arterial and valvular calcification in mice with atherosclerosis and chronic renal disease (CRD) [21]. Using a protease-activatable imaging agent specific for cathepsin S, we used intravital microscopy to detect increased activity of this elastase in regions displaying ostegenic activity (Fig 13.1). CRD-induced calcification was clearly diminished in cathepsin S-deficient mice, even with a similar macrophage accumulation in the valve leaflets. In in vitro experiments with vascular smooth muscle cells, elastin-derived peptides significantly induced the expression of alkaline phosphatase. Taken together, these findings suggest that elastin degradation modulates the calcification potential of myofibroblasts. In this regard, the elastin degradation products—known as matrikines or elastokines—regulate myofibroblastic migration, proliferation, and production of bone-regulating proteins [53–55]. An additional repercussion of the enhanced proteolytic activity can be the activation of proinflammatory precursors deposited in the ECM, which enhances the inflammatory response [56, 57].

Visualization of Early Osteogenic Activity Preceding Valve Calcification

The possibility of detecting nanomolar concentrations of calcium hydroxyapatite crystals through in vivo molecular imaging experiments constitutes one of the greatest technical advancements that have revolutionized our understanding

of cardiovascular calcification. While conventional histological techniques for calcium deposit detection (e.g., Von Kossa and alizarin red stains) are only useful for staining advanced calcific lesions, a bisphosphonate-conjugated fluorescent agent (Osteosense 680/750) allows the localization of active sites of biomineralization in early stages of the calcification process. With the aid of multichannel NIRF microscopy, and the agent either injected into or applied directly on to a tissue section, we have associated osteogenic activity with precise proinflammatory events [21–23, 58]. In our in vivo and ex vivo experiments, osteogenic activity is spatially correlated with macrophage accumulation and proteolytic/elastolytic activity (Fig. 13.1) [21–23]. Of note, NIRF longitudinal studies in the same animals allowed us to monitor dynamic changes in inflammation and osteogenesis simultaneously in vivo. In the second stage of calcification (propagation), these two processes develop in close proximity, and calcification typically appears in areas preceded by macrophage accumulation [22]. Overall, these findings suggest that inflammation precedes calcification. NIRF imaging experiments have been extensively validated through complementary immunohistochemical analysis showing expression of osteopontin, osteocalcin, Runx2, and Notch1 by valvular myofibroblasts [23]. Our results reveal that valve calcification is a highly complex process triggered by inflammation, leading to the expression of osteogenic markers by valvular myofibroblasts. Moreover, these findings provide new insights into the initiation of early calcific lesions in aortic valves (Fig. 13.2). The initial deposition of hydroxyapatite crystals appears to be in the form of microcalcification. These discrete regions of mineralization may cause recurrent activation of an inflammatory response that would enhance ECM degradation and VIC differentiation. Crystal nucleation may start on the surface or lumen of extracellular vesicles released by myofibroblasts [22, 58–60]. The gradual aggregation of microcalcification could result in the large spherical particles composed of highly crystalline hydroxyapatite that recently have been observed in human aortic valves by electron scanning microscopy, even in the absence of macroscopic lesions [61].

Molecular imaging methods offer the great advantage for longitudinal studies to follow the evolution of a biological process over time in the same group of animals. This advantage has been exploited to test the hypothesis that inflammation precedes the events of calcification. Carotid arteries of $ApoE^{-/-}$ mice were imaged to quantify macrophage accumulation and osteogenesis after 10 weeks of a high-cholesterol diet. The carotid arteries showed clear signs of inflammation, but barely any signs of osteogenesis [22]. In a subgroup of these mice, the atherogenic diet was supplemented with atorvastatin and a second imaging session was performed in the same carotid artery region after 10 more weeks. Statin treatment prevented the progression of macrophage burden and osteogenesis, supporting the hypothesis that inflammation promotes osteogenic activity. Similar strategies have been used to find therapeutic targets that block progression of inflammation in the aortic valve [11, 12]. Recently, a role of Notch ligand Delta-like 4 (Dll4) has been proposed in macrophage-mediated inflammation underlying the pathogenesis of cardiometabolic disorders [62]. By ex vivo mapping experiments using FRI, aortic valve calcification was attenuated after blockade of Dll4-Notch signaling with an anti-Dll4 monoclonal antibody [63]. Future work is necessary to understand the mechanisms that promote accumulation of macrophages in the valve leaflets, as well as the signaling pathways involved in inducing the inflammatory response.

Epidemiological surveys have indicated an association among osteoporosis, atherosclerosis, CRD, and cardiovascular calcification [64–66]. In humans, arterial and aortic valve calcification correlates with decreased bone mineral density (BMD). In atherogenic mice, a high-fat diet induces osteoblastic apoptosis, which in turn reduces bone formation [67]. Using 3D micro-CT and optical molecular imaging, we found that in atherosclerotic and CRD mice, the degree of cardiovascular calcification relates inversely to BMD. Most importantly, the bones of these mice also showed signs of inflammatory activity, visualized as uptake of NIRF-conjugated iron nanoparticles. No definitive explanation currently exists for the seemingly disparate responses of cardiac and bone tissue to inflammation.

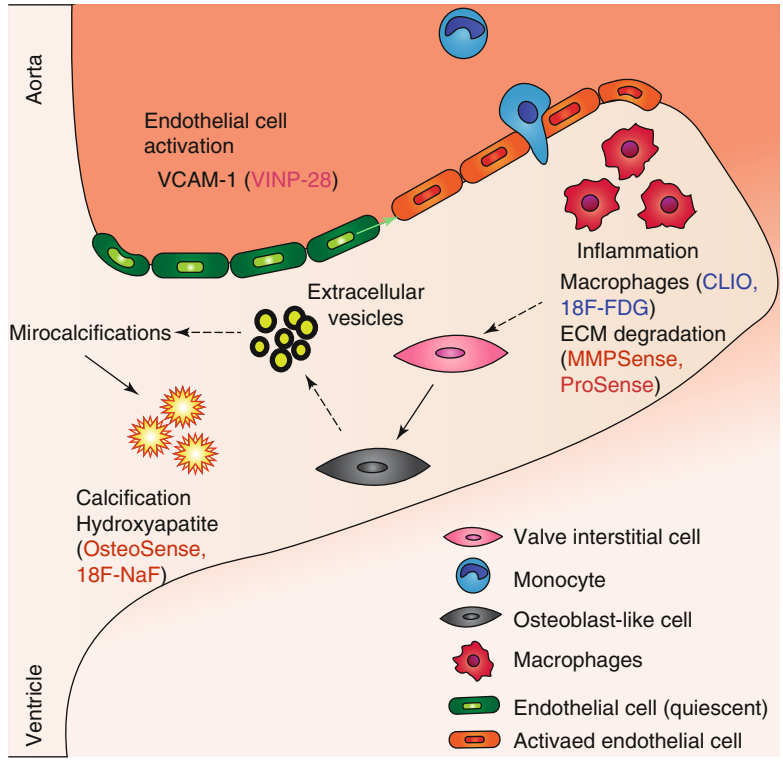

Fig 13.2 Major cellular events underlying calcific aortic valve disease as revealed by molecular imaging. Chronic inflammatory conditions lead to the activation of endothelial cells denoted by an increased expression of adhesion molecules, such as VCAM-1, which can be visualized by NIRF/MRI imaging with magnetofluorescent nanoparticles. The endothelium activation promotes the recruitment of circulating monocytes, which eventually results in macrophage accumulation in the valve interstitium. This process has been analyzed with NIRF macrophage-targeted nanoparticles (CLIO) and a radiolabeled glucose analogue (18F-FDG). The inflammatory process is associated with an extensive remodeling of the extracellular matrix triggered by the release of proteolytic enzymes. Specific probes for matrix metalloproteases and cathepsins have been developed for NIRF applications. Overall the inflammatory environment stimulates the differentiation of valvular myofibroblast into osteoblasts. These osteoblast-like cells release active vesicles capable of nucleating hydroxyapatite on their membranes. Microcalcifications can be identified by a bisphosphonate-conjugated imaging agent before macrospcopic lesions and valvular dysfunction are noted

Osteoporotic bones may release mineralization-promoting signals into the circulation that eventually impact the cardiovascular system [68]. Alternatively, osteoporosis and calcification have been proposed as tissue-specific responses to chronic inflammation [69].

Perspectives for Valve Imaging and Clinical Applications

Despite the enormous utility of IVM, FRI, and other imaging modalities to our understanding of the mechanisms underlying CAVD, these platforms present several disadvantages in their clinical application. Most of these modalities involve an invasive approach and have limited tissue penetration [20]. Considering that the detection of microcalcification formation represents an ideal time point for effective intervention, we need innovative imaging technologies with resolutions capable of their identification. Some promising recent efforts in this direction have combined the widely used technology available in the clinic with molecular imaging agents. Positron emission tomography (PET) combined with CT was used to assess in humans the degree of inflammation and calcification at different stages

of aortic valve disease. A glucose analogue, 18F-Fluorodeoxyglucose (18F-FDG)—uptaken by cells with high metabolic demands, such as macrophages—was used to target inflammatory activity [70, 71]. Sites of active mineralization were identified with 18F-Sodium fluoride (18F-NAF), which directly reacts with hydroxyapatite crystals [72–75]. The results of this study indicate that 18F-NAF allows the detection of regions of microcalcification and consolidated calcific lesions, thus representing a major advance for CAVD diagnostics. The 18F-FDG signal was observed in early stages of the disease, as would be expected from an inflammation marker, but it was also present in calcific regions. The latter may suggest that the incorporation of 18F-FDG may not only reflect inflammatory activity, as macrophages also exhibit increased glucose uptake in response to hypoxia [76]. Thus, additional experiments are needed to validate the use of glucose analogs as markers of inflammation in CAVD [77].

A new technology, micro-optical coherence tomography (μOCT), is one of the most promising approaches in terms of high resolution. This new imaging system allows the visualization of cellular and subcellular features with a resolution of less than 1 μm [78]. The cytoarchitecture of the atherosclerotic artery recently was studied using this technique; remarkably, cholesterol crystals, superficial calcium nodules, and microcalcifications were all visualized. Although conceived as an invasive catheter for its clinical application, μOCT has the potential for improving diagnosis by providing real-time information obtainable only with histological processes.

The advances over the past several years regarding in vivo and ex vivo imaging techniques have accelerated our understanding of cardiovascular calcification. New efforts are oriented to understand better the role of inflammation as an inducer of calcification. Clinical practice soon will benefit from the availability of imaging techniques that will guide the decision of eliminating risk factors from patients showing microcalcification. The need for innovative techniques suitable for the clinic will also aid in the evaluation of drugs with therapeutic potential for aortic valve calcification.

Acknowledgements This work was supported by a National Institute of Health grants (R01HL114805 and R01HL109506 to E.A.) EMM was a Research Fellow supported by Consejo Nacional de Ciencia y Tecnología (CONACYT; Estancias Postdoctorales y Sabáticas al extranjero: 175413) and Fundación México en Harvard, A.C. The authors thank Sara Karwacki for her editorial assistance.

References

1. Li Q, Uitto J. Mineralization/anti-mineralization networks in the skin and vascular connective tissues. Am J Pathol. 2013;183:10–8.
2. Budoff MJ, Shaw LJ, Liu ST, et al. Long-term prognosis associated with coronary calcification: observations from a registry of 25,253 patients. J Am Coll Cardiol. 2007;49:1860–70.
3. Abedin M, Tintut Y, Demer LL. Vascular calcification: mechanisms and clinical ramifications. Arterioscler Thromb Vasc Biol. 2004;24:1161–70.
4. Katz R, Budoff MJ, Takasu J, et al. Relationship of metabolic syndrome with incident aortic valve calcium and aortic valve calcium progression: the Multi-Ethnic Study of Atherosclerosis (MESA). Diabetes. 2009;58:813–9.
5. Nasir K, Katz R, Al-Mallah M, et al. Relationship of aortic valve calcification with coronary artery calcium severity: the Multi-Ethnic Study of Atherosclerosis (MESA). J Cardiovasc Comput Tomogr. 2010;4:41–6.
6. Takasu J, Budoff MJ, O'brien KD, et al. Relationship between coronary artery and descending thoracic aortic calcification as detected by computed tomography: the Multi-Ethnic Study of Atherosclerosis. Atherosclerosis. 2009;204:440–6.
7. Kelly-Arnold A, Maldonado N, Laudier D, et al. Revised microcalcification hypothesis for fibrous cap rupture in human coronary arteries. Proc Natl Acad Sci U S A. 2013;110:10741–6.
8. Osnabrugge RL, Mylotte D, Head SJ, et al. Aortic stenosis in the elderly: disease prevalence and number of candidates for transcatheter aortic valve replacement: a meta-analysis and modeling study. J Am Coll Cardiol. 2013;62:1002–12.
9. Stewart BF, Siscovick D, Lind BK, et al. Clinical factors associated with calcific aortic valve disease. Cardiovascular Health Study. J Am Coll Cardiol. 1997;29:630–4.
10. Allison MA, Cheung P, Criqui MH, et al. Mitral and aortic annular calcification are highly associated with systemic calcified atherosclerosis. Circulation. 2006;113:861–6.
11. Cowell SJ, Newby DE, Prescott RJ, et al. A randomized trial of intensive lipid-lowering therapy in calcific aortic stenosis. N Engl J Med. 2005;352:2389–97.
12. Rossebo AB, Pedersen TR, Boman K, et al. Intensive lipid lowering with simvastatin and ezetimibe in aortic stenosis. N Engl J Med. 2008;359:1343–56.

13. Rajamannan NM, Evans FJ, Aikawa E, et al. Calcific aortic valve disease: not simply a degenerative process a review and agenda for research from the National Heart and Lung and Blood Institute Aortic Stenosis Working Group. Circulation. 2011;124:1783–91.
14. Otto CM. Calcific aortic stenosis – time to look more closely at the valve. N Engl J Med. 2008;359:1395–8.
15. Clark MA, Duhay FG, Thompson AK, et al. Clinical and economic outcomes after surgical aortic valve replacement in Medicare patients. Risk Manag Healthc Policy. 2012;5:117–26.
16. Jaffe IZ, Tintut Y, Newfell BG, et al. Mineralocorticoid receptor activation promotes vascular cell calcification. Arterioscler Thromb Vasc Biol. 2007;27:799–805.
17. Gkizas S, Koumoundourou D, Sirinian X, et al. Aldosterone receptor blockade inhibits degenerative processes in the early stage of calcific aortic stenosis. Eur J Pharmacol. 2010;642:107–12.
18. Elmariah S, Delaney JA, O'brien KD, et al. Bisphosphonate use and prevalence of valvular and vascular calcification in Women MESA (The Multi-Ethnic Study of Atherosclerosis). J Am Coll Cardiol. 2010;56:1752–9.
19. Pittet MJ, Weissleder R. Intravital imaging. Cell. 2011;147:983–91.
20. Weissleder R, Ntziachristos V. Shedding light onto live molecular targets. Nat Med. 2003;9:123–8.
21. Aikawa E, Aikawa M, Libby P, et al. Arterial and aortic valve calcification abolished by elastolytic cathepsin S deficiency in chronic renal disease. Circulation. 2009;119:1785–94.
22. Aikawa E, Nahrendorf M, Figueiredo JL, et al. Osteogenesis associates with inflammation in early-stage atherosclerosis evaluated by molecular imaging in vivo. Circulation. 2007;116:2841–50.
23. Aikawa E, Nahrendorf M, Sosnovik D, et al. Multimodality molecular imaging identifies proteolytic and osteogenic activities in early aortic valve disease. Circulation. 2007;115:377–86.
24. Hjortnaes J, Butcher J, Figueiredo JL, et al. Arterial and aortic valve calcification inversely correlates with osteoporotic bone remodelling: a role for inflammation. Eur Heart J. 2010;31:1975–84.
25. Zaheer A, Lenkinski RE, Mahmood A, et al. In vivo near-infrared fluorescence imaging of osteoblastic activity. Nat Biotechnol. 2001;19:1148–54.
26. Zaheer A, Murshed M, De Grand AM, et al. Optical imaging of hydroxyapatite in the calcified vasculature of transgenic animals. Arterioscler Thromb Vasc Biol. 2006;26:1132–6.
27. Kozloff KM, Volakis LI, Marini JC, et al. Near-infrared fluorescent probe traces bisphosphonate delivery and retention in vivo. J Bone Miner Res. 2010;25:1748–58.
28. Cybulsky MI, Gimbrone Jr MA. Endothelial expression of a mononuclear leukocyte adhesion molecule during atherogenesis. Science. 1991;251:788–91.
29. Nakashima Y, Raines EW, Plump AS, et al. Upregulation of VCAM-1 and ICAM-1 at atherosclerosis-prone sites on the endothelium in the ApoE-deficient mouse. Arterioscler Thromb Vasc Biol. 1998;18:842–51.
30. Obrien KD, Allen MD, Mcdonald TO, et al. Vascular cell-adhesion molecule-1 is expressed in human coronary atherosclerotic plaques – implications for the mode of progression of advanced coronary atherosclerosis. J Clin Invest. 1993;92:945–51.
31. Nahrendorf M, Jaffer FA, Kelly KA, et al. Noninvasive vascular cell adhesion molecule-1 imaging identifies inflammatory activation of cells in atherosclerosis. Circulation. 2006;114:1504–11.
32. Ghaisas NK, Foley JB, O'briain DS, et al. Adhesion molecules in nonrheumatic aortic valve disease: endothelial expression, serum levels and effects of valve replacement. J Am Coll Cardiol. 2000;36:2257–62.
33. Thubrikar MJ, Aouad J, Nolan SP. Patterns of calcific deposits in operatively excised stenotic or purely regurgitant aortic valves and their relation to mechanical stress. Am J Cardiol. 1986;58:304–8.
34. Sun L, Chandra S, Sucosky P. Ex vivo evidence for the contribution of hemodynamic shear stress abnormalities to the early pathogenesis of calcific bicuspid aortic valve disease. PLoS One. 2012;7:e48843.
35. Akahori H, Tsujino T, Naito Y, et al. Intraleaflet haemorrhage is associated with rapid progression of degenerative aortic valve stenosis. Eur Heart J. 2011;32:888–96.
36. Yu Z, Seya K, Daitoku K, et al. Tumor necrosis factor-α accelerates the calcification of human aortic valve interstitial cells obtained from patients with calcific aortic valve stenosis via the BMP2-Dlx5 pathway. J Pharmacol Exp Ther. 2011;337:16–23.
37. Clark-Greuel JN, Connolly JM, Sorichillo E, et al. Transforming growth factor-beta1 mechanisms in aortic valve calcification: increased alkaline phosphatase and related events. Ann Thorac Surg. 2007;83:946–53.
38. Cushing MC, Mariner PD, Liao JT, et al. Fibroblast growth factor represses Smad-mediated myofibroblast activation in aortic valvular interstitial cells. FASEB J. 2008;22:1769–77.
39. Hamilton AM, Rogers KA, Belisle AJ, et al. Early identification of aortic valve sclerosis using iron oxide enhanced MRI. J Magn Reson Imaging. 2010;31:110–6.
40. Šteiner I, Krbal L, Rozkoš T, et al. Calcific aortic valve stenosis: immunohistochemical analysis of inflammatory infiltrate. Pathol Res Pract. 2012;208:231–4.
41. Wallby L, Janerot-Sjoberg B, Steffensen T, et al. T lymphocyte infiltration in non-rheumatic aortic stenosis: a comparative descriptive study between tricuspid and bicuspid aortic valves. Heart. 2002;88:348–51.
42. Otto CM, Kuusisto J, Reichenbach DD, et al. Characterization of the early lesion of 'degenerative' valvular aortic stenosis. Histological and immunohistochemical studies. Circulation. 1994;90:844–53.
43. Olsson M, Dalsgaard CJ, Haegerstrand A, et al. Accumulation of T lymphocytes and expression of interleukin-2 receptors in nonrheumatic stenotic aortic valves. J Am Coll Cardiol. 1994;23:1162–70.

44. Rabkin E, Aikawa M, Stone JR, et al. Activated interstitial myofibroblasts express catabolic enzymes and mediate matrix remodeling in myxomatous heart valves. Circulation. 2001;104:2525–32.
45. Aikawa E, Whittaker P, Farber M, et al. Human semilunar cardiac valve remodeling by activated cells from fetus to adult: implications for postnatal adaptation, pathology, and tissue engineering. Circulation. 2006;113:1344–52.
46. Aikawa M, Rabkin E, Okada Y, et al. Lipid lowering by diet reduces matrix metalloproteinase activity and increases collagen content of rabbit atheroma: a potential mechanism of lesion stabilization. Circulation. 1998;97:2433–44.
47. Helske S, Syvaranta S, Lindstedt KA, et al. Increased expression of elastolytic cathepsins S, K, and V and their inhibitor cystatin C in stenotic aortic valves. Arterioscler Thromb Vasc Biol. 2006;26:1791–8.
48. Deguchi JO, Aikawa E, Libby P, et al. Matrix metalloproteinase-13/collagenase-3 deletion promotes collagen accumulation and organization in mouse atherosclerotic plaques. Circulation. 2005;112:2708–15.
49. Rabkin-Aikawa E, Aikawa M, Farber M, et al. Clinical pulmonary autograft valves: pathologic evidence of adaptive remodeling in the aortic site. J Thorac Cardiovasc Surg. 2004;128:552–61.
50. Rabkin-Aikawa E, Farber M, Aikawa M, et al. Dynamic and reversible changes of interstitial cell phenotype during remodeling of cardiac valves. J Heart Valve Dis. 2004;13:841–7.
51. Masters KS, Shah DN, Walker G, et al. Designing scaffolds for valvular interstitial cells: cell adhesion and function on naturally derived materials. J Biomed Mater Res A. 2004;71:172–80.
52. Rodriguez KJ, Masters KS. Regulation of valvular interstitial cell calcification by components of the extracellular matrix. J Biomed Mater Res A. 2009;90:1043–53.
53. Yip CY, Chen JH, Zhao R, et al. Calcification by valve interstitial cells is regulated by the stiffness of the extracellular matrix. Arterioscler Thromb Vasc Biol. 2009;29:936–42.
54. Simionescu A, Sirnionescu DT, Vyavahare NR. Osteogenic responses in fibroblasts activated by elastin degradation products and transforming growth factor-beta 1 – role of myofibroblasts in vascular calcification. Am J Pathol. 2007;171:116–23.
55. Jacob MP, Fulop T, Foris G, et al. Effect of elastin peptides on ion fluxes in mononuclear-cells, fibroblasts, and smooth-muscle cells. Proc Natl Acad Sci U S A. 1987;84:995–9.
56. Belaaouaj AA, Li AG, Wun TC, et al. Matrix metalloproteinases cleave tissue factor pathway inhibitor – effects on coagulation. J Biol Chem. 2000;275:27123–8.
57. Qin X, Corriere MA, Matrisian LM, et al. Matrix metalloproteinase inhibition attenuates aortic calcification. Arterioscler Thromb Vasc Biol. 2006;26:1510–6.
58. New SE, Goettsch C, Aikawa M, et al. Macrophage-derived matrix vesicles: an alternative novel mechanism for microcalcification in atherosclerotic plaques. Circ Res. 2013;113:72–7.
59. New SE, Aikawa E. Role of extracellular vesicles in de novo mineralization: an additional novel mechanism of cardiovascular calcification. Arterioscler Thromb Vasc Biol. 2013;33:1753–8.
60. Kapustin AN, Davies JD, Reynolds JL, et al. Calcium regulates key components of vascular smooth muscle cell-derived matrix vesicles to enhance mineralization. Circ Res. 2011;109:E1–U41.
61. Bertazzo S, Gentleman E, Cloyd KL, et al. Nano-analytical electron microscopy reveals fundamental insights into human cardiovascular tissue calcification. Nat Mater. 2013;12:576–83.
62. Fung E, Tang SM, Canner JP, et al. Delta-like 4 induces notch signaling in macrophages: implications for inflammation. Circulation. 2007;115:2948–56.
63. Fukuda D, Aikawa E, Swirski FK, et al. Notch ligand delta-like 4 blockade attenuates atherosclerosis and metabolic disorders. Proc Natl Acad Sci U S A. 2012;109:E1868–77.
64. Farhat GN, Cauley JA, Matthews KA, et al. Volumetric BMD and vascular calcification in middle-aged women: the study of women's health across the nation. J Bone Miner Res. 2006;21:1839–46.
65. Farhat GN, Strotmeyer ES, Newman AB, et al. Volumetric and areal bone mineral density measures are associated with cardiovascular disease in older men and women: the health, aging, and body composition study. Calcif Tissue Int. 2006;79:102–11.
66. Frost ML, Grella R, Millasseau SC, et al. Relationship of calcification of atherosclerotic plaque and arterial stiffness to bone mineral density and osteoprotegerin in postmenopausal women referred for osteoporosis screening. Calcif Tissue Int. 2008;83:112–20.
67. Hirasawa H, Tanaka S, Sakai A, et al. ApoE gene deficiency enhances the reduction of bone formation induced by a high-fat diet through the stimulation of p53-mediated apoptosis in osteoblastic cells. J Bone Miner Res. 2007;22:1020–30.
68. Tekin GO, Kekilli E, Yagmur J, et al. Evaluation of cardiovascular risk factors and bone mineral density in post menopausal women undergoing coronary angiography. Int J Cardiol. 2008;131:66–9.
69. Demer LL, Tintut Y. Mechanisms linking osteoporosis with cardiovascular calcification. Curr Osteoporos Rep. 2009;7:42–6.
70. Rudd JH, Warburton EA, Fryer TD, et al. Imaging atherosclerotic plaque inflammation with [18F]-fluorodeoxyglucose positron emission tomography. Circulation. 2002;105:2708–11.
71. Rudd JH, Narula J, Strauss HW, et al. Imaging atherosclerotic plaque inflammation by fluorodeoxyglucose with positron emission tomography: ready for prime time? J Am Coll Cardiol. 2010;55:2527–35.
72. Blau M, Ganatra R, Bender MA. 18F-fluoride for bone imaging. Semin Nucl Med. 1972;2:31–7.
73. Grant FD, Fahey FH, Packard AB, et al. Skeletal PET with 18F-fluoride: applying new technology to an old tracer. J Nucl Med. 2008;49:68–78.

74. Derlin T, Richter U, Bannas P, et al. Feasibility of 18F-sodium fluoride PET/CT for imaging of atherosclerotic plaque. J Nucl Med. 2010;51:862–5.
75. Derlin T, Wisotzki C, Richter U, et al. In vivo imaging of mineral deposition in carotid plaque using 18F-sodium fluoride PET/CT: correlation with atherogenic risk factors. J Nucl Med. 2011;52:362–8.
76. Folco EJ, Sheikine Y, Rocha VZ, et al. Hypoxia but not inflammation augments glucose uptake in human macrophages: implications for imaging atherosclerosis with 18fluorine-labeled 2-deoxy-D-glucose positron emission tomography. J Am Coll Cardiol. 2011;58:603–14.
77. Marincheva-Savcheva G, Subramanian S, Qadir S, et al. Imaging of the aortic valve using fluorodeoxyglucose positron emission tomography increased valvular fluorodeoxyglucose uptake in aortic stenosis. J Am Coll Cardiol. 2011;57:2507–15.
78. Liu L, Gardecki JA, Nadkarni SK, et al. Imaging the subcellular structure of human coronary atherosclerosis using micro-optical coherence tomography. Nat Med. 2011;17:1010–4.

14 Role of Ectonucleotidases and Purinergic Receptors in Calcific Aortic Valve Disease

Patrick Mathieu, Ablajan Mahmut, Philippe Pibarot, Yohan Bossé, and Marie-Chloé Boulanger

Introduction

Calcific aortic valve disease (CAVD) is the most common heart valve disorders [1]. Despite intensive research effort in the last decade or so no medical therapy has emerged to treat patients with CAVD [2]. Studies have underlined that CAVD is characterized by lipid infiltration, inflammation, calcification and extensive tissue remodelling, which leads over the years to a clinically significant stenosis [3]. It should be stressed that mineralization and fibrosis are two major contributors to the development and progression of CAVD. Ectopic valve mineralization involves two mechanisms. First, it is well documented by using in vitro system of cell culture that valve interstitial cells (VICs), the main cellular component of the aortic valve, undergo an osteoblastic transition when exposed to a calcifying medium containing phosphate [4]. During this phenotypic switch VICs express several genes, which are involved in osteoblast development such as Runx2, osteopontin, osteocalcin and bone morphogenetic proteins (BMPs) [5]. It is of interest to note that these osteogenic markers are present in specimen of CAVD retrieved from patients undergoing aortic valve replacements procedures [6]. Second, there is evidence that production of phosphate (Pi), which is of prime importance in controlling mineralization of VICs, promotes apoptosis-mediated mineralization [7]. To this effect, in vitro inhibition of apoptosis prevents phosphate-induced mineralization of VICs [8]. Also, in stenotic aortic valves a high level of apoptotic cells is present in the vicinity of calcific nodules. It should be pointed out that osteoblastic transition and apoptosis-mediated mineralization are not mutually exclusive and probably occur simultaneously in

P. Mathieu, MD (✉)
Department of Surgery, Laboratoire d'Études Moléculaires des Valvulopathies (LEMV), Groupe de Recherche en Valvulopathies (GRV), Quebec Heart and Lung Institute/Research Center, Quebec, QC, Canada

Department of Surgery, Laval University, Québec, QC, Canada

Institut de Cardiologie et de Pneumologie de Québec/ Quebec Heart and Lung Institute, 2725 Chemin Sainte-Foy, Quebec, QC G1V 4G5, Canada
e-mail: patrick.mathieu@chg.ulaval.ca

A. Mahmut, MD, MSc • P. Pibarot, DVM, PhD, FAHA, FACC, FESC, FASE • Y. Bossé, PhD
M.-C. Boulanger, PhD
Laboratoire d'Études Moléculaires des Valvulopathies (LEMV), Groupe de Recherche en Valvulopathies (GRV), Quebec Heart and Lung Institute/Research Center, Quebec, QC, Canada

Department of Surgery,
Laval University, Québec, QC, Canada
e-mail: philippe.pibarot@med.ulaval.ca; yohan.bosse@criucpq.ulaval.ca; marie-chloe.boulanger@criucpq.ulaval.ca

Disclosures
P. Mathieu has patent applications for the use of ectonucleotidase inhibitors and purinergic agonists in the treatment of CAVD.

N.M. Rajamannan (ed.), *Molecular Biology of Valvular Heart Disease*,
DOI 10.1007/978-1-4471-6350-3_14,

different proportions to promote the calcification of the aortic valve. In this regard, studies have highlighted that the stiffness of the substrate on which VICs are grown may determine whether cells will undergo either osteoblastic transition or apoptosis. On this score, a stiffer support largely drives apoptosis of VICs whereas a more compliant matrix will promote mineralization through the expression of bone-related factors [9]. Hence, it could be speculated that during the initial stages of aortic valve mineralization, when the tissues are still relatively compliant, that osteogenic transformation of VICs is dominant, whereas when the process is more advanced apoptosis-mediated mineralization would possibly be major contributor to ectopic valve mineralization.

It is worth to emphasize that both osteogenic transition and apoptosis-mediated mineralization relies largely on availability and production of Pi in the cell environment. To this effect, Pi acts as major modulator of gene expression and, in doing so, contributes to a phenotypic switch of VICs [10]. The ectonucleotidases are a group of membrane bound enzymes, which modulates the extracellular levels of nucleotides and nucleosides and, in doing so, promote the production of phosphate (Pi) and pyrophosphate (PPi), two major molecules that control mineralization [11]. In addition, by changing the bioavailability of nucleotides and nucleosides, the ectonucleotidases exert a control over purinergic signaling [12]. Recently, purinergic signaling has emerged as an important driver of ectopic valve mineralization [13]. Herein, we will review the role and contribution of ectonucleotidases and purinergic receptors in the development of calcific aortic valve disease. The importance of this system in CAVD will be discussed in light of novel therapeutic opportunities that it may offer.

Overview of Ectonucleotidases and Purinergic Receptors

The ectonucleotidases are divided into four families of genes, which encompass: ectonucleotide pyrophosphatase/phosphodiesterases (ENPPs), ectonucleoside triphosphate diphosphohydrolases (ENTPDs), 5′-nucleotidase (NT5E), and alkaline phosphatase (ALP). ENPPs include 7 members, which are involved in different biological processes [14]. While ENPP1-3 have been shown to play roles in different disorders, the role of ENPP4-7 is less clear for the moment. ENPPs are involved in the transformation of ATP into AMP, which also liberate PPi. Also, often less appreciated is the fact that under certain circumstances ENPP can hydrolyze ADP into AMP. It is worth to highlight that ENPP2 is an exception to this rule since it has a poor pyrophophatase/phosphodiesterase activity and is instead a lysophospholipase D, which catalyze the transformation of lysophospholipids into lysophosphatidic acid (LPA) [15]. By allowing the formation of PPi, ENPP1 is an important regulator of mineralization. ENTPDs 1–3 and 8 are located at the cell membrane with the enzymatic site facing the extracellular milieu, whereas ENTPD4-7 are cytosolic proteins. ENTPDs catalyze the hydrolysis of ATP into ADP as well as the transformation of ADP into AMP. ENTPDs have an important control over vascular function, thrombosis and inflammation [16]. NT5E is often co-expressed in tissues where ENTPDs are present and exert a control over the adenosine receptors. To this effect, NT5E uses AMP as a substrate and produce adenosine [17]. ALP is a phosphatase that can use a wide array of substrate and generate therefore a large amount of Pi. By using PPi as a substrate to generate Pi, ALP is also an important regulator of ectopic mineralization [18].

Ectonucleotidases by using different nucleotides and nucleotides as substrates exert a control over purinergic receptors. Hence, each tissue owing to its specific expression of ectonucleotidases may have different responses to nucleotides and nucleosides. A layer of complexity in purinergic signaling is added by the existence of 19 different genes encoding purinergic receptors. It is worth to point out that the ectonucleotidase/purinergic receptor ‘signature’ may change during pathologic process with profound impact on the pathophysiology. The purinergic receptors include the adenosine-sensitive receptors (P1) as well as the nucleotides and nucleosides-responsive

receptors (P2). There are 4 adenosine receptors, which signal through cAMP pathway [19]. A_1 and A_3 receptors are G protein coupled receptors (GPCR), which signals through $G_{i/0}$ and thus lower cAMP production. On the other hand, A_{2a} and A_{2b} receptors are G_s receptors and therefore increase intracellular levels of cAMP. Adenosine receptors control inflammation and participate in the regulation of extracellular matrix synthesis. Therefore, P1 receptors play a role in fibrotic disorders. P2 receptors are divided into two broad categories: the ion channel receptors (P2X) and the G-protein-coupled receptor (P2Y). Upon activation P2X receptor promotes the opening of cation channels, which results in changes of electrical potential and the activation of a signaling cascade. Among the different pathways, P2X receptors have been shown to induce the activation of the protein kinase A (PKA), protein kinase C (PKC), phosphoinositide 3-kinase (PI3K) and the extracellular-signal-regulated kinase 1/2 (ERK1/2) pathways. Currently, 7 different P2X receptor subunits have been described ($P2X_{1-7}$) and their expression have been documented in neuronal cells, T cells, macrophages and endothelial cells [20]. On the other hand, 8 different P2Y receptors have been cloned $P2Y_{(1,2,4,6,11,12,13,14)}$ and their expression has been documented in several cell types including vascular smooth muscle cells (VSMCs) and VICs. P2Y receptors have been shown to signal through phospholipase C (PLC), PKC, PI3K and ERK1/2, which are incidentally pathways that have been previously found implicated in the mineralization of VSMCs/VICs [8]. P2X receptors are stimulated by ATP, whereas P2Y receptors are stimulated by ATP, ADP, UTP and UDP.

ENPP1: Friend or Foe in Ectopic Valve Mineralization?

ENPP1 is a major contributor to the production of PPi, which inhibits the nucleation of hydroxyapatite of calcium (HAC). Hence, in mice a complete knockdown of ENPP1 is associated with ectopic mineralization of tendons and soft tissues [21]. In humans, rare mutations of ENPP1, which greatly affect enzyme function, are associated with generalized arterial calcification of infancy (GACI) [22]. However, it is worth to point out that the latter phenotype is not constant since reports also indicate that same mutations are associated with hypophosphatemic rickets and absence of vascular calcification [23]. The double deficient ENPP1ttw/ttw $ApoE^{-/-}$ mice develop medial calcification but have smaller atherosclerotic lesions when compared to $ApoE^{-/-}$ mice [24]. On the other hand, heterozygote mice for the ttw allele (ENPP1ttw/+ $ApoE^{-/-}$) do not develop medial calcification and also have smaller atherosclerotic lesions compared to $ApoE^{-/-}$ mice. The conclusions of this study are twofold. First, these findings suggest that ENPP1, by still an elusive mechanism, promotes atherosclerosis. Second, considering that the heterozygote ENPP1ttw/+ $ApoE^{-/-}$ mice did not develop medial calcification compared to the homozygote mice for the ttw allele (ENPP1ttw/ttw $ApoE^{-/-}$) it is likely that a minimal production of PPi is required to prevent ectopic vascular mineralization. Noteworthy, isolated VSMCs from ENPP1ttw/ttw $ApoE^{-/-}$ and ENPP1ttw/+ $ApoE^{-/-}$ produced less osteopontin, a negative regulator of mineralization. Hence, these findings highlight that a minimal production of PPi is of foremost importance in preventing ectopic mineralization. In addition, considering that CAVD has to some extent similarities with atherosclerosis it is possible that a dysregulation of ENPP1 in CAVD play a role into the pathobiology.

We recently identified that expression of ENPP1 is increased in stenotic aortic valve. In addition, we documented that ENPP enzyme activity correlated with the amount of calcium in human specimen of CAVD, suggesting a relationship between mineralization and ENPP1 [8]. In vitro, overexpression of ENPP1 in isolated VIC cultures increased mineralization. Similarly, in isolated chondrocytes the transfection of a vector encoding ENPP1 promoted mineralization of cell cultures, suggesting that ENPP1 is a positive regulator of ectopic mineralization when overexpressed [25]. The question that arises is by which mechanism ENPP1 promotes mineralization? Following a series of experiments in isolated VICs we recently underlined that by depleting ATP in the extracellular milieu

ENPP1 contributes to decrease purinergic signaling through $P2Y_2$ receptor (P2Y2R), an important negative regulator of mineralization in VICs. Also, it is worth to emphasize that during pathologic mineralization ALP is co-expressed with ENPP1. Hence, it is likely that PPi that are produced by ENPP1 are transformed by ALP into Pi, which increases the Pi/PPi ratio and therefore promote mineralization. When taken together, these findings suggest that ENPP1 has U-shape relationship with ectopic mineralization. Absence or very low level of ENPP1 expression is conducive to ectopic mineralization by lowering the amount of extracellular PPi, whereas a high level of ENPP1promotes calcification by affecting purinergic signaling. Hence, expression of ENPP1 must be tightly regulated within a certain range in order to prevent ectopic valve/vascular mineralization.

Is ENPP1 the Missing Link Between Visceral Obesity/Type 2 Diabetes and CAVD?

Patients with the metabolic syndrome (MetS) have an increased prevalence of aortic valve calcification [26]. In addition, we previously reported that hemodynamic progression of stenosis is faster in patients with the MetS [27, 28]. Of note, MetS is characterized by the accumulation of ectopic visceral fat, insulin resistance/diabetes, hypertension and an atherogenic dyslipidemia [29]. In this regard, patients with type 2 diabetes (T2D) have an elevated proportion of small, dense low-density lipoprotein (LDL), which is strongly associated with the accumulation of oxidized-LDL within the aortic valve, a powerful promoter of aortic valve calcification [30]. However, it is worth to underscore that the mechanism whereby insulin resistance/T2D promotes CAVD is still poorly understood. Côté et al. found that single nucleotide polymorphisms (SNPs) in the gene encoding ENPP1 are associated with CAVD [8]. More specifically, two SNPs, namely rs1800949 and rs7754586, previously associated with obesity and diabetes respectively, were significantly associated with CAVD (Fig. 14.1) [31, 32]. Of interest, ENPP1 is suspected to be of importance in promoting insulin resistance. To this effect, the content of ENPP1 is increased in skeletal muscle of patients with diabetes [33]. In addition, overexpression of ENPP1 in the liver and adipose tissue promotes insulin resistance [34]. It has been shown that ENPP1 reduces autophosphorylation of the insulin receptor (IR). Studies have highlighted that ENPP1 may interfere with IR by a direct physical interaction. However, whether enzyme activity of ENPP1 is necessary or not in order to interfere with IR activation is controversial [35].

In vitro studies have underlined that insulin is a negative regulator of phosphate-induced

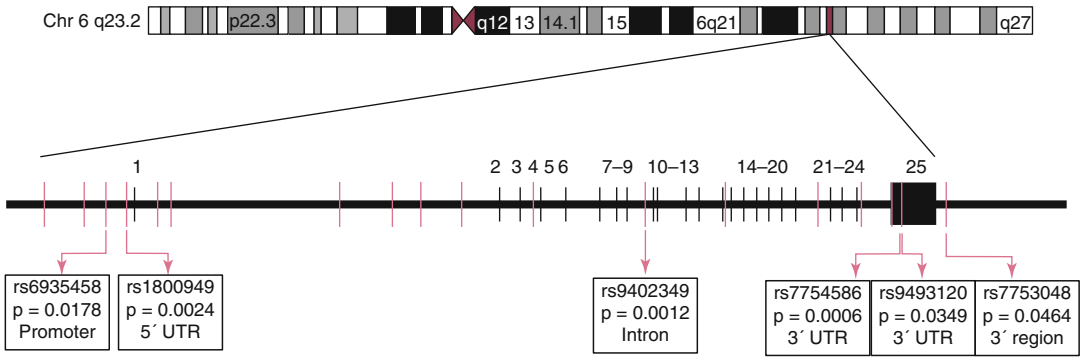

Fig. 14.1 ENPP1gene map on human chromosome 6. SNPs located in the promoter, introns, and 3′UTR region of the gene were associated with CAVD in a case-control study. Three SNPs were significant following correction for multiple testing: rs7754586, rs9402349 and rs1800949 (From Côté et al. [8])

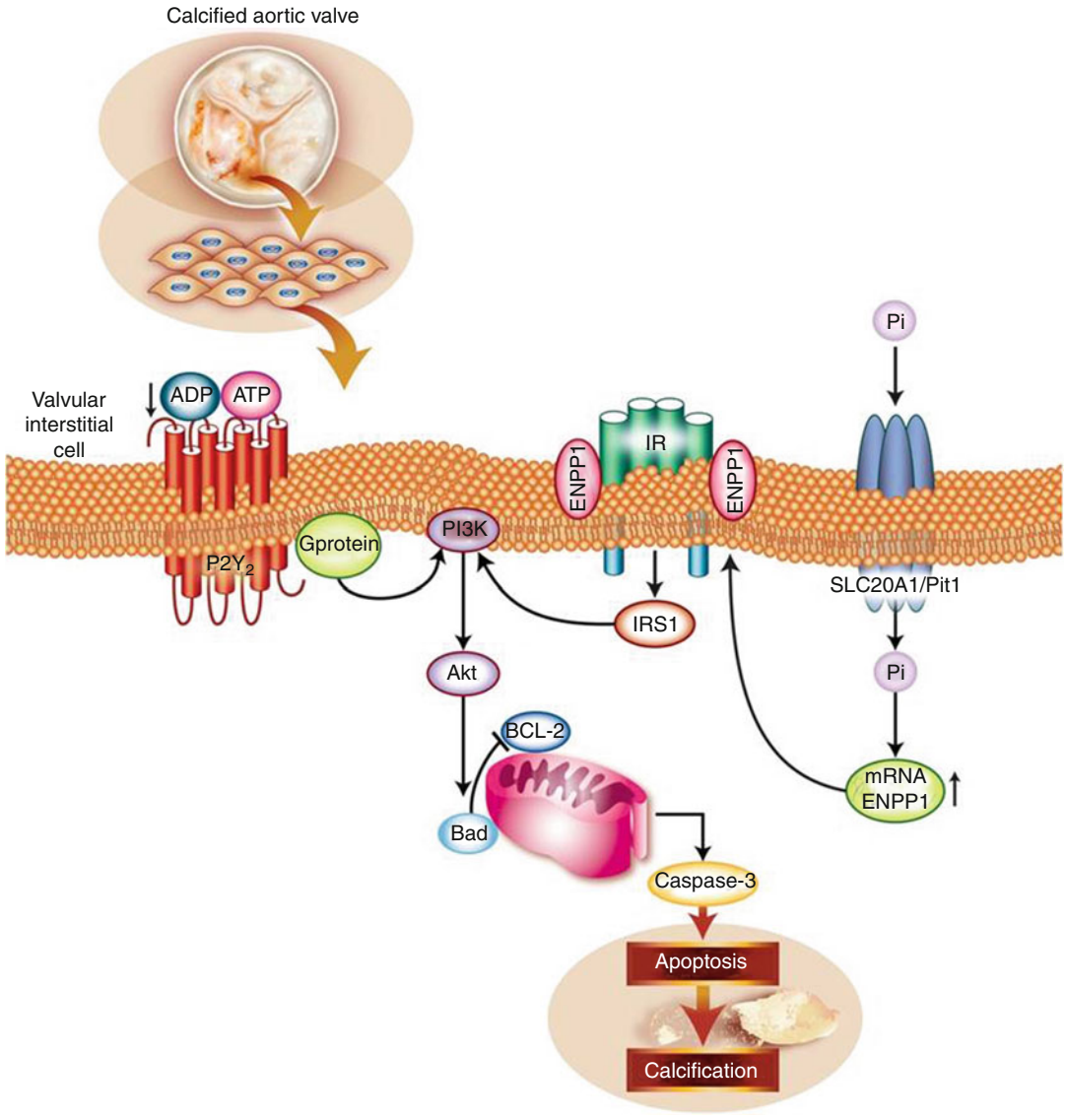

Fig. 14.2 Integrative figure showing interaction of ENPP1 with insulin receptor (*IR*) and P2Y2R as well as with downstream signaling (From Mathieu et al. [13])

mineralization of VSMCs. Downstream signaling of IR such as MAPK and Akt pathways may lower mineralization of VSMCs [36]. We reported that following treatment of VICs with phosphate the levels of mRNA encoding Akt1 and phosphorylated Akt are reduced to a great extent [7]. Although not yet examined in VICs it is possible that insulin may have preventive effect on the mineralization of the aortic valve through Akt pathway. Hence, impediment to insulin signaling, which can be promoted by the overexpression of ENPP1, may contribute to ectopic valve mineralization (Fig. 14.2). However, further work is necessary to examine the relationship between insulin signaling and ENPP1 in the context of aortic valve mineralization.

Phosphate as a Signaling Molecule in Valve Interstitial Cells

Extracellular Pi is generated from the hydrolysis of different nucleotides and nucleosides. As indicated above, ALP can use PPi to generate Pi. Hence, a build-up of Pi occurs when ectonucleotidases are overexpressed and triggers ectopic mineralization. In bone, evidence indicates that extracellular Pi is produced owing to the secretion of matrix vesicles (MVs), which contains a high level of ALP and ENPP1 [37]. It is thought that elevated content of Pi around MVs creates a microenvironment conducive to precipitation of calcium and formation of hydroxyapatite of calcium, which is the predominant calcium-phosphate crystal within CAVD. Of interest, a recent study has found in CAVD the presence of mineralized spheroid microparticles, which are thought to coalesce into larger mineralized structures [38]. Although the exact origin of spheroid microparticles in CAVD has not been identified, it is possible that these particles represent the early phase of mineralization, which may derive from MVs and/or apoptotic cells. Pi is also a potent intracellular signaling molecule in VICs and VSMCs. In this regard, studies have documented that Pi is channeled within the intracellular compartment by the Na^+-Pi co-transporter (Pit1/SLC20A1), which is overexpressed in stenotic aortic valves. El Husseini et al. recently identified that Pit1/SLC20A1 is an important regulator of VICs mineralization [7]. In this regard, it was found that intracellular channeling of Pi by Pit1/SLC20A1 promoted the expression of osteogenic genes. Phosphate-induced expression of osteopontin, osteonectin, osteocalcin, ALP and Runx2 were abrogated by phosphonoformic acid (PFA), an inhibitor of Pit1/SLC20A1 (Fig. 14.3). Moreover, the intracellular transport of Pi reduced the level of Akt and promoted apoptosis-mediated mineralization of VIC cultures. Phosphate-treated VICs exhibited a loss of mitochondrial membrane potential ($\Delta\Psi m$) and expressed activated caspase 3. The apoptosis-mediated mineralization induced by phosphate was prevented by cyclosporin A, an inhibitor of mitochondrial permeability transition pore. Taken together, these findings indicate that

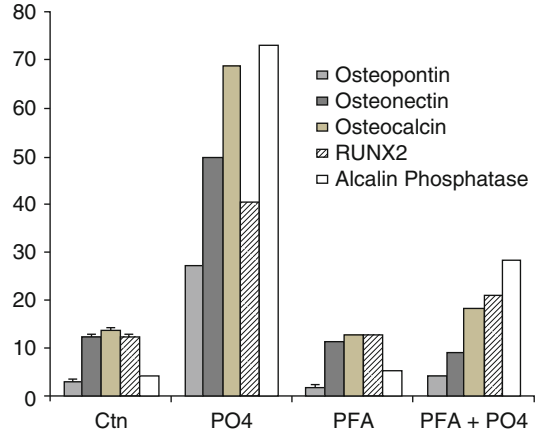

Fig. 14.3 Inhibition of Pit1/SLC20A1 with phosphonoformic acid (*PFA*) prevents the mRNA expression levels of osteoblastic genes to rise following treatment of VIC cultures with phosphate (From El Husseini et al. [7])

phosphate-induced mineralization relies, at least in part, on mitochondrial-dependent apoptosis. Of note, the transfection of VICs with a vector encoding Akt-1 prevented Pi-induced mineralization of VICs. Of interest, in human stenotic aortic valves the level of Akt-1 is greatly reduced compared to control non-mineralized valves. It is likely that in VICs Akt prevents phosphate-induced mineralization by anti-apoptotic mechanism. These findings highlight the importance of Pi as a signaling molecule in promoting mineralization of VICs. However, it should be pointed out that so far the molecular process by which intracellular channeling of Pi promotes osteogenic transition and lower the expression of Akt-1 is still an unresolved issue.

P2Y2 Receptor and Survival of Valve Interstitial Cells

P2Y2R is a G-protein coupled receptor (GPCR) and therefore has 7 transmembrane domains as well as an extracellular N-terminal and an intracellular C-terminal portion. P2Y2R is coupled to $G_{q/0}$ and activates phospholipase C (PLC), which produces inositol triphosphate (IP3) and diacylglycerol (DAG). IP3 promotes liberation of intracellular store of calcium from the endoplasmic reticulum and thus allows signaling through the activation of calcium/calmodulin kinase pathway.

On the other hand, DAG activates protein kinase C (PKC) [39]. It is worth to underline that P2Y2R can also signal through different pathways including MAPK and PI3K. ATP is secreted in the extracellular environment using diverse mechanisms such as connexin, pannexin and ATP-binding cassette (ABC) transporters [40]. As such, ATP is one important molecule used by cells to deliver signals in an auto/paracrine manner. In VICs, minute amount of ATP is liberated in the extracellular environment, where it is sensed by purinergic receptors. Among the different purinergic receptors expressed by VICs we identified that P2Y2R delivers survival signal to VICs through PI3K/Akt pathway. In cell culture experiments, the depletion of extracellular ATP by apyrase (a patato-derived ectonucleotidase) exacerbated Pi-induced mineralization of VIC cultures [8]. On the one hand, the addition of ATPγS to the growth medium of VIC cultures prevented mineralization of VICs. We also observed that gene silencing of P2Y2R in VICs greatly increased mineralization of cell cultures. Hence, ATP is liberated by VICs in the extracellular milieu and delivers survival signals to VICs. Thus, it is worth to highlight that liberation of ATP and the level of ectonucleotidases will modulate purinergic signaling through P2Y2R and thus will determine the fate of VICs with regard to the mineralizing phenotype.

5′nucleotidase (NT5E/CD73) and Ectopic Mineralization

NT5E by promoting the conversion of AMP into adenosine is an important regulator of P1 signaling. St-Hilaire et al. recently reported that loss-of-function mutations of NT5E are associated with rare familial cases of vascular calcifications, which are restricted to the lower-extremity arteries [41]. In this study, the mineralization of skin fibroblast of affected individuals was rescued by the addition of adenosine to the cell culture medium. The authors concluded that P1 signaling has anti-mineralizing properties by possibly lowering the expression of ALP. However, this study should be interpreted with caution as mineralization was not quantified by biochemical methods but documented solely by using alizarin red staining. Recently, Cloyd et al. demonstrated by using micro-Raman spectroscopy that alizarin red staining provides false-positive staining in cell culture experiments when using cells of fibroblastic origin; formation of non-calcified nodules may occur, which take up the alizarin red dye [42]. Also, adenosine was used in cells experiments, which is rapidly metabolized by adenosine deaminase. The use of specific non-hydrolysable P1 agonists may have provided additional insights with regard to the role of adenosine receptors in ectopic vascular mineralization. In lung fibroblasts stimulation of $A2_b$ receptor has been shown to increase inflammation and to promote fibrosis. On the other hand, A1 receptor is preventing inflammation of fibroblasts [43]. Hence, considering that A2 receptors are coupled to G_s and that A1 receptors are G_i it is likely that the pattern of expression of P1 receptors may drive their mineralizing response. Receptors coupled to G_s promote adenylate cyclase activity and the production of cAMP, whereas G_i receptors have the opposite effect. Noteworthy, we recently identified that stimulation of the cAMP pathway is promoting the mineralization of VICs through the expression of ectonucleotidases [44]. Although still unexplored it is possible that specific pattern of P1 receptors in different types of cells, including VICs, may determine their fate upon exposition to mineralizing stimuli. The role of P1 receptors in CAVD is still uninvestigated but certainly deserved further attention.

Ectonucleotidases/Purinergic Receptors as Potential Therapeutic Targets

Works performed in the last several years have contributed to identify that ectonucleotidases and purinergic receptors are important modulators of ectopic valve mineralization. On this score, it is possible that inhibitors of ectonucleotidases may provide benefit in preventing aortic valve mineralization. In a rat model, we recently documented that administration of ARL67156 prevented the development of CAVD [45]. ARL67156 is an

ectonucleotidase inhibitor known to be relatively not specific and poorly absorbed by the digestive tract. Hence, development of potent and selective inhibitors of ectonucleotidases would provide crucial information and would spur translational research in this field. However, the development of isoform specific inhibitors that would not affect purinergic receptors remains a challenging objective. Recently novel oxadiazole derivatives and diadenosine polyphosphate have been described as selective inhibitors of ENPP [13]. We should also emphasize that development of isoform specific inhibitors should be a priority. For instance, inhibition of ENTPD1 may, at least theoretically, worsen inflammation as this ectonucleotidase has been shown to modulate inflammation in different conditions.

Concluding Remarks

The ectonucleotidases/purinergic system is emerging as an important regulator of aortic valve mineralization. A high expression of ectonucleotidase in CAVD promotes mineralization by allowing a high production of Pi and decreasing purinergic signaling through P2Y2R. Co-expression during ectopic valve mineralization of different ectonucleotidases, such as ENPP1 and ALP, entrain the production of a high level of Pi, which is then acting as a strong promoter of mineralization. Pi is acting locally in matrix vesicles and/or in apoptotic remnants and promotes nucleation of hydroxyapatite of calcium. In addition, Pi through Pit1/SLC20A1 promotes the expression of several positive regulators of mineralization such as the bone-related transcription factor Runx2. Hence, Pi appears as a central key player as a signaling molecule in VICs and as a potent promoter of mineralization. Understanding the complex interrelationships between ectonucleotidases, Pi and purinergic signaling is of foremost importance as it may hold promise for further therapeutic development. However, many unresolved issues remain to be studied in order to fuel translational research in this field. In this regard, the role of P1 receptors in the mineralization of the aortic valve is still unknown. In addition, relationships between different ectonucleotidases expressed by VICs such as ENPP1, NT5E and ALP and their impact on the mineralizing process of VICs are still poorly understood. The development of novel isoform specific inhibitors of ectonucleotidases is still lacking. Hence, future research on ectonucleotidases and purinergic signaling will likely provide further important insights with regard to aortic valve mineralization and its pathobiology.

Summary Points

1. Ectonucleotidases by regulating Pi, PPi and ATP levels are important regulators of ectopic valve mineralization.
2. Purinergic signaling through P2Y2R prevents mineralization of VICs by activating the PI3K/Akt pathway.
3. Single nucleotide polymorphisms (SNPs) in the ENPP1 gene are associated with CAVD.
4. Insulin resistance is promoted by ENPP1 and may, at least in part, explain the frequent association of insulin resistance/diabetes with CAVD.
5. Inhibition of ectonucleotidases in a rodent model of CAVD prevents the development of aortic valve mineralization.
6. Ectonucleotidases and/or P2Y2R are potential novel therapeutic targets in CAVD.

Acknowledgements Research of the authors is supported by HSFC grant (P.M., P.P., Y.B.) and CIHR grants MOP245048 (P.M.), MOP 79342 (P.P.), MOP102481 (Y.B.), and Quebec Heart and Lung Institute Fund. P. M. and Y.B. are research scholars from the Fonds de Recherche en Santé du Québec, Montreal, Québec, Canada. P.P. holds the Canada Research Chair in Valvular Heart Diseases, Ottawa, Ontario, Canada.

References

1. Rajamannan NM, Evans FJ, Aikawa E, et al. Calcific aortic valve disease: not simply a degenerative process: a review and agenda for research from the National Heart and Lung and Blood Institute Aortic Stenosis Working Group. Executive summary: calcific aortic valve disease-2011 update. Circulation. 2011;124(16):1783–91.

2. Teo KK, Corsi DJ, Tam JW, Dumesnil JG, Chan KL. Lipid lowering on progression of mild to moderate aortic stenosis: meta-analysis of the randomized placebo-controlled clinical trials on 2344 patients. Can J Cardiol. 2011;27(6):800–8.
3. Freeman RV, Otto CM. Spectrum of calcific aortic valve disease: pathogenesis, disease progression, and treatment strategies. Circulation. 2005;111(24):3316–26.
4. Rattazzi M, Iop L, Faggin E, et al. Clones of interstitial cells from bovine aortic valve exhibit different calcifying potential when exposed to endotoxin and phosphate. Arterioscler Thromb Vasc Biol. 2008;28(12):2165–72.
5. Towler DA. Bone morphogenetic proteins. Blood. 2009;114(10):2012–3.
6. Bosse Y, Miqdad A, Fournier D, Pepin A, Pibarot P, Mathieu P. Refining molecular pathways leading to calcific aortic valve stenosis by studying gene expression profile of normal and calcified stenotic human aortic valves. Circ Cardiovasc Genet. 2009;2(5):489–98.
7. El Husseini D, Boulanger MC, Fournier D, et al. High expression of the Pi-transporter SLC20A1/Pit1 in calcific aortic valve disease promotes mineralization through regulation of Akt-1. PLoS One. 2013;8(1): e53393.
8. Cote N, El HD, Pepin A, et al. ATP acts as a survival signal and prevents the mineralization of aortic valve. J Mol Cell Cardiol. 2012;52(5):1191–202.
9. Yip CY, Chen JH, Zhao R, Simmons CA. Calcification by valve interstitial cells is regulated by the stiffness of the extracellular matrix. Arterioscler Thromb Vasc Biol. 2009;29(6):936–42.
10. Beck Jr GR. Inorganic phosphate as a signaling molecule in osteoblast differentiation. J Cell Biochem. 2003;90(2):234–43.
11. Goding JW, Grobben B, Slegers H. Physiological and pathophysiological functions of the ecto-nucleotide pyrophosphatase/phosphodiesterase family. Biochim Biophys Acta. 2003;1638(1):1–19.
12. Yegutkin GG. Nucleotide- and nucleoside-converting ectoenzymes: important modulators of purinergic signalling cascade. Biochim Biophys Acta. 2008;1783(5): 673–94.
13. Mathieu P. Pharmacology of ectonucleotidases: relevance for the treatment of cardiovascular disorders. Eur J Pharmacol. 2012;696(1–3):1–4.
14. Goding JW. Ecto-enzymes: physiology meets pathology. J Leukoc Biol. 2000;67(3):285–311.
15. Stefan C, Jansen S, Bollen M. NPP-type ectophosphodiesterases: unity in diversity. Trends Biochem Sci. 2005;30(10):542–50.
16. Robson SC, Sevigny J, Zimmermann H. The E-NTPDase family of ectonucleotidases: structure function relationships and pathophysiological significance. Purinergic Signal. 2006;2(2):409–30.
17. Schetinger MR, Morsch VM, Bonan CD, Wyse AT. NTPDase and 5′-nucleotidase activities in physiological and disease conditions: new perspectives for human health. Biofactors. 2007;31(2):77–98.
18. Mathieu P, Voisine P, Pepin A, Shetty R, Savard N, Dagenais F. Calcification of human valve interstitial cells is dependent on alkaline phosphatase activity. J Heart Valve Dis. 2005;14(3):353–7.
19. Koupenova M, Johnston-Cox H, Ravid K. Regulation of atherosclerosis and associated risk factors by adenosine and adenosine receptors. Curr Atheroscler Rep. 2012;14(5):460–8.
20. Burnstock G, Williams M. P2 purinergic receptors: modulation of cell function and therapeutic potential. J Pharmacol Exp Ther. 2000;295(3):862–9.
21. Okawa A, Nakamura I, Goto S, Moriya H, Nakamura Y, Ikegawa S. Mutation in Npps in a mouse model of ossification of the posterior longitudinal ligament of the spine. Nat Genet. 1998;19(3):271–3.
22. Nitschke Y, Baujat G, Botschen U, et al. Generalized arterial calcification of infancy and pseudoxanthoma elasticum can be caused by mutations in either ENPP1 or ABCC6. Am J Hum Genet. 2012;90(1):25–39.
23. Lorenz-Depiereux B, Schnabel D, Tiosano D, Hausler G, Strom TM. Loss-of-function ENPP1 mutations cause both generalized arterial calcification of infancy and autosomal-recessive hypophosphatemic rickets. Am J Hum Genet. 2010;86(2):267–72.
24. Nitschke Y, Weissen-Plenz G, Terkeltaub R, Rutsch F. Npp1 promotes atherosclerosis in ApoE knockout mice. J Cell Mol Med. 2011;15(11):2273–83.
25. Johnson K, Pritzker K, Goding J, Terkeltaub R. The nucleoside triphosphate pyrophosphohydrolase isozyme PC-1 directly promotes cartilage calcification through chondrocyte apoptosis and increased calcium precipitation by mineralizing vesicles. J Rheumatol. 2001;28(12):2681–91.
26. Katz R, Wong ND, Kronmal R, et al. Features of the metabolic syndrome and diabetes mellitus as predictors of aortic valve calcification in the Multi-Ethnic Study of Atherosclerosis. Circulation. 2006;113(17): 2113–9.
27. Briand M, Lemieux I, Dumesnil JG, et al. Metabolic syndrome negatively influences disease progression and prognosis in aortic stenosis. J Am Coll Cardiol. 2006;47(11):2229–36.
28. Capoulade R, Clavel MA, Dumesnil JG, et al. Impact of metabolic syndrome on progression of aortic stenosis: influence of age and statin therapy. J Am Coll Cardiol. 2012;60(3):216–23.
29. Mathieu P, Poirier P, Pibarot P, Lemieux I, Despres JP. Visceral obesity: the link among inflammation, hypertension, and cardiovascular disease. Hypertension. 2009;53(4):577–84.
30. Mohty D, Pibarot P, Despres JP, et al. Association between plasma LDL particle size, valvular accumulation of oxidized LDL, and inflammation in patients with aortic stenosis. Arterioscler Thromb Vasc Biol. 2008;28(1):187–93.
31. Spoto B, Testa A, Parlongo RM, et al. Insulin resistance and left ventricular hypertrophy in end-stage renal disease: association between the ENPP1 gene and left ventricular concentric remodelling. Nephrol Dial Transplant. 2012;27(2):661–6.

32. Valli-Jaakola K, Suviolahti E, Schalin-Jantti C, et al. Further evidence for the role of ENPP1 in obesity: association with morbid obesity in Finns. Obesity (Silver Spring). 2008;16(9):2113–9.
33. Maddux BA, Sbraccia P, Kumakura S, et al. Membrane glycoprotein PC-1 and insulin resistance in non-insulin-dependent diabetes mellitus. Nature. 1995;373(6513):448–51.
34. Kumakura S, Maddux BA, Sung CK. Overexpression of membrane glycoprotein PC-1 can influence insulin action at a post-receptor site. J Cell Biochem. 1998;68(3):366–77.
35. Grupe A, Alleman J, Goldfine ID, Sadick M, Stewart TA. Inhibition of insulin receptor phosphorylation by PC-1 is not mediated by the hydrolysis of adenosine triphosphate or the generation of adenosine. J Biol Chem. 1995;270(38):22085–8.
36. Fadini GP, Pauletto P, Avogaro A, Rattazzi M. The good and the bad in the link between insulin resistance and vascular calcification. Atherosclerosis. 2007;193(2):241–4.
37. Anderson HC. Matrix vesicles and calcification. Curr Rheumatol Rep. 2003;5(3):222–6.
38. Bertazzo S, Gentleman E, Cloyd KL, Chester AH, Yacoub MH, Stevens MM. Nano-analytical electron microscopy reveals fundamental insights into human cardiovascular tissue calcification. Nat Mater. 2013;12(6):576–83.
39. Shaver SR. P2Y receptors: biological advances and therapeutic opportunities. Curr Opin Drug Discov Devel. 2001;4(5):665–70.
40. Lohman AW, Billaud M, Isakson BE. Mechanisms of ATP release and signalling in the blood vessel wall. Cardiovasc Res. 2012;95(3):269–80.
41. St Hilaire, Ziegler SG, Markello TC, et al. NT5E mutations and arterial calcifications. N Engl J Med. 2011;364(5):432–42.
42. Cloyd KL, El-Hamamsy I, Boonrungsiman S, et al. Characterization of porcine aortic valvular interstitial cell 'calcified' nodules. PLoS One. 2012;7(10):e48154.
43. Della Latta V, Cabiati M, Rocchiccioli S, Del RS, Morales MA. The role of the adenosinergic system in lung fibrosis. Pharmacol Res. 2013;76:182–9.
44. Mahmut A, Boulanger MC, El Husseini D, et al. Elevated expression of Lp-PLA2 in calcific aortic valve disease: implication for valve mineralization. J Am Coll Cardiol. 2014;63:460–9.
45. Cote N, El HD, Pepin A, et al. Inhibition of ectonucleotidase with ARL67156 prevents the development of calcific aortic valve disease in warfarin-treated rats. Eur J Pharmacol. 2012;689(1–3):139–46.

In Vitro Model of Drug Testing

15

Nalini M. Rajamannan

Introduction

Valvular heart disease is a significant cause of cardiac morbidity and mortality. Fifteen years ago, there was an epidemic of FenPhen induced valvular heart disease due to overuse for weight loss [1]. Patients developed clinical findings of severe pulmonary hypertension, and left-sided valve lesions similar to those of carcinoid heart disease [1–4]. Previously, we have published the in vitro, and ex vivo mechanism of cellular proliferation secondary to serotonin induced valve disease [5]. The distinctive carcinoid cardiac lesions consist of deposits of fibrous tissue devoid of elastic fibers on the ventricular aspect of the tricuspid valve leaflets and on the arterial aspect of the pulmonic valve cusps. A similar lesion is found in FenPhen valve lesions except on the left side of the heart [1]. Despite the similar plaque formation on the endocardial surface of the cardiac valves in FenPhen patients, the cellular mechanism of this disease is not well known. This chapter will define a novel in vitro assay previously published [5], to determine if FenPhen has a direct effect on the valvular subendothelial cells through a mechanism of increase proliferation, which is responsible for the plaque formation found on these valves.

N.M. Rajamannan, MD
Division of Biochemistry and Molecular Biology,
Visiting Scientist, Mayo Clinic, 200 First St SW,
Rochester, MN 55905, USA
e-mail: rajamannan.nalini@mayo.edu

In Vitro Assay for Direct Drug Effects in the Valvular Subendothelial Myofibroblast Cells and Light Microscopy of Human Carcinoid Valves Versus FenPhen Valves

As described in Chaps. 1 and 2, the isolation of myofibroblast cells were assayed for cell proliferation by testing the different concentrations of serotonin and FenPhen. Carcinoid valve and FenPhen valve removed at the time of surgery were assessed for histology and cell proliferation. An in vitro cell assay was developed using cells isolated from porcine derived myofibroblast cells [6].

The assay tested the incorporation of a radioactive label of thymidine to determine if active cell proliferation would occur during the cell cycle. Quantitative thymidine incorporation after serotonin, Fen, Phen and FenPhen stimulation of the in vitro subendothelial cells reveal a tenfold increase in the amount DNA synthesis over negative control (Table 15.1).

Gross inspection of the carcinoid valves at the time of valve replacement reveal a smooth appearing endocardial surface. There is an associated plaque-like lesion consisting of a thickened subendothelial cell layer. These cells compose the majority of the endocardial plaque

N.M. Rajamannan (ed.), *Molecular Biology of Valvular Heart Disease*,
DOI 10.1007/978-1-4471-6350-3_15, © Springer-Verlag London 2014

Table 15.1 In vitro determination of DNA synthesis by thymidine incorporation secondary to serotonin, Fen, Phen and FenPhen stimulation at 10^{-6} M concentrations

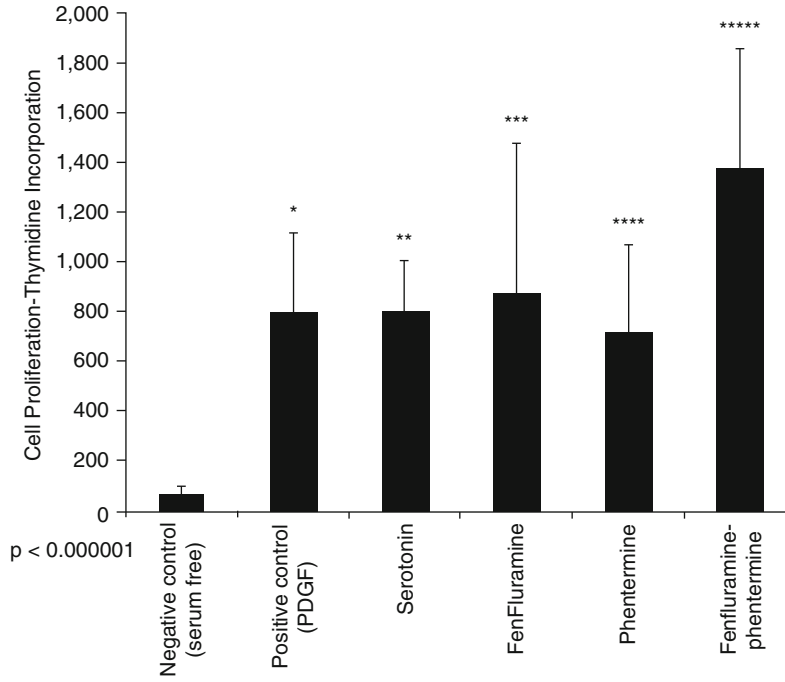

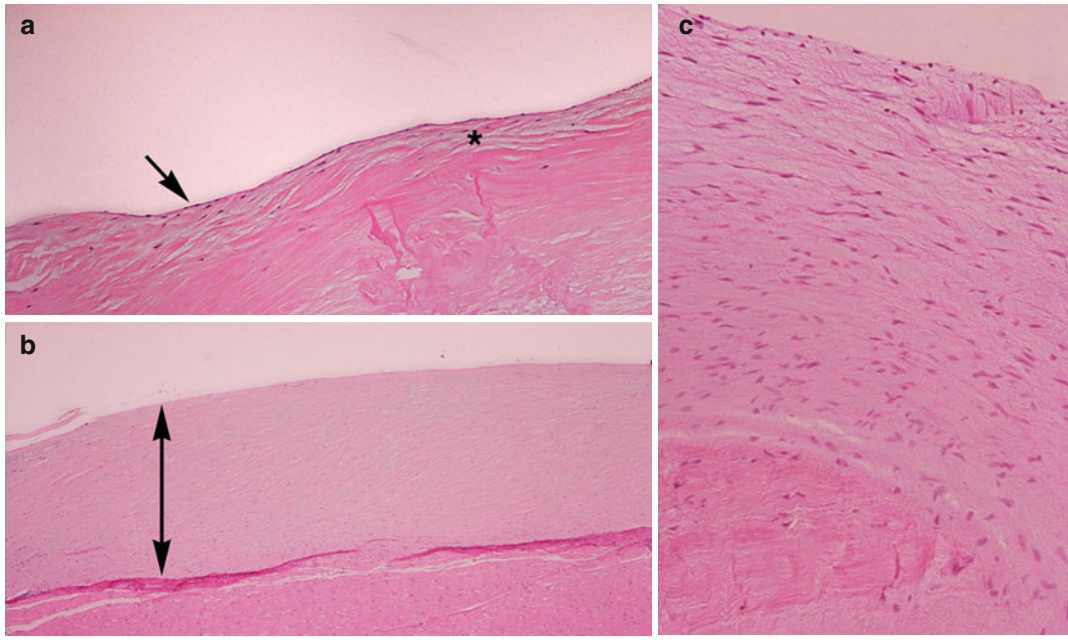

Fig. 15.1 Hematoxylin and Eosin staining, (**a**) normal human valve, (**b**) carcinoid human valve, (**c**) FenPhen Valve Magnification 25×. *Star* indicates myofibroblast. *Double arrow* points to the thickness of the valve lesion. *Single arrow* points to the surface of the valve.

surface. Conversely, normal control valves demonstrated a normal endothelial edge with no visible evidence of endocardial plaque lesions. The valve surface was intact. (Figure 15.1, Hematoxylin and Eosin stain, Panel a, Control, Panel b, Carcinoid and Panel c, FenPhen)

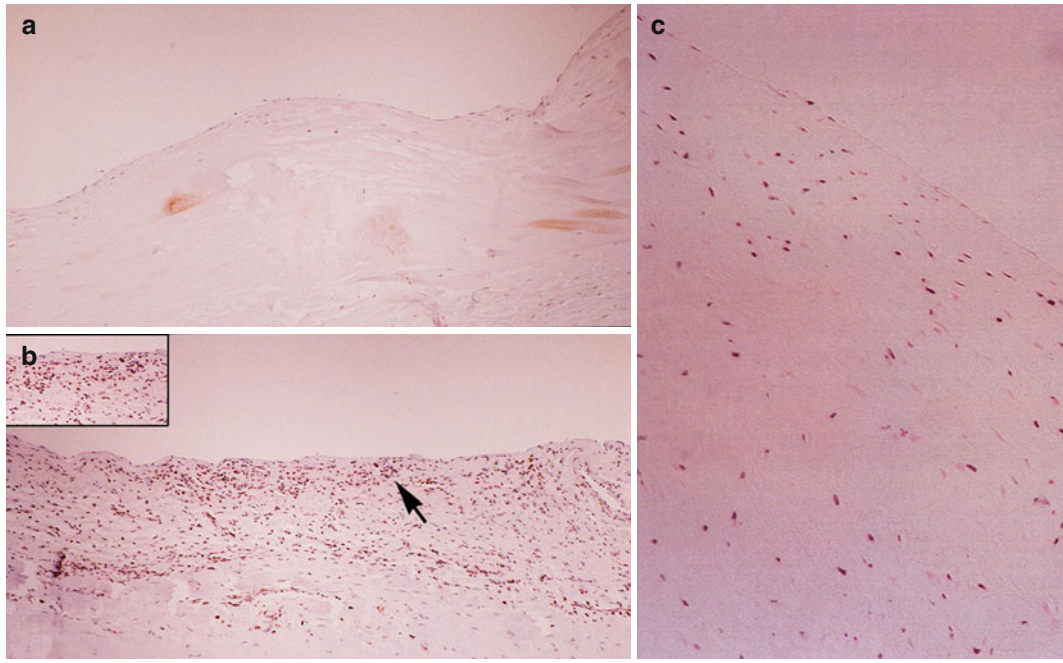

Fig. 15.2 Quantitation of PCNA by digital image analysis, (**a**) normal human valve, (**b**) carcinoid human valve, (**c**) FenPhen Valve, Magnification 50×

In Situ Detection of Proliferation Ex Vivo

Quantitation of the number of PCNA positive staining nuclei in the carcinoid valve demonstrated a 35-fold increase in the number of positive nuclei as compared to the control and 23-fold increase in the number of postive nuclei in FenPhen valve as compared to the controls, which corresponds to an upregulation of DNA (Fig. 15.2).

Summary

Although the histopathology of FenPhen heart disease has been well described as a plaque-like lesion, which consists of proliferating subendothelial cells similar to carcinoid heart disease, the mechanism of this lesion is not well known. The lesion is sometimes perceived as an infiltrative process, despite the location of the plaque superficially on the surface of the endocardium. The actual plaque lesion is composed of smooth muscle cells, myofibroblasts, and an overlying layer of endothelial cells.

Serotonin is a known potent mitogen in the cardiovascular system. Many studies have demonstrated the mitogen effect of serotonin as a direct proliferating agent in the cardiovascular system [5]. Johnson et al. [7], developed an in vitro valvular model and validated that these cells produce matrix proteins and respond to growth factors similarly to coronary artery smooth muscle cells in vitro. This study employed this same model to test the effect of serotonin, Fen, Phen and FenPhen on DNA synthesis and matrix production in cardiac valve cells in vitro.

This chapter provides a foundation for the hypothesis that in the presence of elevated serotonin, and FenPhen there is marked increase in cellular proliferation. This direct stimulation of the valve stimulates plaque formation on the ventricular surface of the atrioventricular valve and vascular surface of the semilunar valves, which is similar to the lesion found in carcinoid valve disease, which is demonstrated in the Fig. 15.3.

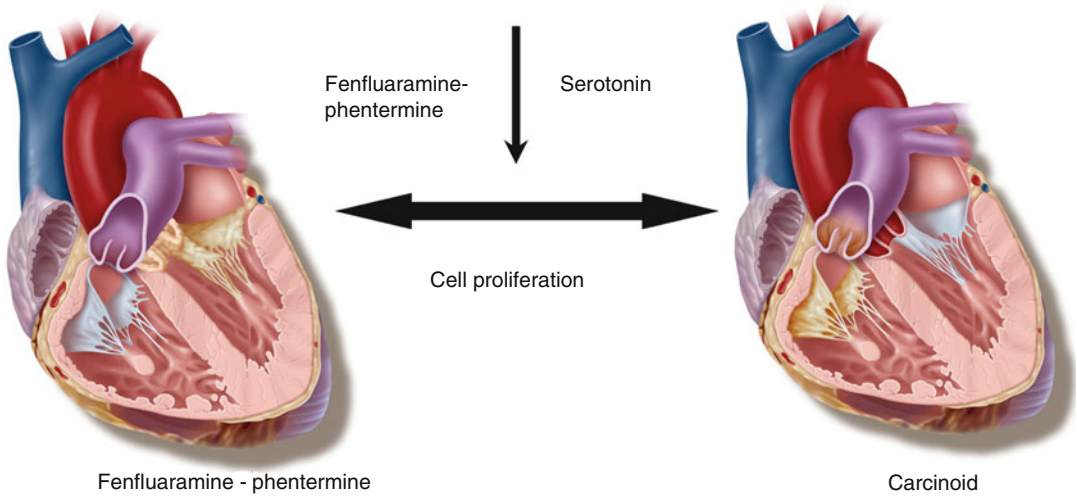

Fig. 15.3 Role of Serotonin and FenPhen in *right sided* versus *left sided* valve lesions

In conclusion, this assay will helpful to determine if drugs for weight loss and/or have serotonin like receptor biology may be helpful for pre-clinical pharmaceutical testing prior to FDA approval [8].

References

1. Connolly HM, Crary JL, McGoon MD, Hensrud DD, Edwards BS, Edwards WD, Schaff HV. Valvular heart disease associated with fenfluramine-phentermine. N Engl J Med. 1997;337(24):1783.
2. Mark EJ, Patalas ED, Chang HT, Evans RJ, Kessler SC. Fatal pulmonary hypertension associated with short-term use of fenfluramine and phentermine. N Engl J Med. 1997;337:602–6.
3. Rich S, Shillington A, McLaughlin V. Comparison of survival in patients with pulmonary hypertension associated with fenfluramine to patients with primary pulmonary hypertension. Am J Cardiol. 2003;92:1366–8.
4. Rothman RB, Ayestas MA, Dersch CM, Baumann MH. Aminorex, fenfluramine, and chlorphentermine are serotonin transporter substrates. Implications for primary pulmonary hypertension. Circulation. 1999;100:869–75.
5. Rajamannan NM, Caplice N, Anthikad F, Sebo TJ, Orszulak TA, Edwards WD, Tajik J, Schwartz RS. Cell proliferation in carcinoid valve disease: a mechanism for serotonin effects. J Heart Valve Dis. 2001;10:827–31.
6. Johnson CM, Hanson MN, Helgeson SC. Porcine cardiac valvular subendothelial cells in culture: cell isolation and growth characteristics. J Mol Cell Cardiol. 1987;19:1185–93.
7. Johnson GJ, Leis LA, Dunlop PC, Weir EK. The effect of the anorectic agent, d-fenfluramine, and its primary metabolite, d-norfenfluramine, on intact human platelet serotonin uptake and efflux. J Thromb Haemost. 2003;1:2663–8.
8. Rajamannan NM. Fenfluaramine-Phentermine valvulopathy is associated with a proliferative phenotype in vitro and ex vivo. J Am Coll Cardiol. 2011;57(14):E2027.

Application of the LDL-Density-Pressure Theory: The Mitral Valve

16

Nalini M. Rajamannan

Introduction

Myxomatous mitral valve regurgitation is the most common indication for surgical valve repair in the world [1]. For years this disease was thought to be a passive degenerative phenomenon. Understanding of the cellular mechanisms of this valve lesion will present improved understanding of this disease and targeted therapy either surgical or medical. Diagnosing mitral regurgitation (MR), and timing to surgical correction is one of the most challenging in the clinical cardiology. Chronic MR, due to increasing prevalence of myxomatous disease and the increasing mean age of population, is presenting as often as aortic stenosis: Moderate or severe MR is found in 1.7 % of the general population and in up to 9.3 % of those over 75 years [1]. Echocardiography is the main tool for MR evaluation. In the modern times of mitral valve (MV) repair surgery, echocardiography has become even more important because the study has to diagnose not only the MR diagnosis, but also the evaluation of the valvular lesions and the mechanisms of disease to guide the election between the different therapeutic options. This combination of aspects related to the complexity of mitral regurgitation is the primary driving force to develop an all encompassing assessment of MR to allow the clinician and surgeon to achieve the important clinical outcomes. One of the key aspects for the elusiveness of this disease, from the clinical perspective, is the understanding of how the mitral valve develops myxomatous changes [2].

Until recently the etiology of valvular heart disease has been thought to be a degenerative process related to the progressive lengthening of the mitral leaflet and the mitral chordae. Recent descriptive studies have demonstrated the critical features of mitral valve degeneration, glycosaminglycan accumulation, proteoglycan expression, and abnormal collagen expression [3]. Studies have demonstrated that specific endochondral bone phenotypes are present in calcifying valve specimens in human specimens [4]. This molecular phenotype is the foundation for the studies focused on determining how the cartilage of how the cartilaginous phenotype is found in the heart and in the future will play a key role in the development of disease, and the timing of surgical correction of regurgitation.

Currently, the treatment strategy for patients with myxomatous mitral valve disease, is to monitor the patients by echocardiography and by symptoms. Once the patients develop severe symptoms the current class I indication for therapy is to repair the valve. There is a rapid goal towards treating patients with severe mitral regurgitation with early repair prior to the onset of symptoms. However between continents the approach towards patients who are asymptomatic

N.M. Rajamannan, MD
Division of Biochemistry and Molecular Biology,
Visiting Scientist, Mayo Clinic, 1601 Guggenheim,
200 First St SW, Rochester, MN 55905, USA
e-mail: rajamannan.nalini@mayo.edu

N.M. Rajamannan (ed.), *Molecular Biology of Valvular Heart Disease*,
DOI 10.1007/978-1-4471-6350-3_16, © Springer-Verlag London 2014

is a difference between a Class IIA(In favor of the early repair) [5] and Class IIB(not strongly in favor of early repair) [6] in the asymptomatic patient population. These recommendations have not changed with the recently published 2014 ACC/AHA guidelines [7]

Timing of Mitral Valve Repair

Since the publication of the guidelines, timing of mitral valve repair in mitral regurgitation has been the center of numerous studies. The most recent is from the Mayo Clinic in which the hypothesis centers around the treatment of patients with Flail Leaflets causing mitral regurgitation. The Mitral Regurgitation International Database (MIDA) [8], which included 2097 consecutive patients with flail mitral valve regurgitation (from 1980–2004), demonstrate that there was no significant difference in early mortality and new-onset heart failure rates (0.9 % for early surgery vs 0.9 % for medical management) between treatment strategies at 3 months. In contrast, long-term survival rates were higher for patients with early surgery (86 % vs 69 % at 10 years, $P<0.001$), associated with a 5-year reduction in mortality of 52.6 % ($P<0.001$). Final conclusions, among registry patients with mitral valve regurgitation due to flail mitral leaflets, performance of early mitral surgery compared with initial medical management was associated with greater long-term survival and a lower risk of heart failure, with no difference in new-onset atrial fibrillation.

Outcomes for Patients with Flail Leaflet Versus Pure Myxomatous Mitral Valve Disease

The timing of the surgical intervention has been defined by the degree of mitral regurgitation and the presence and absence of symptoms in patients. The studies, the guidelines from Europe and America all define the timing based on the degree of regurgitation and symptoms but not on specific mitral valve pathology. The timing of intervention for mitral valve regurgitation is an evolving and controversial topic in the field of valvular medicine. There are two basic approaches in the literature and outlined in the ACC/AHA/ESC [6, 9]. Early surgery for asymptomatic patients with preserved left ventricular function [10, 11], has been recommended by tertiary referral centers and is a Class IIa recommendation in the AHA/ACC guidelines [5]. Early surgery may prevent left ventricular dysfunction from the chronic volume overload secondary to the mitral regurgitation. The ESC [6] guidelines support a more conservative strategy of watchful waiting based on careful monitoring of patients for symptoms, left ventricular dimensions, and signs of changes in clinical status. The Mayo Clinic study found that >90 % of patients needed surgery within 10 years [12]. The study from Vienna demonstrated a much lower rate of surgical valve repair at 8 years with >50 % of patients who did not meet criteria for surgical valve repair. The patient populations are different and as well as the valve lesions causing significant mitral regurgitation. In the study from Vienna [13], watchful waiting for the timing of mitral valve surgical repair, the authors demonstrate an important finding of the long-term outcomes of patients with pure myxomatous mitral valve disease versus patients with flail ruptured leaflet. This is also significant for the differences in approach as outlined in Europe as compared to the American Guidelines. The American (ACC/AHA) [5] guidelines, approach the patient with referral to a tertiary care center when the patient is asymptomatic with preserved ejection fraction without atrial fibrillation or pulmonary hypertension. The European (ESC) [6] guidelines outline a conservative approach.

Hemodynamics in Patients with Flail Leaflet Versus Pure Myxomatous Mitral Valve Disease

Over the past three decades as the role of echo has become the gold standard not only for the color documentation of severe mitral regurgitation, quantitative hemodynamics has become critical for the measurement of severity of the disease [12]. The role of cardiac catheterization hemodynamics has played a lesser role in the pathophysiology understanding of this disease. To further understand the role of hemodynamics,

a study from 1985 [14], 39 patients with symptomatic severe (MR) were studied by cardiac catheterization and two-dimensional echocardiography (2DE) prior to mitral valve replacement. A flail mitral valve was found at surgery in 23 patients (group 1); 16 patients had intact chordae tendineae (chronic MR, group 2). No difference was found between groups 1 and 2 with regard to hemodynamic findings. Left atrial volumes in end systole (LAESV) and end diastole (LAEDV) were determined by 2DE from apical four- and two-chamber views with the use of a biplane area-length method and a light pen system. The LAESV and LAEDV measured 116 ± 66 and 56 ± 48 ml, respectively, in group 1, as compared with 185 ± 101 and 105 ± 62 ml in group 2 ($p < 0.025$). Ten patients from group 1 with LAESV ≤ 100 ml (group 1A) were compared to the remaining 13 patients with LAESV > 100 ml (group 1B). Patients in group 1A had significantly smaller left ventricular volume and higher mean pulmonary wedge pressure, pulmonary artery, and left ventricular end-diastolic pressure compared to patients in groups 1B and 2 ($p < 0.05$). Thus, a subset group of patients with flail mitral leaflets and smaller LAESV has hemodynamic features of acute MR, whereas the remainder with larger LAESV are indistinguishable from patients with chronic MR. The results of this study combined with the watchful waiting study, indicate that hemodynamic pressures, left atrial size and volume, and measurements of pulmonary pressures may play a role in the understanding of the natural history and also the controversy of timing of surgical valve repair. Patients with acute MR hemodynamics from ruptured chords are at higher risk as defined by the Ling and confirmed by the MIDA database which clearly indicate early repair is necessary for improved long-term outcomes [8, 10]. The Vienna Study [13] for Watchful Waiting demonstrates the differences in outcomes for the different pathologies associated with this disease.

Pathologic Classification of Myxomatous Mitral Valve Disease

Over the past decade scientific publications have demonstrated that specific pathologic phenotype is a spectrum of valve pathologies that encompass the disease entity itself. The classification is a based on the pathologic characterization of the mitral valve. Heart valve "degeneration" is the most common pathologic valve disease in the U.S. and Europe. The spectrum of "degenerative" valve lesions have traditionally been thought to be due to a passive disease process developing rapidly within the valve leaflets. The most common location of these diseased valves is the left side of the heart. Myxomatous mitral valve lesions causing mitral regurgitation are believed to be caused by progressive thickening due to activated myofibroblasts [15]. Recent evidence suggests that the aortic valve develops calcification secondary to an osteoblast differentiation pathway [16]. The number of surgical valve replacements and surgical valve repairs are increasing in the U.S. due to rapidly aging population.

The risk factors for the development of mitral valve disease and aortic valve disease have been defined in the past 10 years as traditional cardiovascular disease [17]. The human correlation of cholesterol as a risk factor for the development of mitral valve leaflet thickening is first described in a patient case report of Familial Hypercholesterolemia and mitral valve disease as shown in Fig. 16.1 [19]. We tested this hypothesis in an experimental model of hypercholesterolemia. A 2 months cholesterol diet was fed to rabbits which confirmed the development of atherosclerosis and mitral valve cellular proliferation in the leaflets as shown in Fig. 16.2 [20].

Despite this increase in prevalence and incidence of valvular heart disease, the signaling pathways in human valve disease have not been identified. Our laboratory and others have recently demonstrated in experimental animal models that bone matrix protein expression in the aortic valve and vasculature are regulated by the low-density lipoprotein receptor-related protein 5 (Lrp5) pathway in the presence of elevated hypercholesterolemia [21–23]. The Lrp5, a co-receptor of low-density lipoprotein receptor family, has been discovered as an important receptor in the activation of skeletal bone formation via binding to the secreted glycoprotein Wnt and activating beta-catenin to induce bone formation.

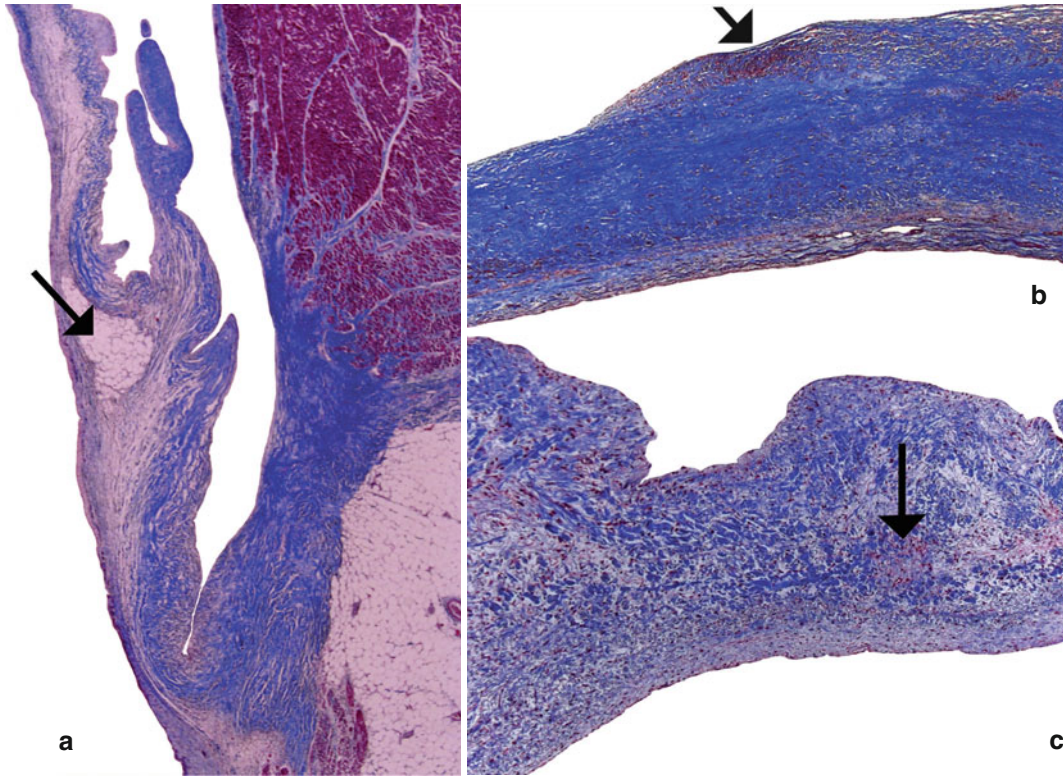

Fig. 16.1 **a–c** Different magnifications of the atherosclerotic mitral valve leaflet, (**a**) 2X, (**b**) 10X, (**c**) 20X *arrows* point to areas of atherosclerosis along the atrial surface of the mitral valve leaflet. Mitral valve atherosclerotic histology from case report of patient with Familial Hypercholesterolemia [18]

Therefore, we hypothesized that the underlying mechanism of "degenerative" valve disease is caused by osteogenic differentiation secondary to the activation of the Lrp5 receptors in human diseased valve leaflets. To test this hypothesis we studied diseased mitral valves, calcified tricuspid, and bicuspid aortic valves to determine if the Lrp5 signaling pathway is expressed in these tissues.

Human Calcified Aortic Valves, Degenerative Mitral Valves, and Control Valves

Figure 16.3 demonstrates the immunohistochemistry stains for the osteoblast signaling markers: Lrp5, Wnt3, and PCNA. Figure 16.3a (panels a1 and a2) and 16.3b (panels b1 and b2) demonstrate a mild amount of Lrp5 and Wnt3 staining in the control valves and in the areas of hypertrophic chondrocytes in the mitral valves. The Lrp5 and Wnt3 staining was increased in the calcified aortic valves (Fig. 16.3a [panels a3 and a4] and 16.3b [panels b3 and b4]). Figure 16.3c, panels c3 and c4, demonstrates the presence of an increase in PCNA protein expression as compared with Fig. 16.3c, panels c1 and c2, which demonstrates a decrease in PCNA protein staining.

Until recently the etiology of valvular heart disease has been thought to be a "degenerative" process related to the passive accumulation of calcium binding to the surface of the valve leaflet. Recent descriptive studies have demonstrated the critical features of aortic valve calcification, including osteoblast expression, cell proliferation, and atherosclerosis [24, 25] and mitral valve degeneration, glycosaminglycan accumulation, proteoglycan expression, and abnormal collagen expression. These studies define the biochemical and histologic characterization of these valve lesions.

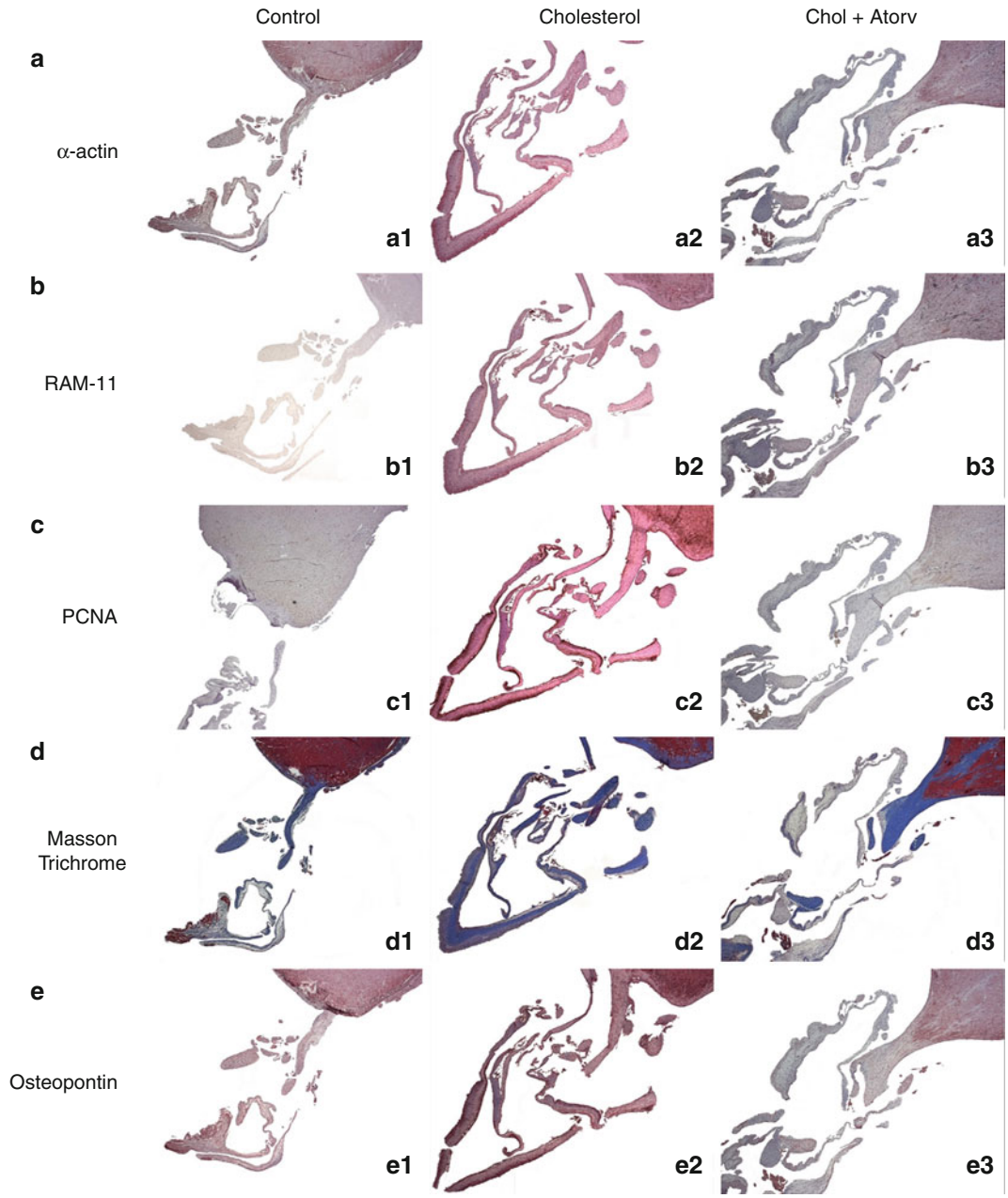

Fig. 16.2 (**a**–**e**) demonstrates the staining of the control, versus cholesterol, versus cholesterol + Atorvastatin mitral valves from the 2 month study protocol. (**a**) a-actin, (**b**) RAM11, (**c**) PCNA, (**d**) Masson Trichrome, (**e**) Osteopontin. Results of 2 months experimental hypercholesterolemia treatment demonstrating atherosclerosis after 2 months and attenuation with Atorvastatin [20]

The most striking phenotypic abnormalities are the formation of cartilaginous structures in the degenerative mitral valves and bone formation in the calcified aortic valves. At the light microscopy level, we were also able to identify hypertrophic chrondrocytes in all of the diseased mitral valves that we studied.

Biochemistry and Pathology of the Myxomatous Mitral Valve Chords

It is well know that myxomatous mitral valve disease is accompanied by lengthening and/or rupture of chordae tendineae. However, the mechanisms and the mode of chordal rupture

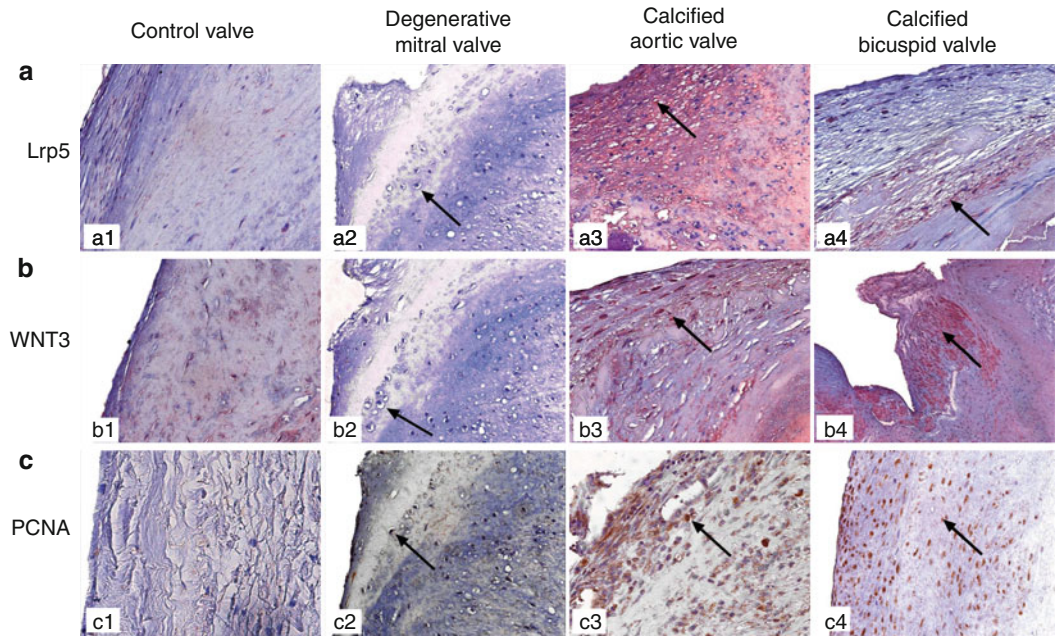

Fig. 16.3 Immunohistochemistry of the human mitral degenerative valves and calcified tricuspid and bicuspid aortic valves for endochondral signaling markers low-density lipoprotein receptor-related protein 5/Wnt and proliferating cell nuclear antigen. Control valve, degenerative mitral valve (*arrow* points to hypertrophic chondrocytes), calcified aortic valves (*arrow* points to positive stain), and bicuspid aortic valve (*arrow* points to positive stain) (magnification 25×). *Insert* within each photo is a high-power magnification to demonstrate cellular staining (magnification 40×). (**a**) lipoprotein receptor-related protein 5 stain. (**b**) Wnt 3 stain. (**c**) Proliferating cell nuclear antigen stain [4]

remain controversial, and the pathologic anatomy of the apparently healthy chordae has mostly been overlooked. The investigators from Italy [26] analyzed the structural aspects of both ruptured and intact chordae tendinae from patients with abnormal chordal pathology. Structural and ultrastructural microscopic analyses indicate that both the extracellular matrix and the interstitial cells are severely affected. Myxomatous chordae show alterations in the synthesis and deposition of collagen and elastin, disorganization of collagen bundles and rupture of collagen fibers, accumulation of proteoglycans and of cellular and vesicular remnants, and cell transformation into a myofibroblast phenotype. Structural disruption makes the spongiosa and the dense collagenous core separate and break. Degeneration of the chordae is segmental, affecting both chordae that are clearly abnormal, and chordae that appear healthy on visual inspection. The authors concluded that surgery corrects the damage, but the underlying causes of the myxomatous changes are not corrected. Thus, progression of the disease and affectation of additional chordae may be at the basis of the late complications and the recurrent mitral regurgitation, which occurs several years after surgery. The study investigators concluded that the early surgical repair is necessary for this patient population.

Application of the LDL-Density-Pressure Theory

Figure 16.4, demonstrates an application of the concepts outlined in this chapter. In the presence of risk factors for left sided valve lesions, aortic valves develop calcification and mitral valves develop cartilage formation. The higher pressure across the aortic valve induces the calcification in the aortic valve and the lower pressure across the mitral valve induces cartilage. Further

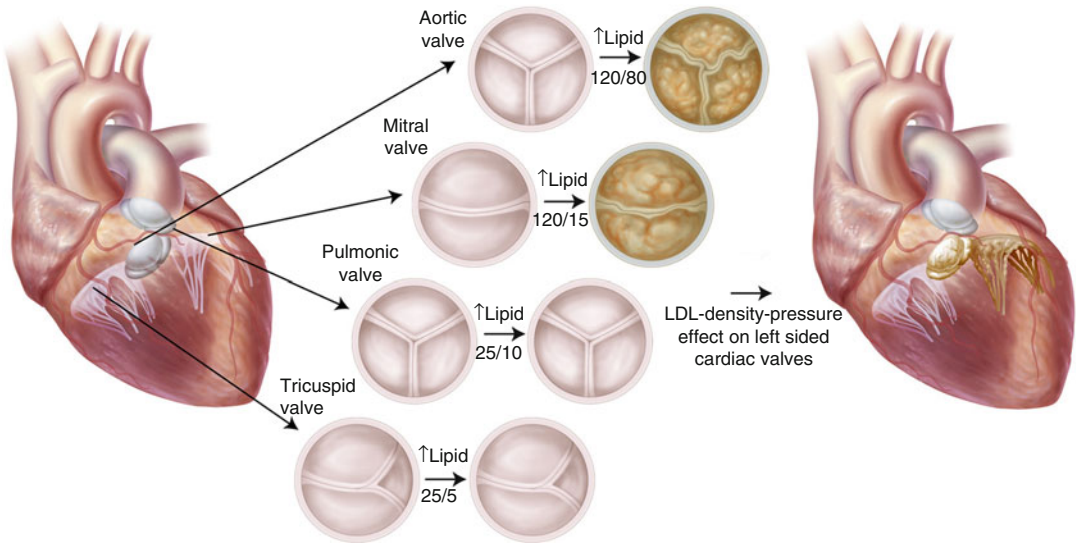

Fig. 16.4 LDL-density-pressure theory [22]

studies are necessary to understand the role of the Lrp5 receptor in inducing these different valve lesions [22].

Summary

Mitral Valve Regurgitation is a complex disease process, which requires expertise in imaging, evaluation and symptom management to diagnose, follow and treat this patient population. Current imaging modalities in echocardiography have vastly improved our understanding of the mechanisms of valve regurgitation, valve pathology and the natural history of this disease. Hemodynamic considerations for the different pathologies associated with myxomatous mitral valve disease will become increasingly more important in defining the timing of surgery and may help to further delineate the controversies that are present in the literature.

References

1. Iung B, Vahanian A. Epidemiology of valvular heart disease in the adult. Nat Rev. 2011;8:162–72.
2. Rajamannan NM. Myxomatous mitral valve disease bench to bedside: LDL-density-pressure regulates Lrp5. Expert Rev Cardiovasc Ther. 2014;12(3):383–92.
3. Grande-Allen KJ, Griffin BP, Calabro A, Ratliff NB, Cosgrove 3rd DM, Vesely I. Myxomatous mitral valve chordae. Ii: selective elevation of glycosaminoglycan content. J Heart Valve Dis. 2001;10:325–32; discussion 332–3.
4. Caira FC, Stock SR, Gleason TG, McGee EC, Huang J, Bonow RO, Spelsberg TC, McCarthy PM, Rahimtoola SH, Rajamannan NM. Human degenerative valve disease is associated with up-regulation of low-density lipoprotein receptor-related protein 5 receptor-mediated bone formation. J Am Coll Cardiol. 2006; 47:1707–12.
5. Bonow RO, Carabello BA, Chatterjee K, de Leon Jr AC, Faxon DP, Freed MD, Gaasch WH, Lytle BW, Nishimura RA, O'Gara PT, O'Rourke RA, Otto CM, Shah PM, Shanewise JS, Smith Jr SC, Jacobs AK, Adams CD, Anderson JL, Antman EM, Fuster V, Halperin JL, Hiratzka LF, Hunt SA, Lytle BW, Nishimura R, Page RL, Riegel B. Acc/aha 2006 guidelines for the management of patients with valvular heart disease: a report of the american college of cardiology/american heart association task force on practice guidelines (writing committee to revise the 1998 guidelines for the management of patients with valvular heart disease) developed in collaboration with the society of cardiovascular anesthesiologists endorsed by the society for cardiovascular angiography and interventions and the society of thoracic surgeons. J Am Coll Cardiol. 2006;48:e1–148.
6. Vahanian A, Baumgartner H, Bax J, Butchart E, Dion R, Filippatos G, Flachskampf F, Hall R, Iung B, Kasprzak J, Nataf P, Tornos P, Torracca L, Wenink A. Guidelines on the management of valvular heart disease: the task force on the management of valvular heart disease of the european society of cardiology. Eur Heart J. 2007;28:230–68.

7. Nishimura RA, Otto C., et al. ACC/AHA 2014 Valvular Guidelines, JACC, In Press
8. Suri RM, Vanoverschelde JL, Grigioni F, Schaff HV, Tribouilloy C, Avierinos JF, Barbieri A, Pasquet A, Huebner M, Rusinaru D, Russo A, Michelena HI, Enriquez-Sarano M. Association between early surgical intervention vs watchful waiting and outcomes for mitral regurgitation due to flail mitral valve leaflets. JAMA. 2013;310:609–16.
9. Bonow RO, Carabello BA, Kanu C, de Leon Jr AC, Faxon DP, Freed MD, Gaasch WH, Lytle BW, Nishimura RA, O'Gara PT, O'Rourke RA, Otto CM, Shah PM, Shanewise JS, Smith Jr SC, Jacobs AK, Adams CD, Anderson JL, Antman EM, Fuster V, Halperin JL, Hiratzka LF, Hunt SA, Nishimura R, Page RL, Riegel B. Acc/aha 2006 guidelines for the management of patients with valvular heart disease: a report of the american college of cardiology/american heart association task force on practice guidelines (writing committee to revise the 1998 guidelines for the management of patients with valvular heart disease): developed in collaboration with the society of cardiovascular anesthesiologists: endorsed by the society for cardiovascular angiography and interventions and the society of thoracic surgeons. Circulation. 2006;114:e84–231.
10. Ling LH, Enriquez-Sarano M, Seward JB, Orszulak TA, Schaff HV, Bailey KR, Tajik AJ, Frye RL. Early surgery in patients with mitral regurgitation due to flail leaflets: a long-term outcome study. Circulation. 1997;96:1819–25.
11. Ling LH, Enriquez-Sarano M, Seward JB, Tajik AJ, Schaff HV, Bailey KR, Frye RL. Clinical outcome of mitral regurgitation due to flail leaflet. N Engl J Med. 1996;335:1417–23.
12. Enriquez-Sarano M, Avierinos JF, Messika-Zeitoun D, Detaint D, Capps M, Nkomo V, Scott C, Schaff HV, Tajik AJ. Quantitative determinants of the outcome of asymptomatic mitral regurgitation. N Engl J Med. 2005;352:875–83.
13. Rosenhek R, Rader F, Klaar U, Gabriel H, Krejc M, Kalbeck D, Schemper M, Maurer G, Baumgartner H. Outcome of watchful waiting in asymptomatic severe mitral regurgitation. Circulation. 2006;113:2238–44.
14. Ren JF, Panidis IP, Kotler MN, Mintz GS, Goel I, Ross J. Flail mitral valve syndrome: comparison with chronic mitral regurgitation of other etiologies. Am Heart J. 1985;109:435–42.
15. Rabkin E, Aikawa M, Stone JR, Fukumoto Y, Libby P, Schoen FJ. Activated interstitial myofibroblasts express catabolic enzymes and mediate matrix remodeling in myxomatous heart valves. Circulation. 2001;104:2525–32.
16. Rajamannan NM, Subramaniam M, Rickard D, Stock SR, Donovan J, Springett M, Orszulak T, Fullerton DA, Tajik AJ, Bonow RO, Spelsberg T. Human aortic valve calcification is associated with an osteoblast phenotype. Circulation. 2003;107:2181–4.
17. Lazaros G, Toutouzas K, Drakopoulou M, Boudoulas H, Stefanadis C, Rajamannan N. Aortic sclerosis and mitral annulus calcification: a window to vascular atherosclerosis? Expert Rev Cardiovasc Ther. 2013; 11:863–77.
18. Rajamannan NM, Spelsberg TC, Moura LM. Mitral valve disease in a patient with familial hypercholesterolemia. Rev Port Cardiol. 2010;29:841–2.
19. Rajamannan NM, Spelsberg TC, Moura LM. Mitral valve disease in a patient with familial hypercholesterolemia. Rev Port Cardiol. 2010;29:841–2.
20. Makkena B, Salti H, Subramaniam M, Thennapan S, Bonow RH, Caira F, Bonow RO, Spelsberg TC, Rajamannan NM. Atorvastatin decreases cellular proliferation and bone matrix expression in the hypercholesterolemic mitral valve. J Am Coll Cardiol. 2005;45:631–3.
21. Rajamannan NM. The role of lrp5/6 in cardiac valve disease: experimental hypercholesterolemia in the apoe-/-/lrp5-/- mice. J Cell Biochem. 2011; 112:2987–91.
22. Rajamannan NM. The role of lrp5/6 in cardiac valve disease: Ldl-density-pressure theory. J Cell Biochem. 2011;112:2222–9.
23. Rajamannan NM. Bicuspid aortic valve disease: the role of oxidative stress in lrp5 bone formation. Cardiovasc Pathol. 2011;20:168–76.
24. Rajamannan NM, Subramaniam M, Caira F, Stock SR, Spelsberg TC. Atorvastatin inhibits hypercholesterolemia-induced calcification in the aortic valves via the lrp5 receptor pathway. Circulation. 2005; 112:I229–34.
25. Rajamannan NM, Subramaniam M, Springett M, Sebo TC, Niekrasz M, McConnell JP, Singh RJ, Stone NJ, Bonow RO, Spelsberg TC. Atorvastatin inhibits hypercholesterolemia-induced cellular proliferation and bone matrix production in the rabbit aortic valve. Circulation. 2002;105:2660–5.
26. Icardo JM, Colvee E, Revuelta JM. Structural analysis of chordae tendineae in degenerative disease of the mitral valve. Int J Cardiol. 2013;167:1603–9.

Application of the LDL-Density-Radius Theory: The Aortic Valve

17

Nalini M. Rajamannan, Francesco Antonini-Canterin, and Kristian Wachtal

Introduction

With the decline incidence of rheumatic carditis, calcific aortic valve disease (CAVD) [1] has become the most common indication for surgical valve replacement in the United States and in Europe [2]. Numerous epidemiologic studies identified risk factors for CAVD, which are similar to those of vascular atherosclerosis, including smoking, male gender, body mass index, hypertension, elevated lipid and inflammatory markers, metabolic syndrome and renal failure [3–19]. For years, this disease process was thought to be due to a degenerative phenomenon by which calcium attached to the surface of the aortic valve leaflet. Understanding calcification, as the critical end-stage process which causes progression to severe stenosis and leads to poor outcomes [20], is becoming important in the results of the randomized trials for treating aortic stenosis with medical therapy. To date, these trials, including SALTIRE, Simvastatin Ezetimibe in Aortic Stenosis (SEAS), Aortic Stenosis Progression Observation: Measuring the Effects of Rosuvastatin (ASTRONOMER), have all been negative [21–23]. Over the past decade, data from several studies have confirmed that all of these traditional risk factors, including metabolic syndrome [13] and renal failure [14], which are important in the development of vascular atherosclerosis, and are also implicated in the development of CAVD [3–19]. These findings provide the foundation to study targeted strategies for medical therapy, including for example, medications for hyperlipidemia, hypertension and diabetes. There are a growing number of experimental in vivo models of calcific AS, which demonstrate primarily that lipids [24–30], diabetes [30] and renal failure [31] are important in the development of this disease. There is also increasing evidence that these cells undergo specific differentiation steps toward the development of this bone phenotype as shown in in vitro studies [32–34]. In addition, there are a growing number of retrospective [35–38] and the large-scale prospective clinical trials [21–23] testing the hypothesis that atherosclerotic CAVD may be targeted with medical therapy. The only clinical trial to date, Rosuvastatin Affecting Aortic Valve Endothelium to Slow the Progression of Aortic Stenosis trial (RAAVE) was a positive study, testing the hypothesis that treating elevated LDL as compared to normal LDL patients slows progression of CAVD [39]. The retrospective studies published to date are shown in Table 17.1 [35–38].

N.M. Rajamannan, MD (✉)
Division of Biochemistry and Molecular Biology, Mayo Clinic, 200 First St SW, Rochester, MN, USA
e-mail: rajamannan.nalini@mayo.edu

F. Antonini-Canterin, MD
Preventive and Rehabilitative Cardiology, Cardiologia ARC, Azienda Ospedaliera "S. Maria degli Angeli", Pordenone, Italy

K. Wachtal, MD, PhD
Department of Medicine, Glostrup Hospital, University of Copenhagen, 57 NDR Ringvej, Glostrup, Denmark
e-mail: kristian@wachtell.net

N.M. Rajamannan (ed.), *Molecular Biology of Valvular Heart Disease*,
DOI 10.1007/978-1-4471-6350-3_17, © Springer-Verlag London 2014

Table 17.1 Application of the LDL-density-radius theory: calculations to demonstrate the significance of the hemodynamic and biologic differences between aortic valve clinical trials versus vascular clinical trials

	LDL (mg/dl)			Aortic valve area (cm^2)		
	Baseline	End of trial	Change in LDL (%)	Baseline	End of trial	Change in AVA (%)
SALTIRE						
Control	133	137	3.00	1.02	0.86	18.60
Atorvastatin 80 mg	137	66	51.82	1.03	0.88	17.04
RAAVE						
Control	119	118	0.84	1.24	1.11	11.70
Rosuvastatin 20 mg	160	94	41.25	1.22	1.16	5.10
SEAS						
Control	139	131	5.75	1.269	1.128	11.11
Simvastatin 40 mg/ ezetimide 10 mg	140	63	55.00	1.292	1.175	9.06

The pioneers in valve clinical trials designed studies prior to the publication of many of the experimental models. The trials were designed with the traditional trial design for lipid lowering using vascular and valvular end-points. The first randomized prospective study testing the effects of statins in CAVD and SALTIRE was published in 2005 [40]. In this double-blind, placebo-controlled trial, patients with calcific aortic stenosis were randomly assigned to receive either 80 mg of atorvastatin daily or a matched placebo. Aortic-valve stenosis and calcification were assessed with the use of Doppler echocardiography and helical computed tomography, respectively. The primary end-points were change in aortic-jet velocity and aortic-valve calcium score, secondary end-points were traditional vascular end-points. The SALTIRE investigators demonstrated a trend in slowing of the progression of the aortic valve stenosis but not a statistically significant study for primary end-points. The vascular end-points demonstrated statistically significant improvement. The SALTIRE investigators concluded that intensive lipid-lowering therapy does not halt the progression of calcific aortic stenosis or induce its regression [40], and the reason for this negative trial is the timing of therapy [41].

The RAAVE trial [39] performed a prospective trial of AS with Rosuvastatin targeting serum LDL slowed progression of echo hemodynamic measurements, and improved inflammatory biomarkers providing the first clinical evidence for targeted therapy in patients with asymptomatic AS. The study's aim was to assess Rosuvastatin on the hemodynamic progression and the inflammatory markers of AS by treating LDL in patients with aortic stenosis according to the NCEP-ATPIII guidelines for 1 year. The clinical characteristics of the RAAVE trial are shown in Table 17.1. Prospective treatment of moderate aortic stenosis with Rosuvastatin targeting serum LDL did slow progression of echocardiographic parameters of aortic stenosis, improved inflammatory biomarkers and improved vascular end-points showing the first clinical evidence for targeted therapy in asymptomatic moderate to severe aortic stenosis [39].

The largest clinical trial was the SEAS trial [22]. This trial is a randomized, double-blind trial involving 1,873 patients with mild-to-moderate, asymptomatic aortic stenosis. Again, similar to SALTIRE [21], there were fewer patients with ischemic cardiovascular events in the Simvastatin–Ezetimibe group (148 patients) than in the placebo group (187 patients); the authors noted that this is mainly because of the smaller number of patients who underwent coronary artery bypass grafting. Cancer occurred more frequently in the Simvastatin–Ezetimibe group (105 vs. 70, $p=0.01$). The investigators concluded that the medication did not reduce the composite outcome of combined aortic-valve events in-patient with aortic stenosis including echo progression

and vascular end-points. ASTRONOMER [23], the most recent trial, also demonstrated negative randomized clinical results and included patients with bicuspid aortic valve disease. This was a randomized, double-blind, placebo-controlled trial in asymptomatic patients with mild to moderate AS and no clinical indications for cholesterol lowering. The patients were randomized to receive either placebo or Rosuvastatin 40 mg daily. A total of 269 patients were randomized: 134 patients to Rosuvastatin 40 mg daily and 135 patients to placebo. Annual echocardiograms were performed to assess AS progression, which was the primary outcome; the median follow-up was 3.5 years. The peak AS gradient increased in patients receiving Rosuvastatin from a baseline of 40.8 ± 11.1–57.8 ± 22.7 mmHg at the end of follow-up and in patients with placebo from 41.6 ± 10.9 mmHg at baseline to 54.8 ± 19.8 mmHg at the end of follow-up. The annualized increase in the peak AS gradient was 6.3 ± 6.9 mmHg in the Rosuvastatin group and 6.1 ± 8.2 mmHg in the placebo group (P = 0.83). This chapter will demonstrate the calculations from the RAAVE and SALTIRE trial to determine the potential role of medical therapy for calcific aortic valve disease and design of the clinical trials using the LDL-Density-Radius Hypothesis [39].

The LDL-Density-Radius Theory is related to two fundamental issues for these two similar but very different disease processes: first, is the LDL effect and second is the difference in the radius between the aortic valve and that of the vessel. These differences must be taken into account toward the final analysis of these trials and for the future trial design for aortic valve disease. From these basic studies and human clinical trials, the lessons learned have evolved into the LDL-Density-Radius theory for future trial design of valvular heart disease, which takes into account two axioms. The first axiom is the LDL-density theory: Low-density lipoprotein is a critical lipoprotein in the development of vascular atherosclerosis and valvular sclerosis. The LDL mechanism by which the disease develops in the vascular lumen and the aortic valve leaflet has two different biological directions. The vascular lesion occludes the lumen inward along the radial axis towards the center, as shown in Fig. 17.1, Panel a. The LDL affects the valvular leaflet to become thickened with decrease mobility. The direction of this disease moves an upward direction along the y-axis along the aortic surface of the aortic valve. Over time, the leaflets fuse which occludes the functional opening of the aortic valve as shown in Fig. 17.1, Panel b. A critical density of LDL that is required to induce this disease initiates the direction of these disease processes. Calculation of the percent lowering of LDL density is important for reducing the biological effect of disease. Figure 17.1, Panel c, demonstrates a formula to calculate the percent reduction of the LDL density. The second axiom is the radius theory of vascular versus valvular disease: to determine the effect of the treatment on the radius for the circumference for this disease. The Bernoulli equation [42] was modified [43] to calculate aortic valve areas by echocardiography using the Doppler technique. The modification of this equation for aortic valve area includes the drop of the calculation for the flow acceleration and the viscous friction because the velocity profile in the center of the lumen is usually flat. For this reason, the viscous friction factor can be ignored in the clinical setting of aortic valve disease. Figure 17.1, Panels d1 and d2, demonstrates the original Bernoulli equation for flow through a pipe [43]. However, the flow in the lumen of a vessel is not flat due to smaller radius: therefore, the viscous friction factor must be taken into account for therapy. Figure 17.1, Panel e, is the calculation of resistance of fluid through a pipe, and demonstrates an inverse r [4] dependence of the resistance to fluid flow, which therefore increases viscosity by a factor of 16. Furthermore reductions of the LDL density will therefore have a quicker effect in the reduction of the vascular lesion depending on the direction of the lesion as shown in Fig. 17.1, Panel a. If the normal diameter of a coronary artery is 4.5 mm, and the normal diameter of the left ventricular outflow tract is 2.0 cm, the calculation of the change in the diameter must take into account these differences in radius and the time it will take to

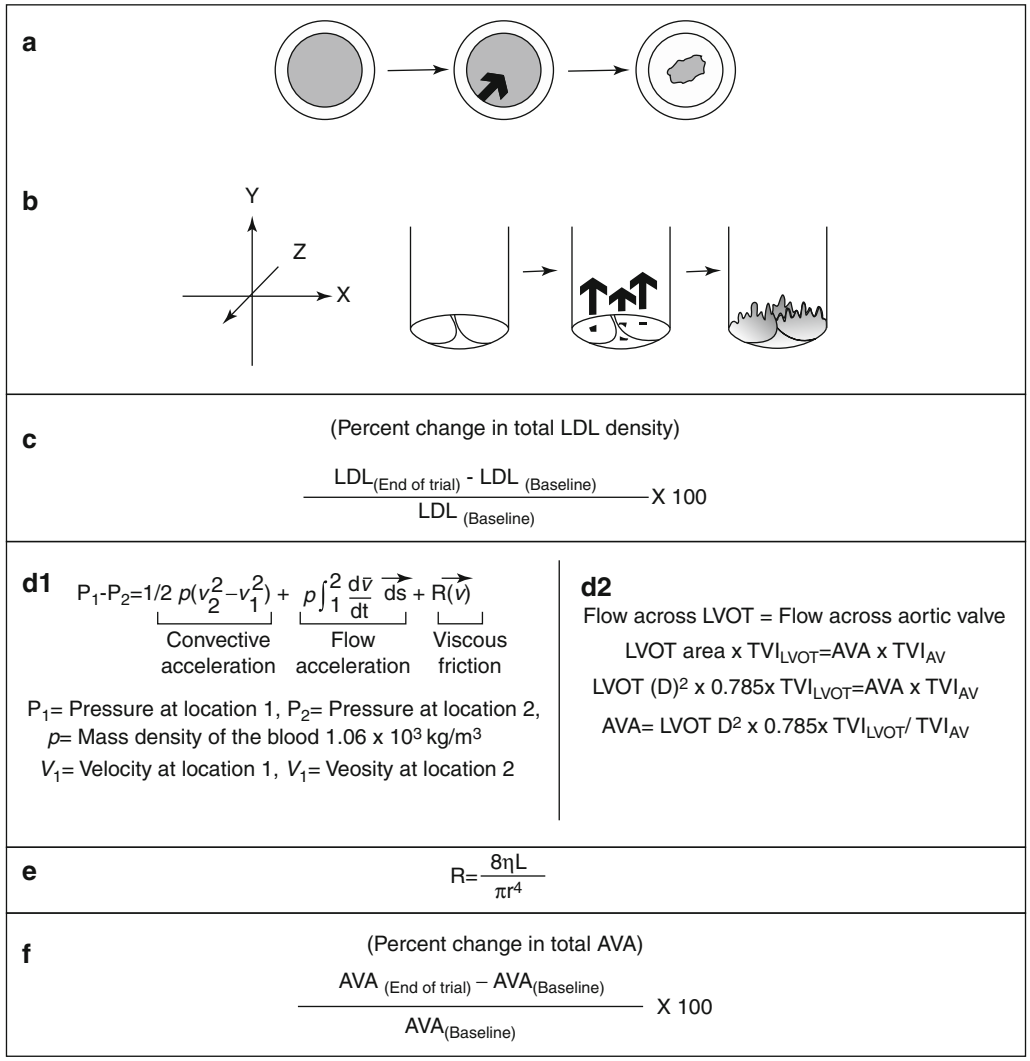

Fig. 17.1 The LDL-density-radius theory. Panel (**a**) Vascular lumen and radial direction of disease. Panel (**b**) Aortic valve leaflet and Y-axis direction of disease. Panel (**c**) Axiom one: LDL-density theory. Panel (*d1*) Bernoulli equation. Panel (*d2*) Modified continuity equation for aortic valve area. Panel (**e**) Resistance for fluid flow. Panel (**f**) Axiom two: radius theory

lower the LDL density to mathematically target the biologic direction of the disease process. Figure 17.1, Panel f, is the calculation for the percent improvement for the aortic valve area. To summarize mathematically and biologically, the clinical trials for aortic valve stenosis need to adopt the following two axioms for targeting the disease biology in terms of the radial direction of disease and the magnitude of the LDL density that is necessary to activate the atherosclerotic process. The importance of LDL lowering and the magnitude of the radius are critical toward treatment efficacy, as viscous resistance cannot be deleted for the vascular radius as it can for the aortic valve radius according to Bernoulli's original formula. SALTIRE and RAAVE are the first two studies to evaluate the use of statins for calcific aortic valve disease (CAVD). This chapter applies the hypothesis of the LDL-Density-Radius Theory.

Clinical Application of the Algorithm

Table 17.1 demonstrates an example of the application of this formula from two of the trials (SALTIRE and RAAVE investigators provided permission to use these data points for this manuscript) [44]. The calculation of the percent change in LDL and the percent change in AVA indicate that the lower the percent change in AVA represents the percent improvement needed to demonstrate the potential to treat atherosclerotic aortic valve disease responsive to medical therapy.

Those patients who received statin therapy had a greater degree of LDL cholesterol lowering seen as the % change in LDL significantly associated with a lower change for aortic valve area demonstrating a slowing of progression with statin therapy ($R^2 = 0.27$ and $p < 0.001$) as shown in Fig. 17.2a. The percent change in the LDL for the treated patients was 47 % and for the not treated was 2 %. The percent change in the AVA for the treated was 5 % and for the not treated was 15 %. The results demonstrate that if the diameter and the LDL lowering percent change do have a significant effect in the slope of the analysis. Figure 17.2b demonstrates a similar analysis for the REVERSAL trial [45] in which intensive lipid lowering therapy and the use of high dose statins slow the progression of vascular atherosclerosis as measured by intravascular ultrasound. The results for both these analyses depend on the point-slope equation of a line. This equation was first published by Renee Descartes in 1637 in the La Geometrie appendix of a textbook entitled Discours de la méthode pour bien conduire sa raison, et chercher la vérité dans les sciences (English Translation: Discourse on the Method of Rightly Conducting One's Reason and of Seeking Truth in the Sciences) [45]. The geometric equation for a line demonstrates that any two points on a nonvertical line can be used to calculate a slope. The equation of the line with a slope m passing through the point (x1, y1) is given by $y - y1 = m(x - x1)$. The comparison of the slopes for the analysis from the combined data points of SALTIRE-RAAVE demonstrate that the negative slope similar to that of REVERSAL [45] indicates slowing of progression for both vascular atherosclerosis and the atherosclerotic biology present in the aortic valve.

Proposed Algorithm for the Approach to Patients with Valvular Heart Disease

This chapter demonstrates the cellular mechanisms, risk factors, and hemodynamic analysis from the perspective of the clinical trials in calcific aortic stenosis. This chapter proposes an approach for the future treatment of this patient population. (1) Symptomatic severe aortic stenosis is a class I indication for surgical valve replacement as defined by Ross and Braunwald and is outlined in the ACC/AHA and ESC current guidelines. (2) Patients with elevated LDL levels, then management of the lipids according to the NCEP ATP III guidelines is appropriate for primary prevention of vascular disease and atherosclerotic mechanisms of valvular disease. (3) Risk stratification of calcification by echo is important for prognostic information for the patient and treating physicians and can be performed routinely in the echocardiographic follow-up of aortic stenosis. (4) Management of other risk factors for this disease process including, blood sugar, weight loss, smoking cessation and risk for metabolic syndrome. (5) Future genetic testing for patients who do not have traditional atherosclerotic risk factors, but have family history of valvular heart disease may play a future role in the clinical management of this complex disease and (6) role for exercise testing to unmask latent symptoms in asymptomatic patients. In summary, this approach suggests applying this calculation, which includes biology and the continuity equation for calculation AVA by applying this calculation, there may be a role for medical therapy in this patient population. However, a full large-scale prospective clinical trial is necessary to prove this hypothesis in patients.

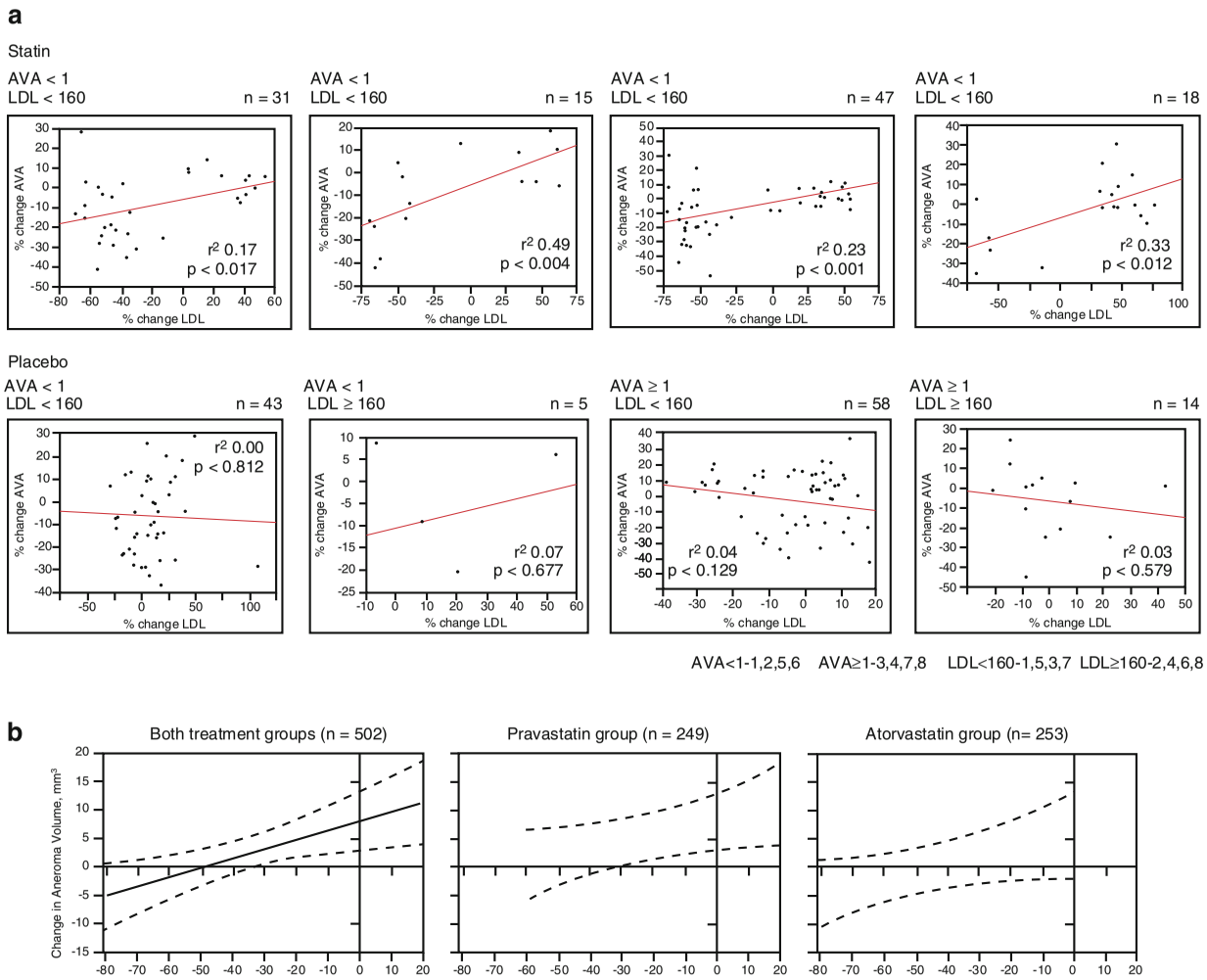

Fig. 17.2 Demonstrates the patients from RAAVE and SALTIRE that were on statin therapy and the effect of LDL lowering as compared to aortic valve area. (**a**) Demonstrates the patients from RAAVE and SALTIRE that were on placebo or no therapy and the effect of the LDL levels as compared to the aortic valve area ($p > 0.05$) and (**b**). Comparison to the Results from the REVERSAL trial (JAMA 2004. Used with Permission) [46]

References

1. Rajamannan NM, Evans FJ, Aikawa E, Grande-Allen KJ, Demer LL, Heistad DD, Simmons CA, Masters KS, Mathieu P, O'Brien KD, Schoen FJ, Towler DA, Yoganathan AP, Otto CM. Calcific aortic valve disease: not simply a degenerative process: a review and agenda for research from the national heart and lung and blood institute aortic stenosis working group. Executive summary: calcific aortic valve disease-2011 update. Circulation. 2011;124:1783–91.
2. Nkomo VT, Gardin JM, Skelton TN, Gottdiener JS, Scott CG, Enriquez-Sarano M. Burden of valvular heart diseases: a population-based study. Lancet. 2006;368:1005–11.
3. Deutscher S, Rockette HE, Krishnaswami V. Diabetes and hypercholesterolemia among patients with calcific aortic stenosis. J Chronic Dis. 1984;37:407–15.
4. Hoagland PM, Cook EF, Flatley M, Walker C, Goldman L. Case-control analysis of risk factors for presence of aortic stenosis in adults (age 50 years or older). Am J Cardiol. 1985;55:744–7.
5. Aronow WS, Ahn C, Kronzon I, Goldman ME. Association of coronary risk factors and use of statins with progression of mild valvular aortic stenosis in older persons. Am J Cardiol. 2001;88:693–5.
6. Aronow WS, Schwartz KS, Koenigsberg M. Correlation of serum lipids, calcium, and phosphorus, diabetes mellitus and history of systemic hypertension with presence or absence of calcified or thickened aortic cusps or root in elderly patients. Am J Cardiol. 1987;59:998–9.
7. Mohler ER, Sheridan MJ, Nichols R, Harvey WP, Waller BF. Development and progression of aortic valve stenosis: atherosclerosis risk factors–a causal relationship? A clinical morphologic study. Clin Cardiol. 1991;14:995–9.
8. Lindroos M, Kupari M, Valvanne J, Strandberg T, Heikkila J, Tilvis R. Factors associated with calcific aortic valve degeneration in the elderly. Eur Heart J. 1994;15:865–70.
9. Boon A, Cheriex E, Lodder J, Kessels F. Cardiac valve calcification: characteristics of patients with calcification of the mitral annulus or aortic valve. Heart. 1997;78:472–4.
10. Chui MC, Newby DE, Panarelli M, Bloomfield P, Boon NA. Association between calcific aortic stenosis and hypercholesterolemia: Is there a need for a randomized controlled trial of cholesterol-lowering therapy? Clin Cardiol. 2001;24:52–5.
11. Wilmshurst PT, Stevenson RN, Griffiths H, Lord JR. A case-control investigation of the relation between hyperlipidaemia and calcific aortic valve stenosis. Heart. 1997;78:475–9.
12. Chan KL, Ghani M, Woodend K, Burwash IG. Case-controlled study to assess risk factors for aortic stenosis in congenitally bicuspid aortic valve. Am J Cardiol. 2001;88:690–3.
13. Briand M, Lemieux I, Dumesnil JG, Mathieu P, Cartier A, Despres JP, Arsenault M, Couet J, Pibarot P. Metabolic syndrome negatively influences disease progression and prognosis in aortic stenosis. J Am Coll Cardiol. 2006;47:2229–36.
14. Palta S, Pai AM, Gill KS, Pai RG. New insights into the progression of aortic stenosis: implications for secondary prevention. Circulation. 2000;101:2497–502.
15. Peltier M, Trojette F, Sarano ME, Grigioni F, Slama MA, Tribouilloy CM. Relation between cardiovascular risk factors and nonrheumatic severe calcific aortic stenosis among patients with a three-cuspid aortic valve. Am J Cardiol. 2003;91:97–9.
16. Stewart BF, Siscovick D, Lind BK, Gardin JM, Gottdiener JS, Smith VE, Kitzman DW, Otto CM. Clinical factors associated with calcific aortic valve disease. Cardiovascular health study. J Am Coll Cardiol. 1997;29:630–4.
17. Otto CM, Lind BK, Kitzman DW, Gersh BJ, Siscovick DS. Association of aortic-valve sclerosis with cardiovascular mortality and morbidity in the elderly. N Engl J Med. 1999;341:142–7 [comment].
18. Faggiano P, Antonini-Canterin F, Baldessin F, Lorusso R, D'Aloia A, Cas LD. Epidemiology and cardiovascular risk factors of aortic stenosis. Cardiovasc Ultrasound. 2006;4:27.
19. Pohle K, Maffert R, Ropers D, Moshage W, Stilianakis N, Daniel WG, Achenbach S. Progression of aortic valve calcification: association with coronary atherosclerosis and cardiovascular risk factors. Circulation. 2001;104:1927–32.
20. Rosenhek R, Binder T, Porenta G, Lang I, Christ G, Schemper M, Maurer G, Baumgartner H. Predictors of outcome in severe, asymptomatic aortic stenosis. N Engl J Med. 2000;343:611–7.
21. Cowell SJ, Newby DE, Prescott RJ, Bloomfield P, Reid J, Northridge DB, Boon NA; Scottish Aortic Stenosis and Lipid Lowering Trial, Impact on Regression (SALTIRE) Investigators. A randomized trial of intensive lipid-lowering therapy in calcific aortic stenosis. N Engl J Med. 2005;352(23):2389–97.
22. Rossebo AB, Pedersen TR, Boman K, Brudi P, Chambers JB, Egstrup K, Gerdts E, Gohlke-Barwolf C, Holme I, Kesaniemi YA, Malbecq W, Nienaber CA, Ray S, Skjaerpe T, Wachtell K, Willenheimer R. Intensive lipid lowering with simvastatin and ezetimibe in aortic stenosis. N Engl J Med. 2008;359:1343–56.
23. Chan KL, Teo K, Dumesnil JG, Ni A, Tam J. Effect of lipid lowering with rosuvastatin on progression of aortic stenosis: results of the aortic stenosis progression observation: measuring effects of rosuvastatin (astronomer) trial. Circulation. 2010;121:306–14.
24. Rajamannan NM, Subramaniam M, Springett M, Sebo TC, Niekrasz M, McConnell JP, Singh RJ, Stone NJ, Bonow RO, Spelsberg TC. Atorvastatin inhibits hypercholesterolemia-induced cellular proliferation and bone matrix production in the rabbit aortic valve. Circulation. 2002;105:2260–5.
25. Rajamannan NM, Sangiorgi G, Springett M, Arnold K, Mohacsi T, Spagnoli LG, Edwards WD, Tajik AJ, Schwartz RS. Experimental hypercholesterolemia

induces apoptosis in the aortic valve. J Heart Valve Dis. 2001;10:371–4.
26. Drolet MC, Arsenault M, Couet J. Experimental aortic valve stenosis in rabbits. J Am Coll Cardiol. 2003;41:1211–7.
27. Weiss RM, Ohashi M, Miller JD, Young SG, Heistad DD. Calcific aortic valve stenosis in old hypercholesterolemic mice. Circulation. 2006;114:2065–9.
28. Aikawa E, Nahrendorf M, Sosnovik D, Lok VM, Jaffer FA, Aikawa M, Weissleder R. Multimodality molecular imaging identifies proteolytic and osteogenic activities in early aortic valve disease. Circulation. 2007;115:377–86.
29. Drolet MC, Roussel E, Deshaies Y, Couet J, Arsenault M. A high fat/high carbohydrate diet induces aortic valve disease in c57bl/6j mice. J Am Coll Cardiol. 2006;47:850–5.
30. Shao JS, Cheng SL, Pingsterhaus JM, Charlton-Kachigian N, Loewy AP, Towler DA. Msx2 promotes cardiovascular calcification by activating paracrine wnt signals. J Clin Invest. 2005;115:1210–20.
31. Palta S, Pai AM, Gill KS, Pai RG. New insights into the progression of aortic stenosis: implications for secondary prevention. Circulation. 2000;101(21):2497–502.
32. Blevins TL, Peterson SB, Lee EL, Bailey AM, Frederick JD, Huynh TN, Gupta V, Grande-Allen KJ. Mitral valvular interstitial cells demonstrate regional, adhesional, and synthetic heterogeneity. Cells Tissues Organs. 2008;187:113–22.
33. Liu AC, Joag VR, Gotlieb AI. The emerging role of valve interstitial cell phenotypes in regulating heart valve pathobiology. Am J Pathol. 2007;171:1407–18.
34. Yip CY, Chen JH, Zhao R, Simmons CA. Calcification by valve interstitial cells is regulated by the stiffness of the extracellular matrix. Arterioscler Thromb Vasc Biol. 2009;29:936–42.
35. Antonini-Canterin F, Popescu BA, Huang G, Korcova-Miertusova R, Rivaben D, Faggiano P, Pavan D, Piazza R, Bolis A, Ciavattone A, Ruggiero A, Nicolosi GL. Progression of aortic valve sclerosis and aortic valve stenosis: what is the role of statin treatment? Ital Heart J. 2005;6:119–24.
36. Bellamy MF, Pellikka PA, Klarich KW, Tajik AJ, Enriquez-Sarano M. Association of cholesterol levels, hydroxymethylglutaryl coenzyme-a reductase inhibitor treatment, and progression of aortic stenosis in the community. J Am Coll Cardiol. 2002;40:1723–30 [comment].
37. Shavelle DM, Takasu J, Budoff MJ, Mao S, Zhao XQ, O'Brien KD. Hmg coa reductase inhibitor (statin) and aortic valve calcium. Lancet. 2002;359:1125–6 [comment].
38. Rosenhek R, Rader F, Loho N, Gabriel H, Heger M, Klaar U, Schemper M, Binder T, Maurer G, Baumgartner H. Statins but not angiotensin-converting enzyme inhibitors delay progression of aortic stenosis. Circulation. 2004;110:1291–5.
39. Moura LM, Ramos SF, Zamorano JL, Barros IM, Azevedo LF, Rocha-Gonçalves F, Rajamannan NM. Rosuvastatin affecting aortic valve endothelium to slow the progression of aortic stenosis. J Am Coll Cardiol. 2007;49(5):554–61.
40. Cowell SJ, Newby DE, Prescott RJ, Bloomfield P, Reid J, Northridge DB, Boon NA. A randomized trial of intensive lipid-lowering therapy in calcific aortic stenosis. N Engl J Med. 2005;352:2389–97.
41. Newby DE, Cowell SJ, Boon NA. Emerging medical treatments for aortic stenosis: statins, angiotensin converting enzyme inhibitors, or both? Heart. 2006;92:729–34.
42. Nissen SE, Tuzcu EM, Schoenhagen P, Brown BG, Ganz P, Vogel RA, Crowe T, Howard G, Cooper CJ, Brodie B, Grines CL, DeMaria AN; REVERSAL Investigators. Effect of intensive compared with moderate lipid-lowering therapy on progression of coronary atherosclerosis: a randomized controlled trial. JAMA. 2004;291(9):1071–80.
43. Bernoulii D. Hydrodynamica Sive De Viribus et Motibus Fluidorum Commentarrii. Strasbourg: Argentoratum, St 31. 1738.
44. Rajamannan NM. Mechanisms of aortic valve calcification: the ldl-density-radius theory: a translation from cell signaling to physiology. Am J Physiol Heart Circ Physiol. 2010;298:H5–15.
45. Descartes, La Geometrie appendix: Discours de la Methode pour bien condiuire sa raison, et chercher la verite dans les sciences, 1637.
46. Rajamannan NM, Best P, Antonini-Canterin F, Moura LM, Saltire-raave subanalysis: a role for statins in aortic valve disease. J Am Coll Cardiol. 2011;57(14): E1317.

Index

N.M. Rajamannan (ed.), *Molecular Biology of Valvular Heart Disease*,
DOI 10.1007/978-1-4471-6350-3, © Springer-Verlag London 2014